FRACTURE ANALYSIS, HYDRODYNAMIC PROPERTIES AND MINERAL ABUNDANCE IN THE ALTERED IGNEOUS WALL ROCKS OF THE MAYFLOWER MINE, PARK CITY DISTRICT, UTAH

by

Raimundo Netuno Nobre Villas

A dissertation submitted to the faculty of the
University of Utah in partial fulfillment of the requirements
for the degree of

Doctor of Philosophy

in

Geology

Department of Geology and Geophysics

University of Utah

Spring 1975

UNIVERSITY OF UTAH GRADUATE SCHOOL

SUPERVISORY COMMITTEE APPROVAL

of a dissertation submitted by

Raimundo Netuno Nobre Villas

I have read this dissertation and have found it to be of satisfactory quality for a doctoral degree.

April 9, 1975
Date

Denis L. Norton
Chairman, Supervisory Committee

I have read this dissertation and have found it to be of satisfactory quality for a doctoral degree.

April 9, 1975
Date

Mathew P. Nackowski
Member, Supervisory Committee

I have read this dissertation and have found it to be of satisfactory quality for a doctoral degree.

April 9, 1975
Date

Mead LeRoy Jensen
Member, Supervisory Committee

I have read this dissertation and have found it to be of satisfactory quality for a doctoral degree.

April 9, 1975
Date

Jonathan H. Goodwin
Member, Supervisory Committee

I have read this dissertation and have found it to be of satisfactory quality for a doctoral degree.

April 9, 1975
Date

Jan D. Miller
Member, Supervisory Committee

I have read this dissertation and have found it to be of satisfactory quality for a doctoral degree.

April 9, 1975
Date

Frank Stenger
Member, Supervisory Committee

UNIVERSITY OF UTAH GRADUATE SCHOOL

FINAL READING APPROVAL

To the Graduate Council of the University of Utah:

I have read the dissertation of Raimundo Netuno Nobre Villas in its final form and have found that (1) its format, citations, and bibliographic style are consistent and acceptable; (2) its illustrative materials including figures, tables, and charts are in place; and (3) the final manuscript is satisfactory to the Supervisory Committee and is ready for submission to the Graduate School.

April 18, 1975
Date

Jonathan H. Goodwin
Member, Supervisory Committee

Approved for the Major Department

S. H. Ward
Chairman/Dean

Approved for the Graduate Council

Sterling M. McMurrin
Dean of the Graduate School

ACKNOWLEDGEMENTS

I wish to express my most profound gratitude to Dr. Denis Norton, Chairman of the Supervisory Committee, for his constant assistance during all phases of this research. His guidance, moral support, patience, fruitful discussions and financial aid are deeply appreciated. I am glad this work brought us together as friends.

I would like also to acknowledge the Department of Geology and Geophysics, especially Dr. Stanley Ward who made possible my coming to the University of Utah and gave financial assistance in the manner of a Research Fellowship and Teaching Assistantship. I am also thankful to Dr. Jonathan Goodwin and Dr. Matthew Nackowski for their criticism and suggestions regarding this dissertation manuscript.

My parents and friends from Brazil were of vital importance to the accomplishment of this study. Their help is deeply appreciated.

My friends from Salt Lake City and Tucson enabled me to cope with the rigors of this work which could not have been terminated without their vitality and dedication shown outside the academic realm.

A special thanks goes to Mr. John Simos, former Chief Geologist of the Mayflower Mine, and the additional members of the Hecla Mining Company who assisted me during the field work. I would also like to thank Mr. Bill Reed who assisted with field work and sample analysis.

Acknowledgement is also due to the Department of Geosciences at the University of Arizona, Tucson, in whose laboratory facilities a

great part of the analytical work was done.

The final phase of this work could not have been possible without the financial assistance provided by the Research Corporation and the National Science Foundation (grant n. GA41136). The Geological Research Fund of the Geology and Geophysics Department of the University of Utah also provided financial assistance in the form of travel expenses and means for confection of petrographic material.

TABLE OF CONTENTS

	Page
ACKNOWLEDGEMENTS	iv
LIST OF TABLES	ix
LIST OF ILLUSTRATIONS	xi
ABSTRACT	xv
INTRODUCTION	1
Chapter	
I. GENERAL ENVIRONMENT OF THE MAYFLOWER STOCK	3
Geologic Setting of the Park City District	3
Regional geology	3
Geology of the Park City District	5
II. THE MAYFLOWER MINE	19
Geology of the Mayflower Mine Area	19
Mine Stratigraphy	19
Igneous Rocks	22
The Mayflower-Pearl Fault Zone	24
Mayflower fissure-vein	25
Pearl fissure-vein	26
Alteration and Base-Metal Mineralization	26
III. DATA COLLECTION	28
Field Work	28
Sample Numeration and Location	29
Analytical Work	30
IV. FRACTURING OF THE IGNEOUS ROCKS	35
V. FRACTURE CHARACTERISTICS AND HYDRODYNAMIC PROPERTIES OF THE ROCKS	47
Parallel Plate Model for Fractured Media	48
Fracture Abundance	52

Chapter Page

Aperture Characteristics 60
Porosity 63
Permeability 77

VI. PETRO-CHEMISTRY OF THE IGNEOUS ROCKS 80

Occurrence and General Petrographic Description 80
The Mayflower stock 80
The Ontario stock 82
The Valeo stock 82
Bulk Chemistry 83
Major components 83
Transition elements 84
Mineral Chemistry 87
Primary and alteration assemblages 87
Chemical compositions of the mineral phases 88
Average Modes of the Unaltered Igneous Rocks 112
Petrogenetic Relationships Among the Stocks 114

VII. MASS ABUNDANCE OF REACTANT AND PRODUCT MINERALS 116

Mass Abundance Calculations 117
Distribution 121
Description of Phase Relationships 138
Initial solution 139
Phase stability relationships 141
Gains and Losses 172
Alteration and Its Relation To Fracturing 177

VIII. CONCLUSIONS 180

Appendices

A. BULK CHEMICAL COMPOSITION OF THE ROCKS 185

B. CHEMICAL COMPOSITION OF MINERALS 195

C. BULK AND GRAIN DENSITIES OF THE ROCKS 197

D. FRACTURE APERTURE DETERMINATIONS 200

E. QANMIN PROGRAM FUNDAMENTALS 203

F. DIST PROGRAM FUNDAMENTALS 206

G. THERMODYNAMIC DATA FOR BIOTITE AND PLAGIOCLASE COMPOSITIONS FOUND IN THE MAYFLOWER STOCK 209

H. MINERAL ABUNDANCE AND GAINS AND LOSSES 217

Page

BIBLIOGRAPHY 251

VITA 255

LIST OF TABLES

Table		Page
1.	Mine Stratigraphy	23
2.	Characteristics of Continuous Fractures in Mayflower Mine	53
3.	Fracture Apertures of the Mayflower and Ontario Rocks	61
4.	Grain and Bulk Densities, Porosity and Bulk Chemical Composition of the Igneous Rocks of the Mayflower Mine	65
5.	Estimated Composition of the Unaltered Mayflower, Ontario and Valeo Rocks	85
6.	Ore Production, Mayflower Mine	86
7.	Chemical Composition of Mineral Phases -- Mayflower, Ontario and Valeo Stocks	89
8.	Chemical Composition of Feldspars -- Mayflower, Ontario and Valeo Stocks	93
9.	Structural Formulas of Minerals Used in Mass Abundance Calculations -- Mayflower, Ontario and Valeo Stocks	94
10.	Fine-grained Biotite Compositions	106
11.	Estimated Initial Composition of the Mayflower Hydrothermal System	142
12.	Initial Solution Composition at 300^{o}C After Partitioning Among Most Important Complexes	143
13.	Range of Mineral Gains and Losses Resulting from the Alteration of the Mayflower and Ontario Stocks	175
14.	Overall Component Gains and Losses Resulting from the Alteration of the Mayflower and Ontario Stocks	176
15.	Operational Conditions for Rock Chemical Analysis with XRF Instrumentation	189

Table Page

16. Indication of the Accuracy of the Analyses for the Major Oxides (Except H_2O) Composing the Altered Mayflower and Ontario Rocks 190

17. Equilibrium Constant (LogK) of the Average Mayflower Biotite (X_{phl} = 0.64; X_{ann} = 0.36; X_{PDoxy} = 0.00) at Temperatures from 25°C to 350°C. 212

18. Equilibrium Constant (LogK) of the Average Plagioclase (0.6 Ab and 0.4 An) at Temperatures from 25°C to 350°C 216

19. Mineral Abundance and Gains and Losses in the Altered Mayflower and Ontario Rocks 217

LIST OF ILLUSTRATIONS

Figure		Page
1.	Map of Location of the Park City District and Mayflower Mine	4
2.	Regional Geology Map of the Areas Surrounding the Park City District	7
3.	Bedrock Geology Map of the Park City District	8
4.	Stratigraphic Column of the Park City District	11
5.	E-W Cross-section of the Park City District	12
6.	Stereogram of the Major Fissures Present in the Park City District	37
7A.	Stereogram of Shear Planes Compiled from Hecla Mining Co. Maps	37
7B.	Stereogram of Fractures Observed in the Mayflower and Ontario Stocks	37
8.	SSE-NNW Cross-section of the Mayflower Mine Area	21
9.	Sample Location (on N-S cross-section)	32
10.	Sample Location (on WSW-ENE cross-section)	33
11.	Diagram of the Stress Field that Generated the Fractures of the Mayflower and Ontario Stocks	42
12.	Hypothetical Mohr's Diagram Applied to the Mayflower and Ontario Fracturing Patterns	45
13.	Parallel Plate Model for Fracture Media	50
14A.	Frequency Distribution of Fracture Abundance	57
14B.	Cumulative Frequency Distribution of the Fracture Abundance.	57
15.	Fracture Abundance Distribution on a N-S Cross-section of the Mine	58

Figure Page

16. Porosity Contributors Sketched from a Rock Slab 73

17. Frequency Distribution of Bulk Density, Grain Density and Total Porosity 74

18. Total Porosity Distribution on a N-S Cross-section of the Mine 76

19. Biotite Geothermometer Diagram 101

20. Composition of Biotites and Chlorites as Functions of the MgO/(MgO + FeO) and $SiO_2/(SiO_2 + Al_2O_3)$ Ratios 104

21. Composition of Biotites as Functions of Their Phlogopitic Fraction and the TiO_2 and (F + Cl) wt.% 105

22. Diagram for the Amphibole Compositions 109

23. Diagram of the Feldspar Compositions 110

24. Abundance of the Major Mineral Constituents on a N-S Cross-section of the Mine--Andesine 123

25. Abundance of the Major Mineral Constituents on a N-S Cross-section of the Mine--K-feldspar 124

26. Abundance of the Major Mineral Constituents on a N-S Cross-section of the Mine--Kaolinite 125

27. Abundance of the Major Mineral Constituents on a N-S Cross-section of the Mine--Quartz 126

28. Abundance of the Major Mineral Constituents on a N-S Cross-section of the Mine--Biotite 127

29. Abundance of the Major Mineral Constituents on a N-S Cross-section of the Mine--Chlorite 128

30. Abundance of the Major Mineral Constituents on a N-S Cross-section of the Mine--Calcite 129

31. Abundance of the Major Mineral Constituents on a N-S Cross-section of the Mine--Anhydrite 130

32. Abundance of the Major Mineral Constituents on a N-S Cross-section of the Mine--Pyrite 131

Figure Page

33. Mineral Abundance Variation on the 2,800' Level 134

34. Mineral Abundance Variation on the 3,000' Level 135

35. Mineral Abundance Variation on the 2,600' Level 136

36. Mineral Abundance Variation on the 2,600' Level 137

37. Mass of Products/Mass of Unaltered Rock Ratio on a N-S Cross-Section of the Mayflower Mine 146

38A. Phase Stability Relations of Phlogopite, Biotite, Annite, Mg-montmorillonite and Microcline in the System MgO-FeO-K_2O-Al_2O_3-SiO_2-HCl-H_2O at 300°C. 150

38B. Phase Stability Relations of Phlogopite, Biotite, Annite, Mg-montmorillonite and Muscovite in the System MgO-Feo-K_2O-Al_2O_3-SiO_2-HCl-H_2O at 200°C. 151

38C. Phase Stability Relations of Phlogopite, Biotite, Annite and Kaolinite in the System MgO-FeO-K_2O-Al_2O_3-SiO_2-HCl-H_2O at 100°C. 152

39A. Phase Stability Relations of Chlorite, Phlogopite, Biotite, Annite and Mg-montmorillonite in the System MgO-FeO-K_2O-Al_2O_3-SiO_2-HCl-H_2O at 300°C. 153

39B. Phase Stability Relations of Chlorite, Phlogopite, Microcline, Muscovite, K-montmorillonite and Mg-montmorillonite in the System MgO-Feo-K_2O-Al_2O_3-SiO_2-HCl-H_2O at 200°C. 154

39C. Phase Stability Relations of Chlorite, Phlogopite, Microcline, Muscovite and Kaolinite in the System MgO-FeO-K_2O-Al_2O_3-SiO_2-HCl-H_2O at 100°C. 155

40A. Phase Stability Relations of Low-albite, Microcline, Na-montmorillonite, K-montmorillonite and Kaolinite in the System K_2O-Na_2O-Al_2O_3-SiO_2-HCl-H_2O at 300°C. 159

40B. Phase Stability Relations of Low-albite, Microcline, Muscovite, K-montmorillonite, Na-montmorillonite and Kaolinite in the System K_2O-Na_2O-Al_2O_3-SiO_2-HCl-H_2O at 200°C. . . . 160

40C. Phase Stability Relations of Low-albite, Microcline, Muscovite, Na-montmorillonite and Kaolinite in the System K_2O-Na_2O-Al_2O_3-SiO_2-HCl-H_2O at 100°C. 161

Figure Page

41A. Phase Stability Relations of Anorthite, Plagioclase, Low-albite, Na-montmorillonite, Ca-montmorillonite and Kaolinite in the System $CaO-Na_2O-Al_2O_3-SiO_2-HCl-H_2O$ at 300^oC. 162

41B. Phase Stability Relations of Anorthite, Plagioclase, Low-albite, Na-montmorillonite, Ca-montmorillonite and Kaolinite in the System $CaO-Na_2O-Al_2O_3-SiO_2-HCl-H_2O$ at 200^oC. 163

41C. Phase Stability Relations of Low-albite, Ca-montmorillonite, Na-montmorillonite and Kaolinite in the System $CaO-Na_2O-Al_2O_3-SiO_2-HCl-H_2O$ at 100^oC. 164

42A. Phase Stability Relations of Magnetite, Chalcopyrite, Bornite, Covelite and Pyrite in the System $Cu_2S-FeS-H_2S-H_2SO_4-HCl-H_2O$ at 300^oC. 169

42B. Phase Stability Relations of Magnetite, Chalcopyrite, Bornite, Covelite and Pyrite in the System $Cu_2S-FeS-H_2S-H_2SO_4-HCl-H_2O$ at 200^oC. 170

42C. Phase Stability Relations of Chalcopyrite, Bornite, Covelite and Pyrite in the System $Cu_2S-FeS-H_2S-H_2SO_4-HCl-H_2O$ at 100^oC. 171

ABSTRACT

A 670-meter vertical section of the igneous wall rocks of the Mayflower Mine, Park City District, Utah, was studied with the purpose of documenting quantitatively some fluid flow parameters and the mineral abundance in the altered igneous rocks. Fracture abundance and fracture aperture determinations allowed an estimation of the permeability and flow porosity of the igneous rocks by using a parallel plate model for a fractured medium. Values for the permeability fell in the range of 0.1 to 10 darcies, whereas flow porosity values ranged from 0.05 to 0.4%. Total porosity was calculated from bulk and grain densities of the rocks and analyzed in a model in which flow, diffusion and residual porosities are its major contributing parts. Residual porosity accounted for most of the total porosity of the fractured igneous rocks. Mapping of the fractures revealed two prominent fracture directions, N50°E/80°NW and N50°W/80°SW, which apparently constitute a conjugate set of shear fractures supposed to have been formed soon after the stocks crystallized (solidus temperature) and under a high confining pressure.

Mineralogical compositions of the rocks were determined by a computer technique which requires chemical composition of the rocks and mineral phases as input data. The rocks were analyzed for Si, Al, Fe (total iron as Fe++), Mg, Ca, Na, K, Mn and Ti with X-ray flourescence instrumentation, and for sulfide sulfur, sulfate sulfur and carbon

dioxide with LECO equipment. The mineral phases were analyzed for the same components, except for the last three, with an electron microprobe. Chemically simple phases were considered to be stoichiometric. The resulting mineral abundances disclosed two broad zonings over the sampled N-S cross-section of the mine: one lateral, characterized by both an increase of the K-feldspar, kaolinite and quartz abundances and a decrease of andesine, biotite and chlorite towards the main veins; and the other vertical, characterized by major deposition of K-feldspar, anhydrite, pyrite and kaolinite below the 2,200' level; and calcite, quartz and biotite more abundantly precipitated above. Mineral and component gains and losses were also computed and agreed with the abundance of reactant and product minerals.

Estimated initial solution composition was derived from available fluid inclusion data and constraints imposed by equilibrium relationships of the alteration assemblages at 300°C. The interpretation of the major alteration mineral constitutents was based upon a physicochemical model in which H+ ion consumption was the major chemical change of the solution composition and was also based upon a sequence of isothermal conditions for the wall rocks. Activity diagrams depicting chemical equilibrium among the major alteration phases at 100°C, 200°C, and 300°C and 1 bar total pressure were used for such an interpretation.

INTRODUCTION

Hydrothermal mineral deposits are a consequence of heat anomalies in the earth's crust generated by the emplacement of igneous intrusions into colder water-saturated host rocks. As these intrusions fracture, they may become sufficiently permeable to allow flow of aqueous solutions through their continuous fractures. As a result of the rock-solution interaction, the rocks are chemically altered and frequently mineralized. The extent and nature of the alteration and mineralization depends upon (1) the chemical composition of the rocks and solutions, (2) the physical conditions of the environment, (3) the rates of fluid flow and the pore availability in the rocks, and (4) the time span of the hydrothermal event.

Information on these sets of parameters is fundamental in understanding the formation of a hydrothermal mineral deposit. Rock composition can be obtained directly from conventional analytical techniques, but the other parameters need indirect determination. The physical conditions of the hydrothermal environment can be estimated by any of the available geothermometers or geobarometers (fluid inclusions, hydrothermal biotite, etc.) or from geological evidence on the depth of emplacement of the intrusions. Fluid flow characteristics require the knowledge of the rock permeability, whereas data on the solution composition are mainly derived from the alteration mineral assemblages, in particular the abundances with which the mineral constituents participate in the altered rocks.

The present research was proposed to document quantitatively some controlling parameters of the alteration of the igneous wall rocks of the Mayflower mine, Park City district, Utah. The mine is mostly excavated in the Tertiary Mayflower stock whose porphyritic quartz-dioritic rocks hosted most of the vein-filling sulfide ore deposits along the Mayflower-Pearl fissure zone. The 670-meter exposed vertical section of the underground mine offered a unique opportunity for collecting data from a representative volume of its igneous rocks which permitted the effects of the alteration to be studied on a broad scale. The field work was done during the last three months of operational existence of the mine just before its shutdown in December, 1972.

Abundance of continuous fractures and their corresponding apertures served as the basis for the application of a permeability model for fractured media, so that some fluid flow characteristics of the Mayflower hydrothermal system could be evaluated. Fluid inclusions studies by Nash (1973) provided adequate information on the temperature and pressure of the system. Mineral abundances were calculated by a computer technique which used the chemical composition of the rocks and mineral phases as raw data. Equilibrium relationships among the various minerals were studied with the aid of activity diagrams at 300°C, 200°C and 100°C and 1 bar total pressure.

The results obtained during this investigation were found to be compatible with field observations. Significantly, the mass abundance of alteration minerals uncovered possibilities of being used as a prospecting guide, at least for the type of ore found in the Mayflower mine.

CHAPTER I

GENERAL ENVIRONMENT OF THE MAYFLOWER STOCK

Geologic Setting of the Park City District

Regional geology

The Park City District is located in the central-northern part of the State of Utah (Fig. 1), approximately 50 km southeast of Salt Lake City, at the intersection of the north-south trending Wasatch Range and the east-west trending Uinta Range. It occupies the central part of a roughly defined quadrilateral bounded on the north by the Mount Raymond Thrust, on the south by the Charleston Thrust, on the east by the Uinta Uplift and on the west by the Wasatch Fault (Fig. 2). This structural framework is mostly related to the Uinta and Cottonwood Uplifts both of Laramide age, and the Basin and Range diastrophism. A third uplift, the Antelope-Farmington, northwest of that quadrilateral, and the Oquirrh Range, west of the Wasatch Mountains, complete the major tectonic features of the region surrounding the Park City District.

This region exposes rocks from Precambrian to Quaternary age in a fairly complete stratigraphic sequence. Gneisses, quartzites, schists and granitized rocks make up most of the Precambrian terrains which occupy the central parts of the mentioned uplifts (Grant 1966). The Paleozoic sedimentary rocks, which flank all three uplifts, are

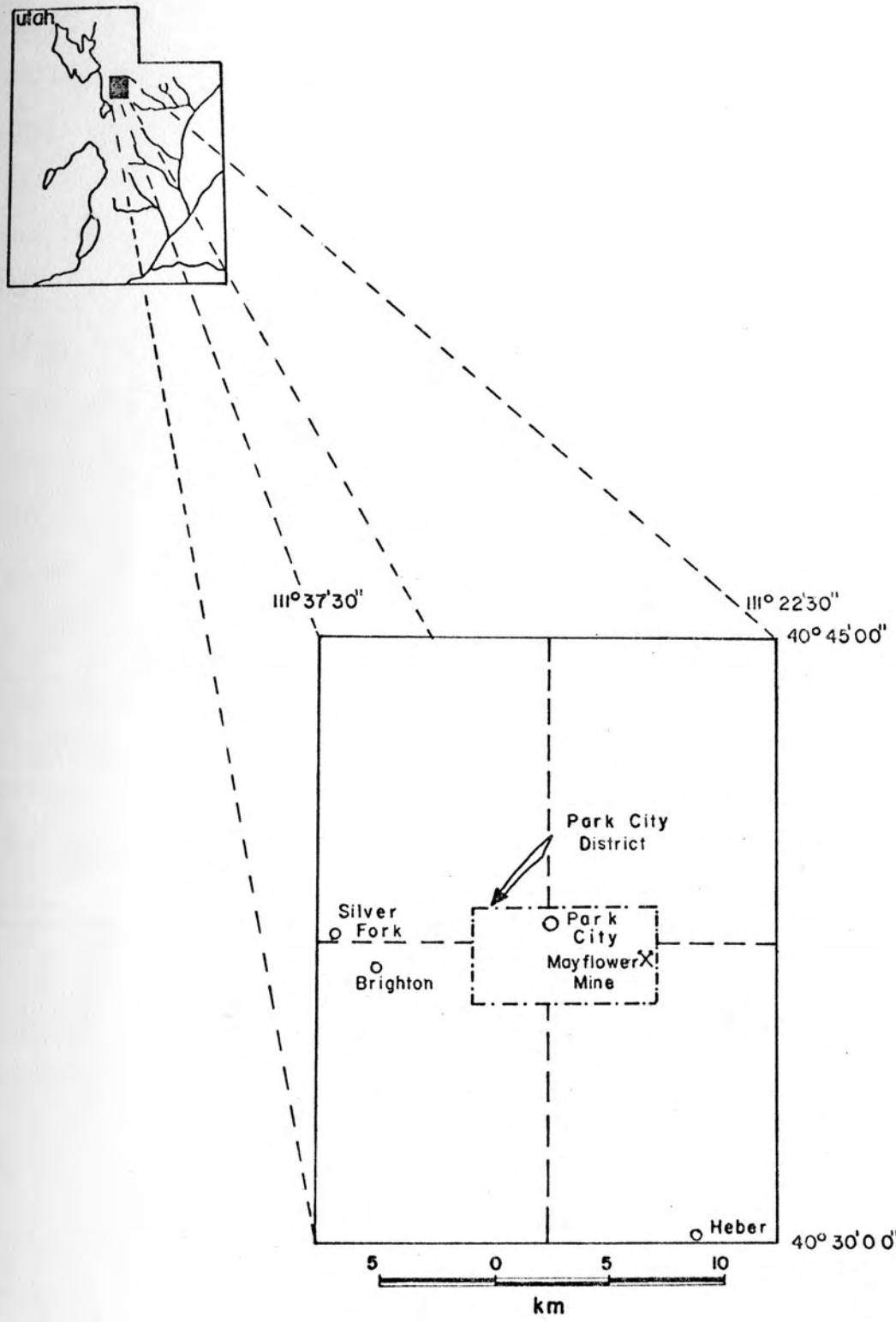

FIG. - Index Map: Location of the Park City District and Mayflower Mine

largely composed of limestone, dolomite, and sandstone and their recrystallized equivalents. Mesozoic rocks crop out away from the uplifts and include conglomerate, sandstone, shale, and limestone of diverse sedimentary environments (Grant 1966). Cenozoic rocks are irregularly distributed and include both intrusive and extrusive igneous rocks and sedimentary units. These units include Eocene conglomerates and Pleistocene glacial deposits accumulated in the valleys of the Uinta and Wasatch mountains. Oligocene plutonic igneous bodies of granitic to dioritic composition occur along a line coincident with the east-northeast trend of the Uinta axis. They include the Last Chance and Bingham stocks in the Oquirrh Mountains, the Cottonwood and Alta stocks in the Cottonwood-American Fork area and the Clayton Peak and Park City stocks in the Park City district (Fig. 2). Absolute age determinations show these intrusions to be of about the same age, 24 m.y. to 41 m.y., and that they become progressively younger westward (Crittenden et al. 1973) suggesting a migration of the magmatic center to the west. The Eocene-Oligocene volcanic counterparts of these plutonic rocks filled up two major sags, one between the Uinta and Cottonwood uplifts (Keetley volcanics) and the other between the Wasatch and the Oquirrh mountains (Traverse volcanics).

Geology of the Park City District

The Park City District is one of the large bonanza mining camps of the Western United States. It ranks as one of the three great base-metal districts of Utah with a production that has been almost continuous since 1870.

Fig. 2. Regional geology of the area surrounding the Park City District. Numbers refer to known stocks emplaced in the area: (1) Last Chance; (2) Bingham; (3) Cottonwood; (4) Alta; (5) Clayton Peak; (7) Pine Creek and (6) Mayflower, Ontario, Valeo, Glencoe and Flagstaff (modified after Eardley 1968).

Fig. 3. Bedrock geology of the Park City District showing major structural features. The densest pattern of the intrusives refers to the outcropping area of the Mayflower stock. The small circle corresponds to the Mayflower mine shaft projected vertically from the 800' level (modified after Barnes and Simos 1968).

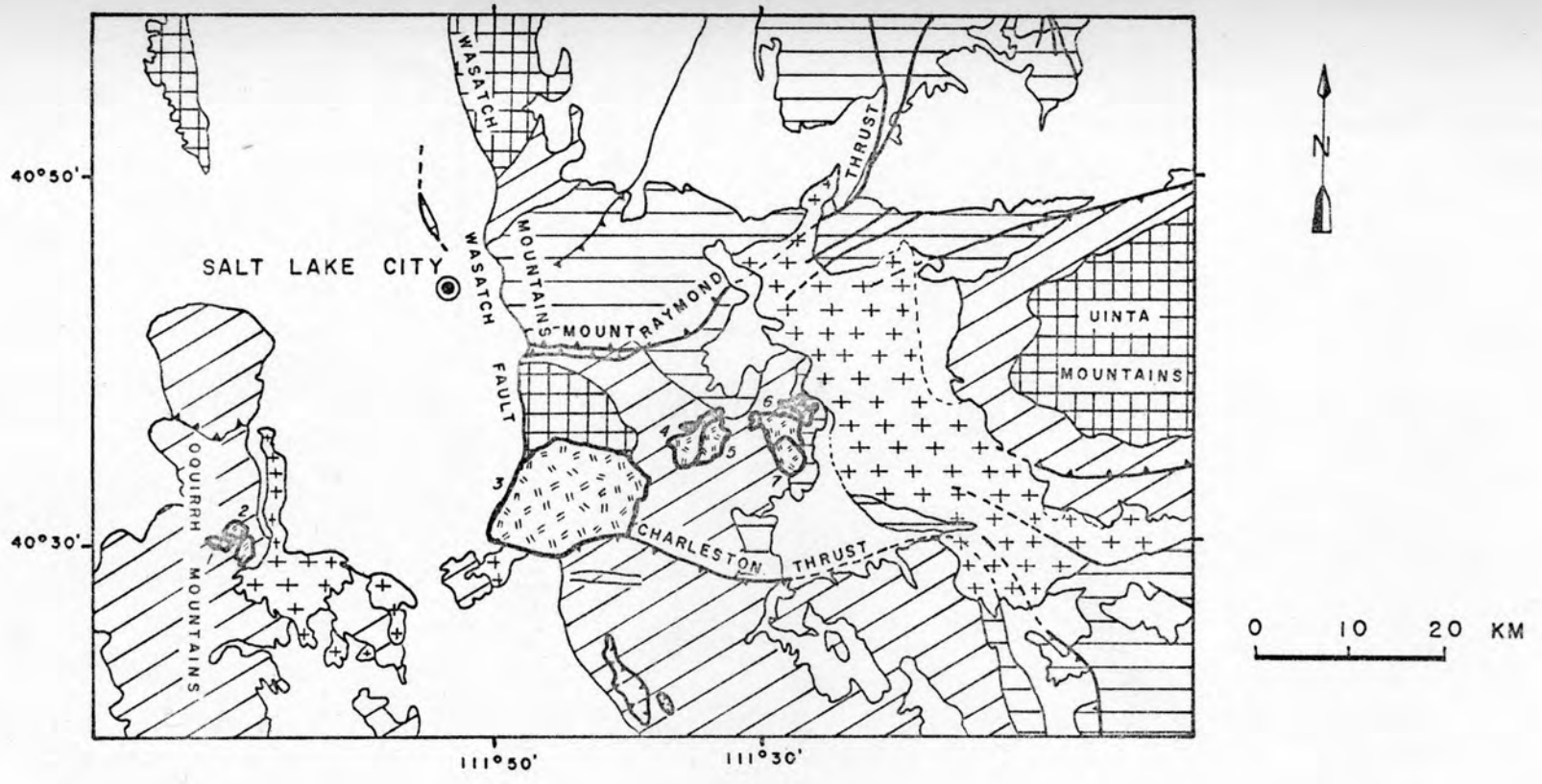
WASATCH MOUNTAINS
THRUST
SALT LAKE CITY
WASATCH FAULT
MOUNTRAYMOND
UINTA MOUNTAINS
OQUIRRH MOUNTAINS
CHARLESTON THRUST
40°50'
40°30'
111°50'
111°30'
N
0 10 20 KM
Cenozoic rocks and deposits
Intrusive Tertiary rocks
Volcanic Tertiary rocks
Mesozoic rocks
Paleozoic rocks
Precambrian rocks
Normal faults
Thrust faults
Contact

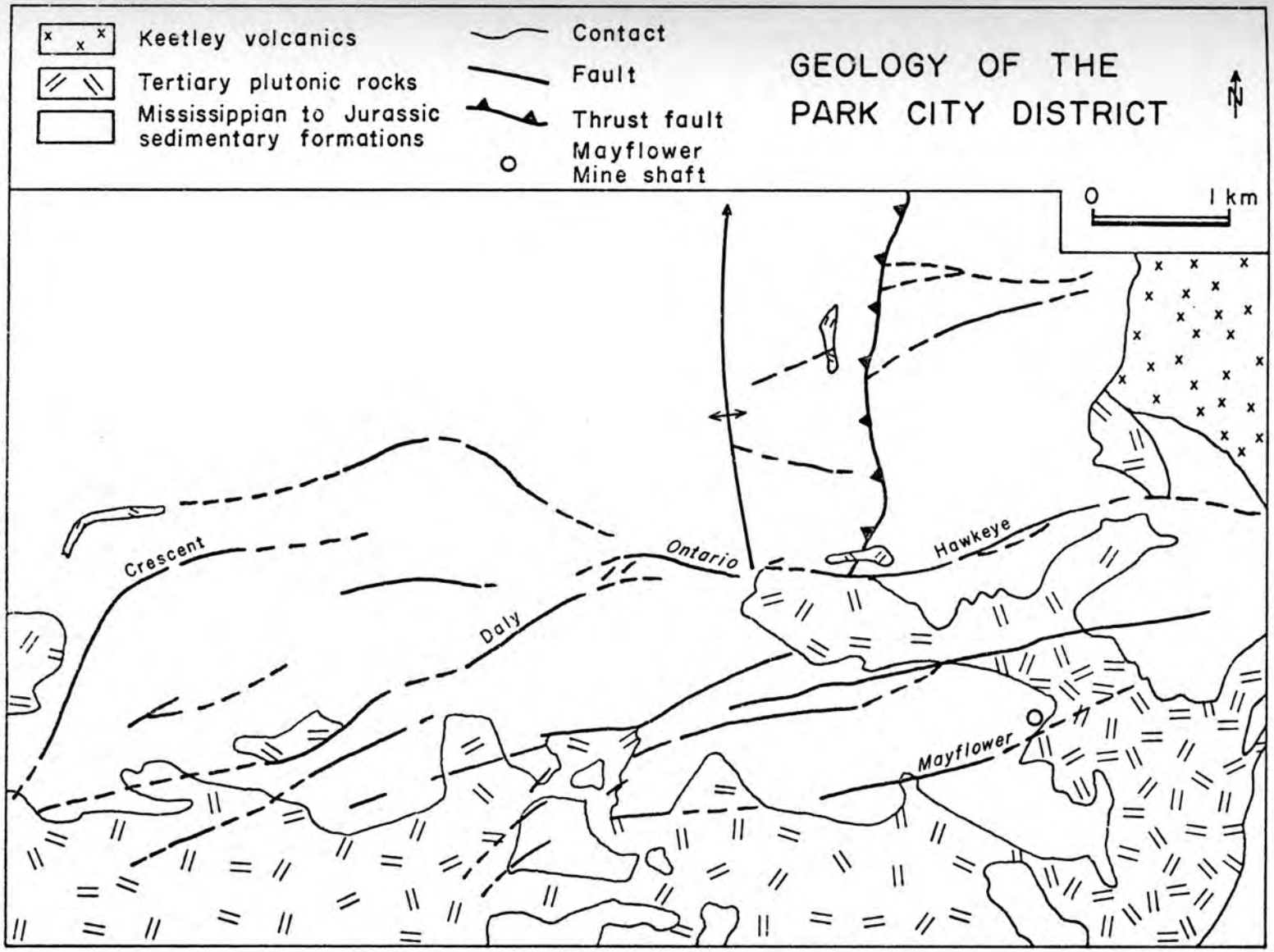
Keetley volcanics
Tertiary plutonic rocks
Mississippian to Jurassic sedimentary formations
Contact
Fault
Thrust fault
Mayflower Mine shaft
GEOLOGY OF THE PARK CITY DISTRICT
N
0
1 km
Crescent
Daly
Ontario
Hawkeye
Mayflower

Sedimentary rocks, ranging in age from Cambrian to Triassic, early Tertiary intrusives, and the Keetley volcanics make up the rocks of the district which have been partly concealed under recent fluvial and glacial deposits (Fig. 3). These rocks are exposed on the surface and in the underground workings of several mines of the area. The sedimentary sequence has an aggregate thickness of approximately 2,200 meters (Barnes & Simos 1968). It consists of clastic rocks intercalated with limestone and dolomite folded into a broad anticlinal structure. The stratigraphic column of the district is presented in Figure 4 and a generalized schematic E-W cross-section of the district is shown in Figure 5.

As a result of the igneous events, most of the rocks of the area have been hydrothermally altered to a lesser or greater extent. The emplacement of the intrusives in part caused the broad tilting of the region in the early Tertiary times and also produced large faults and fissure systems where mineralizing solutions deposited significant quantities of ore in both sedimentary and igneous host rocks. Subsequent uplifts coupled with stream and glacial erosion denuded the folded structures to expose large areas of Paleozoic and intrusive rocks and to produce the present rugged topography of the district.

Sedimentary rocks. The Permian Weber Quartzite and the Triassic Thaynes formation have the largest outcrop areas in the district. The Weber Quartzite outcrops over most of the north-central part of the district extending southeastward where it is interrupted by intrusive rocks. The Weber Quartzite is the oldest formation exposed on the crest of the Park City anticline. The Thaynes formation

Fig. 4. Stratigraphic column of the Park City District. Prepared by A. J. Erickson, 1972 (unpublished).

Fig. 5. Schematic east-west cross section of the Park City District showing major geological features.

STRATIGRAPHIC COLUMN OF THE PARK CITY DISTRICT, UTAH

COMPILED FROM SURFACE AND UNDERGROUND MAPPING
AND D.D.HOLE DATA FROM UNITED PARK CITY MINES
COMPANY FILES. LOWER PALEOZOIC DATA: U.G.S., GUIDEBOOK 22.

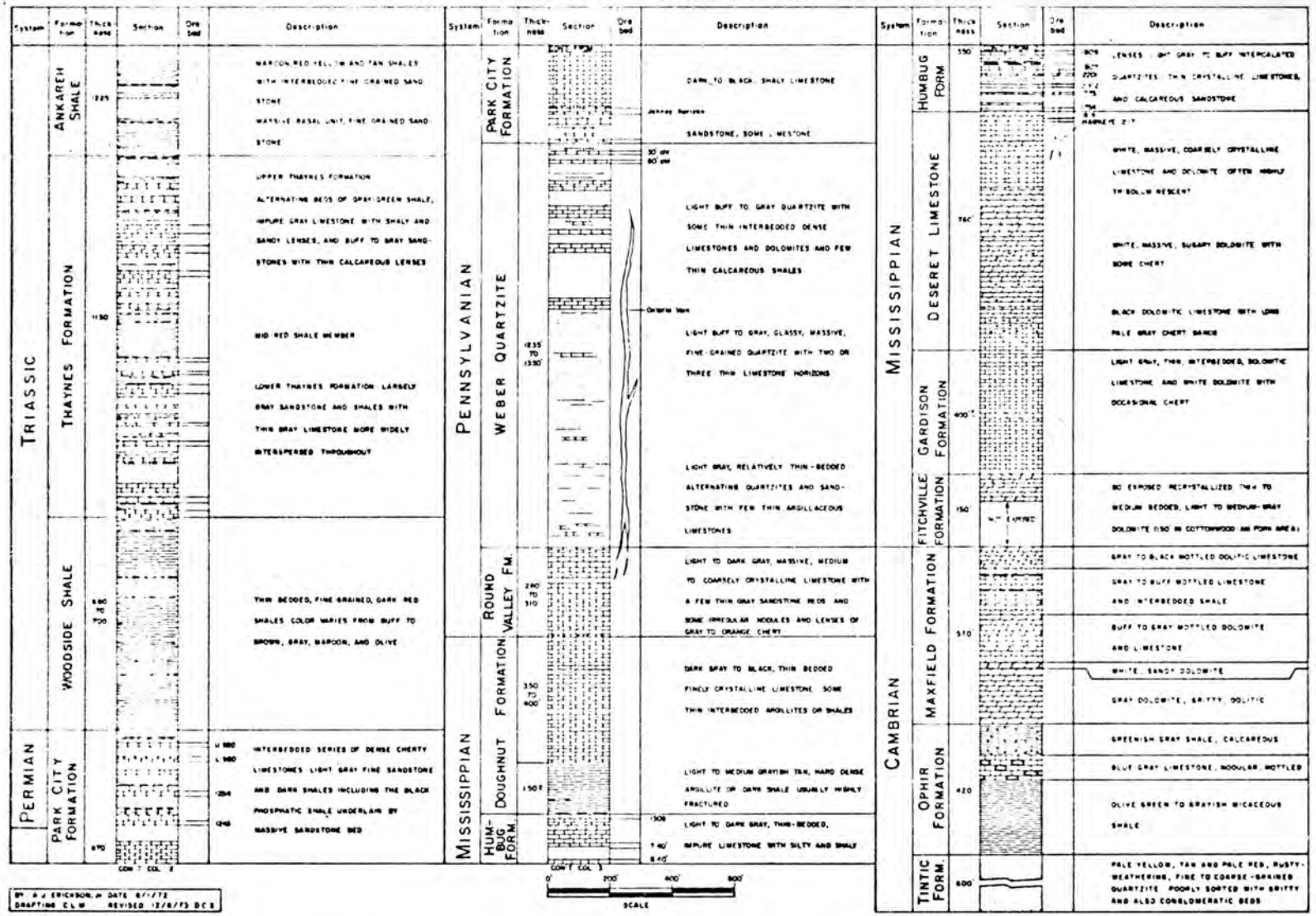

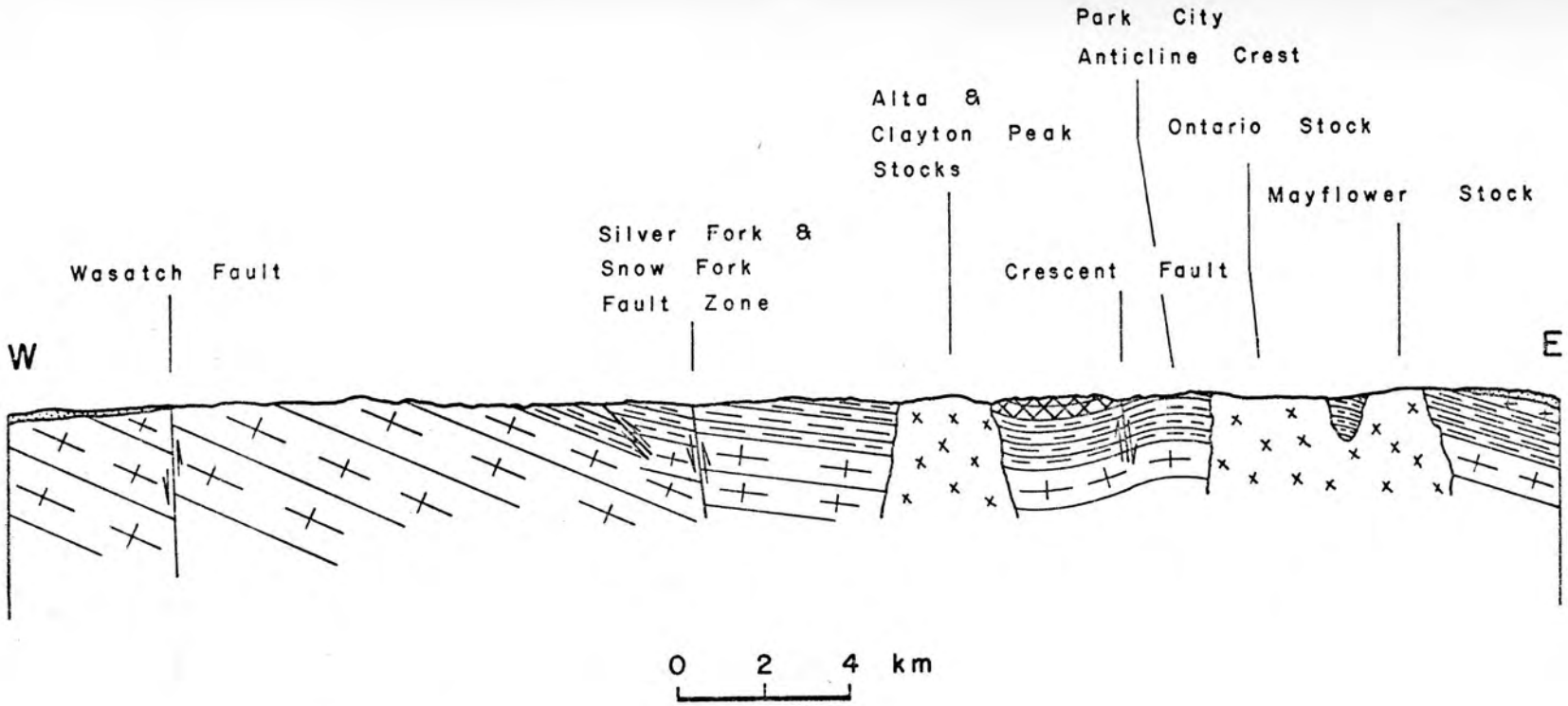
Park City
Anticline Crest
Alta &
Clayton Peak
Stocks
Ontario Stock
Mayflower Stock
Silver Fork &
Snow Fork
Fault Zone
Wasatch Fault
Crescent Fault
W
E
0 2 4 km
Recent
Extrusives
Paleozoic
Intrusives
Mesozoic
Precambrian

occurs on both flanks of the anticline but is partly buried on the east side by the Keetley volcanics. The other sedimentary formations are more restricted in occurrence, especially the lower Pennsylvanian and Mississippian units which are irregularly distributed in the southeast corner of the district.

All these formations have been truncated by faulting and to a lesser or greater extent, mineralized. The Park City formation was the most extensively mineralized of all as evidenced by production records. However, lower carbonate units below the Weber Quartzite may be equally productive. Ore production has also come from the Weber Quartzite where a fissure-filling type of ore is dominant.

Igneous rocks. Igneous rocks dominate most of the southern and extreme eastern parts of the district. They have intruded the sedimentary rocks as stocks and dike-like bodies and their volcanic counterparts have concealed an extensive portion of the pre-Tertiary formations. Intrusive igneous rocks of the Clayton Peak and Park City stocks are closely associated with many of the ore bodies. Calcareous and shale host rocks are generally altered to rocks composed of skarn or hornfelsic mineral assemblages along the contact with these intrusions. The Clayton Peak porphyry stock occupies the southwest portion of the district. Mineralogically it is composed of plagioclase, potassic feldspar, quartz and mafics (hornblende, biotite, etc.) in such proportions as to classify it as a syenodiorite (Bromfield 1968). Radiometric dating by independent investigators has assigned basically the same age of emplacement. Jaffe, et al. (in Hashad 1964) found it to be emplaced 40 to 48 m.y. ago, while the results of Crittenden Jr.,

et al. (1973) indicated an absolute age of 37 ± 1.5 m.y. to 41 ± 2.2 m.y. The Clayton Peak stock has an outcropping area of approximately 13 km^2 and consists of rocks showing a general equigranular texture with an average grain size of 3 mm (Boutwell 1912).

East of the Clayton Peak stock lies a composite igneous body where six separate porphyry intrusions have been recognized: the Mayflower, the Glencoe, the Valeo, the Pine Creek, the Flagstaff Mountain, and the Ontario. Together they constitute the so-called Park City stock. Bromfield, et al. (1970) described them as follows:

Mayflower Porphyry, light to medium-gray granodiorite porphyry containing phenocrysts of plagioclase, hornblende and locally biotite, commonly 1 to 3 mm in size, in a micro- to microcrystalline groundmass of orthoclase, quartz and plagioclase. Some facies are fine-grained, nearly equigranular rocks.

Glencoe Porphyry, light to medium-gray granodiorite porphyry containing 1- to 3-mm phenocrysts of plagioclase, hornblende, biotite and quartz in a microcrystalline groundmass.

Valeo Porphyry, medium to dark-gray granodiorite porphyry containing conspicuous plagioclase phenocrysts generally 5 to 10 mm in length, and phenocrysts of hornblende, biotite and rounded quartz "eyes" 1 to 3 mm in size in a fine-grained matrix of plagioclase, orthoclase and quartz.

Pine Creek Porphyry, light-gray granodiorite porphyry containing abundant phenocrysts of plagioclase, hornblende, biotite and scarce quartz in a fine-grained matrix of plagioclase, orthoclase and quartz.

Flagstaff Mountain Porphyry, dark-gray to gray-green granodiorite porphyry containing abundant phenocrysts of plagioclase 1 to 3 mm in size, and in some outcrops, scattered plagioclase phenocrysts as much as 1 cm in length, hornblende, and locally, some biotite.

Ontario Porphyry, light to yellowish-gray quartz monzonite porphyry containing phenocrysts of plagioclase, biotite, and hornblende 2 to 4 mm in size, in a microcrystalline groundmass of orthoclase, quartz, and plagioclase. Locally some facies are seriate porphyritic to nearly equigranular.

These stocks rank in order of estimated decreasing outcropping areas as follows: Pine Creek (8 km^2), Valeo (3 km^2), Mayflower and Flagstaff (1.7 km^2), Ontario (0.8 km^2) and Glencoe (0.4 km^2). Absolute age data are available only for the Pine Creek stock, which give an age of 37 m.y. ago (Crittenden Jr., et al. 1973) determined by K-Ar method applied to biotite crystals.

Extrusive rocks are exposed in the extreme northeast corner of the district and are collectively called the Keetley volcanics. They consist of more than 900 m of rhyodactic to andesitic flows, breccias and tuffs. Radiometric determinations indicate 32 ± 1.0 m.y. to 35.1 ± 1.1 m.y. as the range of age of these volcanics (Crittenden Jr., et al. 1973). These data were provided by dating biotite crystals by the K-Ar method.

The Park City District tectonics. The tectonic framework of the Park City District is characterized by folding, thrusting, faulting, extensive fracturing and emplacement of igneous masses.

In analyzing the structural elements of the district it is

possible to recognize three successive periods of deformation (Nackowski, verbal communication): (a) a compressive stage forming north-south trending folds and thrusts; (b) a stage characterized by east-northeast trending normal faulting and emplacement of stocks and dikes in the same direction; and, (c) a stage in which east-northeast trending left-lateral transcurrent faults were formed.

A fourth stage can be recognized and includes post-mineralization displacements. These movments, however, may well represent small or local tectonic adjustments resulting from earlier deformation periods.

During the compressive stage the sedimentary layers were folded into the north-plunging Park City anticline and its corresponding, but much less impressive, syncline. The Frog Valley thrust, dipping gently to the west, was also formed east of the anticlinal axis.

Following this compressive period, the rocks of the district underwent an extensive normal faulting along roughly defined east-west zones of weakness. The emplacement of the stocks and dikes was prior to or simultaneous with the forming of some of these structures. These fault zones dip either northwest or southeast. The former include the Daly, Hawkeye-McHenry, Naildriver, Mayflower-Pearl, and Ontario fissures while the Crescent,Back Vein and Massachusetts-McGregor fissures belong to the latter group. Southeast dipping fault zones generally exhibit wider scatter in their strike directions, ranging from N25°E to almost E-W, than northwest dipping faults. The angle of dip is also variable from moderate (45°-55°) to steep (80°-85°) for both groups. The variation of the structural attitudes of these fault zones is shown in Figure 6. Data for the preparation of this sterogram

were compiled from available publications. Rich ore deposits of the Park City District commonly are localized along these normal faults.

The third, but less important, period of deformation of the district is characterized by transcurrent displacements which may have reactivated many of the early normal faults.

Nearly all these fault zones are associated with abundant fracturing but little or no movement took place along the joints. Some of these structures are very continuous, both laterally and vertically, and they account for most of the permeability of the rocks, especially the igneous types.

Ore deposits. Veins or lodes, replacement ore deposits and mineralized breccias have been recognized in the Park City District. However, only the vein or lode and the replacement deposits are of large enough tonnage and high enough grade to afford continuous productive mining. The two major types of ore occur in both sedimentary and intrusive host rocks, and are commonly associated with each other. Vein deposits also occur independently and are intimately related to the igneous intrusions and fissure systems. Mineralized breccias have been mined but account for only 5% of the ore production (Garmoe and Erickson 1968).

Replacement deposits exist as bedded and irregular ore masses. They are found in the calcareous beds of the many sedimentary formations of the district and are localized by stratigraphic parameters such as bedding, lithology, etc. Most production of the camp has come from the highest grade replacement deposits in the Park City, the Thaynes, and the Mississippian formations. The vein deposits are

usually in quartzites, shales and igneous rocks. The Weber Quartzite and the Park City stock have apparently hosted the deposits with largest tonnage and highest grade. Structural control is commonplace to all ore deposits of the Park City camp. Even in those mining areas where replacement deposits dominate such as the Silver King, Ontario, Judge and Daly West mines the faults and related fracture systems rendered the rocks permeable enough to allow the flow of the hydrothermal solutions and, as a consequence, ore deposition in favorable beds.

The mineralogy of the district is simple. Five major minerals are present in nearly all ore bodies: pyrite, galena, sphalerite, quartz and calcite, although their relative abundance varies from mine to mine. Important minor minerals are tetrahedrite, gold, chalcopyrite, argentite and barite.

CHAPTER II

THE MAYFLOWER MINE

Geology of the Mayflower Mine Area

The Mayflower Mine is located on the eastern flank of the Park City anticline on the easternmost protuberance of the Mayflower stock. It is the only mine in the district to date whose ore production has come primarily from veins in igneous host rocks. Only about 20% of the production has been provided by veins and replacement deposits in sedimentary host rocks (Barnes & Simos 1968). Intrusive rocks and the Weber Quartzite occupy most of the surface area surrounding the mine site, but, on its east side, volcanics and Quaternary deposits become dominant.

The Mayflower and Pearl fissure zones are the most important mineralized structures extending across this mining area and vicinity. The ore deposits of the Mayflower Mine which are primarily fissure-filling lead-zinc sulfide veins with high content in gold, copper and silver occur along these fracture zones. Figure 8 shows the major geologic features of the mine in a schematic geologic cross section.

Mine Stratigraphy

The only sedimentary rocks present in the mine are exposed on the west extensions of the mine. They range from the Mississippian Gardison Formation on the 2,005' level to the Permian Weber Quartzite

Fig. 8. Schematic SSE-NNW cross section of the Mayflower Mine showing major geologic features. Sedimentary units are represented with their maximum thickness (see stratigraphic column of Figure 4). T = Triassic; P = Permian; $\mathbb{P}$ = Pennsylvanian; M = Mississippian; $\mathfrak{C}$ = Cambrian and P$\mathfrak{C}$ = Precambrian.

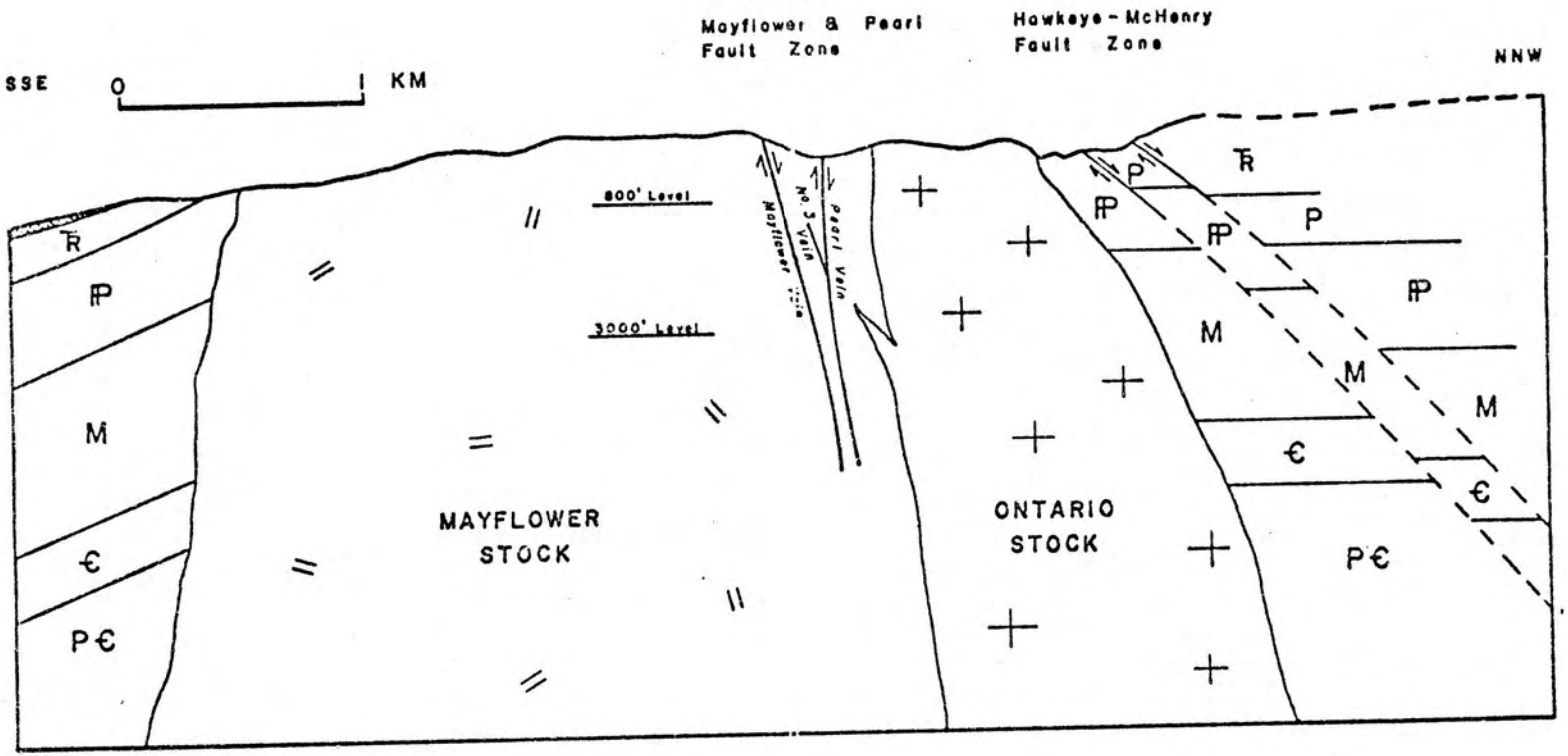
Mayflower & Pearl
Fault Zone
Hawkeye - McHenry
Fault Zone
SSE
0
1 KM
NNW
800' Level
3000' Level
No. 3 Vein
Mayflower Vein
Pearl Vein
MAYFLOWER
STOCK
ONTARIO
STOCK
R
PP
M
€
P€
P
T
R

on the surface, and are occasionally intercalated with sill-like bodies of igneous rocks. Table 1 shows the complete stratigraphic section of the mine.

Igneous intrusions produced an irregular contact zone some tens of meters wide along calcareous formations. This zone is characterized by the development of a calc-silicate mineral assemblage in the sedimentary rocks, especially tremolite-actinolite and diopside, and by more anorthitic plagioclase on the igneous side as compared to the normal plagioclase of the main porphyry body (Holt 1953). These mineralogical changes were accompanied by a conspicuous increase in the mineral grain size in that zone. The contact of the intrusives with the Weber Quartzite is sharp in striking contrast with that of the calcareous beds.

All stratigraphic units show some degree of mineralization, especially the Humbug Formation which seems to have been the most susceptible to interaction with the ore solutions. The Weber Quartzite and the Gardison Formation, however, have not contributed to the ore production of the mine (Quinlan & Simos 1968).

Igneous Rocks

Three different intrusive porphyry bodies have been recognized in the Mayflower Mine: the Mayflower, the Ontario and the Valeo. This order corresponds tentatively to a chronological sequence of emplacement from the oldest to the youngest. Field observations and analysis of some geologic maps of the district corroborate that interpretation. On the 3,000' level dikes of the Ontario stock can be seen

TABLE 1

MINE STRATIGRAPHY

Age	Formation	Thickness in Feet	Description
Penn.	Weber quartzite	+1,160	Top not exposed--generally gray to buff quartzite, intercalated with buff to blue gray limestone in lower portion.
Penn.	Round Valley limestone	350	Pale gray limestone, intercalated sandy, quartzite and shale beds.
Miss.	Doughnut formation	400	Massive gray-buff limestone alternating with horizons of black-white banded limestones and some shale, 98 ft. of hackly green-brown argillite at base.
Miss.	Humbug formation	300	Upper 150 ft.--white to light gray marmorized limestone, some dolomite, and sandy horizons. Lower 150 ft.--fine to medium grained limestone with thin quartzite horizons, dolomitic near base.
Miss.	Deseret limestone	460	Upper 310 ft.--massive white sugary dolomite, some chert. Lower 150 ft. black dolomitic limestone with pale colored chert bands.
Miss.	Gardison limestone	120	Top 40 ft. is thin to medium bedded black shaley limestone, then 80 ft. gray to white dolomite, chert occurs throughout, base not exposed.

(After Quinlan & Simos 1968)

cutting across Mayflower rocks. Likewise, in the geologic map by Bromfield, et al. (1970), a dike of the Valeo porphyry intrudes the Mayflower stock. However, age relationships for the Ontario and Valeo stocks are not evident.

The porphyritic rocks of all three stocks are petrologically quite similar with a composition ranging from granodiorite to diorite. They consist of andesine, biotite, hornblende, quartz and orthoclase but differ in their varietal mineralogy, bulk chemical composition and texture. The Mayflower porphyry has an aphanitic to fine-grained groundmass where phenocrysts with an average size of 2 mm are always present. The Valeo porphyry contains the largest phenocrysts (up to 1 cm in length) and well rounded quartz grains. The Ontario, on the other hand, shows the strongest tendency towards equigranularity due to the relatively coarser grain size of its matrix. In fact, these stocks may represent different facies of the same general magmatic episode. All three intrusions have been mineralized and altered and the Valeo pluton is the least altered. Ore production has been dominantly from the Mayflower porphyry and lesser quantities from the Ontario rocks.

The Mayflower-Pearl Fault Zone

The Mayflower-Pearl fault zone is the most important structural feature of the mine since it is the locus for the metallic mineralization which gave rise to the Mayflower ore zone. This fault zone is readily identified where it is altered and mineralized, but beyond the mineralized areas it becomes indistinct (Barnes and Simos 1968).

The Mayflower ore zone consists of a complex anastomosing vein

system bounded by two major parallel mineralized fissures. The southernmost is the Mayflower and the northernmost is the Pearl. This ore zone strikes N60°E through the sedimentary formations shifting to an almost east-west trend in the intrusives. In both rock types, however, it dips steeply either due northwest or vertically. Hence, the Mayflower and Pearl fissures can be considered as the footwall and hangingwall of the Mayflower ore zone respectively. A third mineralized fissure, named the Number Three vein, seems to connect the two major veins. There is no major displacement offsetting the ore bodies, but small post-mineralization faulting occurred along and across the ore zone. The three main veins exhibit the same general characteristics, although important differences in their mineralogy, strength and structure are noticeable.

Mayflower fissure-vein

This structure is a narrow well-defined fracture zone showing sharp contacts with the host rocks along most of its extent. The vein structure is cymoidal and locally, especially on the western mine front in sedimentary rocks,splits into numerous thin individual veins forming an irregularly defined zone encompassing large blocks of country rocks (Williams 1952). The Mayflower fissure strikes N60°E to N80°E dipping 80°NW or vertically and mostly occurs in the intrusives.

Above the 1,020' mine level, the Mayflower vein was the only ore producer. Although it is a persistent structure, it decreases in metal content in the lower levels.

Pearl fissure-vein

This fissure has similar structural behavior to that of the Mayflower fissure, but its dip changes gradually from northwestly to southeastly although always at high angles. Economic mineralization associated with this fracture is only present from the 1,020' mine level down.

This structure defines a narrow (a few centimeters to 2.5 meters wide) vein "characterized by a band of friable, sugary quartz with lacing strands of sulfides" (Quinlan & Simos 1968). Internally it exhibits successive dichotomous branches some of which merge subsequently into a major veinlet lending an irregular aspect to the vein structure.

Alteration and Base-Metal Mineralization

Williams (1952) recognized five stages of alteration in the Mayflower stock rocks during his studies of the ore zone between the 800' and the 1,380' mine levels. Veinward these stages are: (1) host rock, (2) chlorite, (3) argillic, (4) local quartz-sericite and (5) migratory quartz-sericite, with the first four stages more or less symmetrically arranged, in that order, around the veins and other mineralized fractures. Kaolinite is the dominant mineral in the argillic zone, but minor amounts of montmorillonite and dickite are also present. Serpentine, epidote and magnetite are minor constituents of the chlorite zone. The zoning is attributed to successive reaction of the hydrothermal solutions with an earlier alteration stage, except

for the migratory quartz-sericite episode which transects all other zones. The alteration envelope is commonly a few inches wide and seldom extends more than a few feet into the wall rock. In the limestones, Williams recognized an irregular zone of alteration composed dominantly of montmorillonite but also containing kaolinite, halloysite and sericite. Nash (1973) identified another stage of alteration associated with what he refers to as deep early veins. These veins, exposed in crosscuts between the shaft and the Pearl veins on the 2,005' and lower levels, display K-feldspar and biotite alteration envelopes and are associated with quartz crystals which contain high salinity fluid inclusions.

Metal sulfide deposition in the Mayflower-Pearl fissure zone occurred simultaneously with alteration. Pyrite, galena and sphalerite are the major sulfide minerals, although chalcopyrite and gold added great economic significance to the ore zone. The minerals are considered to have been deposited by relatively dilute solutions as opposed to the early brines of the potassic alteration (Nash 1973).

Paragenetic studies by Nash have indicated four stages in the evolution of the Mayflower ore zone. During the first stage sugary quartz, pyrite, hematite and anhydrite were deposited. This was followed by massive deposition of sphalerite, galena and chalcopyrite. In the third stage anhydrite, carbonate, sugary quartz, barite and hematite dominated with minor amounts of sulfides. The last stage was marked by major precipitation of sphalerite and sugary quartz and subordinate chalcopyrite. Except for minor differences, this paragenetic sequence agrees with William's version in which an early sulfide, a carbonate-quartz and a late sulfide stage were recognized.

CHAPTER III

DATA COLLECTION

Field Work

The field work was done during the Fall of 1972. It consisted of mapping the fracture abundance and sampling the igneous wall rocks on several levels of the Mayflower Mine. The field work also included reconnaissance trips throughout the district and geological observations around the surface mine site.

The Mayflower Mine exposures at that time consisted of a vertical section of approximately 670 m between the 800' and the 3,000' level. The mine was inaccessible above the 800' level. The levels mapped and the extent of sampling depended on physical safety and operational conditions prevalent at that time, thus only nine levels out of sixteen were studied. Approximately 2.0 km of drifts and crosscuts were examined of which 0.6 km were sampled in laterals parallel to the vein system along ENE-WSW directions; the remaining 1.4 km were mapped along N-S directions through the mine shaft. Other few traverses included NW-SE directions as on the 2,005' level. Also 305m of core samples from a vertical diamond drill hole located near the shaft (DDH-41) on the 3,000' level were analyzed.

Observations were made at intervals of 15 meters or less along drifts and laterals where the most obvious through-going mineralized fractures were recorded. At the beginning of each interval the

structural attitude of fractures, representative of a particular set, was measured. All other fractures visually parallel to measured fractures were assumed to have the same attitude and were counted over the interval. Hence, for every interval, the frequency of fractures of a specific set was determined. The procedure was repeated for other fracture sets identified in the interval. The fracture abundance was then calculated by dividing the total number of fractures of all sets in the interval over its lateral distance.

Rock sampling in each interval consisted of collecting chip rock samples, hand specimens and large blocks of rocks. Continuous chip rock samples covered the whole extension of each interval; a few were restricted to the immediate vicinity of veins. They were used to determine the bulk chemical composition of the rocks. Hand specimens provided petrographic thin-sections and microprobe mounts, but were also used to determine the bulk and grain density of the rocks. For each interval one or two hand specimens were taken. The large blocks (about 30 cm x 20 cm x 15 cm) were collected in such a way as to contain the most important sets of mineralized fractures and were intended for fracture aperture determinations. A block, in some cases, was considered to represent more than one interval as long as it was taken on the same level and in the immediate adjacency.

Sample Numeration and Location

The samples analyzed represent the Mayflower, Ontario and Valeo stock rocks exposed in the mine. Each sample was given a number composed of two letters and four digits. The letters stand for the stock

name (MF = Mayflower; ON = Ontario; VL = Valeo); the first two digits identify the mine level (08 = 800' level; 16 = 1,630' level; 22 = 2,200' level; etc.) and the last two digits refer to the different intervals. In a few instances a "V" was added to the end of the number to specify that the sample came from a vein present in the interval in question. The six core samples were labelled with the letters DDH (diamond drill hole) followed by three digits representing the depth in feet below the 3,000' level from which they came.

Figures 9 and 10 are key diagrams for locating intervals and identifying samples.

Analytical Work

The analytical work carried out during the present research involved qualitative and quantitative evaluations of both the mineralogy and chemistry of the igneous rocks of the Mayflower Mine. Bulk and grain densities and fracture apertures were also determined.

The qualitative part dealt with primary identification of minerals in the rocks with hand lens, magnet and acid tests. For further identification, all rock pulps were analyzed under a binocular microscope and forty thin sections were examined with a petrographic microscope. Thin sections were made from rock samples collected nearby and a distance from the ore zone at the different levels studied. X-ray technique was also used in some instances for identification of clays and other alteration minerals. The microscopic examination also served as a semi-quantitative analysis of the relative proportion of minerals and the major phases present. The relative amount of K-feldspar, however, was checked in some rock slabs with appropriate staining

Fig. 9. Sample location on a N-S cross section of the Mayflower Mine.

Fig. 10. Sample location on a WSW-ENE cross section of the Mayflower Mine.

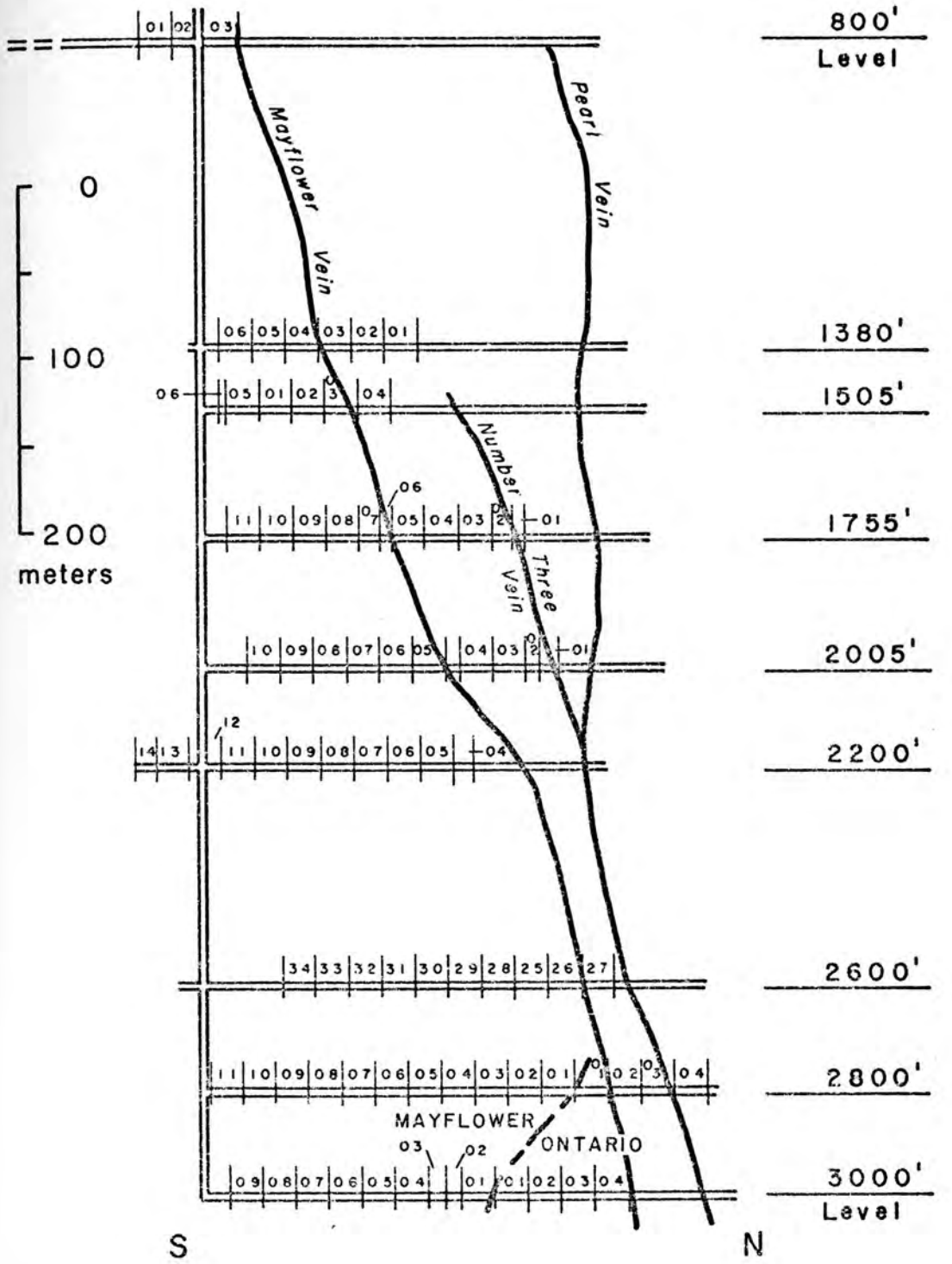
800'
Level
Pearl Vein
Mayflower Vein
0
100
200
meters
1380'
1505'
Number Three Vein
1755'
2005'
2200'
2600'
2800'
MAYFLOWER
ONTARIO
3000'
Level
S
N

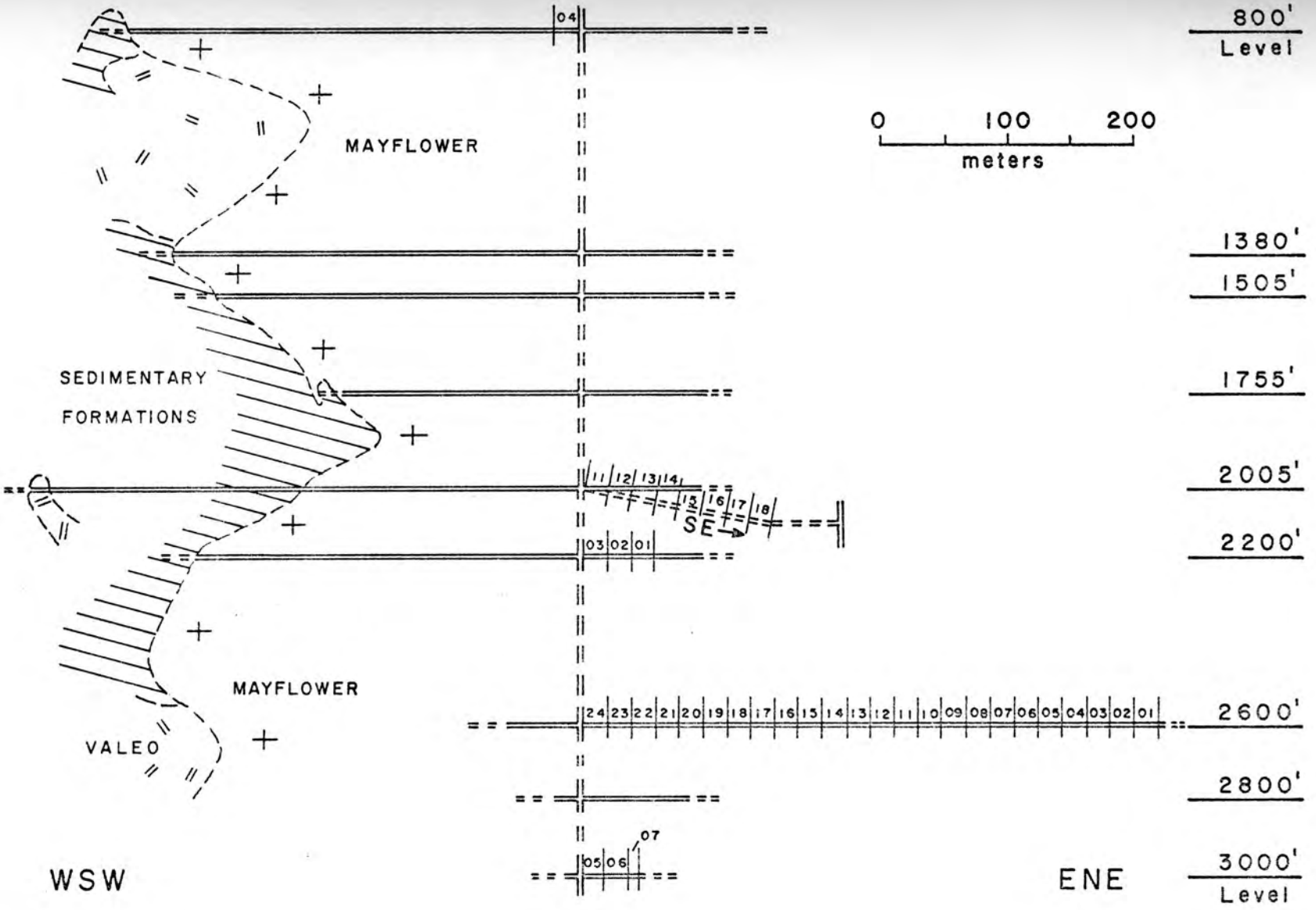
800' Level
0 100 200
meters
MAYFLOWER
1380'
1505'
SEDIMENTARY FORMATIONS
1755'
2005'
2200'
SE
MAYFLOWER
VALEO
2600'
2800'
07
WSW
ENE
3000' Level

techniques (Bailey and Stevens 1960).

The quantitative analysis comprised the determination of the bulk chemical compositions of rocks, the chemical composition of mineral phases, bulk and grain densities of rocks and fracture aperature in rock slabs. One hundred thirty-three chip rock samples were analyzed for twelve major components. Si, Al, Fe (total iron as Fe^{++}), Mg, Ca, Na, K, Mn and Ti were determined by X-ray fluorescence technique, and S, SO_3 and CO_2 were analyzed with LECO equipment. Chemical compositions of minerals were determined with an electron microprobe. Eighteen polished thin sections were examined to determine the compositions of biotite, chlorite, hornblende, actinolite, epidote, salite, augite, K-feldspar and plagioclase grains. Nine major elements, Si, Al, Fe (total iron as Fe^{++}), Mg, Ca, Na, K, Mn and Ti were determined. Biotite grains were also analyzed for Cl, F and Ba whereas the feldspar grains were only analyzed for Ca, Na and K. Bulk and grain densities were determined for one hundred thirty rock samples for the estimation of their total porosity and aperture determinations served for calculation of the permeabilities of the rocks.

Analytical procedures, operational conditions and analysis precision are reported in appendices at the end of the text.

CHAPTER IV

FRACTURING OF THE IGNEOUS ROCKS

The Mayflower and the Ontario stocks are thoroughly fractured. The relations of the fracturing pattern of these igneous intrusions to the major fissure zones of the Park City District were studied to establish any possible genetic association on a district-wide scale. Poles of 1100 fracture planes, mostly shear planes present in the Mayflower porphyry, were plotted as shown in Fig. 7A. Mine maps prepared by the Hecla Mining Company geologists provided the necessary data for the construction of that stereogram. A similar plot was prepared with the fracture orientation data obtained during the field work. The result is the stereogram of Fig. 7B, where 2106l poles of fracture planes were recorded with the aid of a Schmidt equal area computer program. Both diagrams exhibit, with striking similarity, three distinctive regions where fracture poles preferentially concentrated although a small difference in the position of the corresponding domains of the stereograms 7a and 7b is noted. Nevertheless, the two independent plots show two prominent sets of fractures developed in the plutons. One trends NE-SW dipping either NW or SE; the other is NW-SE trending and dips dominantly SW. The steep dipping character of the fractures is evident. The representative structural attitudes of these two sets were considered to be N50°E/80°NW and N50°W/80°SW.

Comparison between Figs. 6, 7A and 7B suggests, almost

Fig. 6. Stereographic plot of the poles of the major fissure zones present in the Park City District. Encircled areas show the variation of the fissure structural attitude. X represents the axis of the Park City anticline. Lower hemisphere projection.

Fig. 7. Per cent plot of the poles of fractures in the Mayflower and Ontario stocks. 1% counting areas. Lower hemisphere projection on equal area net. A. Approximately 1,100 shear planes compiled from mine maps (all levels below the 700' level). Dark areas: 5.5-75.%; hachured areas: 3.5-5.5%; dotted areas: 1.5-3.5% and blank encircled areas: 0.5-1.5%. B. 21,061 poles of mineralized fractures (800', 1,380', 1,505', 1,755', 2,005', 2,200', 2,600', 2,800' and 3,000 levels). Dark areas: 8.0-11.0%; hachured areas: 5.0-8.0%; dotted areas: 2.0-5.0% and blank encircled areas: 0.8-2.0%.

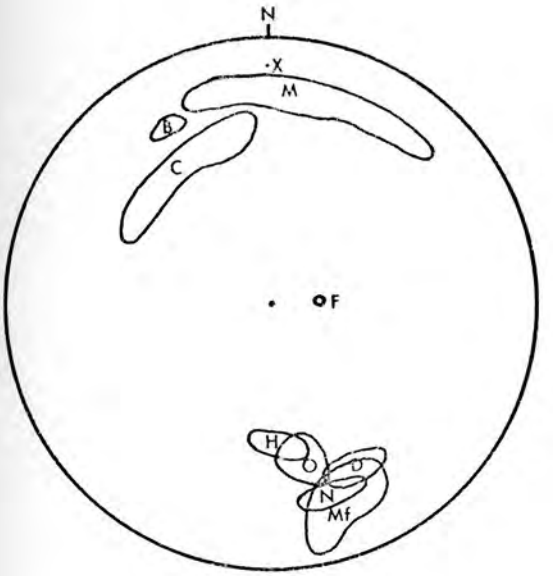

KEY

M Massachusetts
B Back
C Crescent
F Frog Valley
H Hawkeye
O Ontario
D Daly
N Naildriver
Mf Mayflower – Pearl

Fig. 6

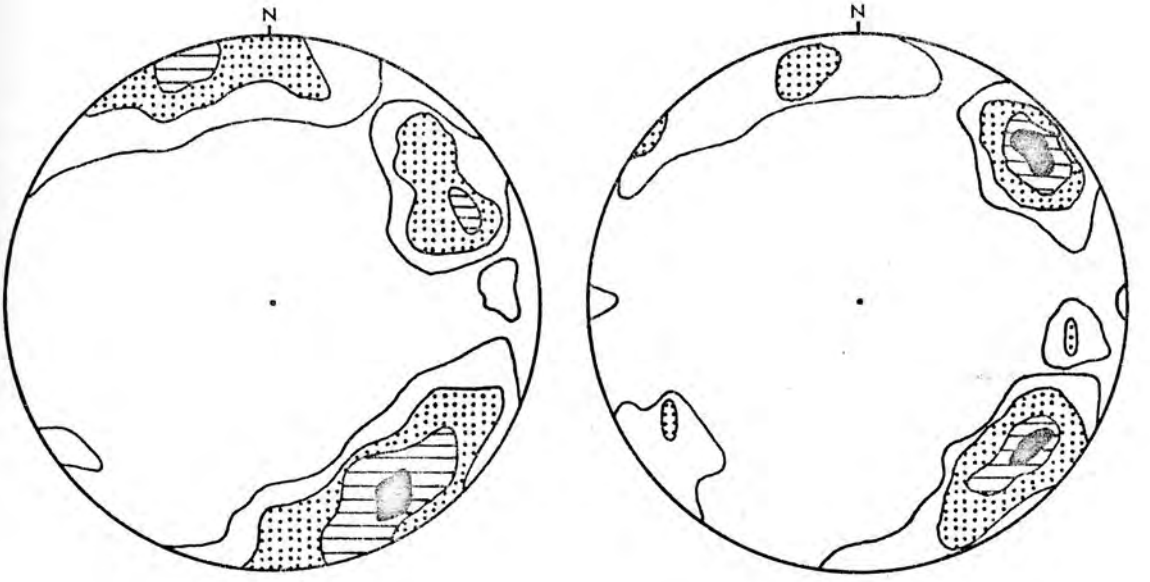

A B

Fig. 7

unequivocally, that the NE-trending fissure system is genetically related to the major fissure zones on the district scale and developed during the period of deformation when NE-SW faulting activity prevailed. The NW trending fractures do not show any obvious relation to the major structural features of the district. If this is the case, they may represent a local structural manifestation in the area of the Mayflower Mine whose cause is unknown. A possibility is the assumption that each set was developed by distinct unidirectional stress fields. However, the mineralized character of fractures of both sets would require the existence of two stress fields in the span of time taken to mineralize the igneous rocks of the Mayflower Mine, which does not seem to be geologically conceivable. Heidrick (verbal communication) has used the unidirectional hypothesis to explain the development of two dominant sets of fractures at approximately 90° commonly found in Tertiary intrusions in the southwestern United States. He assumes an interchange in the orientations of the minimum (σ_3) and intermediate (σ_2) principal stress directions, while the maximum (σ_1) principal stress direction remains vertical. This implies that σ_2 and σ_3 would have to have the same magnitude at a certain time before they could switch position and, as a consequence, the rocks would exhibit multidirectional fracturing instead of only two preferential fracture directions.

Conversely, if the NE-trending and the NW-trending fracture sets intersecting the igneous rocks of the Mayflower Mine are also tied to the structural framework of the Park City district, they should represent a conjugate set of shear fractures. The presence of gouge material along some of the fracture planes points to their shear nature. This

evidence, however, may be ambiguous since the gouge material could have been produced by subsequent movements not related to the stress field that generated the fractures. Lack of significant offsetting between these two fractures sets, on the other hand, supports evidence for their contemporaneity. The conjugate shear angle (2θ) of these two sets is approximately 80° ± 5° and was measured on the stereograms (Fig. 7A and 7B) between points located inside the areas with the densest fracture poles. Also, the intersection of the representative fracture planes for these sets is not vertical.

Interpreting the fracture pattern of the Mayflower and Ontario stocks with a stress theory of failure, or using Anderson's approach for fracture analysis (1951), requires further assumptions; otherwise, no simple model for fracturing under the same stress conditions is applicable. The most critical assumption perhaps is that present-day fault characteristics may not reflect original conditions of fracturing. Secondly, one of the principal stress directions may deviate from verticality despite the shallow depths (0.9 to 1.2 km; Nash 1973) of fracturing of the two plutons. Billings (1972, p. 273) stresses that "the orientation of strike-slip faults and the displacement along them is not systematically disposed about a vertical to the surface of the earth . . . . Heterogeneity of the rocks and pre-existing fractures generally influences the stress distribution." Also, the shape of an unfractured rock body affects the distribution of stress around it (Roberts 1970) so that the deviation of a principal stress direction from verticality may be a common circumstance in igneous intrusions. Thirdly, it is assumed that pure (non-rotational) shear as opposed to

simple (rotational) shear was the dominant kind of stress.

The interpretation of conjugate fracture sets in the igneous rocks of the Mayflower Mine implies that the stress field under which they were developed was characterized by a nearly vertically oriented σ_2 that induced the formation of strike-slip faults (Fig. 11). Field observations indicate the Mayflower-Pearl fault zone (a NE-trending fissure zone) to be a normal fault (Quinlan & Simos 1968). Therefore, this fault zone might have been reactivated and abundant fracturing occurred under conditions which produced strike-slip fault movements modifying the earlier normal faulting character of the Mayflower-Pearl fault zone. Post-mineralization displacements, although of small scale, have been observed in the Mayflower ore zone. Moreover, the lateral expansion of the Mayflower-Pearl fissure zone to receive a 5-meter wide ore zone may be also an indication of such movements. On the other hand, the pinch-and-swell nature of this ore zone suggests original irregular fracture surfaces capable of generating the ore zone without any later expansion. Also, this ore zone could have been, at least partially, a result of the dissolution of the host rocks by alteration minerals.

If the Navier-Coulomb criterion of failure (Jaeger 1964) is used to explain the fracturing of the stocks, the large 2θ angle measured (80°) implies a very low angle of friction, ϕ, approximately 10°, or a coefficient of internal friction, μ, of about 0.18. Most data on granitic rocks at room temperature show μ to be approximately equal to 1.0. At higher temperature μ decreases appreciably. Calculated values of μ for the Westerly granite at 800°C (Griggs 1960) are of the order of

Fig. 11. Stress field diagram for the formation of strike-slip faults in Mayflower stock.

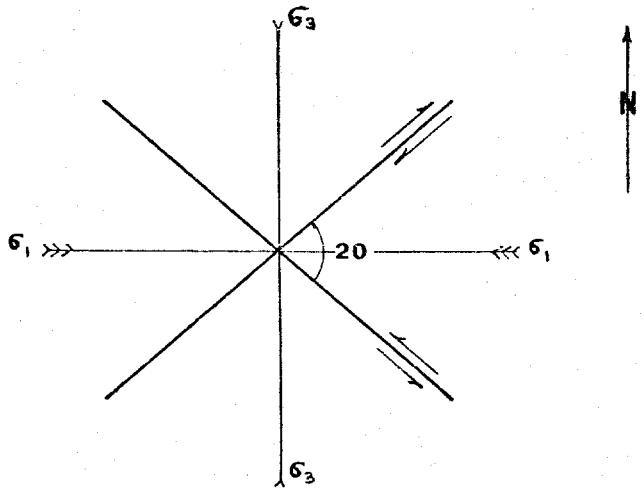
σ3
σ1
20
σ1
σ3
N

0.4 corresponding to calculated values for 2θ of approximately 68°. Observed values during his experiment, however, revealed larger 2θ angles of the order of 76° to 82° at the same temperature. The latter values would allow for even lower values of μ for the Westerly granite. Calculated values of μ for the Eskdale Granite (Cumberland, Ireland) range from 0.37 to 1.43 corresponding to dihedral angels of 70° and 34° respectively (Aucott 1970). Therefore, although large 2θ angles for shear fractures are not very common, they have been systematically reported in the rock mechanics literature. And, at least quantitatively, it is possible to envisage low coefficients of friction when a rock fractures at high temperatures.

The interpretation of the fracture pattern of the Mayflower and Ontario stocks based on Mohr's criterion of shear fracture entails a large confining pressure (σ_3) and evidently, a shear difference ($\sigma_1 - \sigma_3$) sufficiently large to cause movement on potential shear planes. This means that the Mohr circle representing $\sigma_1 - \sigma_3$ at failure must be bigger at higher confining pressures, so that 2θ angles similar to those found in the present fracture analysis can be obtained. Data on the Oil Creek Sandstone (Badgley 1965) point to larger 2θ angles at higher confining pressures (at 1,000 atm and 24°C, 2θ = 28°; at 2,000 atm and 24°C, 2θ = 58°; at 2,000 atm and 150°C, 2θ = 54°' at 2,000 atm and 300°C, 2θ = 64°).

The hypothetical diagram of Fig. 12 shows qualitatively how ϕ decreases as the confining pressure increases. It also shows the effects of pore fluid pressure (P_f) which reduces the total resistance to shear and allow rocks at depth to fail at differential stresses lower

Fig. 12. Idealized Mohr's diagram of failure showing how the conjugate shear angle (2θ) increases with decreasing ϕ as the confining pressure (σ_3) increases. Larger circles than the ones shown on the diagram would be required to cause fracture at a fluid pressure P'_f.

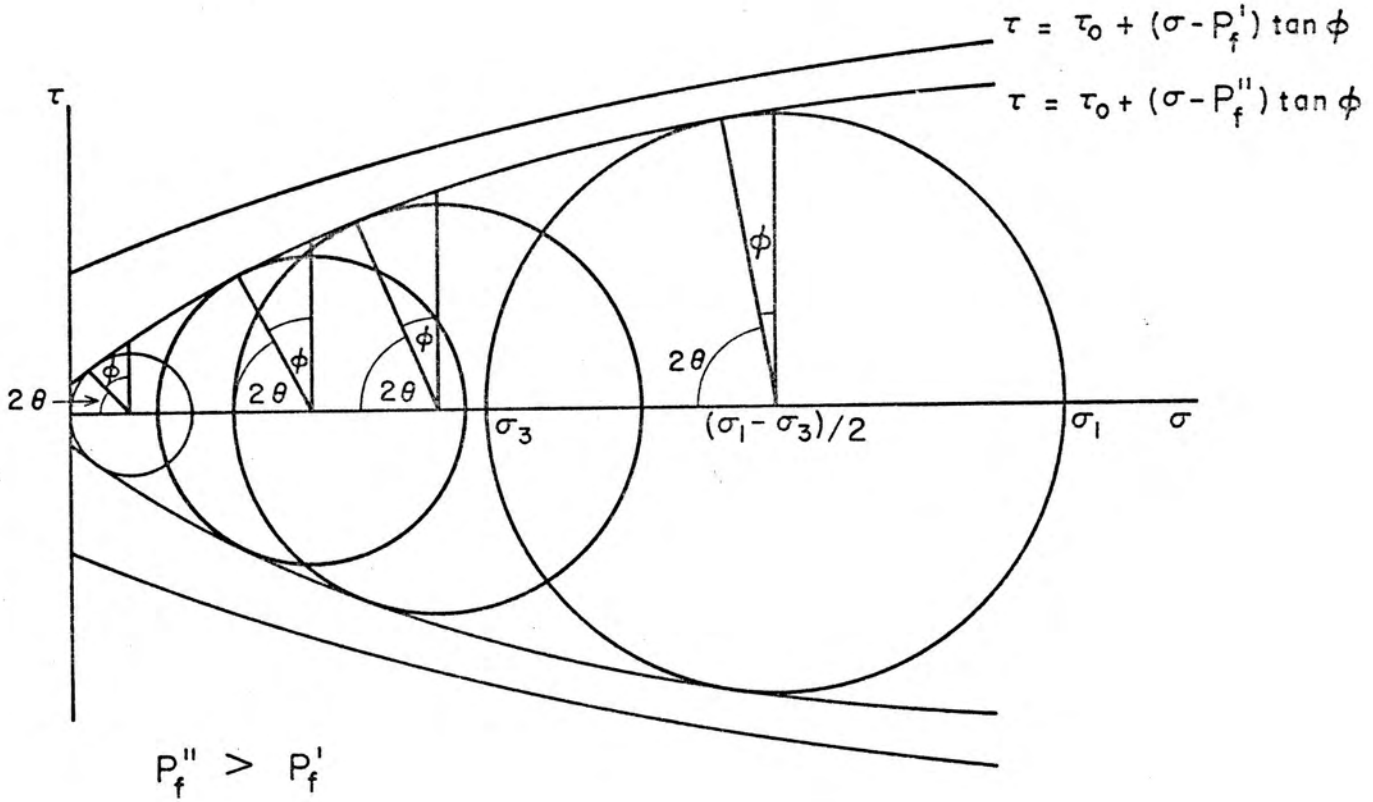
$\tau = \tau_0 + (\sigma - P_f') \tan\phi$
$\tau = \tau_0 + (\sigma - P_f'') \tan\phi$
τ
2θ
ϕ
2θ
ϕ
2θ
ϕ
2θ
ϕ
σ_3
$(\sigma_1 - \sigma_3)/2$
σ_1
σ
$P_f'' > P_f'$

than those required for fracturing relatively drier rocks. In the diagram P''_f is greater than P'_f.

The above considerations allow the suggestion that the Mayflower and the Ontario stocks may have been fractured approximately at their solidus temperature (750° ± 50°) under a large confining pressure in order to produce the observed conjugate-shear angle between the two most prominent sets of fractures transecting the rocks. They most likely ruptured at the ductile-brittle transition when they were brittle enough to break but also still ductile enough to render a low coefficient of friction to their rocks.

In the absence of a more effective criterion to analyze the fracture pattern of these plutons, the present proposition seems to be useful to explain the observed data with available models for rock fracturing.

CHAPTER V

FRACTURE CHARACTERISTICS AND HYDRODYNAMIC PROPERTIES OF THE ROCKS

Many ore deposits have been interpreted as being formed from hydrothermal solutions flowing through channelways available in rocks. Despite this almost universal recognition, only recently have investigators attempted to measure some hydraulic parameters for modelling ore-forming processes. Allusions to these parameters may be found in the literature on the genesis of hydrothermal mineral deposits. "Plumbing system" is the common qualitative terminology used when, in fact, permeability is the fundamental quantitative parameter required to fully define the movements of fluids in rocks. Indeed, to model any hydrothermal system with reference to its geometry, temperature and fluid density distributions in the pluton-host rock domain, cooling rate of the hydrothermal episode, fluid velocities and mass flow rates (Norton unpublished), requires a knowledge of rock porosity and permeability. Through-going fractures account for the major flow channels in crystalline rocks particularly in mineralized igneous rocks in which fractures are, in a lesser or greater degree, always present. Because permeability must have been related to fracture properties at the time of the hydrothermal solution flow, models describing fluid flow in fractured media should include fracture properties as significant parameters.

For the Mayflower stock, a thoroughly fractured medium, fracture

abundance and fracture aperture were measured and used with the model described below to evaluate the flow porosity and permeability of the rocks.

Parallel Plate Model for Fractured Media

Snow (1965) developed a model for fluid flow in fractured media consisting of equidistant, planar, parallel plates of infinite extent (Fig. 13A), but randomly oriented. The model was proposed to predict the role of geometric variables controlling flow, especially the variation in conduit orientation and aperture, and conduit spacing.

Equations (1) and (2) describe flow in a single parallel-plate conduit (Fig. 13B) and have been derived from the Navier-Stokes formulation for a slow, non-turbulent Newtonian fluid (for which the rate of strain is proportion to stress). V is the average velocity of flow, b is the half-aperture of the conduit, g is the gravitational acceleration, μ is the kinematic viscosity of the fluid, $\nabla\Phi$ is the effective potential gradient expressed in terms of unit weight, and G is the discharge per unit width of conduit (Snow 1965; Bianchi & Snow 1969).

$$V = - \frac{b^2 g}{3\mu} \nabla\Phi \qquad (1)$$

$$Q = - \frac{2b^3 g}{3\mu} \nabla\Phi \qquad (2)$$

The total discharge Q of a set of N parallel conduits present in a given volume of a cubic body may, therefore, be expressed by

$$Q = - \frac{2}{3} \frac{b^3}{\mu} g N W \nabla\Phi \qquad (3)$$

Fig. 13. A. Planar parallel plate model for permeability and flow porosity--a cube of edge W (after Snow 1965). B. Poisseulle flow along a conduit of aperture 2b.

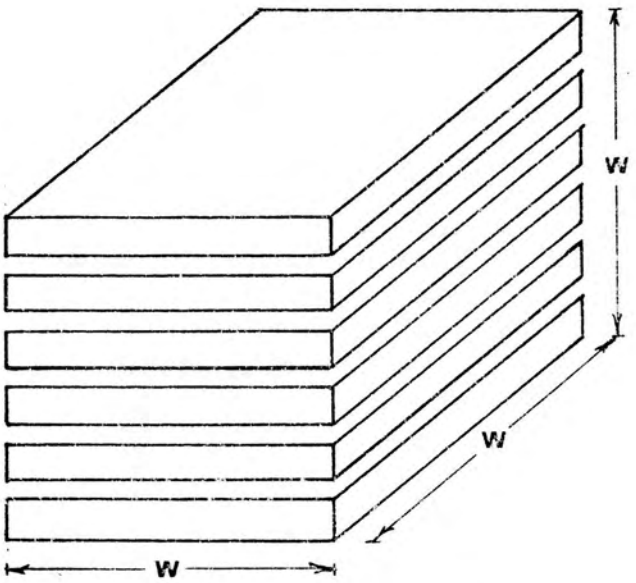

(A)

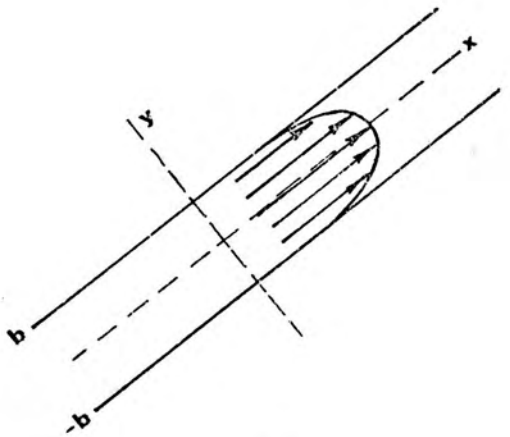

(B)

where W is the length of the unit cube edge.

The flow Q through an equivalent continuous medium is given by Darcy's Law (Hubbert 1940)

$$Q = -kA \frac{dh}{dl} \tag{4}$$

where k is the permeability, A is the cross-sectional area and dh/dl is the potential gradient. Combination of equations (3) and (4) gives

$$k = \frac{2}{3} b^3 \frac{N}{W} \tag{5}$$

provided the necessary adaptations are made for the cube of Fig. 13A. N/W expresses exactly the abundance of conduits per unit of width. If n represents this relationship and $2b = d_i$ where d_i is the aperture of the i^{th} fracture, equation (5) may be written as

$$k = \frac{d_i^3}{12} n \tag{6}$$

This equation describes flow through a single set of conduits composed of i fractures and is a functional expression for the permeability in fractured media that can be used as a first approximation, if the frequency of through-going fractures and their apertures are known for a representative volume of rock. Worthwhile noting is the dimensional equation for this relationship given by L^2 which, for the CGS system, is expressed in cm^2, where $10^{-8} cm^2 = 1$ darcy.

The flow porosity (ϕ_f) per unit length of fracture for the corresponding case of equation (6) may be written as

$$\phi_f = d_i n \tag{7}$$

Therefore, for each set of fractures the permeability is given by

$$k = \frac{d^2_i \phi_f}{12} \qquad (8)$$

Fracture Abundance

In Chapter III the method used to determine the fracture abundance for the several intervals mapped in the Mayflower Mine was described. The drift and lateral orientations, mostly along N-S and ENE-WSW directions, afforded a good opportunity to sample a significant volume of the stocks, so that a representative statistical counting of the fractures was readily possible.

The fracture abundance values (Table 2) are reported in relation to two planes representing the main NE-trending and the NW-trending fracture sets that transect the Mayflower and Ontario stocks (N50°E/80° NW and N50°W/80° SW). Fractures located in the NE quadrant or trending N-S were assigned to the former plane whereas the fractures located in the NW quadrant or trending E-W were ascribed to the latter one.

The frequency of the n values (Fig. 14A) describes a positively skewed sampling distribution. Its corresponding cumulative distribution (Fig. 14B), on the other hand, approaches the characteristic sigmoid shape of the normal distribution. Geologically more significant, however, is the variation of n over the N-S cross-section of the mine (Fig. 15). There is a substantial decrease in the fracture abundance below the 2,600' level and at distances from the Mayflower vein to the to the north and south. This trend to the south might have been expected,

TABLE 2

CHARACTERISTICS OF CONTINUOUS FRACTURES IN MAYFLOWER MINE

SAMPLE MF-	N40E / 80NW PERMEABILITY CM**2	N40E / 80NW POROSITY PER CENT	N40E / 80NW ABUNDANCE FRCT/CM	N40W / 80SW PERMEABILITY CM**2	N40W / 80SW POROSITY PER CENT	N40W / 80SW ABUNDANCE FRCT/CM
801	0.72E-07	.203	0.98E-01	0.29E-07	.081	0.39E-01
802	0.42E-07	.118	0.57E-01	0.41E-07	.116	0.56E-01
803	0.11E-07	.030	0.15E-01	0.37E-07	.105	0.51E-01
804	0.23E-07	.064	0.31E-01	0.34E-07	.097	0.47E-01
1301	0.28E-08	.054	0.70E-01	0.39E-08	.077	0.98E-01
1302	0.35E-08	.069	0.89E-01	0.42E-08	.082	0.10E+00
1303	0.39E-08	.078	0.10E+00	0.34E-08	.067	0.85E-01
1304	0.35E-08	.069	0.89E-01	0.30E-08	.059	0.75E-01
1305	0.35E-08	.070	0.89E-01	0.30E-08	.059	0.75E-01
1306	0.38E-08	.074	0.95E-01	0.31E-08	.060	0.77E-01
1501	0.33E-08	.069	0.93E-01	0.21E-08	.044	0.59E-01
1502	0.21E-08	.044	0.59E-01	0.31E-08	.066	0.89E-01
1503	0.40E-08	.085	0.11E+00	0.28E-08	.059	0.79E-01
1504	0.31E-08	.066	0.89E-01	0.29E-08	.061	0.81E-01
1505	0.45E-08	.095	0.13E+00	0.35E-08	.074	0.98E-01
1701	0.27E-07	.130	0.82E-01	0.13E-07	.062	0.39E-01
1703	0.33E-07	.158	0.10E+00	0.16E-07	.078	0.49E-01
1704	0.22E-07	.107	0.68E-01	0.23E-07	.109	0.69E-01
1705	0.29E-07	.140	0.89E-01	0.25E-07	.122	0.77E-01
1706	0.19E-07	.093	0.59E-01	0.29E-07	.140	0.89E-01
1708	0.19E-07	.093	0.59E-01	0.34E-07	.163	0.10E+00
1709	0.19E-07	.093	0.59E-01	0.32E-07	.156	0.98E-01
1710	0.19E-07	.091	0.58E-01	0.26E-07	.124	0.79E-01
1711	0.22E-07	.104	0.66E-01	0.19E-07	.093	0.59E-01
1712	0.22E-07	.104	0.66E-01	0.23E-07	.109	0.69E-01
2001	0.60E-08	.034	0.23E-01	0.18E-07	.103	0.71E-01
2002	0.31E-08	.017	0.12E-01	0.19E-07	.104	0.72E-01
2003	0.63E-08	.035	0.24E-01	0.19E-07	.106	0.73E-01
2004	0.94E-08	.053	0.36E-01	0.12E-07	.068	0.47E-01
2005	0.15E-07	.086	0.59E-01	0.24E-07	.134	0.92E-01
2006	0.28E-07	.160	0.11E+00	0.17E-07	.096	0.66E-01
2007	0.95E-08	.054	0.37E-01	0.26E-07	.144	0.98E-01
2008	0.16E-07	.091	0.62E-01	0.20E-07	.115	0.79E-01
2009	0.11E-07	.060	0.41E-01	0.18E-07	.101	0.69E-01
2010	0.13E-07	.073	0.50E-01	0.20E-07	.114	0.78E-01
2011	0.61E-08	.034	0.24E-01	0.21E-07	.117	0.80E-01
2012	0.11E-07	.059	0.41E-01	0.12E-07	.067	0.46E-01
2013	0.11E-07	.062	0.43E-01	0.11E-07	.062	0.43E-01

	.....N40E / 80NW.....			*****.....	N40W / 80SW.....	
SAMPLE MF-	PERMEABILITY CM**2	POROSITY PER CENT	ABUNDANCE FRCT/CM	****PERMEABILITY CM**2	POROSITY PER CENT	ABUNDANCE FRCT/CM
2014	0.13E-07	.074	0.51E-01	0.11E-07	.060	0.41E-01
2015	0.12E-07	.066	0.45E-01	0.16E-07	.088	0.60E-01
2016	0.13E-07	.072	0.49E-01	0.22E-07	.124	0.85E-01
2017	0.15E-07	.086	0.59E-01	0.20E-07	.115	0.79E-01
2018	0.19E-07	.104	0.72E-01	0.15E-07	.086	0.59E-01
2019	0.18E-07	.101	0.69E-01	0.14E-07	.081	0.56E-01
2201	0.36E-07	.131	0.72E-01	0.29E-07	.107	0.59E-01
2202	0.23E-07	.083	0.46E-01	0.36E-07	.131	0.72E-01
2203	0.20E-07	.072	0.40E-01	0.41E-07	.148	0.82E-01
2204	0.15E-07	.053	0.30E-01	0.31E-07	.113	0.62E-01
2205	0.28E-07	.102	0.56E-01	0.21E-07	.077	0.43E-01
2206	0.59E-07	.215	0.12E+00	0.32E-07	.118	0.65E-01
2207	0.54E-07	.197	0.11E+00	0.47E-07	.172	0.95E-01
2208	0.51E-07	.185	0.10E+00	0.37E-07	.137	0.75E-01
2209	0.47E-07	.173	0.96E-01	0.38E-07	.139	0.77E-01
2210	0.46E-07	.167	0.93E-01	0.36E-07	.133	0.73E-01
2211	0.49E-07	.178	0.98E-01	0.42E-07	.156	0.86E-01
2212	0.29E-07	.107	0.59E-01	0.38E-07	.140	0.77E-01
2213	0.00E+00	.000	0.00E+00	0.10E-06	.368	0.20E+00
2601	0.23E-07	.121	0.80E-01	0.68E-08	.036	0.24E-01
2602	0.00E+00	.000	0.00E+00	0.28E-07	.148	0.98E-01
2603	0.17E-07	.091	0.60E-01	0.11E-07	.055	0.37E-01
2604	0.27E-07	.145	0.96E-01	0.12E-07	.062	0.41E-01
2605	0.66E-08	.035	0.23E-01	0.29E-07	.155	0.10E+00
2606	0.56E-08	.030	0.20E-01	0.27E-07	.140	0.93E-01
2607	0.94E-08	.050	0.33E-01	0.33E-07	.173	0.11E+00
2608	0.24E-07	.127	0.84E-01	0.15E-07	.081	0.54E-01
2609	0.66E-08	.035	0.23E-01	0.27E-07	.140	0.93E-01
2610	0.94E-08	.050	0.33E-01	0.21E-07	.111	0.73E-01
2611	0.75E-08	.040	0.26E-01	0.20E-07	.105	0.70E-01
2612	0.94E-08	.050	0.33E-01	0.24E-07	.129	0.85E-01
2613	0.13E-07	.066	0.44E-01	0.18E-07	.094	0.62E-01
2614	0.14E-07	.074	0.49E-01	0.23E-07	.119	0.79E-01
2615	0.12E-07	.065	0.43E-01	0.18E-07	.093	0.62E-01
2616	0.13E-07	.069	0.46E-01	0.15E-07	.077	0.51E-01
2617	0.12E-07	.064	0.43E-01	0.14E-07	.076	0.51E-01
2618	0.94E-08	.050	0.33E-01	0.23E-07	.121	0.80E-01
2619	0.10E-07	.054	0.36E-01	0.20E-07	.107	0.71E-01
2620	0.43E-08	.023	0.15E-01	0.24E-07	.129	0.85E-01
2621	0.18E-07	.095	0.63E-01	0.12E-07	.061	0.41E-01
2622	0.17E-07	.089	0.59E-01	0.14E-07	.074	0.49E-01

	N40E / 80NW			N40W / 80SW		
SAMPLE MF-	PERMEABILITY CM**2	POROSITY PER CENT	ABUNDANCE FRCT/CM	PERMEABILITY CM**2	POROSITY PER CENT	ABUNDANCE FRCT/CM
2623	0.85E-08	.045	0.30E-01	0.18E-07	.096	0.64E-01
2624	0.24E-07	.129	0.85E-01	0.00E+00	.000	0.00E+00
2625	0.63E-08	.033	0.22E-01	0.12E-07	.061	0.41E-01
2626	0.32E-07	.168	0.11E+00	0.11E-07	.059	0.39E-01
2628	0.17E-07	.089	0.59E-01	0.12E-07	.064	0.43E-01
2629	0.14E-07	.074	0.49E-01	0.13E-07	.069	0.46E-01
2630	0.13E-07	.066	0.44E-01	0.16E-07	.084	0.56E-01
2631	0.30E-07	.159	0.10E+00	0.47E-08	.025	0.16E-01
2632	0.14E-07	.074	0.49E-01	0.27E-07	.142	0.94E-01
2633	0.17E-07	.089	0.59E-01	0.16E-07	.084	0.56E-01
2634	0.21E-07	.109	0.72E-01	0.21E-07	.111	0.73E-01
2801	0.38E-07	.190	0.12E+00	0.37E-07	.187	0.12E+00
2802	0.12E-07	.062	0.40E-01	0.13E-07	.067	0.43E-01
2803	0.17E-07	.084	0.54E-01	0.14E-07	.069	0.45E-01
2804	0.15E-07	.076	0.49E-01	0.13E-07	.064	0.41E-01
2805	0.11E-07	.058	0.37E-01	0.11E-07	.054	0.35E-01
2806	0.60E-08	.030	0.20E-01	0.13E-07	.064	0.41E-01
2807	0.12E-07	.059	0.38E-01	0.90E-08	.045	0.30E-01
2808	0.22E-07	.112	0.73E-01	0.10E-08	.005	0.33E-02
2809	0.10E-07	.051	0.33E-01	0.90E-08	.045	0.30E-01
2810	0.80E-08	.040	0.26E-01	0.12E-07	.061	0.39E-01
2811	0.70E-08	.035	0.23E-01	0.10E-07	.052	0.33E-01
3001	0.14E-07	.071	0.47E-01	0.59E-09	.003	0.20E-02
3002	0.12E-07	.063	0.41E-01	0.98E-08	.050	0.33E-01
3003	0.47E-08	.024	0.16E-01	0.33E-08	.017	0.11E-01
3004	0.47E-08	.024	0.16E-01	0.33E-08	.017	0.11E-01
3005	0.20E-08	.010	0.66E-02	0.80E-08	.041	0.27E-01
3006	0.20E-08	.010	0.66E-02	0.85E-08	.044	0.29E-01
3007	0.31E-08	.016	0.10E-01	0.88E-08	.045	0.30E-01
3008	0.31E-08	.016	0.10E-01	0.18E-07	.090	0.59E-01
3009	0.74E-08	.038	0.25E-01	0.20E-07	.100	0.66E-01
ON-						
2801.	0.11E-07	.045	0.26E-01	0.18E-07	.082	0.50E-01
2802.	0.81E-08	.024	0.12E-01	0.41E-07	.122	0.60E-01
2804.	0.53E-08	.034	0.25E-01	0.14E-07	.090	0.66E-01
3001.	0.81E-08	.042	0.28E-01	0.77E-08	.040	0.26E-01
3000.	0.00E+00	.000	0.00E+00	0.58E-09	.003	0.20E-02
3002.	0.65E-08	.034	0.22E-01	0.21E-07	.110	0.72E-01
3003.	0.31E-08	.031	0.29E-01	0.50E-08	.051	0.47E-01
3004.	0.13E-08	.017	0.18E-01	0.35E-08	.045	0.47E-01
3005.	0.26E-09	.003	0.33E-02	0.39E-08	.049	0.50E-01
3006.	0.42E-09	.008	0.10E-01	0.19E-08	.037	0.48E-01

Fig. 14. Fracture abundance distribution in the Mayflower and Ontario stocks. A. Hystogram of frequency describing a positively skewed sampling distribution. B. Cumulative distribution which approaches the characteristic sigmoid shape of the normal distribution.

Fig. 15. Fracture abundance distribution on a N-S cross section of the Mayflower Mine showing the substantial decrease of n on the lower levels and zones of higher fracture abundance frequency related to the Mayflower vein on the upper levels.

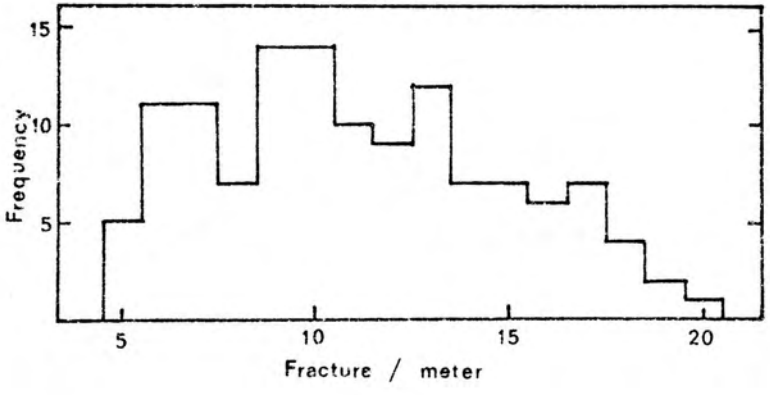
15
10
5
Frequency
5
10
15
20
Fracture / meter

A

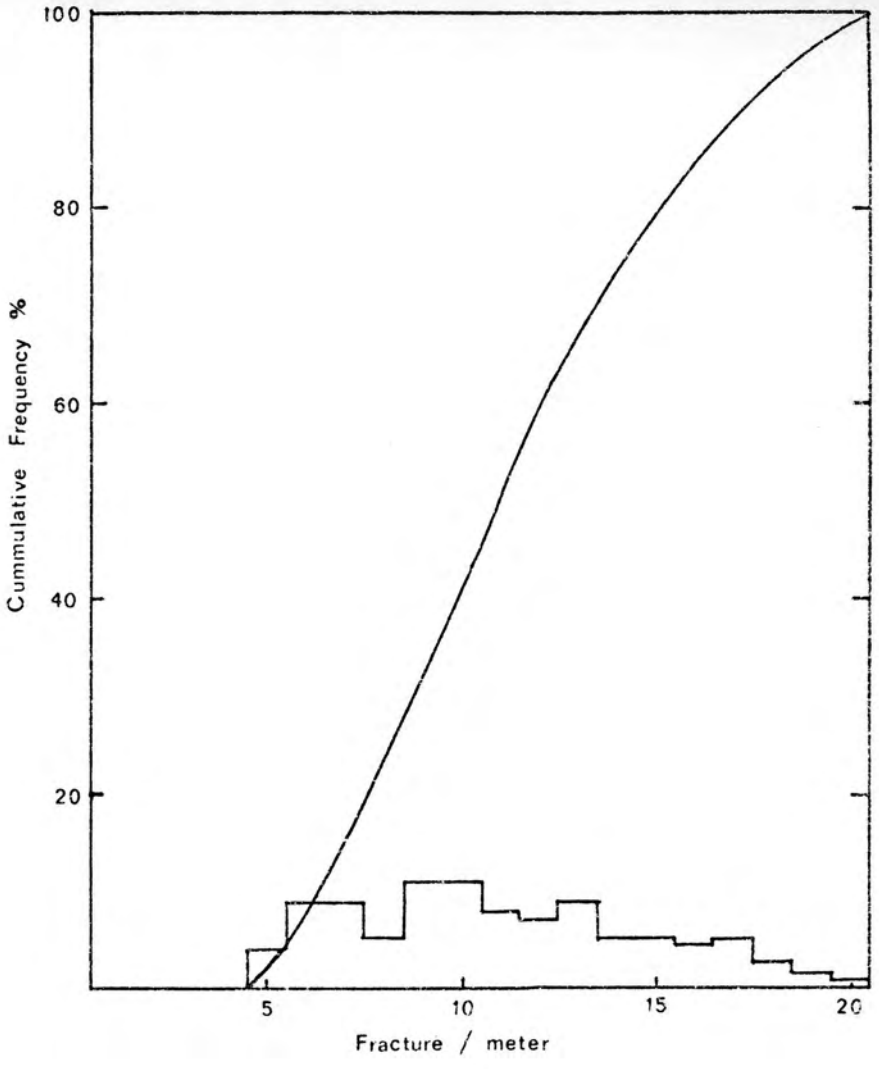
100
80
60
40
20
Cummulative Frequency %
5
10
15
20
Fracture / meter

B

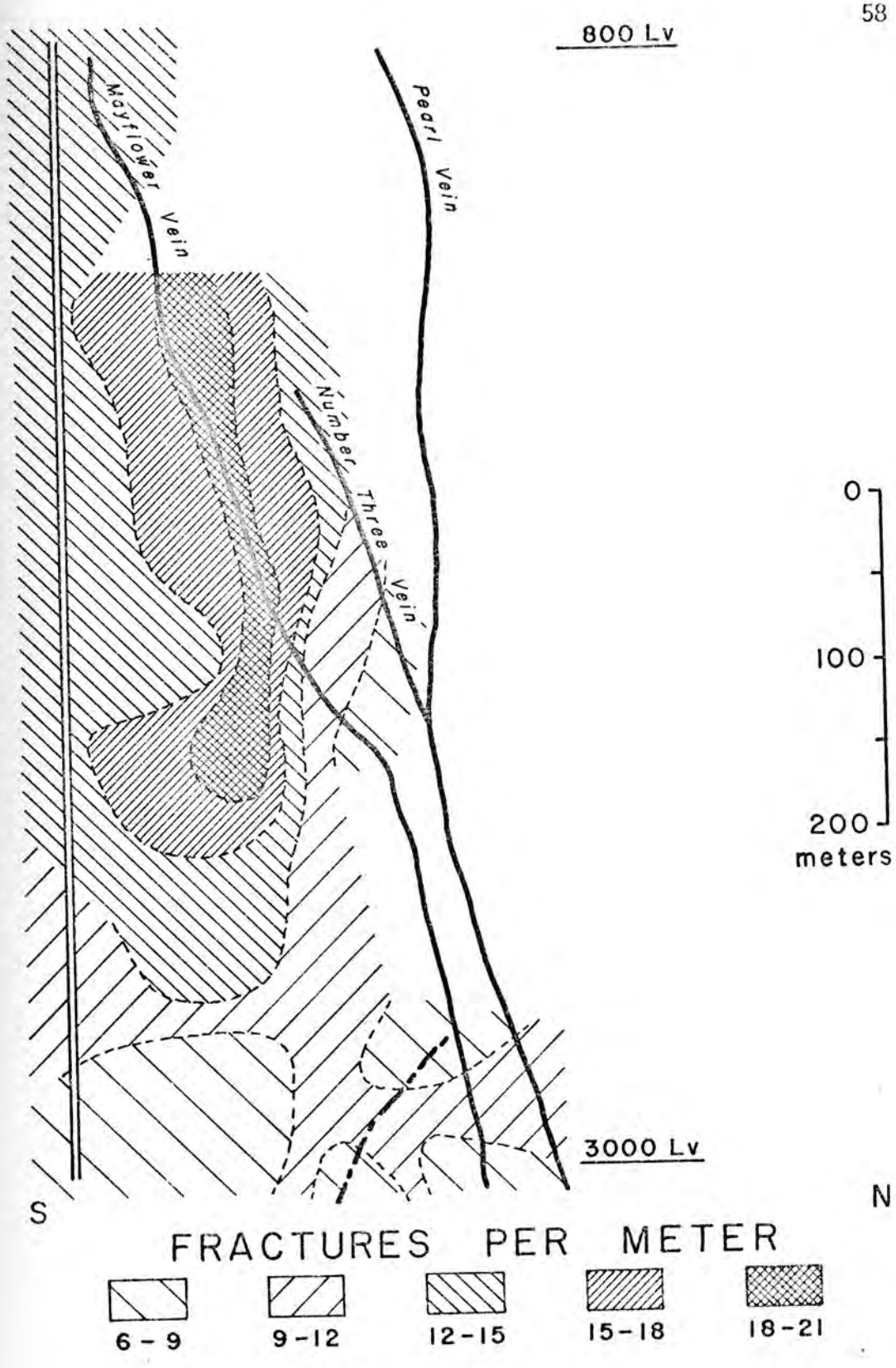
800 Lv
Mayflower Vein
Pearl Vein
Number Three Vein
0
100
200
meters
3000 Lv
S
N
FRACTURES PER METER
6 - 9
9 - 12
12 - 15
15 - 18
18 - 21

considering that the contact zones (Fig. 8) represent earlier solidified domains in the cooling history of the stock, and consequently, have been exposed longer to fracturing than other domains. Decreases in n with depth are due to the average stress effects on fracturing. The present level of exposure of most plutons in the Park City District is suggestive of a shallow sub-volcanic environment and near the pluton roofs, as evidenced by the presence of volcanics having similar chemical composition to the plutons and the presence of roof-pendants (Nash 1973). Lithostatic pressure may be a factor tending to hamper the development of fractures or decrease their aperture or close them completely at greater depths. On the other hand, on the hangingwall side of the ore zone, between the 1,380' and 2,200' level, n values decrease away from the Mayflower vein, however lack of data toward the Pearl vein and pluton contact does not permit any interpretation.

Greater fracture abundances occur on the upper levels in the vicinity of the Mayflower vein, notably between the 1,380' and 2,005' levels where they are symmetrically arranged around it. If this occurrence, although limited to a restricted extension of the vein, is not sufficient to imply a causal relationship with the vein system, the appearance of the Number Three vein exactly in that region may justify special conditions of fracturing that led to more abundant cracks in that zone. Unfortunately, it was possible to make only a few observations in the vicinity of the Number Three and Pearl veins, so that any inference related to fracture abundance trends in those regions may be misleading.

Relating fractures to rock permeability requires an estimate of

their through-going nature. Observations in the Mayflower Mine were made on 2.5 meter high vertical walls and roofs of drifts and laterals, so that examination of fracture continuity beyond that limit was not possible. Field experience, in regions where rocks expose large outcropping areas, has shown that some cracks extend for only some tens of meters and suddenly stop or connect to other major channels through less prominent cracks or with micro-fractures. Although selective counting recorded only the most obvious flow-fractures, the n values determined in this study are most likely overestimated.

Aperture Characteristics

The through-going fractures mapped in the Mayflower Mine were invariably filled with alteration minerals. Nevertheless, some space inside the cracks has been left open, either preserved or produced by dissolution of minerals at later stages of the hydrothermal event. Whatever the case may have been, these voids are the only indication of the fracture apertures during the hydrothermal event. Veinlet widths are not appropriate indication since they may extend into the edges of host rocks that have been replaced by the veinlet minerals. Accordingly, the data obtained for fracture aperture of the Mayflower Mine igneous rocks express present-day apertures which were assumed to represent the fracture opening during the hydrothermal episode. In the absence of a more adequate way to quantify paleo-fracture apertures, this seems to be a reasonable initial estimate.

Aperture values (Table 3) were obtained by the method described in Appendix D. The capricious nature of the fracture, widening and

TABLE 3

FRACTURE APERTURES OF THE MAYFLOWER

AND ONTARIO ROCKS

Sample	Aperture μm	Sample	Aperture μm	Sample	Aperture μm
MF- 801	206	MF- 2602	102	MF- 3004	228
MF- 1303	78	MF- 2603	125	MF- 3005	157
MF- 1507	65	MF- 2604	188	MF- 3006	197
MF- 1702	160	MF- 2605	131	MF- 3008	184
MF- 1711	156	MF- 2606	115	ON- 3001	152
MF- 2001	189	MF- 2607	223	ON- 3003	109
MF- 2002	105	MF- 2608	162	ON- 3004	96
MF- 2004	175	MF- 2610	112	ON- 3005	98
MF- 2005	101	MF- 2613	98	ON- 3007	78
MF- 2006	106	MF- 2614	214	DDH- 45	185
MF- 2007	109	MF- 2617	104	DDH- 162	114
MF- 2008	197	MF- 2620	224	DDH- 262	101
MF- 2009	164	MF- 2622	218	DDH- 275	130
MF- 2010	97	MF- 2624	190	DDH- 304	131
MF- 2011	195	MF- 2627	122	DDH- 325	123
MF- 2012	118	MF- 2629	136	DDH- 390	134
MF- 2013	218	MF- 2631	97	DDH- 438	40
MF- 2014	84	MF- 2634	156	DDH- 468	166
MF- 2015	91	MF- 2803	188	DDH- 484	190
MF- 2016	165	MF- 2805	155	DDH- 506	148
MF- 2018	218	MF- 2806	121	DDH- 598	72
MF- 2202	206	MF- 2807	134	DDH- 642	69
MF- 2204	150	MF- 2808	182	DDH- 668	87
MF- 2206	196	ON- 2810	102	DDH- 713	112
MF- 2207	131	ON- 2801	164	DDH- 749	124
MF- 2209	92	ON- 2802	202	DDH- 767	51
MF- 2211	268	MF- 2804	137	DDH- 855	123
MF- 2213	227	MF- 3001	186	DDH- 923	163
MF- 2601	145	MF- 3003	202	DDH- 953	191

NOTE: Average per level: 800', 206 μm; 1,380', 78 μm; 1,505', 75 μm; 1,755', 158 μm; 2,005', 146 μm; 2,200', 181 μm; 2,600', 151 μm; 2,800', 154 μm; 3,000', 153 μm.

narrowing or displaying irregular and rough walls, contributed largely to possible incorrect evaluations. An error of ± 45 μm is to be expected in the reported values. Nevertheless, they afford a satisfactory estimation of the crack openings which is compatible with the deviation from the natural system inherent to the simplified model described earlier.

Aperture values range from 40 to 268 μm and average 145 μm. On the levels where larger number of samples were examined, namely the 2,005', 2,200', 2,600', 2,800', and 3,000' levels, the average values (146, 181, 151, 154, and 153 μm respectively) are remarkably uniform except for the 2,200' level which is,nonetheless, still within the limits of the indicated error. No variations in aperture with depth were found.

Indirect fracture opening measurements obtained from drill-hole pump tests in fractured hard rocks at damsites, ranged from 75 to 400 μm in the upper 12 meters, but they decrease from 100 to 50 μm in the interval between 15 and 61 meters (Snow 1968). Bianchi (1968) performed direct surface measurements of fracture apertures and found an average value of 905 μm for the Pikes Peak granite. The comparatively larger value obtained by Bianchi may be the result of surface conditions (topography, weathering, etc.) as opposed to subsurface determinations. Comparison between Snow's work and the present research is more problematic considering all the differences involved in the two methods. Despite the significant overlap in the values obtained by the two independent approaches, Snow's data show a marked decrease of fracture aperture with depth in a relatively shorter depth interval, whereas

the values for the Mayflower rocks exhibit a more scattered pattern over a relatively greater depth interval. This disparity may reflect the differences of geological environments and different procedures under which the measurements were carried out. Alternatively, that discrepancy may be the result of perturbation of the natural stress field in underground excavation tending to enlarge the fracture opening. As Bianchi and Snow (1969) stated, "Fracture apertures measured in underground excavation would meet the same problems as do surface measurements." This statement is, however, an overestimation of the stress factor. Undoubtedly it contributes to the separation of the rock walls into distinct blocks by pulling the fracture walls apart, but the cracks measured in these blocks showed no apparent signs of post-hydrothermal event separation. The average value of the fracture aperture for the Pikes Peak granite being six times as great as the average value of the fracture aperture measured for the Mayflower Mine rocks, is an indication that surface and underground measurements are not comparable.

Porosity

The porosity of a fractured crystalline rock is a qualitative measure of its potentiality to be altered provided sufficient hot circulating fluids are available and are in chemical disequilibrium with the rock. The porosity geometry and distribution defines the contact area between fluids and reactant minerals. Understanding of the mass transfer mechanisms between reactant minerals and aqueous solutions requires knowledge of the pores available in rocks. It is convenient, therefore, to discriminate the major contributing parts of the rock

porosity. Norton (1975) relates the nature of the pores to specific porosities as expressed in equation 9, where ϕ_T is the total porosity of the rock, ϕ_F, the flow porosity,

$$\phi_T = \phi_F + \phi_D + \phi_R \qquad (9)$$

refers to the open spaces along fractures where aqueous ions are transported primarily by fluid flow, ϕ_D, the diffusion porosity, regards pores or dead-end fractures connected to flow channels; these fluid-saturated voids constitute a stationary medium through which ions are transported primarily by diffusion; and ϕ_R, the residual porosity, is that part of the porosity associated with pores not connected to flow or diffusion voids such as fluid inclusions, mineral grain boundaries, etc. Figure 16 is a reproduction from a slab of a Mayflower rock (MF-3003) where these different kinds of pores are sketched from observations under a binocular microscope, except residual voids that have been arbitrarily added.

Values of total porosity (Table 4) were obtained indirectly by using an expression that relates this parameter to the bulk and grain densities of the rocks (Appendix C). Extrapolating the values obtained from a hand sample at each interval to represent the total porosity of that interval is probably inadequate. A better estimation would require measurements of some tens of hand samples for each interval that was beyond the scope of the present research. Average total porosity values were calculated for the several traverses on the studied levels of the mine. Those oriented along ENE-WSW directions, at approximately 15 m south of the Mayflower vein, showed the highest porosity values

TABLE 4

GRAIN AND BULK DENSITIES, POROSITY AND BULK CHEMICAL COMPOSITION

OF THE IGNEOUS ROCKS OF THE MAYFLOWER MINE

	G/CM**3		PER CNT	WEIGHT PER CENT											
SAMPLE	GRDENS	BKDENS	PRSTY	SIO2	AL203	FEO	MGO	CAO	NA2O	K2O	S	CO2	MNO	SO3	TIO2	TOTAL
MF-0401	2.821	2.78	1.45	58.20	16.70	4.25	3.61	5.60	3.67	3.27	.58	1.32	.15	.19	.86	99.40
MF-0402	2.819	2.79	1.03	54.40	17.40	4.85	4.18	7.01	3.30	2.77	.93	1.87	.21	.22	.95	98.08
MF-0403	2.849	2.74	3.83	56.50	17.60	4.43	4.31	6.08	3.56	2.55	.34	1.21	.13	.22	.95	97.83
MF-0404	2.835	2.75	4.68	57.00	18.00	4.97	3.90	5.97	3.62	2.61	.81	1.49	.12	0.00	.93	99.42
MF-1301	2.761	2.70	2.21	61.50	17.20	3.67	2.50	4.74	3.27	3.62	.47	1.31	.17	.02	.69	99.19
MF-1302	2.785	2.73	1.97	61.50	17.20	3.89	2.50	4.00	3.16	3.72	.41	.70	.29	0.00	.71	99.08
MF-1303	2.754	2.70	1.96	61.50	15.30	3.92	2.30	4.04	2.87	3.43	1.74	1.07	.35	1.02	.53	99.07
MF-1304	2.759	2.73	1.05	61.70	17.20	4.18	2.77	3.81	3.03	3.92	.54	.66	.30	.11	.74	99.26
MF-1305	2.827	2.70	4.49	59.10	16.70	4.00	2.52	5.62	3.58	2.95	.60	1.12	.10	.35	.73	97.37
MF-1501	2.811	2.78	1.10	60.40	17.10	3.72	2.78	4.87	3.10	3.15	.20	1.19	.11	.16	.72	97.50
MF-1502	2.825	2.75	2.65	59.70	16.80	3.78	2.71	4.53	3.24	3.05	1.22	1.04	.12	0.00	.66	96.85
MF-1503	2.746	2.71	1.31	60.30	16.50	3.82	2.79	3.92	3.10	3.33	.81	.89	.36	.17	.62	96.63
MF-1504	2.759	2.72	1.41	61.50	16.20	4.14	2.72	3.93	2.98	3.65	.85	.90	.33	.15	.67	98.02
MF-1505	2.821	2.75	2.52	59.40	17.50	4.40	3.32	5.36	3.52	3.05	.24	.42	.10	.13	.94	98.38
MF-1506	2.691	2.61	2.65	43.50	13.50	4.59	1.74	19.74	1.44	2.34	1.11	9.81	.38	2.17	.48	100.90
MF-1701V	2.765	2.72	1.63	56.90	13.30	7.53	1.74	4.42	1.90	2.55	6.18	2.52	.39	1.49	.49	99.41
MF-1702	2.795	2.76	1.25	58.20	16.80	5.16	3.39	3.69	2.41	4.30	1.40	.97	.51	.33	.80	97.95
MF-1703	2.755	2.72	1.27	57.40	17.80	4.36	3.37	4.76	3.24	3.44	.27	1.03	.23	.67	.83	97.40
MF-1704	2.783	2.74	1.44	58.80	17.90	4.27	3.60	4.74	3.36	3.37	.40	.72	.19	.20	.83	98.38
MF-1705	2.777	2.74	1.33	58.30	17.30	4.44	3.52	4.52	2.96	3.69	.49	.67	.35	.33	.77	97.34
MF-1706	2.750	2.71	1.45	54.70	16.50	4.10	2.89	7.80	2.53	3.49	1.74	4.77	.26	0.00	.57	99.35
MF-1707	2.798	2.75	1.72	56.70	17.50	4.29	3.39	6.20	3.04	3.09	.43	1.66	.24	.30	.82	97.66
MF-1708	2.794	2.74	1.93	55.00	15.90	4.22	3.23	7.79	2.79	2.84	.82	2.67	.21	.75	.78	97.00
MF-1709	2.784	2.73	1.94	57.50	17.20	4.39	3.45	6.06	3.27	2.96	.22	.96	.13	.24	.85	97.23

TABLE 4 (CONT.)

	G/CM**3		PER CNT	WEIGHT PER CENT											
SAMPLE	GRDENS	BKDENS	PRSTY	SIO2	AL2O3	FEO	MGO	CAO	NA2O	K2O	S	CO2	MNO	SO3	TIO2	TOTAL
MF-1710	2.774	2.76	.50	58.70	16.90	4.45	3.60	5.18	3.21	3.33	.49	.69	.12	.01	.44	97.22
MF-1711	2.791	2.72	2.54	61.60	17.70	4.26	2.96	4.90	3.79	3.25	.27	.40	.10	.17	.82	100.22
MF-1712	2.745	2.71	.91	58.90	17.20	4.34	3.17	5.83	3.41	2.99	.98	1.74	.10	.11	.77	98.54
VL-2001	2.733	2.70	1.21	63.00	17.70	1.96	2.70	2.48	2.70	6.01	1.09	.96	.16	0.00	.45	99.21
VL-2002	2.664	2.59	2.78	62.10	18.40	2.02	3.54	2.20	2.33	6.37	1.34	.84	.14	0.00	.46	99.44
MF-2001	2.733	2.67	4.40	59.10	18.10	3.47	2.71	4.10	3.04	3.57	.96	1.25	.15	.94	.64	97.93
MF-2002	2.834	2.77	2.26	60.20	18.00	3.53	2.36	3.58	3.07	3.82	1.43	1.09	.16	.13	.59	97.96
MF-2003	2.788	2.74	1.72	53.60	16.40	5.03	4.36	6.50	2.16	3.61	1.38	2.76	.65	.48	.64	97.37
MF-2004	2.687	2.59	3.61	58.10	17.30	4.97	3.86	3.16	2.16	3.86	1.47	1.15	.52	.42	.74	97.71
MF-2005	2.774	2.74	1.23	61.30	17.50	3.89	3.42	3.68	3.70	3.25	.90	.60	.12	.46	.72	99.54
MF-2006	2.868	2.76	3.77	55.70	17.20	4.91	4.88	5.22	3.24	2.74	.66	.40	.10	1.14	1.00	97.19
MF-2007	2.836	2.76	2.68	53.58	17.40	4.87	4.53	6.36	3.04	2.88	1.00	.75	.08	2.58	.92	97.99
MF-2008	2.798	2.78	.64	53.66	16.80	4.75	4.32	6.31	3.01	2.61	1.08	.68	.06	2.51	.87	96.66
MF-2009	2.797	2.74	2.04	51.43	16.00	3.91	4.17	8.26	2.76	2.18	2.28	1.11	.09	3.86	.60	96.65
MF-2010	2.744	2.73	.51	52.36	16.20	4.89	4.67	6.96	2.84	2.42	2.82	1.45	.06	3.18	.64	98.49
MF-2011	2.824	2.74	2.97	59.20	16.70	4.96	3.15	3.69	2.41	3.70	1.37	1.30	.72	0.00	.72	97.92
MF-2012	2.751	2.73	.76	60.17	15.50	4.98	2.90	3.92	1.93	3.70	2.27	1.70	.63	.89	.60	99.19
MF-2013	2.798	2.74	2.07	58.40	17.50	4.34	3.29	5.36	3.65	3.19	.24	.64	.15	.40	.76	97.92
MF-2014	2.744	2.72	1.59	57.90	16.90	4.07	3.43	5.17	3.06	3.66	.73	1.12	.25	.35	.76	97.40
MF-2015	2.854	2.76	3.29	58.10	17.60	4.34	4.11	5.73	3.21	2.94	.28	.87	.15	0.00	.90	98.23
MF-2016	2.792	2.73	1.47	59.50	17.50	4.28	4.04	5.79	3.21	2.98	.16	.97	.12	.67	.89	100.11
MF-2017	2.777	2.71	2.41	59.50	18.00	4.27	3.43	6.14	3.35	3.08	.22	1.32	.12	0.00	.88	100.31
MF-2018	2.822	2.75	2.55	61.10	18.20	3.93	3.04	5.10	3.94	2.95	.12	.48	.10	.58	.82	100.36
MF-2201	-0.000	-0.00	0.00	59.90	16.80	3.10	2.08	4.65	2.19	3.80	1.49	2.10	.34	.76	.49	97.70
MF-2202	2.761	2.65	4.02	62.48	18.27	3.00	3.00	3.38	3.79	3.11	.80	.53	.08	.65	.60	99.69
MF-2203	2.784	2.64	5.17	56.93	17.30	5.19	4.07	4.07	4.16	3.31	1.48	.50	.12	1.24	.79	98.16

TABLE 4 (CONT.)

	G/CM**3	PER CNT		WEIGHT PER CENT										
SAMPLE	GRDENS	DKDENS	PRSTY	SIO2	AL203	FEO	MGO	CAO	NA2O	K2O	S	CO2	MNO	SO3	TIO2	TOTAL
MF-2204	-0.000	-0.00	0.00	59.10	19.40	4.52	4.64	4.37	4.09	2.51	.53	.70	.19	.42	.76	100.31
MF-2205	2.781	2.71	2.55	55.70	17.60	5.16	4.85	4.91	2.77	3.25	1.25	.83	.31	.67	.74	99.24
MF-2206	2.800	2.74	2.14	57.10	18.00	4.51	3.79	5.72	4.16	2.40	.57	.57	.07	2.02	.75	99.64
MF-2207	2.753	2.72	1.20	57.40	17.80	4.30	3.49	5.79	3.76	2.69	.64	.54	.07	2.04	.81	99.32
MF-2208	2.793	2.76	1.18	56.60	16.30	4.26	3.54	6.56	3.06	2.36	1.03	.77	.11	3.16	.67	98.32
MF-2209	2.844	2.85	1.52	53.54	15.30	3.97	4.61	9.44	2.92	1.71	1.09	1.95	.07	4.59	.56	99.75
MF-2210	2.772	2.70	2.60	54.90	17.20	4.96	4.32	6.94	3.57	2.47	.59	1.00	.10	.79	.96	97.90
MF-2211	2.766	2.64	4.56	54.40	17.30	4.81	4.46	7.97	3.43	1.91	.60	.53	.12	.71	1.04	97.28
MF-2212	2.760	2.75	.36	57.10	18.00	4.64	4.14	6.11	4.45	2.70	.27	.45	.12	.32	.98	99.24
MF-2213	2.801	2.77	1.11	55.80	17.40	4.99	4.43	6.70	3.36	2.75	.23	.76	.12	.38	1.00	97.92
MF-2214	2.779	2.72	2.09	56.60	17.30	5.23	4.36	6.12	3.36	2.95	.44	.84	.14	.06	1.04	98.44
MF-2601	2.727	2.63	3.56	60.70	17.46	4.95	3.11	3.18	3.43	2.90	2.48	.45	.05	.51	.66	99.85
MF-2602	2.709	2.61	3.65	60.90	17.95	4.36	3.15	3.19	3.94	2.61	2.03	.49	.35	.34	.67	99.98
MF-2603	2.824	2.74	2.97	60.10	17.57	5.38	3.15	3.17	3.57	2.62	2.70	.36	.05	.79	.68	100.14
MF-2604	2.834	2.72	4.02	60.03	16.99	5.37	3.40	3.85	3.58	2.62	2.67	.37	.05	1.20	.65	100.78
MF-2605	2.785	2.72	2.33	57.60	17.00	5.32	3.23	4.34	3.79	2.70	2.67	.53	.07	1.20	.62	99.07
MF-2606	2.755	2.69	2.36	59.23	17.09	4.63	3.11	4.13	3.79	2.91	2.24	.47	.05	1.52	.63	99.80
MF-2607	2.775	2.72	1.99	59.10	17.18	5.08	3.47	3.56	3.14	2.49	2.47	.69	.05	2.07	.69	99.99
MF-2608	2.776	2.72	2.02	60.10	16.51	4.60	4.11	3.91	3.21	2.88	2.05	.28	.05	1.14	.75	99.59
MF-2609	2.813	2.71	3.66	60.06	16.69	5.46	3.96	2.94	3.14	3.04	2.62	.36	.06	.39	.73	99.45
MF-2610	2.801	2.63	6.10	58.10	17.20	6.61	3.38	3.20	3.00	3.45	3.43	.35	.05	.89	.82	101.49
MF-2611	2.782	2.66	4.19	59.17	17.41	5.93	4.39	2.65	3.21	2.88	2.48	.49	.06	.70	.74	100.11
MF-2612	2.779	2.75	1.04	59.57	16.64	5.82	3.72	3.29	3.94	2.54	2.27	.23	.05	1.10	.72	99.89
MF-2613	2.756	2.72	1.31	57.74	16.12	5.39	3.47	5.51	3.53	2.69	2.40	.57	.04	2.90	.64	101.03
MF-2614	2.782	2.74	1.51	58.88	16.18	4.66	2.90	4.89	3.72	3.13	2.00	.43	.04	2.90	.64	100.37
MF-2615	2.832	2.75	2.90	55.80	16.30	5.30	3.47	6.00	3.65	2.90	2.27	.40	.04	3.19	.63	99.95

TABLE 4 (CONT.)

	G/CM**3		PER CNT	WEIGHT PER CENT											
SAMPLE	GRDENS	BKDENS	PRSTY	SIO2	AL2O3	FEO	MGO	CAO	NA2O	K2O	S	CO2	MNO	SO3	TIO2	TOTAL
MF-2616	2.765	2.75	.54	57.50	17.50	4.73	3.29	5.07	3.57	2.98	1.98	.33	.04	2.62	.66	100.17
MF-2617	2.835	2.78	1.94	59.85	16.99	4.13	3.43	4.41	3.94	2.99	1.24	.63	.05	1.67	.68	100.01
MF-2618	2.727	2.64	3.19	52.90	17.95	3.07	2.04	3.73	3.50	3.55	.65	.42	.04	1.10	.57	93.54
MF-2619	2.768	2.62	5.35	61.25	17.66	4.55	2.65	3.18	2.99	3.52	1.50	.47	.09	.71	.63	99.20
MF-2620	2.811	2.69	4.30	60.45	17.02	4.49	2.53	3.95	3.35	3.66	1.33	.59	.11	1.33	.61	99.41
MF-2621	2.811	2.79	.75	61.10	17.10	4.06	2.29	4.08	3.21	3.29	1.75	.39	.07	1.72	.54	99.59
MF-2622	2.742	2.69	1.90	61.40	17.20	2.93	2.22	4.58	3.86	3.10	.75	.36	.08	.86	.58	97.92
MF-2623	2.728	2.70	1.03	60.55	17.55	4.00	2.72	4.29	4.37	2.49	1.30	.45	.06	1.52	.56	99.46
MF-2624	2.735	2.63	3.84	58.50	16.90	3.01	2.61	5.84	3.14	2.80	.90	.64	.10	3.39	.56	98.33
MF-2625	2.724	2.70	.88	61.60	18.00	3.14	2.11	4.53	3.79	3.06	.82	.57	.08	1.50	.55	99.75
MF-2626	2.830	2.73	3.53	54.80	16.90	4.22	2.90	6.60	4.01	2.46	1.22	.47	.06	3.63	.66	97.93
MF-2627	2.797	2.72	2.75	61.70	17.40	3.07	1.65	5.11	2.99	3.40	1.28	1.18	.11	2.21	.54	100.64
MF-2628	2.753	2.65	3.95	62.10	17.80	3.12	1.97	3.96	2.55	3.98	1.34	.83	.14	1.86	.51	100.16
MF-2629	2.755	2.74	.54	56.30	15.90	3.03	2.79	7.02	2.84	3.24	1.06	1.33	.05	5.43	.59	99.58
MF-2630	2.797	2.74	2.04	59.86	16.79	4.52	3.34	4.04	2.74	3.50	2.10	1.52	.17	.46	.72	99.76
MF-2631	2.769	2.75	.69	55.70	17.70	3.82	3.15	6.28	3.50	2.44	1.03	.83	.05	2.83	.80	99.13
MF-2632	2.797	2.76	.97	56.30	17.60	3.60	2.76	6.25	3.57	2.75	1.17	.64	.11	2.80	.75	98.30
MF-2633	2.824	2.76	2.27	55.10	17.40	3.95	3.97	7.12	3.24	2.73	1.06	1.06	.10	1.76	.87	98.40
MF-2634	2.804	2.78	.86	53.30	17.30	5.29	4.61	6.03	2.29	2.65	2.51	.67	.06	2.37	.86	97.94
MF-2401	2.742	2.72	2.23	54.21	17.65	5.34	2.75	5.28	1.68	4.13	2.84	2.13	.34	1.80	.53	99.68
MF-2402	2.730	2.70	3.23	59.30	17.10	3.43	2.83	4.75	2.92	2.91	1.28	.66	.06	2.06	.66	97.96
MF-2403	2.813	2.75	2.24	56.60	16.50	3.98	3.40	5.91	3.21	2.79	1.49	.65	.06	3.90	.62	99.13
MF-2404	2.819	2.78	1.38	56.20	17.20	4.92	4.75	5.59	3.87	2.61	2.53	.60	.04	1.93	.80	101.04
MF-2405	2.799	2.76	1.39	51.70	15.70	6.85	4.33	6.67	2.97	2.78	3.79	1.77	.24	1.47	.80	99.47
MF-2406	2.829	2.78	1.73	55.50	16.40	5.51	4.61	5.91	2.92	2.49	2.07	.62	.06	2.42	.74	99.25
MF-2407	2.822	2.76	2.20	56.80	16.32	4.86	5.25	5.63	3.14	2.83	1.39	1.32	.06	2.57	.79	100.96

TABLE 4 (CONT.)

	G/CM**3		PER CNT	WEIGHT PER CENT											
SAMPLE	GRDENS	IKDENS	PRSTY	SIO2	AL2O3	FEO	MGO	CAO	NA2O	K2O	S	CO2	MNO	SO3	TIO2	TOTAL
MF-2408	2.775	2.76	.54	56.20	15.90	5.39	4.50	5.57	3.06	2.55	2.84	.65	.07	1.79	.73	99.25
MF-2409	2.749	2.67	4.27	55.16	16.30	5.54	5.28	5.61	3.21	2.57	2.13	.56	.11	2.78	.81	99.76
MF-2410	2.811	2.78	1.10	52.60	14.90	7.06	4.95	6.17	2.72	2.81	3.85	.90	.11	2.77	.83	99.57
MF-2411	2.734	2.76	1.22	55.70	15.90	5.63	5.89	5.89	3.28	2.79	1.48	.61	.06	1.85	.88	99.55
ON-2401	2.754	2.70	1.96	61.30	17.50	3.25	2.36	4.24	3.21	3.94	1.32	.77	.12	1.76	.57	100.34
ON-2402	2.697	2.63	2.48	62.30	18.30	3.30	2.26	2.96	3.43	3.70	1.36	.43	.05	.90	.59	99.54
ON-2404	2.927	2.84	2.97	59.60	17.60	5.63	2.90	2.69	2.55	3.62	2.94	.38	.12	.82	.59	99.44
MF-3301	2.845	2.76	2.99	55.32	16.00	5.45	4.06	5.53	3.52	2.81	2.12	.28	.05	2.50	.77	98.41
MF-3302	2.808	2.77	1.35	56.46	16.14	4.93	4.04	5.70	3.72	2.57	1.79	.33	.05	1.40	.76	98.23
MF-3303	2.817	2.74	2.73	54.90	14.90	6.07	4.16	5.68	3.38	2.87	2.84	.43	.05	2.62	.74	98.64
MF-3304	2.815	2.75	2.31	55.80	15.40	5.16	4.16	5.82	3.55	2.52	1.62	1.20	.05	2.59	.75	98.62
MF-3305	2.873	2.78	3.24	54.70	14.80	6.23	3.96	5.70	3.43	2.80	3.24	.48	.09	2.80	.69	98.32
MF-3306	2.771	2.74	1.12	54.90	15.40	5.92	4.89	6.43	3.38	2.47	1.36	.40	.06	2.85	.79	98.85
MF-3307	2.792	2.75	1.50	52.70	15.60	6.91	5.38	5.98	3.18	2.54	1.54	.70	.10	2.00	.80	98.43
MF-3308	2.795	2.77	.89	53.70	16.50	5.65	5.66	5.83	2.81	3.04	1.64	.59	.10	2.12	.94	98.54
MF-3309	2.822	2.76	2.20	53.90	17.10	5.78	5.84	6.07	3.33	2.78	1.78	.52	.09	1.53	.89	99.61
ON-3301	2.882	2.79	3.19	58.90	17.70	4.56	2.95	4.49	3.36	3.26	1.81	.46	.09	.41	.63	98.62
ON-3302	2.745	2.68	3.77	60.60	17.20	3.32	2.52	4.27	3.41	3.55	1.14	.51	.06	1.25	.58	98.41
ON-3303	2.769	2.70	2.49	61.70	16.90	3.21	2.24	4.21	2.71	4.44	1.27	1.04	.13	.90	.59	99.34
ON-3304	2.834	2.76	2.61	60.70	16.70	3.20	2.24	4.52	3.06	4.32	1.66	1.16	.17	1.77	.55	100.35
ON-3305	2.750	2.69	2.18	59.40	18.10	3.91	2.25	3.75	2.33	5.17	2.24	1.19	.14	.27	.58	99.73
ON-3305V	-0.000	-0.00	0.10	58.10	17.60	4.59	2.31	3.08	2.02	5.04	3.27	1.29	.18	1.22	.58	99.23
ON-3306	2.776	2.72	2.02	59.50	16.80	3.45	2.71	4.55	3.47	4.07	1.15	.56	.10	1.88	.53	98.77
ON-3307	2.753	2.72	1.20	57.90	17.30	5.24	3.32	4.25	2.13	3.74	2.00	1.06	.35	1.36	.59	99.28
DDH-216	2.794	2.78	.50	55.80	16.10	4.09	5.35	6.35	4.23	2.45	.50	.38	.06	2.95	.40	99.06
DDH-350	2.803	2.78	.82	56.20	16.60	4.23	5.33	6.06	3.72	2.75	.77	.36	.08	1.14	.83	97.77

TABLE 4 (CONT.)

	G/CM**3		PER CNT	WEIGHT PER CENT											
SAMPLE	GRDENS	BKDENS	PRSTY	SIO2	AL2O3	FEO	MGO	CAO	NA2O	K2O	S	CO2	MNO	SO3	TIO2	TOTAL
DDH-839	2.753	2.70	1.93	62.00	17.30	2.86	2.26	4.38	4.37	2.54	.29	.33	.05	1.36	.62	98.33
DDH-770	2.819	2.68	4.93	63.00	17.70	2.72	2.23	4.04	4.44	3.37	.29	.34	.04	1.36	.54	100.06
DDH-812	2.747	2.70	1.71	62.10	17.20	3.34	1.33	3.33	3.59	3.14	1.26	.35	.04	1.39	.49	97.76
DDH-992	2.856	2.77	3.01	55.10	16.40	5.31	5.10	6.05	3.21	2.64	1.16	.33	.05	3.53	.79	99.63

(3.24%, 4.50% and 2.72% for the 2,005', 2,200' and 2,600' levels respectively). N-S traverses for the levels exhibit averages of 2.20%, 1.93% and 1.25% respectively. The ENE-WSW traverses, as it will be shown later, correspond to strongly altered zones where clay minerals, among others, are very abundant and render the rocks more porous.

Figure 17 shows the frequency distribution of total porosity for the Mayflower Mine igneous rocks which approaches a Poisson distribution, as opposed to the skewed and normal distributions of the corresponding bulk and grain densities respectively, shown on the same figure.

When ϕ_T values are plotted in a N-S cross-section of the veins (Fig. 18), the only meaningful trend noticed is the dominant occurrence of higher values below the 2,005' level. This may bear some significance in the assortment of certain alteration minerals in the mine, as will be discussed later.

Data for flow porosity (Table 2) were calculated by equation 7 and, similarly to the fracture abundance, were resolved into components projected on the N50°E/80°NW and N50°W/80°SW structural planes. Hence, the reported values refer to directional flow porosity along those planes. Aperture values used in the equation correspond to average values for the mine levels rather than for individual intervals. Incompleteness of the aperture data as well as uncertainties regarding the significance of present-day openings relative to pre-alteration apertures suggest that the error induced by the use of the average value probably do not exceed the error inherent in the latter assumptions.

The calculated values for flow porosity (ϕ_F) for the Mayflower

Fig. 16. Reproduction from a Mayflower rock slab depicting the different kinds of porosities represented on equation 9. Residual voids were arbitrarily added.

Fig. 17. Hystogram of frequency of bulk density (ρ_β), grain density (ρ_g) and total porosity (ϕ_T) of 131 samples of the Mayflower and Ontario rocks.

residual voids
d_i
d_i
f = 1/n

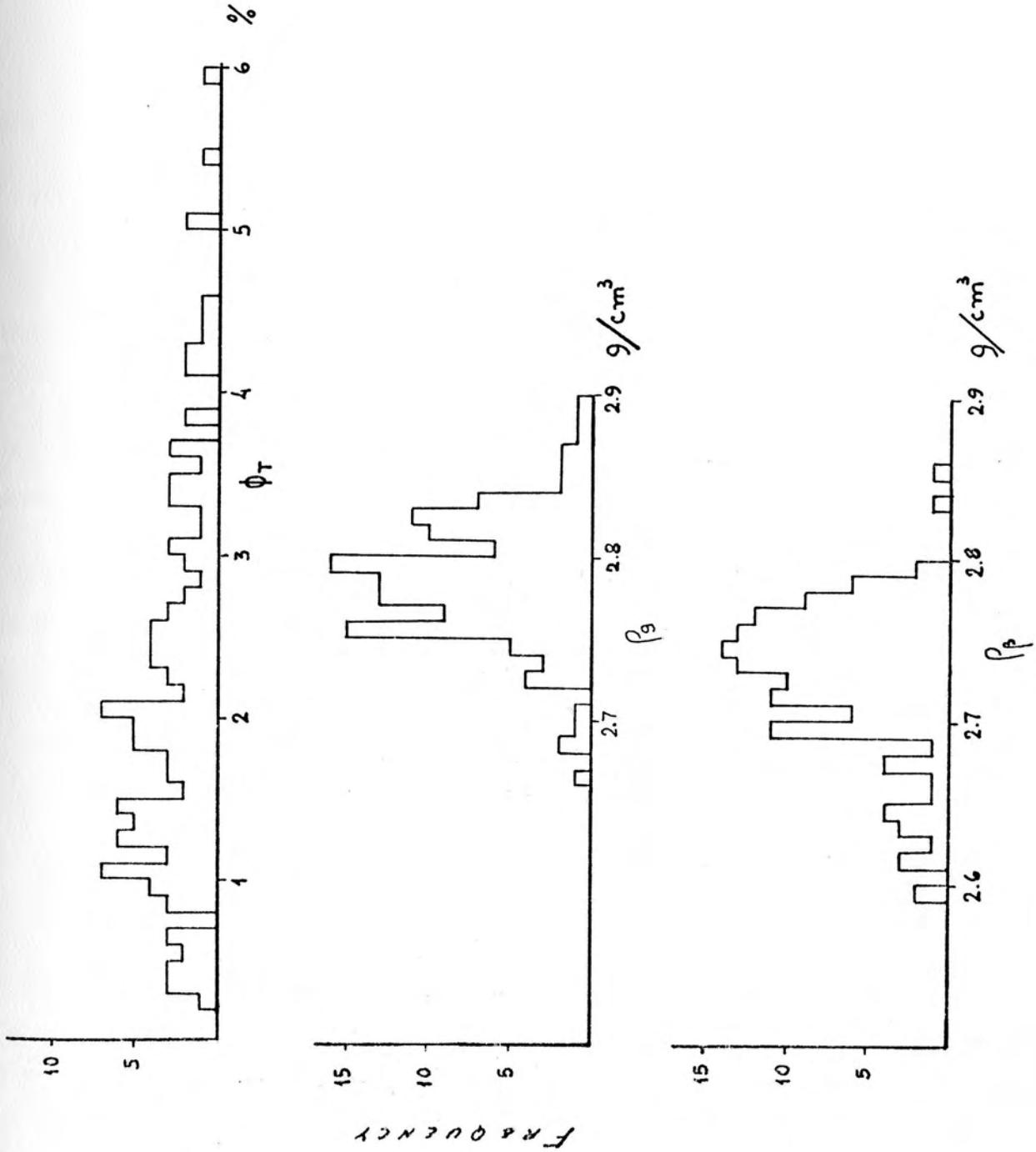
FREQUENCY
10
5
1
2
3
4
5
6
%
ϕ_T
15
10
5
2.7
2.8
2.9
g/cm³
ρ_g
15
10
5
2.6
2.7
2.8
2.9
g/cm³
ρ_b

Fig. 18. Distribution of total porosity (ϕ_T) on a N-S section of the Mayflower Mine showing overall higher values on the lower levels than on the upper levels.

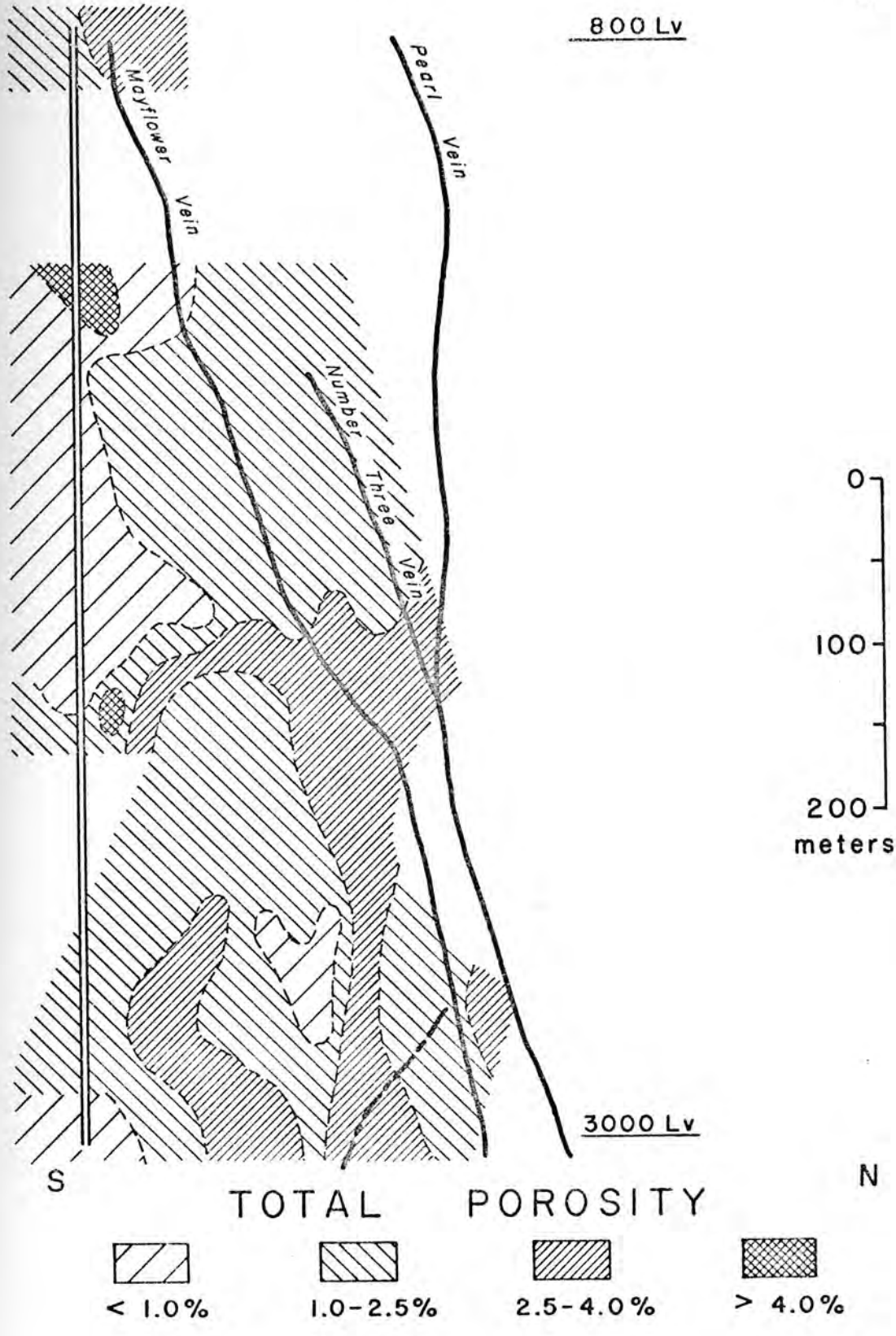
800 Lv
Mayflower Vein
Pearl Vein
Number Three Vein
3000 Lv
S
N
0
100
200
meters
TOTAL POROSITY
< 1.0%
1.0-2.5%
2.5-4.0%
> 4.0%

and Ontario stocks range from about 0.05% to approximately 0.4%. The significant aspect derived from these figures is that the residual porosith (ϕ_R) accounts for most of the total porosity (ϕ_T) of these igneous rocks, since the contribution of the diffusion porosity (ϕ_D) seems to be very small. Indeed, preliminary data on diffusion porosity of fractured granitic rocks (Knapp, verbal communication) point to the same order of magnitude revealed by these flow porosity data.

An independent test was carried out in order to find out how realistic were the results obtained by using Snow's method for flow porosity. The test consisted of measuring the total porosity of a rock slab (MF-2601) transected by several fractures, which was found to be 3.92%. Then a small piece, containing no visible fractures, was cut from the rock slab and its total porosity was also determined and found to be 3.77%. The 0.15% difference, evidently, corresponds to pores other than residual pores existing in the rocks, and agrees by the same order of magnitude with the values found for both the flow and diffusion porosities. This test also indicated the major control exerted by the residual porosity over the total porosity of an igneous rock. Scanning electron microscope study of pore systems in rocks (Timur et al. 1971) reveals enough details of the abundance, shape and size of residual pores, both intergranular and intragranular, in rocks to make the above conclusion seem inescapable.

Permeability

Permeability is the ability of a porous medium to transmit fluids through it. For a fractured crystalline rock, permeability is

essentially associated with flow fractures and, therefore, with its flow porosity. The largest amount of alteration per unit of volume occurring adjacent to flow fractures is generally an indication of the amounts of fluids circulating through them, and, as a result, of the permeability of the rock.

The permeability data for the Mayflower and Ontario plutons (Table 2) refer to directional permeability and were calculated according to equation 6 of the mathematical model. The same constraints imposed on the computation of the flow porosity were also applied on the permeability calculations.

Most values for the calculated permeabilities of these pluton rocks have an order of magnitude between 10^{-7} to $10^{-8} cm^2$ along both the N50°E/80°NW and N50°W/80°SW structural planes, suggesting that the permeabilities lie on a plane of anisotropy within the stocks. More significant, however, is their range of variation from 0.4 to 10 darcies with an average value of approximately 4.0 darcies. Earlier estimates for the permeabilities of igneous rocks ranged from 0.01 to 1.0 millidarcy. The present calculations indicated higher rates of fluid flux, if the measured apertures are representative along the whole extension of the fractures. The equation below shows that the flux q varies according

$$\bar{q} = \frac{k}{\nu} \nabla\phi = \frac{d_i^3 n/12}{\nu} \nabla\phi \qquad (10)$$

to changes in d_i and n in case both the potential gradient ($\nabla\phi$) and the viscosity (ν) are held constant.

At the time of the hydrothermal event, the picture might have

been quite different. It is obvious that the fracture apertures varied as minerals were replaced and/or deposited along cracks. Thus, the present-day fracture openings may be an overestimation of the paleo-apertures and most likely the calculated permeabilities deviate from more realistic values. Likewise, as pointed out earlier, some of the fractures counted for determination of their abundance may have not been continuous fractures, and have led to an overestimation of the permeabilities. However, even a reduction of 50% in both the fracture aperture and abundance values would not modify the order of magnitude found for the permeabilities of the Mayflower and Ontario rocks to any significant extent. Furthermore, the extrapolation of these values to represent the permeabilities of the rocks at the time of the hydrothermal event is meant only to test the model and does not replace more elaborate experimental determinations.

CHAPTER VI

PETRO-CHEMISTRY OF THE IGNEOUS ROCKS

Occurrence and General Petrographic Description

The Mayflower stock

The Mayflower stock is the predominant rock unit exposed within the limits of the underground excavation of the mine. Its composition ranges from diorite to granodiorite, but generally falls into the quartz-diorite category. The Mayflower rocks are prophyritic with large phenocrysts embedded in an aphanitic to fine-grained, and even cryptocrystalline, groundmass. These phenocrysts consist essentially of plagioclase and biotite, and minor quartz, hornblende and K-feldspar. The groundmass exhibits basically the same mineralogy with relative enrichment of K-feldspar.

Subhedral to anhedral plagioclase phenocrysts are mostly andesine with an anorthite content ranging from 34% to 44% (microprobe analysis). Optical observation of twinning lamellae in combined albite-carlsbad twins indicate a composition range of 33% to 48% anorthite. In most instances they show zoning but the enrichment in albite content does not occur in a uniform way towards the phenocryst edges. They comprise up to 80% of all phenocrysts and show amounts of alteration ranging from 0% up to 80%. Anhedral plagioclase crystals are the major

component of the groundmass. The most common alteration products replacing plagioclase are kaolinite, sericite, epidote, calcite, anhydrite and chlorite.

Biotite is present in varying amounts and constitutes the second most abundant phenocrysts in the rocks. In the groundmass it occurs as scattered flakes less than 0.5 mm in length. It is from 10% to almost 100% altered especially to chlorite. In some instances it is found replacing hornblende. Most samples contain clusters of fine-grained biotite, about 0.1 mm long, believed to be caused by recrystallization of earlier biotite phenocrysts. These clusters are also chloritized. Besides chlorite, the most common alteration products of biotite are epidote, fine-grained calcite and sphene.

Hornblende has an occurrence similar to that of the biotite with which it is usually associated. Generally it is present as an accessory mineral, although in a few cases it comprises up to 15% of the rock. It appears usually in subhedral crystals frequently altered to chlorite.

Quartz exists both as phenocrysts and small grains in varying amounts. Some crystals, however, have been introduced by the several veinlets that transect the rock. In general it forms small anhedral equant crystals, especially in the groundmass.

K-feldspar occurs rarely as phenocrysts. When present, it shows anhedral crystals slightly altered to kaolinite or sericite. In the groundmass it is more abundant, especially as a secondary product.

Augite, apatite, sphene and zircon occur as accessories.

The Ontario stock

The Ontario stock is exposed only on the 2,800' and 3,000' levels of the Mayflower Mine. The Ontario rocks are porphyritic although some facies are nearly equigranular and their composition ranges from quartz-monzonite to quartz-diorite. Rocks of the Ontario stock are coarser grained than the Mayflower rocks, which in part may be the reason for the lighter color of the Ontario rocks. The Ontario stock may represent a later pulse of the magmatic events with a comparatively slower rate of cooling than the first pulse that formed the Mayflower stock.

No marked difference was noticed in both the primary and alteration mineralogies of the two stocks, but K-feldspar and biotite seem to be more abundant and hornblende less abundant in the Ontario porphyry. Petrographically the stocks look alike, their minerals displaying essentially the same textural characteristics, except for some plagioclase phenocrysts having edges studded with a myrmekitic intergrowth of quartz.

The Valeo stock

The Valeo porphyry rocks are exposed on the west side of the mine between the 800' and the 1,270' levels, forming a thick sill-like body between sedimentary walls. It reappears on the 2,005' level as small dikes or tongue-shaped intrusions cutting through calcareous units.

The Valeo stock did not serve as host for the main ore zones of the Mayflower Mine, although it contains disseminated pyrite. In fact its sub-economic nature largely limited the west extension of some mine

levels.

The Valeo rocks have a distinctive porphyritic texture with phenocrysts of white plagioclase and quartz (some with rounded outlines) embedded in a fine-grained groundmass which lends a gray color to the rocks. Plagioclase phenocrysts are tabular reaching up to 1 cm in length. Mafic minerals, particularly biotite, are present as scattered small crystals but are not abundant. K-feldspar occurs in larger amounts than in the other two stocks and some grains are perthitic.

Pyrite and minor kaolinite, sericite, calcite and chlorite are the alteration minerals of the Valeo stock.

Bulk Chemistry

Major components

The volumetric distribution of those stocks within the underground limits of the mine conditioned the extension of sampling of each igneous body. Of the 133 intervals sampled, a total of 117, 14 and 2 samples were collected from the wall rocks of the Mayflower, Ontario and Valeo porphyries respectively.

All major components in these samples except chemically bound water were determined (Table 4). Considering the fact that these stocks are geologically contemporaneous and have been integral parts of the hydrothermal system that generated the Mayflower ore zone, they must have interacted with similar aqueous solutions responsible for their alteration. Their present-day chemical composition should, therefore, reflect the extent to which their rocks reacted with the hydrothermal fluids. The extent of these thermo-chemical processes and the

petrogenetic relationships among these stocks necessitate the knowledge of their original chemical composition. Unaltered specimens of these rocks were not found in the mine. Samples from surface outcrops of the Valeo and Ontario stocks have been analyzed and are believed to represent the unaltered equivalents of these rocks (Norton, unpublished), Table 5.

Analyses of unaltered rocks of the Mayflower porphyry were not available, however, examinations of thin sections and calculations of mineral abundance for less altered intervals of the Mayflower rock walls (see Chapter VII) allowed an estimation of what their original modal composition might have been. An approximation of their original chemical composition was then possible, since their major primary minerals have been chemically analyzed (see next section). Also, the analysis of the Mayflower interval (MF-2018) that revealed the least amount of hydrothermal minerals was taken to be a good indication of its composition before alteration (Table 5). The calculated composition and the determined least altered Mayflower rock composition agree fairly well within the expected margin of error.

Transition elements

Some transition element geochemical anomalies in the igneous wall rocks at the Mayflower Mine were investigated by Al-Shaieb (1972). From trace element distributions he concluded that lead and zinc anomalies are confined mainly to the vicinity of the veins, while the aureoles of gold, silver and copper were more extensive especially in the eastern part of the mine. On the 2,600' level, in a 67 meter interval

TABLE 5

ESTIMATED COMPOSITION OF THE UNALTERED

MAYFLOWER, ONTARIO AND VALEO ROCKS

	Valeo*	Ontario*	Mayflower	
			Calculated	MF- 2018+
SiO_2	60.70	60.80	59.40	61.11
Al_2O_3	17.50	16.70	20.60	18.20
FeO	1.89	1.20	4.30	3.93
Fe_2O_3	3.05	3.96	. .	. .
MgO	2.49	1.81	1.90	3.04
CaO	4.10	3.15	5.90	5.10
Na_2O	4.46	5.39	4.90	3.94
K_2O	2.54	3.60	2.10	2.95
S	0.02	0.07	. .	0.12
H_2O^+	0.64	0.73	0.45	. .
H_2O^-	0.36	0.44	. .	. .
CO_2	. .	. .	. .	0.48
SO_3	. .	. .	. .	0.58
MnO	. .	. .	0.05	0.10
TiO_2	. .	. .	0.40	0.82
Total	98.20 %	97.80 %	100.00 %	100.37 %

*Norton's Analyses (unpublished).
+Present research.

Note: figures are in weight per cent

TABLE 6

ORE PRODUCTION, MAYFLOWER MINE

Year	Operator	Tons of Ore	Average Grade					
			Au oz/ ton	Ag oz/ ton	Pb %	Zn %	Cu %	Cd %
1870-1932	Various	±35,000	. .	. .	. .	. .	. .	. .
1932-1961	New Park	1,397,912	0.28	6.5	5.6	7.0	0.7	n.a.
1961-1967	Hecla	565,722	0.39	4.1	4.5	4.3	0.7	n.a.
1968	Hecla*	122,357						
1969	Hecla**	117,452	0.49	6.33	5.23	3.14	0.98	n.a.
1970	Hecla**	115,762	0.48	5.2	4.51	2.85	1.01	0.02
Total		2,354,205	0.33	5.74	5.18	5.88	0.73	0.02

SOURCE: Quinlan and Simos, 1968.
*New Park Mining Company files.
**New Park Mining Company Annual Report, 1970.
n.a. = not available.

along a longitudinal section 15 meters south of the Mayflower vein, the average concentrations calculated from Al-Shaieb's tables were 478 ppb Ag, 131 ppb Au, 511 ppm Cu, 43 ppm Pb and 66 ppm Zn. One very anomalous concentration in that interval was not computed. In a 100-meter interval along a N-S section on the same level the averages obtained were 428 ppb Ag, 188 ppb Au, 275 ppm Cu, 44 ppm Pb and 74 ppm Zn. Values for lead and zinc are very uniform along both intervals, whereas those for gold, silver and copper show a more pronounced scattering. Sections sampled on other levels do not change this pattern appreciably.

For the ore zone, the concentrations of these metals were calculated using a weighted average from production figures given on Table 6

Mineral Chemistry

Primary and alteration assemblages

Plagioclase, quartz, K-feldspar, biotite and hornblende constitute the major primary minerals present in the stocks exposed in the Mayflower Mine. The alteration assemblage of the wall rocks, on the other hand, is much more varied, but only a few minerals occur in significant quantities over the studied vertical section of the mine. These most abundant alteration products are kaolinite, K-feldspar, quartz, biotite, chlorite, anhydrite, calcite and pyrite. Minor alteration components include actinolite, epidote, salite, zeolites, rhodochrosite, gypsum, schorlite, magnetite, etc. which locally may become abundant especially as vein-filling minerals. Sericite, although ubiquitous, is not abundant except occasionally in the immediate vicinity of the main vein system. Albite, likewise, is not widespread but becomes

a major hydrothermal mineral a few meters away from the Mayflower vein. Montmorillonite was not found, but it has been reported to occur ubiquitously in small amounts (Williams 1952).

Chemical compositions of the mineral phases

Only silicate minerals that usually exhibit significant compositional variation, e.g., members of a solid solution series, were analyzed. Accordingly, the chemical compositions of biotite, chlorite, hornblende, actinolite, epidote, salite, augite, plagioclase and K-feldspar grains were determined (Tables 7 and 8). Corresponding structural formulas of these minerals are given in Table 9.

General chemical characteristics of individual mineral phases are as follows:

Biotite. Three distinct textural kinds of biotite were recognized in the igneous rocks of the Mayflower Mine: 1) large isolated phenocrysts, 2) replacing hornblende and 3) aggregates of diminute flakes. The arrangement of these flake aggregates preserved, in many instances, the outlines of the longitudinal and basal sections of some phenocrysts so as to indicate a thorough recrystallization of the phenocrysts. It was thought, therefore, that these textural varieties could represent distinct generations of biotite (primary and secondary). Chemical compositions of fine-grained biotite of four different samples are given below (Table 10). Comparison of these results with the analyses of biotite phenocrysts present in the same samples (see Table 7), however, reveals no discernible chemical difference, unless they

TABLE 7

CHEMICAL COMPOSITION OF MINERAL PHASES

MAYFLOWER, ONTARIO AND VALEO ROCKS

	WEIGHT PERCENT												
MINERAL	SIO2	AL2O3	FEO	MGO	CAO	NA2O	K2O	MNO	TIO2	F	CL	BAO	TOTAL
BIOTITE													
MF-0801	38.16	12.93	15.50	14.11	.14	.28	8.89	.34	5.17	.46	.19	1.62	97.55
MF-1306	38.65	12.52	15.50	15.56	.07	.22	9.08	.32	3.52	.45	.27	.39	96.30
MF-1504	37.42	13.67	14.77	15.69	.18	.19	9.01	.31	3.63	.32	.29	.62	95.91
MF-1704	38.98	12.47	15.24	15.44	.07	.15	9.49	.24	3.86	.50	.25	.20	96.62
MF-2011	38.50	13.59	15.08	16.05	.04	.25	8.49	.13	3.70	.41	.33	.23	96.55
MF-2201	39.18	14.31	14.70	14.78	.09	.32	9.18	.17	4.24	.59	.35	.85	98.43
MF-2204	37.78	12.11	15.05	15.63	.17	.29	8.99	.20	3.28	.86	.21	.17	94.33
MF-2206	38.76	12.44	15.43	15.37	.17	.19	9.15	.31	3.37	.51	.25	.21	95.89
MF-2211	37.89	13.40	16.23	13.86	.21	.26	9.32	.29	4.19	.32	.33	1.34	97.43
MF-2603	37.10	14.80	16.40	13.72	.09	.34	9.17	.27	3.83	.30	.37	1.14	97.32
MF-2614	36.31	13.04	13.51	16.17	.26	.30	8.74	.19	3.62	.37	.25	.34	92.93
MF-2802	39.17	14.33	14.26	14.73	.05	.24	9.49	.08	4.45	.63	.25	.33	97.66
MF-3005	37.30	13.20	16.05	14.03	.14	.24	9.51	.16	3.91	.35	.27	.62	95.57
OOH-177	37.31	13.35	12.56	17.88	.19	.22	8.75	.19	3.07	.65	.20	.37	94.42
OOH-812	37.97	14.58	16.03	14.95	.04	.33	9.30	.15	3.60	.83	.28	.73	98.36
ON-3005	36.31	14.34	15.39	14.76	.04	.30	9.11	.13	4.25	.80	.32	.73	96.07
VL-2002	37.60	15.12	5.95	23.26	.02	.15	9.06	.16	2.63	1.22	.10	.08	94.82

TABLE 7 (CONT.)

WEIGHT PERCENT

MINERAL	SIO2	AL2O3	FEO	MGO	CAO	NA2O	K2O	MNO	TIO2	F	CL	BAO	TOTAL
CHLORITE													
MF-0801	27.84	16.88	18.68	20.71	.24	.10	0.00	.39	.04				84.88
MF-0801V	28.04	17.30	16.67	22.25	.14	.12	0.00	.35	0.00				84.87
MF-0804	27.58	16.44	14.75	24.03	.15	.12	0.00	.44	.03				83.54
MF-1306	26.79	16.80	18.90	21.38	.13	.09	0.00	.47	.06				84.62
MF-1504	26.82	16.40	18.06	21.92	.08	.09	.05	.21	.15				83.78
MF-1708	27.09	16.64	19.13	20.87	.09	.06	.13	.41	.06				84.48
MF-2011	27.40	16.97	19.79	21.06	.12	.11	.04	.22	.05				85.76
MF-2201	28.01	18.18	20.56	18.58	.08	.03	.05	.94	.06				86.79
MF-2204	27.09	15.84	18.98	20.31	.18	.14	.02	.37	.09				83.02
MF-2206	26.96	16.49	19.83	20.85	.07	.05	.06	.72	.08				85.11
MF-2211	27.20	16.56	19.77	19.97	.24	.10	.05	.38	.08				84.35
MF-2603	26.93	18.25	17.38	22.83	.07	.09	.03	.32	.02				85.92
MF-2634	26.34	16.33	19.48	20.12	.21	.10	0.00	.26	.06				82.90
MF-2802	27.05	17.17	20.07	20.33	.08	.04	.02	.14	.04				84.94
MF-3005	26.89	16.55	20.23	19.16	.19	.12	.14	.26	.07				83.61
OOH-177	27.08	15.81	19.57	20.58	.16	.07	.09	.21	.04				83.61
OOH-177V	26.89	15.73	21.99	18.80	.29	.02	0.00	.28	0.00				84.00
OOH-812	25.97	17.77	19.70	21.63	.08	.08	.02	.35	.07				85.67
ON-3005	25.53	17.26	20.74	20.36	.10	.03	.06	.28	.03				84.39
VL-2002	27.18	17.26	10.24	27.59	.04	.05	.06	1.00	.07				83.49

TABLE 7 (CONT.)

	WEIGHT PERCENT											
MINERAL	SIO2	AL2O3	FEO	MGO	CAO	NA2O	K2O	MNO	TIO2	F	CL	BAO	TOTAL
ACTINOLITE													
MF-0801	56.09	2.34	10.50	16.84	12.33	.36	.12	.63	.19				98.40
MF-1336	51.55	5.25	13.76	14.10	11.56	.87	.52	.55	.49				99.05
MF-2011	52.92	4.55	11.20	16.42	11.62	.67	.41	.33	.41				98.53
MF-2204	52.63	3.67	12.31	16.46	12.53	.63	.31	.33	.43				99.30
MF-2206	53.69	3.91	11.53	16.05	11.98	.59	.28	.57	.27				98.87
MF-2211	52.22	4.50	12.68	15.51	11.33	.80	.40	.58	1.03				99.05
MF-2634	52.90	3.09	12.88	15.84	12.79	.31	.15	.28	.11				98.35
MF-3005	54.81	3.05	10.14	16.88	12.48	.40	.26	.44	.35				98.81
DDH-177	52.32	3.84	17.20	12.47	12.63	.46	.25	.28	.13				99.58
EPIDOTE													
MF-0801	39.54	21.49	13.18	.08	23.23	.07	.03	.22	.03				97.87
MF-1336	37.83	22.39	14.57	.11	22.62	.07	.12	.37	.21				98.29
MF-2011	36.92	22.46	13.84	.09	23.06	.04	.11	.09	.28				96.89
MF-2204	38.45	23.52	11.28	.05	24.83	.08	0.00	.32	.05				98.98
MF-2603	38.37	23.24	13.31	.02	23.85	.06	0.00	.08	.08				99.01
MF-2634	39.46	20.99	14.57	.04	23.01	.01	.02	.10	.10				98.30
MF-2802	36.57	23.09	14.16	.06	23.78	.05	.09	.13	.21				98.14
DDH-177	38.66	21.27	15.02	.24	23.07	.01	.02	.10	.04				98.43

TABLE 7 (CONT.)

	WEIGHT PERCENT											
MINERAL	SIO2	AL2O3	FEO	MGO	CAO	NA2O	K2O	MNO	TIO2	F	CL	BAO	TOTAL
SALITE													
MF-3401	52.51	1.08	8.78	14.31	21.90	.41	.06	.57	.21				99.83
MF-2204	52.08	1.10	7.78	14.03	23.87	.42	.04	.47	.10				99.89
AUGITE													
MF-1708	53.31	1.19	9.22	13.80	21.61	.49	.04	.42	.27				100.35
HORNBLENDE													
MF-1708	42.31	12.14	10.16	16.21	11.30	2.13	1.14	.24	2.13				97.76
MF-3005	43.26	11.14	14.16	12.56	11.91	1.35	1.10	.22	1.64				97.34

TABLE 8

CHEMICAL COMPOSITIONS OF FELDSPARS

MAYFLOWER, ONTARIO AND VALEO STOCKS

FELDSPAR	WEIGHT PER CENT CAO	NA2O	K2O	ANORT	ALBIT	ORTHO	TOTAL	RECALCULATED TO 100 PER CENT MOLE PER CENT ANORT	ALBIT	ORTHO
PLAGIOCLASE										
MF-0804	8.52	6.48	.22	42.26	54.79	1.30	98.36	41.54	57.18	1.28
MF-1306	8.58	6.35	.29	42.56	53.69	1.71	97.97	42.02	56.28	1.69
MF-1504	9.01	6.13	.20	44.70	51.83	1.18	97.71	44.29	54.54	1.17
MF-1708	8.17	6.67	.23	40.53	56.40	1.36	98.29	39.83	58.84	1.33
MF-2011	8.16	6.63	.24	40.48	56.06	1.42	97.96	39.91	58.69	1.40
MF-2206	7.31	7.11	.32	36.26	60.12	1.89	98.27	35.56	62.59	1.85
MF-2603	7.18	7.25	.32	35.62	61.30	1.89	98.81	34.72	63.44	1.84
MF-2802	7.09	7.35	.29	35.17	62.15	1.71	99.03	34.19	64.14	1.67
MF-3005	8.35	6.53	.22	41.42	55.22	1.30	97.94	40.87	57.84	1.28
DDH-812	7.48	6.82	.22	37.11	57.67	1.30	96.07	37.24	61.45	1.30
ON-3005	7.33	6.73	.29	36.36	56.91	1.71	94.98	36.92	61.34	1.74
VL-2002	6.69	7.56	.29	33.19	63.93	1.71	98.92	32.29	66.04	1.67
ORTHOCLASE										
MF-0804	.26	1.26	14.09	1.29	10.65	83.21	95.15	1.35	11.80	86.85
MF-1306	.17	1.26	14.54	.84	10.65	85.86	97.36	.86	11.54	87.60
MF-1708	.22	1.46	13.94	1.09	12.35	81.73	95.17	1.14	13.66	85.20
MF-2011	.17	1.28	13.63	.84	10.82	80.49	92.16	.91	12.38	86.71
MF-2206	.18	1.46	14.29	.89	12.35	84.39	97.63	.91	13.32	85.77
MF-2802	.10	1.82	13.38	.50	15.39	79.01	94.90	.52	17.04	82.44
MF-3005	.09	1.20	13.80	.40	10.15	81.49	92.04	.43	11.62	87.95
DDH-812	.11	1.29	14.74	.55	10.91	87.05	98.50	.55	11.68	87.77
ON-3005	.13	1.36	14.63	.64	11.50	86.40	98.54	.65	12.30	87.05
VL-2002	.06	1.06	15.10	.30	8.96	89.17	98.43	.30	9.61	90.09

TABLE 9

STRUCTURAL FORMULAS OF MINERALS USED IN MASS ABUNDANCE CALCULATIONS

MAYFLOWER, ONTARIO AND VALEO STOCKS

	GRAM.ATOM/MOLE												
MINERAL	SI	AL	FE	MG	CA	NA	K	MN	TI	BA	O	S	C	H2O
ANALYSED WITH THE ELECTRON MICROPROBE														
BIOTITE														
MF-0801	2.837	1.133	.964	1.563	.011	.040	.842	.021	.289	.047	11.0			1.0
MF-1306	2.887	1.103	.968	1.732	.005	.031	.876	.020	.198	.011	11.0			1.0
MF-1504	2.808	1.207	.920	1.751	.014	.028	.861	.020	.204	.018	11.0			1.0
MF-1708	2.898	1.090	.947	1.710	.004	.018	.902	.013	.214	.004	11.0			1.0
MF-2011	2.842	1.182	.931	1.765	.003	.035	.799	.008	.205	.007	11.0			1.0
MF-2201	2.852	1.228	.895	1.604	.007	.045	.852	.010	.232	.024	11.0			1.0
MF-2204	2.881	1.089	.960	1.776	.014	.043	.874	.013	.188	.005	11.0			1.0
MF-2206	2.901	1.098	.966	1.714	.013	.028	.873	.020	.190	.006	11.0			1.0
MF-2211	2.832	1.180	1.014	1.543	.017	.038	.888	.018	.235	.039	11.0			1.0
MF-2603	2.772	1.303	1.204	1.528	.007	.049	.873	.017	.215	.033	11.0			1.0
MF-2634	2.793	1.183	.869	1.854	.021	.044	.858	.012	.209	.012	11.0			1.0
MF-2902	2.840	1.210	.856	1.578	.040	.035	.864	.004	.285	.009	11.0			1.0
MF-3005	2.830	1.180	1.019	1.587	.011	.036	.920	.010	.223	.018	11.0			1.0
DDH-177	2.799	1.198	.788	1.998	.015	.032	.837	.012	.173	.011	11.0			1.0
DDH-812	2.793	1.264	.986	1.639	.003	.047	.872	.009	.199	.021	11.0			1.0
ON-3305	2.740	1.276	.971	1.660	.003	.043	.878	.008	.241	.022	11.0			1.0
VL-2002	2.727	1.293	.361	2.514	.001	.021	.839	.010	.143	.002	11.0			1.0

TABLE 9 (CONT.)

	GRAM.ATOM/MOLE													
MINERAL	SI	AL	FE	MG	CA	NA	K	MN	TI	BA	O	S	C	H2O
CHLORITE														
MF-0401	5.871	4.197	3.295	6.509	.054	.041	0.000	.070	.006		28.0			8.0
MF-0401V	5.844	4.251	2.905	6.911	.031	.048	0.000	.062	0.000		28.0			8.0
MF-0804	5.803	4.078	2.595	7.535	.034	.049	0.000	.078	.005		28.0			8.0
MF-1306	5.697	4.212	3.362	6.775	.030	.037	0.000	.085	.010		28.0			8.0
MF-1504	5.726	4.127	3.224	6.974	.018	.036	.007	.038	.024		28.0			8.0
MF-1708	5.773	4.181	3.410	6.630	.020	.024	.032	.074	.010		28.0			8.0
MF-2011	5.756	4.203	3.477	6.594	.027	.044	.010	.040	.078		28.0			8.0
MF-2201	5.829	4.461	3.578	5.856	.017	.012	.012	.166	.009		28.0			8.0
MF-2204	5.886	4.058	3.449	6.518	.042	.058	.005	.068	.014		28.0			8.0
MF-2206	5.734	4.135	3.527	6.609	.016	.020	.016	.129	.012		28.0			8.0
MF-2211	5.822	4.179	3.539	6.370	.055	.041	.014	.069	.013		28.0			8.0
MF-2603	5.578	4.457	3.011	7.047	.015	.036	.008	.056	.003		28.0			8.0
MF-2634	5.741	4.196	3.551	6.535	.049	.042	0.000	.048	.010		28.0			8.0
MF-2802	5.744	4.298	3.564	6.433	.018	.016	.004	.025	.006		28.0			8.0
MF-3005	5.848	4.227	3.665	6.185	.044	.050	.038	.047	.011		28.0			8.0
ODH-177	5.846	4.024	3.534	6.622	.037	.029	.025	.038	.006		28.0			8.0
ODH-177V	5.856	4.038	4.006	6.102	.068	.008	0.000	.051	0.000		28.0			8.0
ODH-812	5.492	4.422	3.478	6.804	.018	.033	.005	.062	.011		28.0			8.0
ON-3005	5.510	4.392	3.744	6.549	.023	.012	.017	.051	.005		28.0			8.0
VL-2002	5.544	4.151	1.747	5.387	.009	.019	.016	.172	.010		28.0			8.0

TABLE 9 (CONT.)

GRAM.ATOM/MOLE

MINERAL	SI	AL	FE	MG	CA	NA	K	MN	TI	BA	O	S	C	H2O
ACTINOLITE														
MF-0801	7.731	.389	1.241	3.550	1.868	.098	.020	.076	.019		23.0			1.0
MF-1306	7.398	.888	1.651	3.015	1.777	.242	.095	.067	.096		23.0			1.0
MF-2011	7.514	.761	1.330	3.474	1.768	.184	.074	.040	.043		23.0			1.0
MF-2204	7.488	.615	1.464	3.491	1.908	.172	.054	.039	.045		23.0			1.0
MF-2206	7.607	.653	1.366	3.389	1.819	.162	.050	.068	.029		23.0			1.0
MF-2211	7.407	.752	1.504	3.279	1.722	.220	.071	.070	.110		23.0			1.0
MF-2634	7.601	.523	1.547	3.392	1.969	.086	.026	.028	.011		23.0			1.0
MF-3005	7.711	.506	1.193	3.539	1.881	.109	.047	.052	.037		23.0			1.0
DDH-177	7.571	.654	2.082	2.690	1.958	.129	.045	.028	.014		23.0			1.0
EPIDOTE														
MF-0801	3.221	2.064	.898	.010	2.028	.011	.002	.015	.001		12.5			.5
MF-1306	3.099	2.162	.988	.013	1.985	.011	.013	.025	.013		12.5			.5
MF-2011	3.605	2.198	.960	.011	2.051	.006	.012	.006	.017		12.5			.5
MF-2204	3.116	2.224	.756	.006	2.134	.013	0.000	.021	.003		12.5			.5
MF-2603	3.099	2.213	.899	.002	2.064	.010	0.000	.005	.002		12.5			.5
MF-2634	3.221	2.020	.995	.005	2.012	.001	.002	.007	.003		12.5			.5
MF-2802	3.012	2.242	.975	.007	2.007	2.099	.009	.009	.009		12.5			.5
DDH-177	3.164	2.052	1.028	.029	2.023	.002	.002	.007	.002		12.5			.5

TABLE 9 (CONT.)

	GRAM.ATOM/MOLE												
MINERAL	SI	AL	FE	MG	CA	NA	K	MN	TI	BA	O	S	C	H2O
SALITE														
MF-0901	1.962	.047	.274	.797	.877	.030	.003	.018	.060		6.0			0.0
MF-2204	1.947	.048	.243	.797	.956	.030	.002	.015	.030		6.0			0.0
AUGITE														
MF-1709	1.981	.052	.287	.764	.861	.035	.002	.013	.007		6.0			.0
HORNBLENDE														
MF-1708	6.196	2.096	1.244	3.538	1.773	.604	.212	.030	.234		23.0			1.0
MF-3005	6.453	1.959	1.766	2.792	1.904	.390	.208	.022	.184		23.0			1.0
PLAGIOCLASE														
MF-0804	2.585	1.415			.415	.572	.013				8.0			0.0
MF-1306	2.580	1.420			.420	.563	.017				8.0			0.0
MF-1504	2.557	1.443			.443	.545	.012				8.0			0.0
MF-1709	2.602	1.398			.398	.588	.014				8.0			0.0
MF-2011	2.601	1.399			.399	.587	.014				8.0			0.0
MF-2206	2.644	1.356			.356	.626	.018				8.0			0.0
MF-2503	2.640	1.360			.360	.621	.019				8.0			0.0
MF-2802	2.658	1.342			.342	.641	.017				8.0			0.0
MF-3005	2.591	1.409			.409	.578	.013				8.0			0.0
ODH-912	2.628	1.372			.372	.614	.014				8.0			0.0
ON-3005	2.641	1.359			.369	.613	.018				8.0			0.0
VL-2002	2.677	1.323			.323	.660	.017				8.0			0.0

TABLE 9 (CONT.)

	GRAM.ATOM/MOLE													
MINERAL	SI	AL	FE	MG	CA	NA	K	MN	TI	BA	O	S	C	H2O
K-FELDSPAR														
MF-0404	2.986	1.014			.014	.118	.868				8.0			0.0
MF-1306	2.991	1.009			.009	.115	.876				8.0			0.0
MF-1708	2.989	1.011			.011	.137	.852				8.0			0.0
MF-2011	2.991	1.009			.009	.123	.868				8.0			0.0
MF-2206	2.991	1.009			.009	.134	.857				8.0			0.0
MF-2402	2.995	1.005			.005	.170	.825				8.0			0.0
MF-3005	2.996	1.004			.004	.117	.879				8.0			0.0
DDH-812	2.995	1.005			.005	.117	.878				8.0			0.0
ON-3005	2.994	1.006			.006	.123	.871				8.0			0.0
VL-2002	2.997	1.003			.003	.096	.901				8.0			0.0
ASSUMED TO BE STOICHIOMETRIC														
KAOLINITE	4.000	4.000	0.000	0.000	0.000	0.000	0.000	0.000	0.000	0.000	14.0	0.00	0.00	4.0
ALBITE	3.000	1.000	0.000	0.000	0.000	1.000	0.000	0.000	0.000	0.000	8.0	0.00	0.00	0.0
QUARTZ	1.000	0.000	0.000	0.000	0.000	0.000	0.000	0.000	0.000	0.000	2.0	0.00	0.00	0.0
CALCITE	0.000	0.000	0.000	0.000	1.000	0.000	0.000	0.000	0.000	0.000	3.0	0.00	1.00	0.0
ANHYDRITE	0.000	0.000	0.000	0.000	1.000	0.000	0.000	0.000	0.000	0.000	4.0	1.00	0.00	0.0
PYRITE	0.000	0.000	1.000	0.000	0.000	0.000	0.000	0.000	0.000	0.000	0.0	2.00	0.00	0.0
MAGNETITE	0.000	0.000	3.000	0.000	0.000	0.000	0.000	0.000	0.000	0.000	4.0	0.00	0.00	0.0

++++++++++++++++

095- NUMBER OF IONS WERE CALCULATED ON THE BASIS OF 11, 28, 23 AND 12.5 ATOMS OF OXYGEN FOR BIOTITE,CHLORITE, AMPHIBOLES AND EPIDOTE RESPECTIVELY.

differ in the Fe^{+3} content for which they were not analyzed. Indeed the relative proportions of the annite (Fe^{++}), phlogopite (Mg^{++}) and proton-deficient oxy-annite (Fe^{+3}) fractions in the biotites in equilibrium with K-feldspar and magnetite, defines the temperature of formation of the ferro-magnesian mica solid solution series. The fundamentals of this temperature-dependent composition scheme have been set forth by Beane (1972 and 1974) who investigated the stability of biotite for a parabolic athermal solution model. This geothermometer constitutes to date the only reliable criterion to distinguish primary from hydrothermal biotite. Ferric and ferrous iron were not determined in this study and therefore the biotite geothermometer could not be used. It was assumed, nonetheless, that there has been re-equilibration of the primary biotite with the hydrothermal solutions that altered the igneous rocks of the Mayflower Mine.

The Mayflower stock biotites show a uniform composition with a phlogopite content ranging from 0.60 to 0.72 (the mean is 0.64) over a 725-meter observed vertical section of the mine. Minor components are less uniform with BaO showing surprisingly high values in some samples.

The chemical compositions of the Ontario and Valeo biotites were obtained from analyses performed in just one sample from each stock. No noticeable chemical contrast was found to exist between the Mayflower and Ontario biotites. The composition of the Valeo biotite, on the other hand, deviates significantly from the composition of biotites from the other two stocks notably in its phlogopitic content which is 0.87. This chemical parameter points to a minimum temperature of formation of 500°C (Fig. 19) if a minimum mole fraction PDoxyannite of 0.001 is

Fig. 19. Biotite geothermometer as a function of the phlogopite and PDoxyannite mole fractions (after Beane 1974). A temperature of 500°C is indicated for the Valeo biotite ($X_{phl} = 0.87$) if a minimum X_{PDoxy} of 0.001 is assumed.

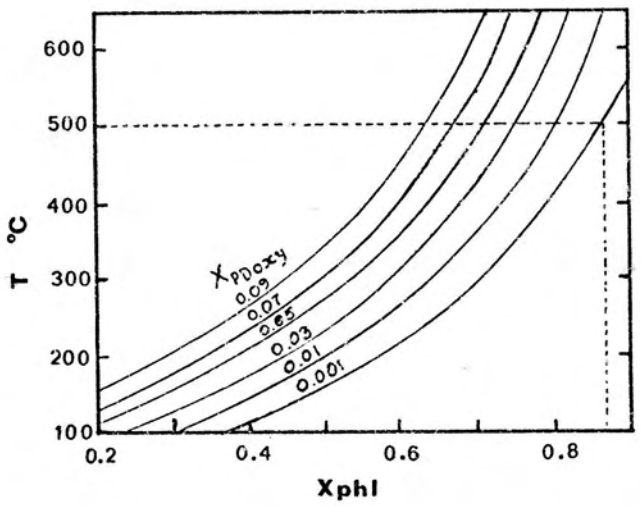
600
500
400
300
200
100
T °C
0.2
0.4
0.6
0.8
Xphl
X_{PDoxy}
0.09
0.07
0.05
0.03
0.01
0.001

assumed for the Valeo biotite.

Figures 20 and 21 demonstrate the homogeneous character of the Mayflower biotite and compare them to both the Ontario and Valeo ferromagnesian micas.

Chlorite. This mineral is present in the igneous rocks of the Mayflower Mine as a secondary product, either replacing mafic minerals and plagioclase or as a vein mineral. Its most common occurrence is as a replacement product of biotite. Chemical compositions were determined for all varieties, except chlorite forming after plagioclase. Those derived from biotite show a remarkably uniform composition with MgO/(MgO + FeO) mole ratios ranging from 0.62 to 0.68. The ratios for vein-chlorites are more variable, but are in general higher than 0.70. This general compositional homogeneity may suggest an equilibration of the chlorites with the hydrothermal solutions over different domains of alteration of the Mayflower stock rocks.

The Ontario chlorites are chemically indistinguishable from the Mayflower ones, whereas the Valeo chlorites constitute a very distinct variety with a MgO/(MgO + FeO) mole ratio of 0.83. Comparative illustration of the variability of the chemical composition of chlorites of all three stocks is given in Fig. 20 which relates these phyllosilicates to their four major components.

Actinolite and hornblende. From inspection of the composition of the amphiboles found in the Mayflower stock, it can be seen that they can be expressed in terms of the Ca-amphibole end members since they do not show any marked deviation towards the alkali-amphibole group.

Fig. 20. Compositional variation of the Mayflower biotites and chlorites as a function of the MgO/(MgO + FeO) and $SiO_2/(SiO_2 + Al_2O_3)$ mole ratios. Analyzed samples were collected at different mine levels over a 670-meter vertical section. Analyses of the Ontario and Valeo biotite and chlorite are shown for comparison.

Fig. 21. Compositional variation of the Mayflower biotites as a function of their phlogopite mole fraction and wt.%TiO_2 and their phlogopite mole fraction and wt.% (F + Cl). Analyzed samples were collected at different mine levels over a 670-meter vertical section. Symbols are the same as for Fig. 20.

Biotite
Chlorite (after mafics)
Vein-chlorite
Mayflower Rocks
Ontario Rocks
Valeo Rocks
MgO/(MgO+FeO)
1.0
0.9
0.8
0.7
0.6
.70
.72
.74
.76
.78
.80
.82
.84
SiO2/(SiO2 + Al2O3)

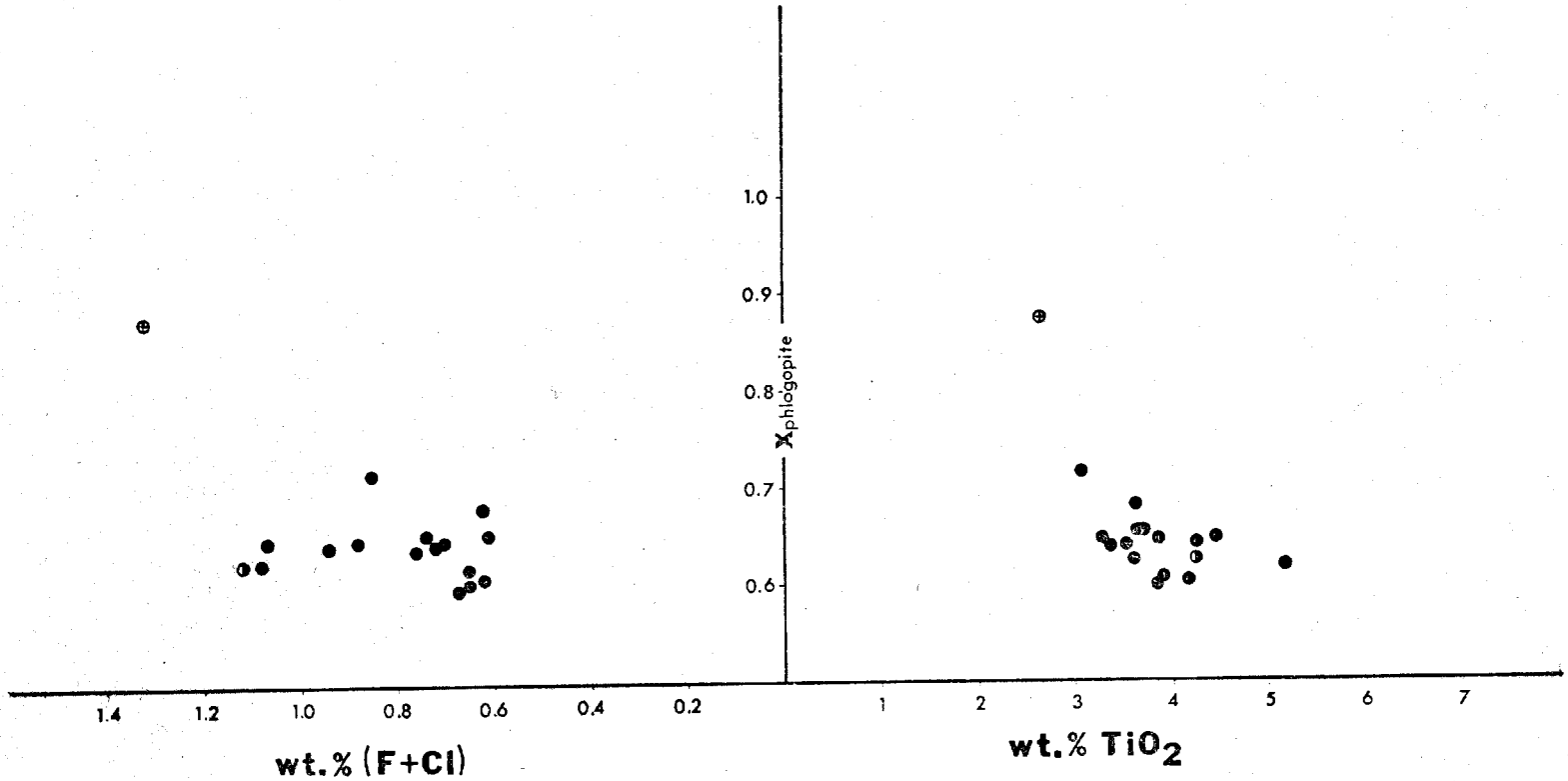
1.0
0.9
0.8
0.7
0.6
$X_{phlogopite}$
1.4
1.2
1.0
0.8
0.6
0.4
0.2
wt.% (F+Cl)
1
2
3
4
5
6
7
wt.% TiO_2

TABLE 10

FINE-GRAINED BIOTITE COMPOSITIONS

	MF- 2011	MF- 2603	MF- 2802	MF-3005
SiO_2	38.57	38.13	39.14	37.29
Al_2O_3	13.62	14.63	14.54	13.22
FeO	15.43	15.56	14.74	16.00
MgO	16.21	14.90	14.50	14.25
CaO	0.04	0.09	0.06	0.14
Na_2O	0.24	0.21	0.29	0.24
K_2O	8.31	9.21	9.40	9.30
MnO	0.14	0.24	0.11	0.15
TiO_2	3.37	2.87	3.95	3.57
Totals	95.95 %	95.84 %	97.00 %	94.16 %

Note: figures are in weight per cent

Variations in the compositions of the Mayflower amphiboles are illustrated by Hallimond's (1943) triangular diagram (Fig. 22). Most of them occupy an area near the tremolite-ferrotremolite corner, but two compositions are displaced towards the pargasite-ferrohastingisite and tschermakite-ferrotschermakite side of the diagram. The analyzed amphiboles, therefore, range from actinolite through actinolitic hornblende to a hornblende rich in aluminum.

Where actinolite and hornblende are present in the same sample, the former is generally replacing the latter. This may also explain the very inhomogeneous character of the actinolites with respect to SiO_2 and Al_2O_3 as analysis spots with the electron microprobe disclosed. It seems likely that submicroscopic intergrowths of actinolite and hornblende may give rise to this inhomogeneity. The actinolite analyses in Table 7 represent averages of inhomogeneous counts.

Actinolite exists commonly as a biotite replacement and as a vein mineral, but no significant chemical difference was noticed among any of the distinct occurrences of this mineral, although the sample DDH-177 revealed vein actinolite with a much higher FeO/(FeO + MgO) ratio than any other analysis. Similarly to the case of the chlorites, actinolite might have equilibrated with the hydrothermal solutions regardless of its spatial position in the alteration system.

The two hornblende compositions, on the other hand, show a marked chemical variation, but reasons for it were not sought.

Epidote. This mineral occurs as an alteration product of biotite, hornblende and plagioclase and as a vein mineral. Electron-microprobe analyses of epidote represent relatively homogeneous single

Fig. 22. Compositional variation of the Mayflower amphiboles represented on a triangular diagram for Ca-amphibole end members (after Hallimond 1943). □ = actinolite; ◉ = hornblende.

Fig. 23. Compositional variation of both the plagioclase and K-feldspar from analyzed samples of the Mayflower, Ontario and Valeo stocks.

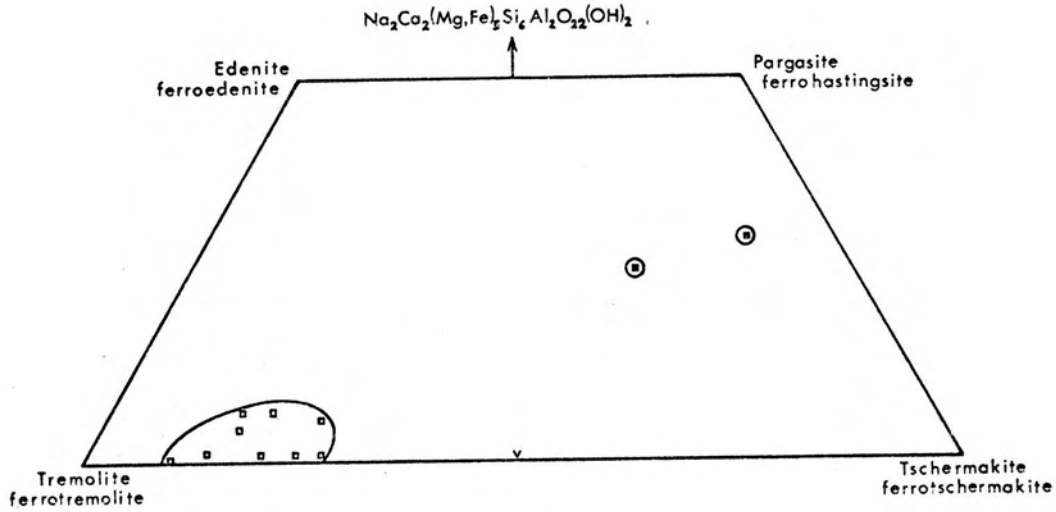
$Na_2Ca_2(Mg,Fe)_5Si_8Al_2O_{22}(OH)_2$
Edenite
ferroedenite
Pargasite
ferrohastingsite
Tremolite
ferrotremolite
Tschermakite
ferrotschermakite

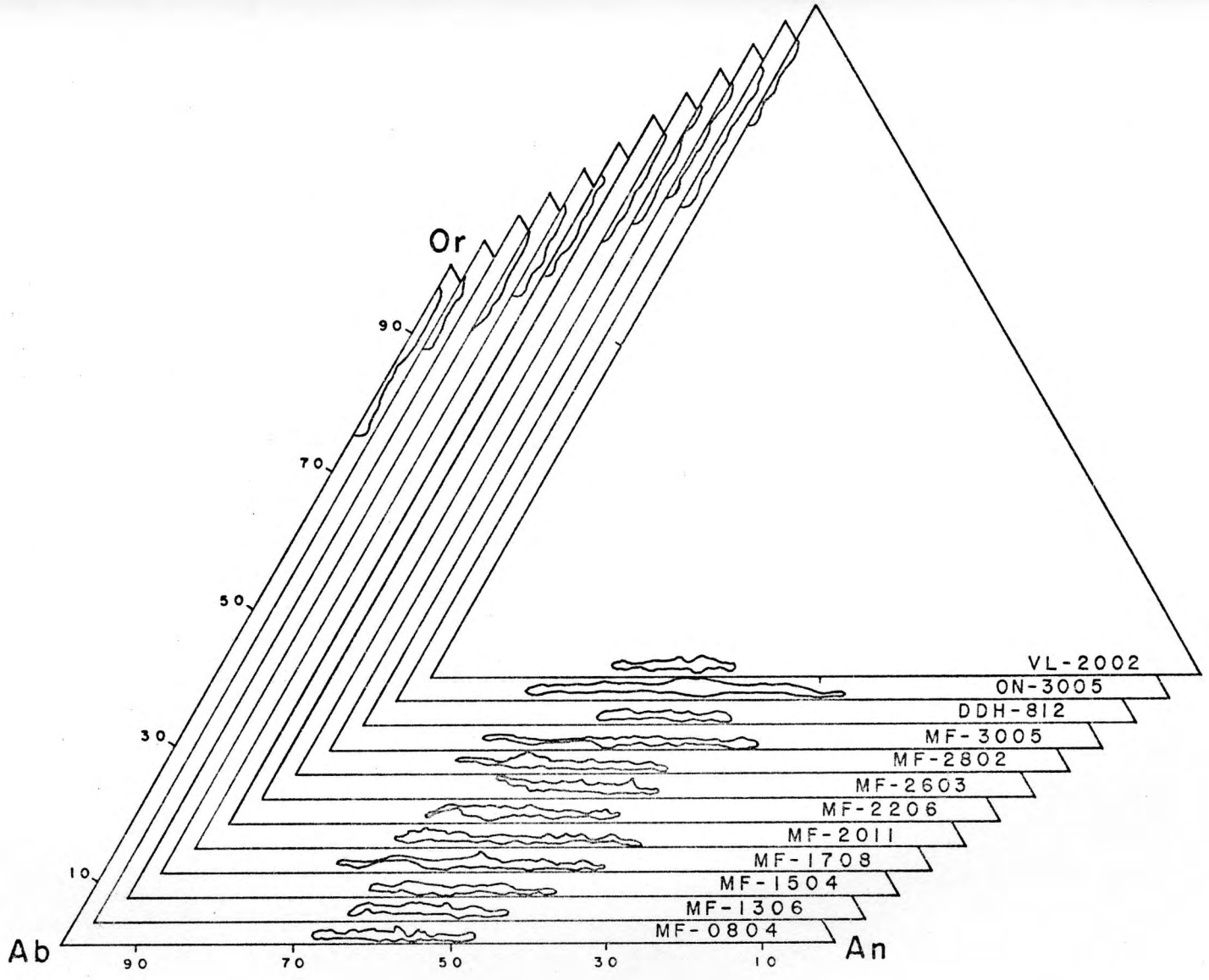
Or
90
70
50
30
10
Ab
90
70
50
30
10
An
VL-2002
ON-3005
DDH-812
MF-3005
MF-2802
MF-2603
MF-2206
MF-2011
MF-1708
MF-1504
MF-1306
MF-0804

grains or groups of grains with a very uniform pistacite content, despite its distinct modes of occurrence.

Salite and augite. Pyroxenes are not widespread minerals in the Mayflower stock rocks. However, two phases were recognized, each having a distinct mode of occurrence: One exists as a primary mineral whereas the other occurs as a vein constituent. The primary pyroxene composition plotted in a conventional enstatite-diopside-hedenbergite-ferrosilite diagram lies at the boundary between augite and salite, but the vein pyroxene compositions fall distinctly in the area reserved for salite. Evidently, there is no significant compositional variation among these minerals to permit a sharp separation between augite and salite. However, the distinction is maintained to suggest once more the re-equilibration of a primary mineral with the hydrothermal solutions.

Plagioclase. Analysis spots with the electron microprobe in plagioclase phenocrysts of the Mayflower rocks, show a compositional variation from oligoclase to labradorite (Fig. 23). The average of all phenocrysts for each sample, however, represents compositions of the andesine member with an anorthite content ranging from 34% to 44% (Table 8). Considering their zoned character, this range points to a fairly homogeneous composition over the vertical section of the mine. The plagioclase composition of the sample of the Ontario stock falls within the range found for the Mayflower plagioclases, whereas in the Valeo stock this feldspar is more albite enriched than the plagioclases of the other two stocks. All plagioclase phenocrysts exhibit low K_2O contents which range from 0.20 to 0.32 weight percent. Analyses for

Fe, Ba and Sr, three minor but frequently present elements in this feldspar structure, were not done. Albite crystals were observed in some veinlets transecting the Mayflower rocks. Semi-quantitative microprobe analyses showed them to be essentially pure albite grains.

K-feldspar. Both primary and secondary K-feldspar are present in the igneous rocks of the Mayflower Mine. Most crystals are orthoclase, but minor amounts of adularia were identified in some veinlets. Only orthoclase grains were examined for chemical composition determination. Primary and secondary varieties do not differ appreciably in the K, Na and Ca contents for which they were analyzed. As a consequence, the compositions reported on Table 8 and Fig. 23 represent the average composition of all orthoclase crystals analyzed in each sample. There is a considerable amount of soda in them--much more than there is potash in the plagioclase as seems to be the case in many hydrothermal systems. Mayflower and Ontario compositions match fairly well, but the Valeo orthoclase seems to be more enriched in Na_2O content.

Average Modes of the Unaltered Igneous Rocks

Examination of several thin sections of the Mayflower and Ontario rocks indicated andesine, orthoclase, quartz, biotite and hornblende to be the quantitatively most important primary igneous minerals. Petrographic observations of some of the least altered rock samples of both stocks permitted an estimate of what might have been the original mineral modes for these rocks. For orthoclase, in particular, the estimated mode was based also on K-feldspar staining

techniques used in some unaltered-looking rock slabs.

Considering the remarkable similarities in both the bulk and mineral chemistry of the Mayflower and Ontario plutons, they were assumed to have had essentially the same modal composition, which was estimated as follows:

Andesine	69% ± 5.0%
Orthoclase	5% ± 2.0%
Quartz	10% ± 3.0%
Biotite	12% ± 3.0%
Hornblende	3% ± 1.0%
Magnetite	1% ± .5%

Magnetite was included due to its universal occurrence in most igneous rocks in similar proportions.

In order to test the validity of this estimate, it was compared with the calculated mineral composition of the interval MF-2018 which was found to contain the least abundant amounts of alteration minerals among all intervals. Its calculated mineral modes (see next chapter and Table 19) agrees very reasonably with the estimate above, if some assumptions are observed. First, calcite and anhydrite were formed with calcium derived from the reactant plagioclase. This implies that 5 wt% anorthite had to be destroyed, what corresponds to 12 wt% of plagioclase characterized by 40% anorthite and 60% albite contents (the average Mayflower plagioclase composition). A minimum original mode for andesine could then be set at 65 wt% (53 wt% + 12 wt%). Second, hornblende was assumed to be totally destroyed for purposes of calculations of the mineral modes for the altered rocks. As a result, the calculated mode for biotite, the only ferromagnesian mineral present in that interval, should be subtracted from the estimated hornblende to represent the maximum original amount of biotite, i.e., 16 wt% (19wt% - 3 wt%). The

recalculated mineral modal composition of the interval MF-2018, except for quartz, would then be

Andesine	65.0%
Orthoclase	7.5%
Biotite	16.0%
Hornblende	3.0%
Magnetite	1.0%

which corresponds to approximately 50 wt% bulk silica. Inasmuch as the chemical analyses of unaltered samples of the igneous rocks of the Park City District average 60 wt% silica (Table 5), the 10 wt% difference was considered to account for the presence of quartz.

The two independent methods, therefore, give equivalent modal analyses for the unaltered Mayflower and Ontario rocks within the assumptions indicated.

Petrogenetic Relationships Among the Stocks

If the analyses given in Table 5 do correspond to the original composition of the Mayflower, Ontario and Valeo plutons, they suggest that these rocks may have had a common parental magma, each representing a different facies of the magmatic evolution.

The data on the chemical composition of the various mineral phases present in the igneous rocks, add more evidence for that petrogenetic link. The chemical similarities between the Mayflower and the Ontario stocks are so striking in terms of both their bulk compositions and compositions of their mineral constituents, that a co-parental magma seems to be the most reasonable explanation. Although the analyses of the minerals may not represent their original compositions (except

plagioclase), since they seem to have been re-equilibrated with the hydrothermal solutions that altered the stocks, it is unlikely that so similar conditions would recur in rocks containing minerals of quite diverse chemical compositions. It is likely that the pulse that gave rise to the Ontario rocks came soon after the Mayflower pluton was crystallized, but long before the co-parental magma had had time to undergo any appreciable differentiation. The Valeo stock, on the other hand, shows some chemical differences, but not petrogenetically significant as to point to derivation from another magmatic center. Its higher K-feldspar and quartz contents and the slightly more albitic character of its plagioclase may indicate it to be a differentiate from the same magma that generated both the Mayflower and Ontario rocks.

Petrochemical evidence, therefore, supports the chronological order of intrusion assumed earlier, in which the Mayflower, the Ontario and the Valeo stocks were successively emplaced.

CHAPTER VII

MASS ABUNDANCE OF REACTANT AND PRODUCT MINERALS

The quantitative evaluation of the minerals present in a representative volume of an altered rock is fundamental to understanding the processes responsible for the rock alteration. The following considerations stress this importance.

Hydrothermal alteration is a path dependent phenomenon and entails the progressive reaction of rocks and aqueous solutions, if they are in chemical disequilibrium. The nature of the mineral assemblages formed and the relative amounts of the phases precipitated depend upon the composition of the aqueous solutions which varies as the reaction progresses (Helgeson 1970). The most important chemical changes in the hydrothermal solutions are related to the consumption or production of H^+. The H^+ balance determines the distribution pattern of the alteration minerals that is conducive to the interpretation of the sequence of hydrothermal events that occurred in the system. Both the amount of H^+ involved in the rock-solution interaction and the distribution of product phases require the knowledge of the mass abundance of reactant and product minerals so that the extent of the hydrothermal processes can be evaluated in time and space. Furthermore, the abundance of certain minerals reflects the prevailing thermochemical conditions governing the equilibrium among the co-existing phases and solutions.

As a result, important constraints can be imposed upon the entire system.

As significant as these theoretical considerations is the fact that the mass abundance of alteration minerals can be used as a guide for ore-prospecting, considering the common occurrence of hydrothermal ore deposits in altered rocks. That fact was found to be valid during the development of the present research.

Mass Abundance Calculations

Many techniques have been used to determine the relative proportions of minerals in rocks. The most common is the point-counting method used with a conventional petrographic microscope. This method has been proven to be very efficient for modal analyses of unaltered rocks in which the mineral grains are large enough to be identified. For volcanic and subvolcanic rocks this technique becomes quite time-consuming considering the difficulties of examining aphanitic groundmasses even with the most powerful microscope. The problem is similar for altered rocks and aggravated for those rocks in which clay and other fine-grained minerals are widespread and intimately associated. Good modal analyses have been obtained by this method even in those extensively altered rocks, but following long time and tedious work. In general, modal analyses of altered rocks by the point-counting method leave much to be desired both in terms of time and precision.

Theoretical calculations have been largely applied to estimate the chemistry of rocks for which the mineral constituents are considered to be stoichiometric and are assigned approximate modes. As expected,

the calculated bulk chemical composition gives only approximate results and deviates significantly from the true values in most cases. A similar, somewhat inverse approach can be used to calculate mineral modes for solution of geochemical problems in which more precise and refined data are needed. Mineral modes of a rock can be determined if 1) its qualitative mineral assemblage, 2) its bulk chemical composition and 3) the chemical compositions of the minerals present in that assemblage are known. The mathematical operations involving these three parameters require the use of computers for complex rock systems as it is the general case of hydrothermally altered environments. The accuracy of the results obtained by this mathematical method depends on the accuracy of the chemical analyses of rocks and minerals and on the selection of a representative mineralogy for the rock.

The relative amounts of reactant and product minerals characterizing the altered igneous rocks of the Mayflower Mine were calculated by using a Fortran IV program (QANMIN) developed by Norton and Kolvoord (unpublished). A brief description of the QANMIN program is given in Appendix E.

The calculations were performed after thoroughly scrutinizing the major minerals composing the altered rocks. Accordingly, each rock pulp, representing 15 meters of igneous wall sampling, was examined under the binocular microscope and several petrographic thin sections prepared from samples collected throughout the vertical section of the mine were also examined. In addition to this, microprobe inspection helped identifying phases present in the groundmass and veinlets, as well as minerals not readily recognizable with a petrographic microscope.

Complex silicate minerals present in the rocks in amounts less than 1% were excluded from the calculations. The reasons relate to the nature of the computer program solution that utilizes the least square method as the best fit. If these minor mineral constituents are considered, the linear approximation of this numerical method tends to include their composition in the fit. This tendency causes large deviations and may affect heavily the values assigned for the amounts of the major mineral constituents. This was particularly true for those minor minerals having in their structures many of the same analyzed components as do the major mineral constituents. By the same token, manganese was not computed due to its small amounts in both the rock and mineral compositions characterizing the igneous walls of the Mayflower Mine. Rhodochrosite has been reported to be only very locally abundant.

On the other hand, minerals chemically distinguished by some of the analyzed components (but not partioned among many phases) were included in the calculations even when their presence in certain mine intervals was found to be not significant. This was the case of pyrite, calcite and anhydrite for which S, CO_2 and SO_3 analyses were available as major components in the bulk chemical compositions of the rocks. Pyrite, calcite and anhydrite were the only minerals to be calculated to account for the analyzed S, CO_2 and SO_3 respectively. Copper, lead and zinc occur in the igneous rocks of the Mayflower Mine in amounts less than 0.06% (600 ppm). These transition elements were the only ones contributing to the sulfide assemblage of the ore zone in the form of chalcopyrite, galena and sphalerite respectively. Other carbonate minerals (siderite, dolomite, etc.) are never present in the igneous

wall rocks in significant amounts, even locally. Barite has been described (Nash 1973) only in the main vein selvage, but is not quantitatively important either. Gypsum, on the other hand, has been found to be locally important. However, the unavailability of bound-water analyses for the igneous rocks of the Mayflower Mine did not permit a distinction between anhydrite and gypsum during the calculations, which were done on an anhydrous basis for all minerals. As a result, for some intervals, the reported amounts of anhydrite should represent the proportions of both anhydrite and gypsum. Likewise, zeolites were included in the computed amounts for albite since no chemical compositions were determined for them. This approximation might have given slightly larger values for the calculated plagioclase than really present in rocks containing zeolites.

The calculated mineral modes of the altered igneous rocks of the Mayflower Mine (Table 19) turned out to be very consistent with the field observations, especially the distribution of alteration minerals in relation to the vein system (see next section). Furthermore, the method used revealed many practical aspects, in particular the possibility of evaluating mineralogically a large volume of rocks in a relatively short period of time. Although the data collection is a slow process, it is nonetheless indispensable for any elaborate geochemical research. The method, however, has a few disadvantages. It cannot be used either for rocks in which polymorphic minerals occur together or when the equations describing mineral and rock compositions are not independent.

Distribution

Figures 24 through 32 present the distribution of the nine major minerals occurring over a north-south cross-section of the igneous walls of the Mayflower Mine. Andesine, K-feldspar, kaolinite and quartz distributions are obviously controlled by the main vein system whereas biotite, chlorite, pyrite, calcite and anhydrite distributions seem to bear generally no significant dependency on it.

Andesine decreases in abundance away from the Mayflower vein both northward and southward. This zoning was also found around the Number Three vein wherever it was sampled. Clearly, andesine was more thoroughly destroyed in the vicinity of the main vein, but persisted as a reactant mineral to the end of the hydrothermal event. Within the sampled rock volume, therefore, the aqueous solutions never equilibrated with andesine even in the regions where it was apparently less dissolved.

Quartz, K-feldspar and kaolinite show an opposite trend. They are more abundant in the zones surrounding the Mayflower and Number Three veins and decrease towards the host rocks. Furthermore, kaolinite and K-feldspar seem to have been more massively precipitated below the 2,600' level, whereas quartz seems to have been deposited more abundantly on the upper levels, especially between the 1,380' and 1,755' levels.

Biotite and chlorite, which are usually associated with each other, have no definite pattern of distribution over the whole north-south cross-section. However, below the 2,600' level, a zoning is

Figs. 24 through 32. Distribution of the abundance of the major mineral constituents found in the igneous wall rocks of the Mayflower and Ontario stocks exposed over a N-S 670-meter vertical section of the Mayflower Mine.

Fig. 24. Andesine.

Fig. 25. K-feldspar.

Fig. 26. Kaolinite.

Fig. 27. Quartz.

Fig. 28. Biotite.

Fig. 29. Chlorite.

Fig. 30. Calcite.

Fig. 31. Anhydrite.

Fig. 32. Pyrite.

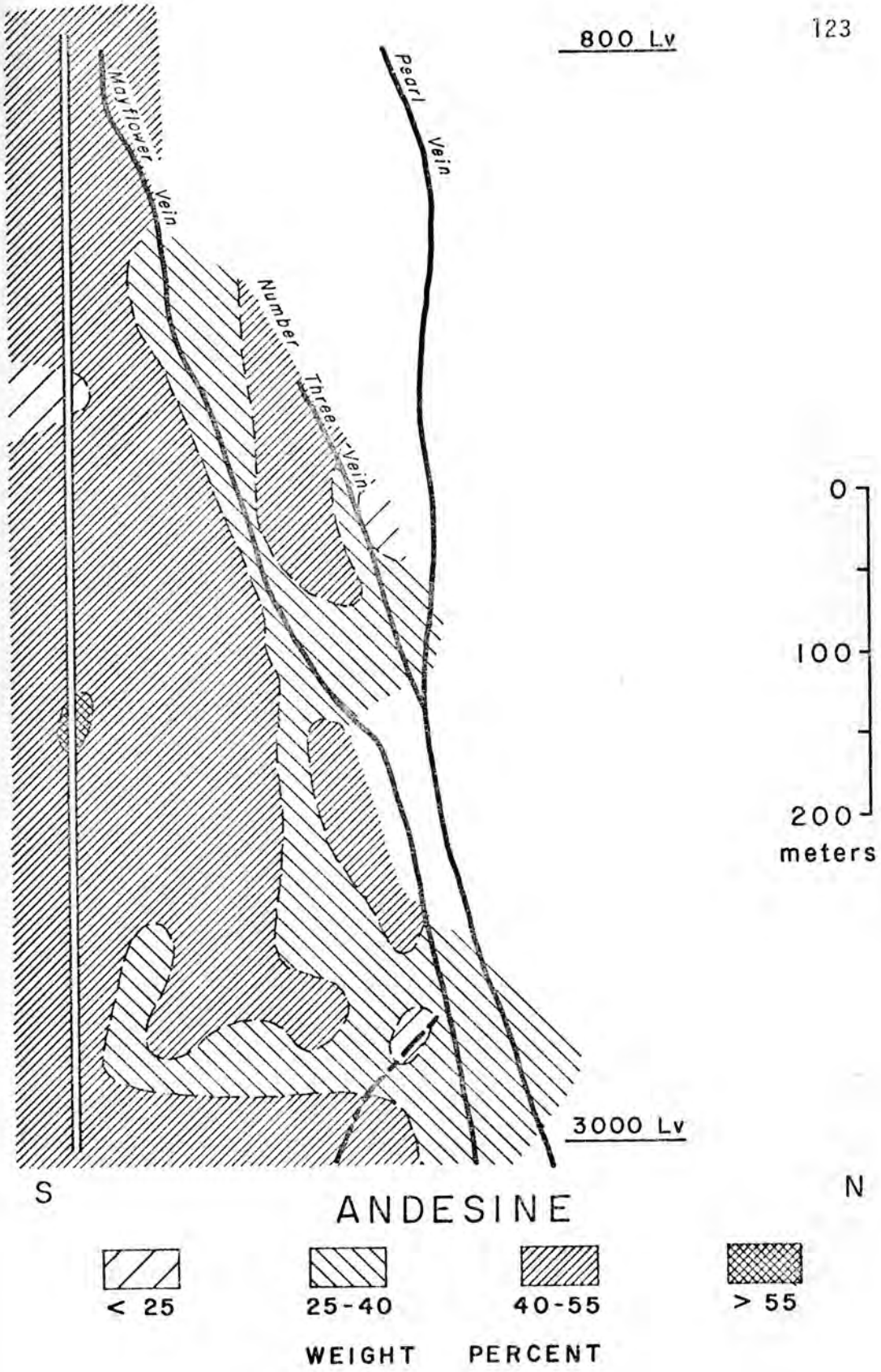
800 Lv
Pearl Vein
Mayflower Vein
Number Three Vein
0
100
200
meters
3000 Lv
S
N
ANDESINE
< 25
25-40
40-55
> 55
WEIGHT PERCENT

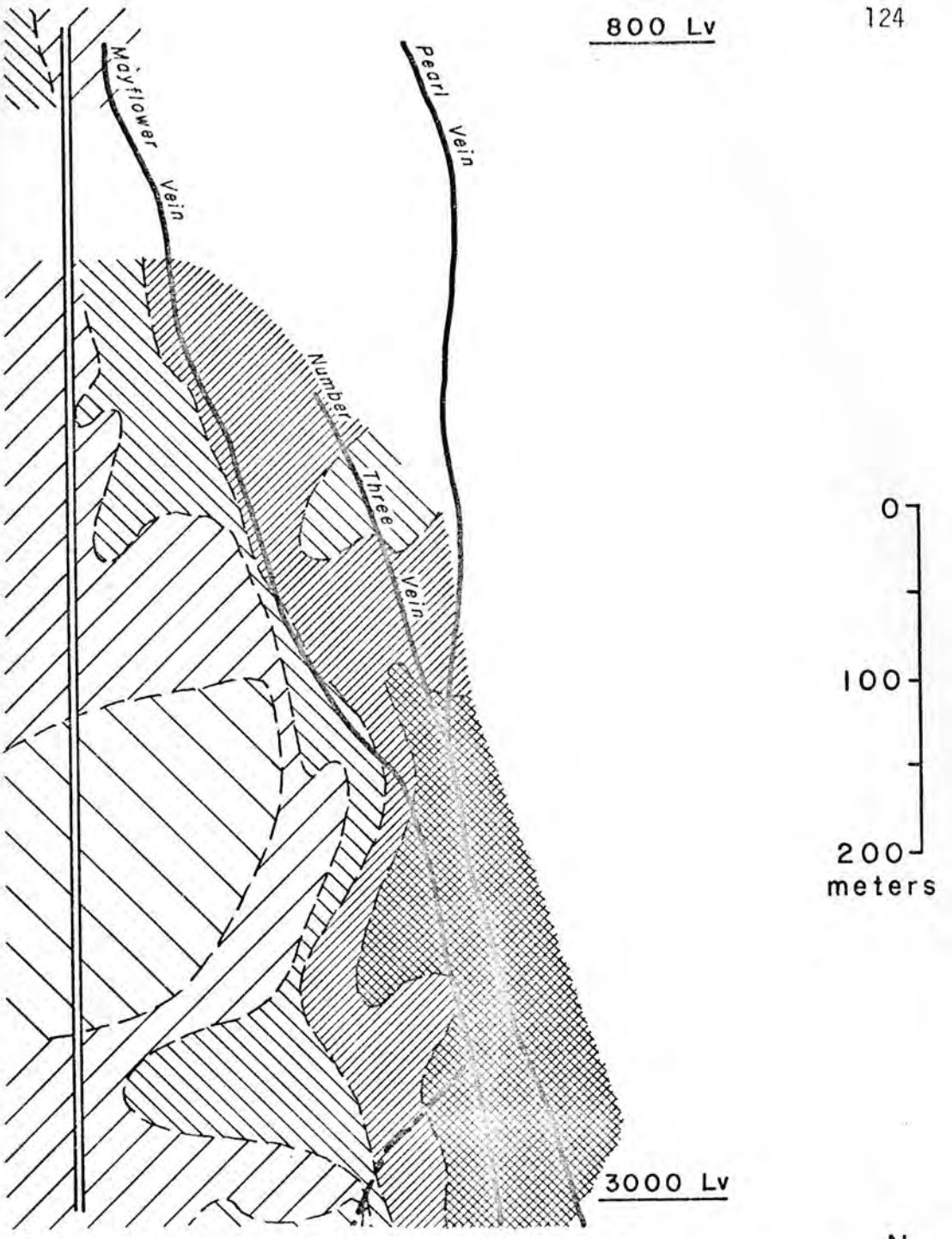
800 Lv
Mayflower Vein
Pearl Vein
Number Three Vein
0
100
200
meters
3000 Lv
S
N
K - FELDSPAR
< 3
3 - 7
7 - 11
11 - 15
> 15
WEIGHT PERCENT

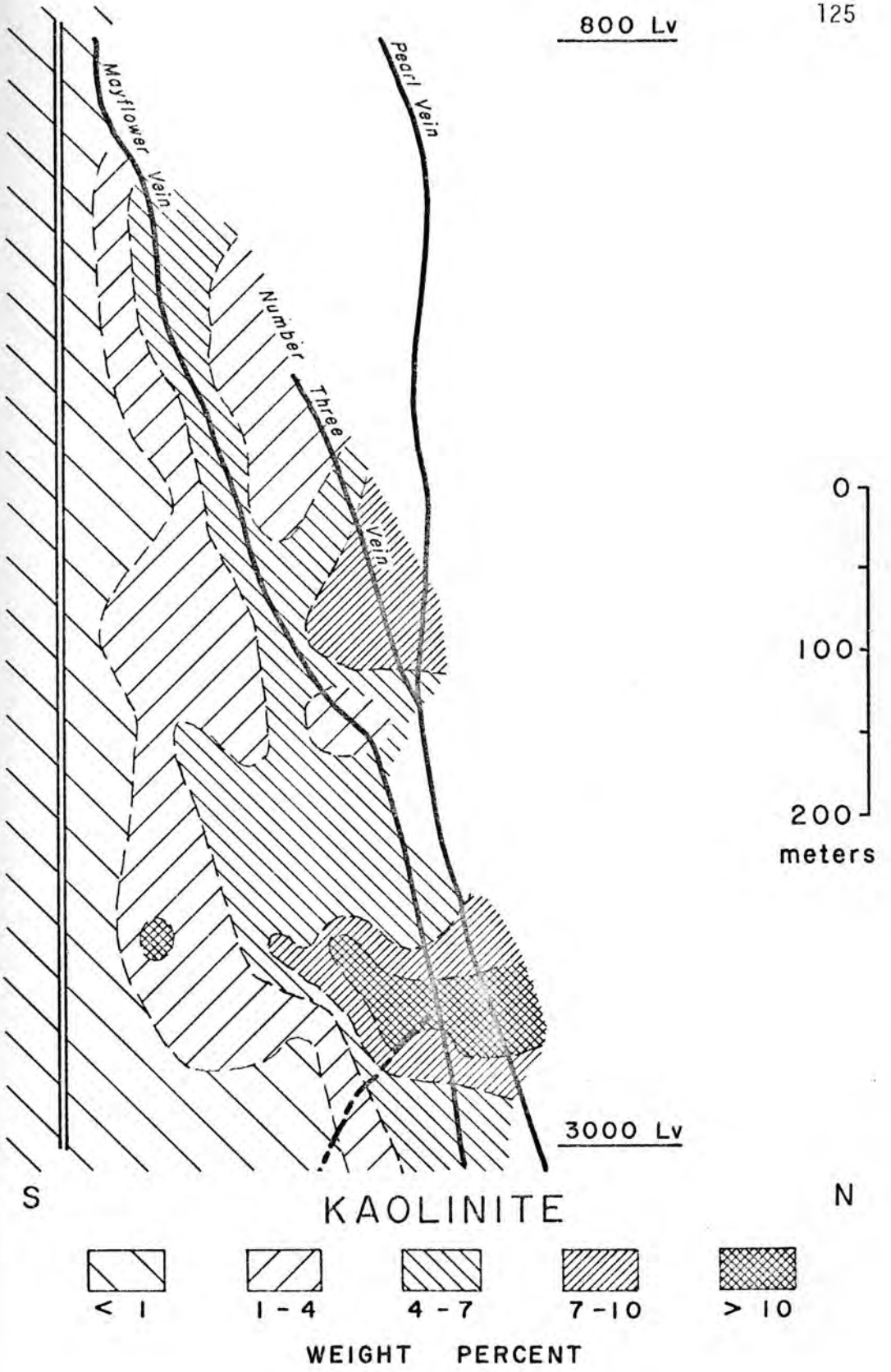
800 Lv
Mayflower Vein
Pearl Vein
Number Three Vein
0
100
200
meters
3000 Lv
S
N
KAOLINITE
< 1
1 - 4
4 - 7
7 - 10
> 10
WEIGHT PERCENT

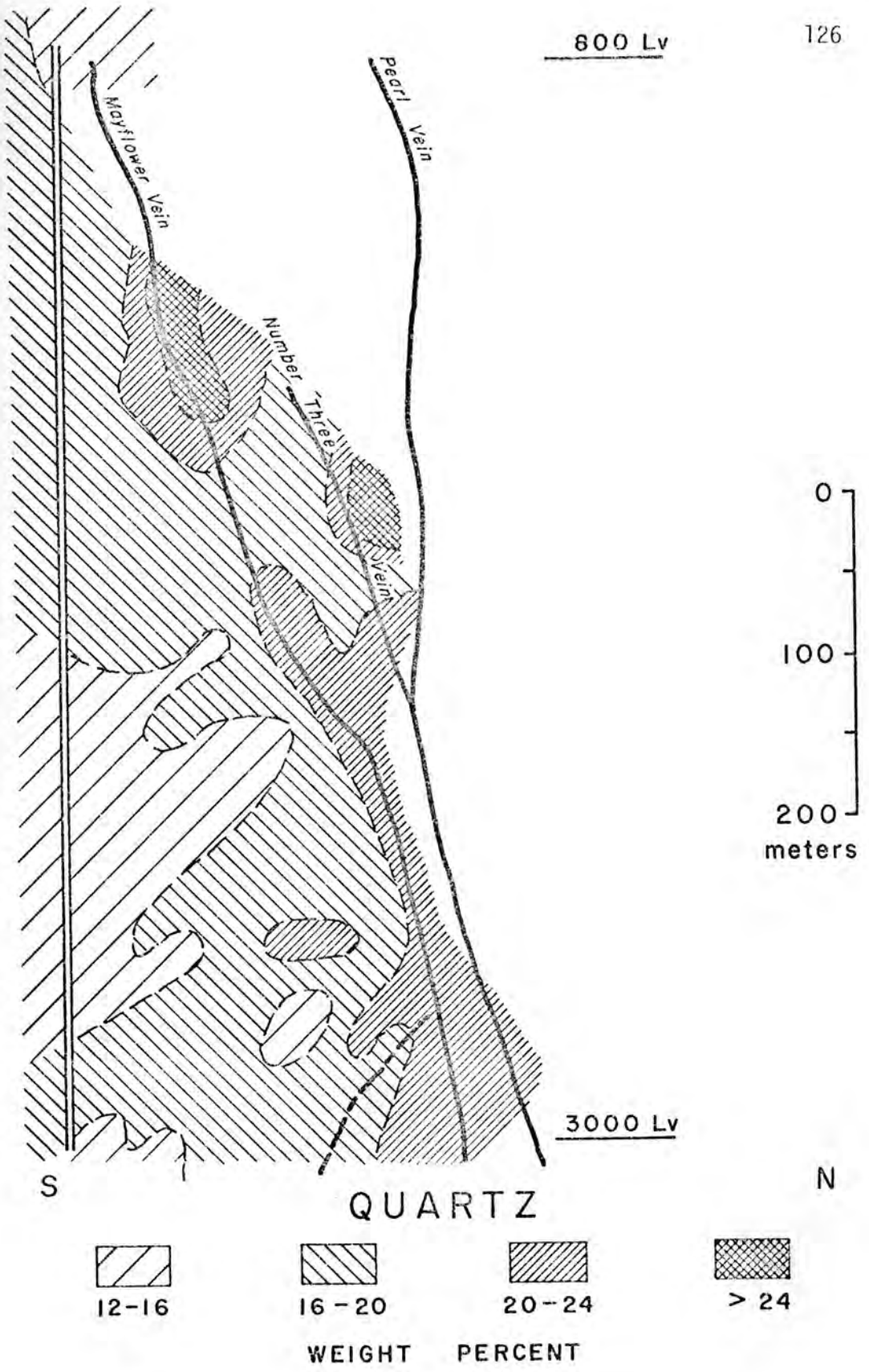
800 Lv
Pearl Vein
Mayflower Vein
Number Three Vein
0
100
200
meters
3000 Lv
S
N
QUARTZ
12-16
16-20
20-24
> 24
WEIGHT PERCENT

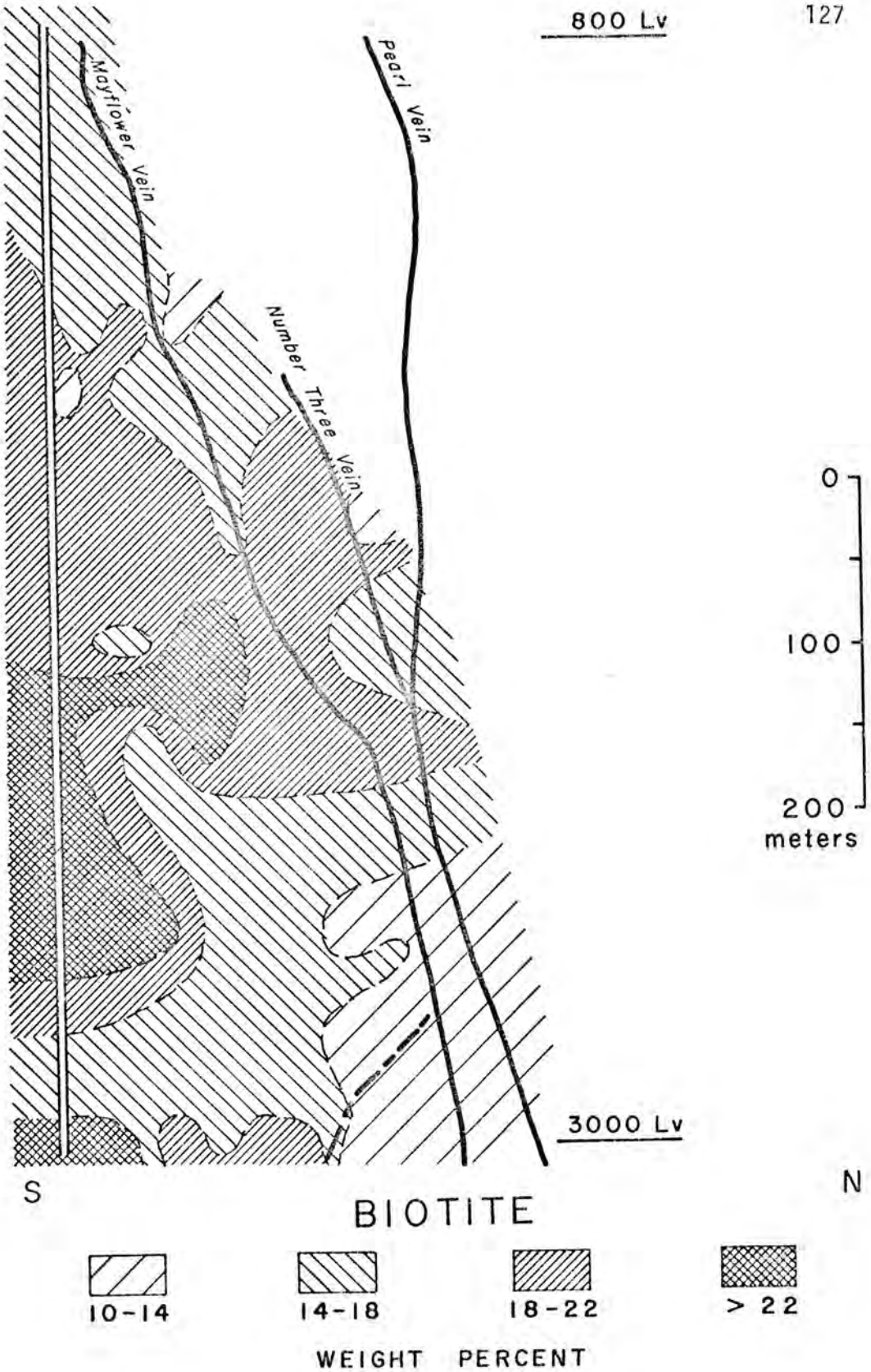
800 Lv
Mayflower Vein
Pearl Vein
Number Three Vein
3000 Lv
S
N
0
100
200
meters
BIOTITE
10-14
14-18
18-22
> 22
WEIGHT PERCENT

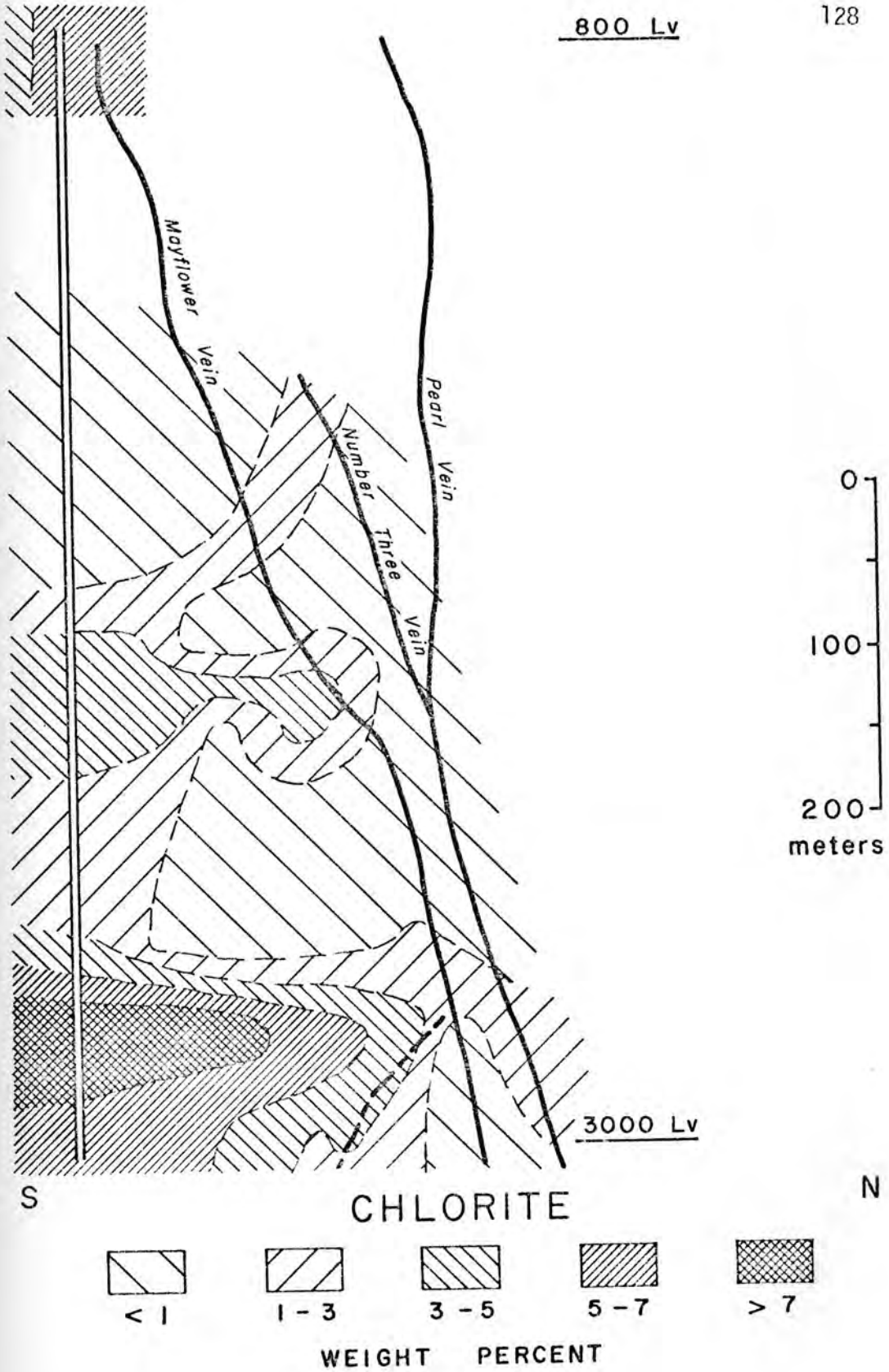
800 Lv
Mayflower Vein
Pearl Vein
Number Three Vein
0
100
200
meters
3000 Lv
S
N
CHLORITE
< 1
1 - 3
3 - 5
5 - 7
> 7
WEIGHT PERCENT

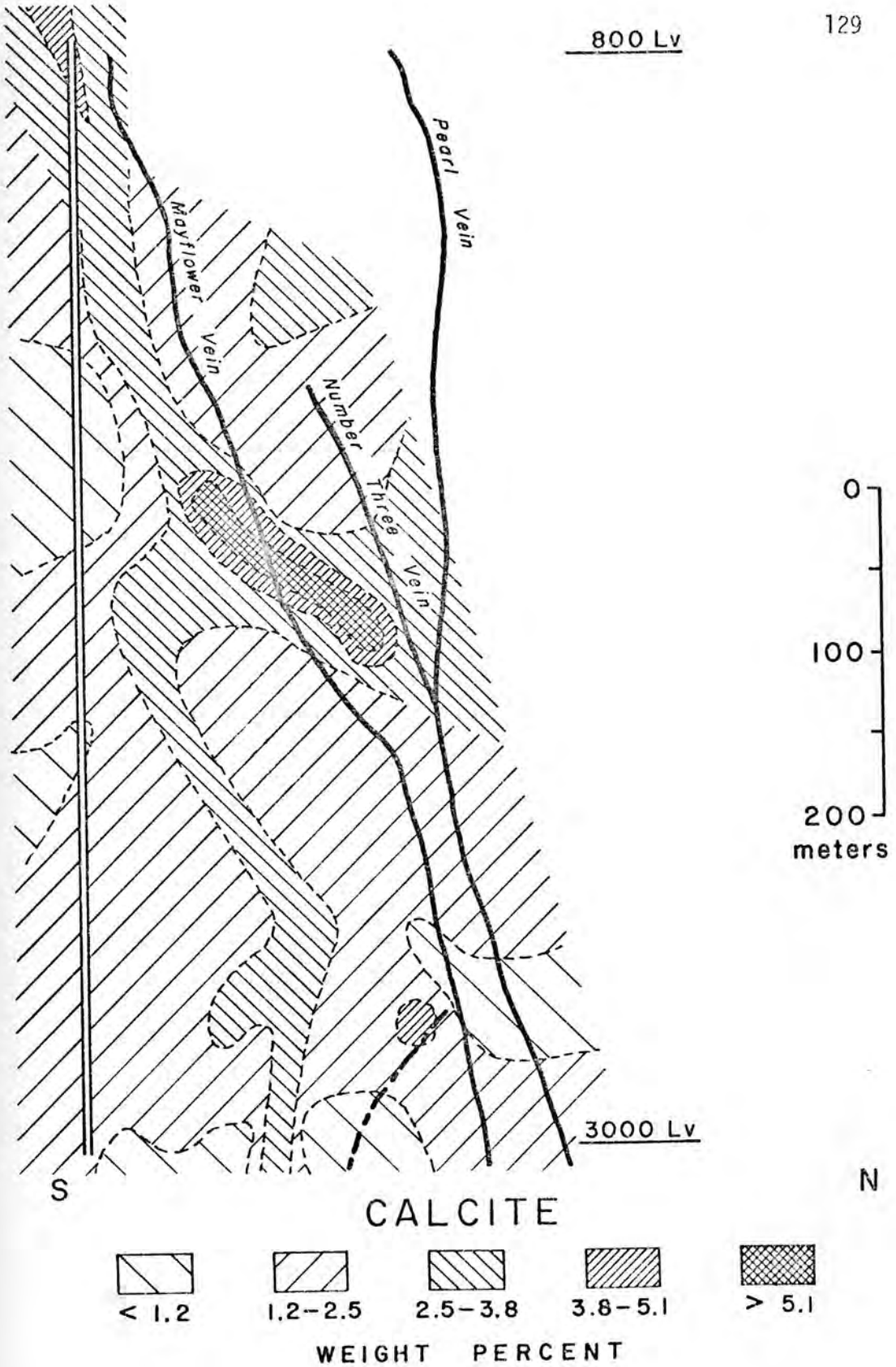
800 Lv
Pearl Vein
Mayflower Vein
Number Three Vein
3000 Lv
S
N
0
100
200
meters
CALCITE
< 1.2
1.2–2.5
2.5–3.8
3.8–5.1
> 5.1
WEIGHT PERCENT

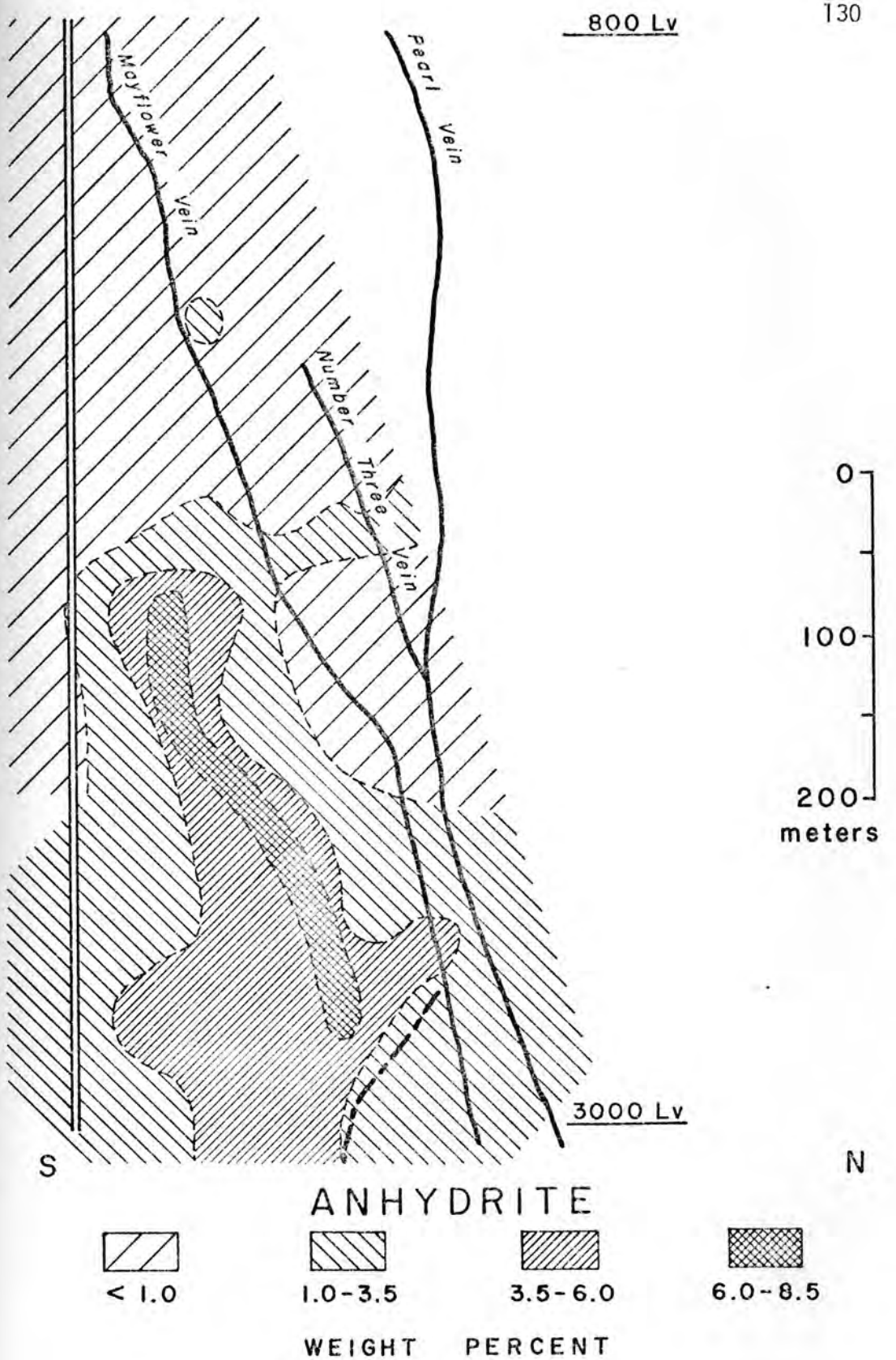
800 Lv
Pearl Vein
Mayflower Vein
Number Three Vein
0
100
200
meters
3000 Lv
S
N
ANHYDRITE
< 1.0
1.0-3.5
3.5-6.0
6.0-8.5
WEIGHT PERCENT

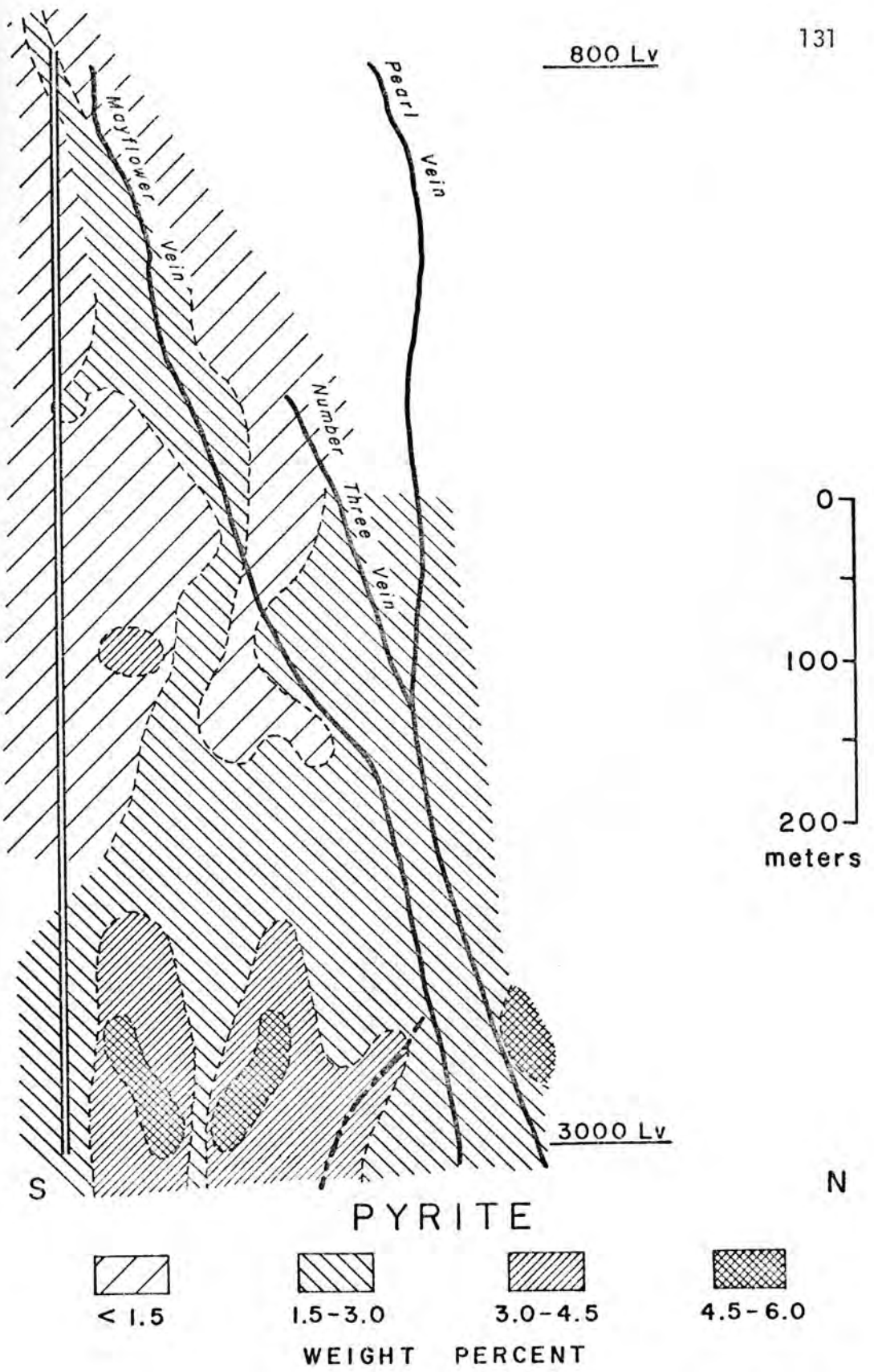
800 Lv
Pearl Vein
Mayflower Vein
Number Three Vein
0
100
200
meters
3000 Lv
S
N
PYRITE
< 1.5
1.5-3.0
3.0-4.5
4.5-6.0
WEIGHT PERCENT

manifested and both minerals decrease in abundance towards the major veins.

Anhydrite and calcite appear as reaction products over the sampled vertical section of the mine, but vary in abundance and distribution. Anhydrite is more abundant than calcite below the 2,200' level decreasing upwards. Calcite becomes more abundant than anhydrite above that level. Such a change reflects a decrease in the $a_{SO_4^{=}} / a_{CO_3^{=}}$ ratio in solution which tends to favor the precipitation of calcite as the CO_2 pressure increases.

Pyrite was found to be most abundant below the 2,600' level at some distance from the main vein system. The pyrite distribution obtained from individual vein samples was not included in order to better demonstrate the bulk distribution of FeS_2 in the host rocks.

A more detailed variation of the distribution of the nine major mineral constituents can be seen along north-south traverses on the 2,800' and 3,000' levels (Figs. 33 and 34). The figures were intended to provide a collective picture of the variational trends of these minerals and facilitate the comparison between reactant and product phases with distance from the main vein structure. The greatest abundance of K-feldspar, kaolinite and quartz and the lowest abundance for andesine coincide with both the nearness of the major veins and the contact between the Mayflower and the Ontario stocks, and could be partly attributed to the effects brought up by the later Ontario intrusion. Observations on the 3,000' level (Fig. 34), however, indicate this interpretation to be erroneous, since similar abundance patterns for K-feldspar, kaolinite, quartz and andesine relate to the major veins

Figs. 33 through 36. Lateral variation of the abundance of the major mineral constituents found in the igneous wall rocks of the Mayflower and Ontario stocks exposed on a 670-meter vertical section of the Mayflower Mine.

Fig. 33. 2,800' level (N-S cross-section).

Fig. 34. 3,000' level (N-S cross-section).

Figs. 35 and 36. 2,600' level (WSW-ENE cross-section).

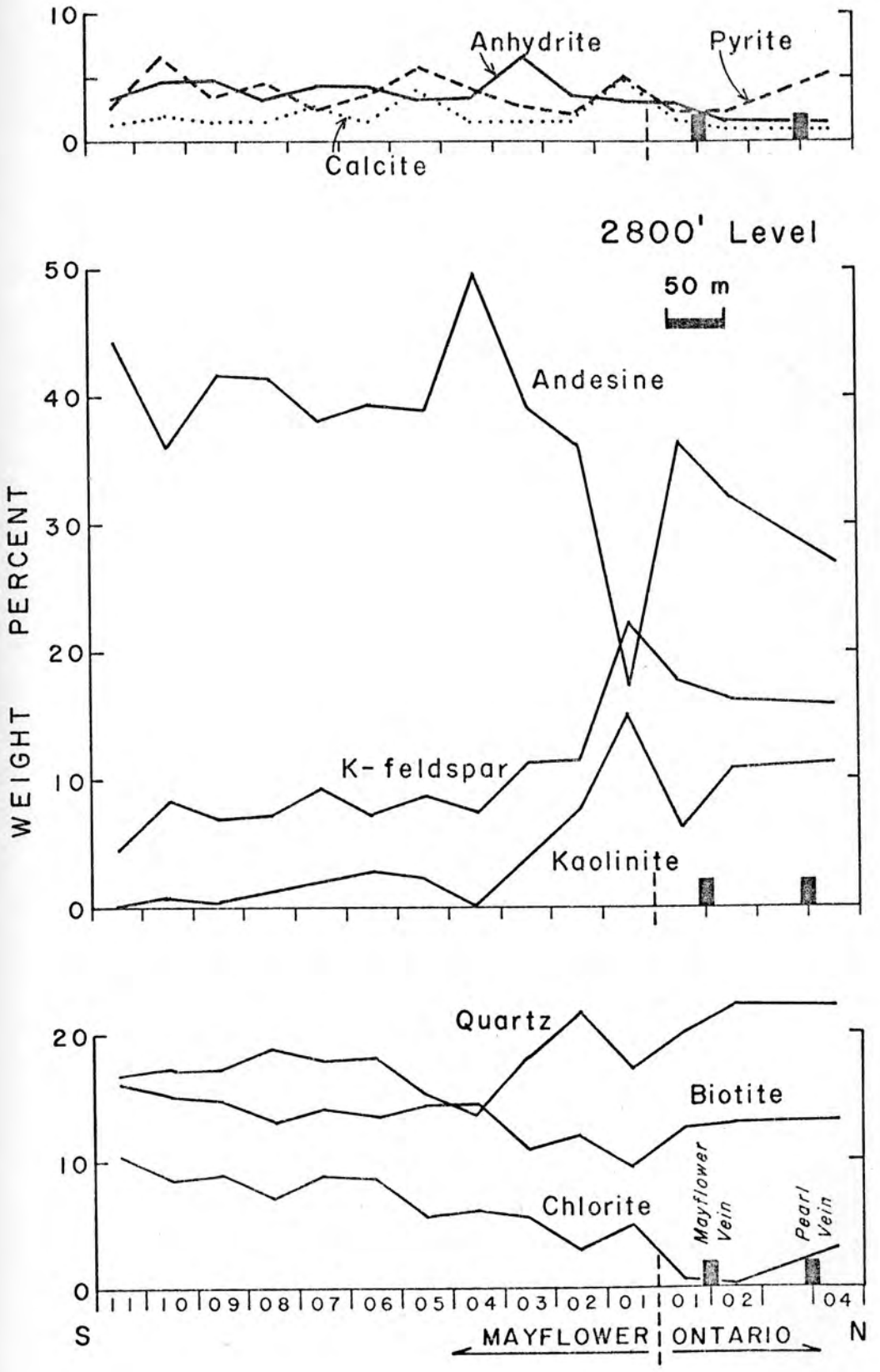
10
0
Anhydrite
Pyrite
Calcite
2800' Level
50 m
50
40
30
20
10
0
WEIGHT PERCENT
Andesine
K-feldspar
Kaolinite
20
10
0
Quartz
Biotite
Chlorite
Mayflower Vein
Pearl Vein
11 10 09 08 07 06 05 04 03 02 01 01 02 04
S
MAYFLOWER
ONTARIO
N

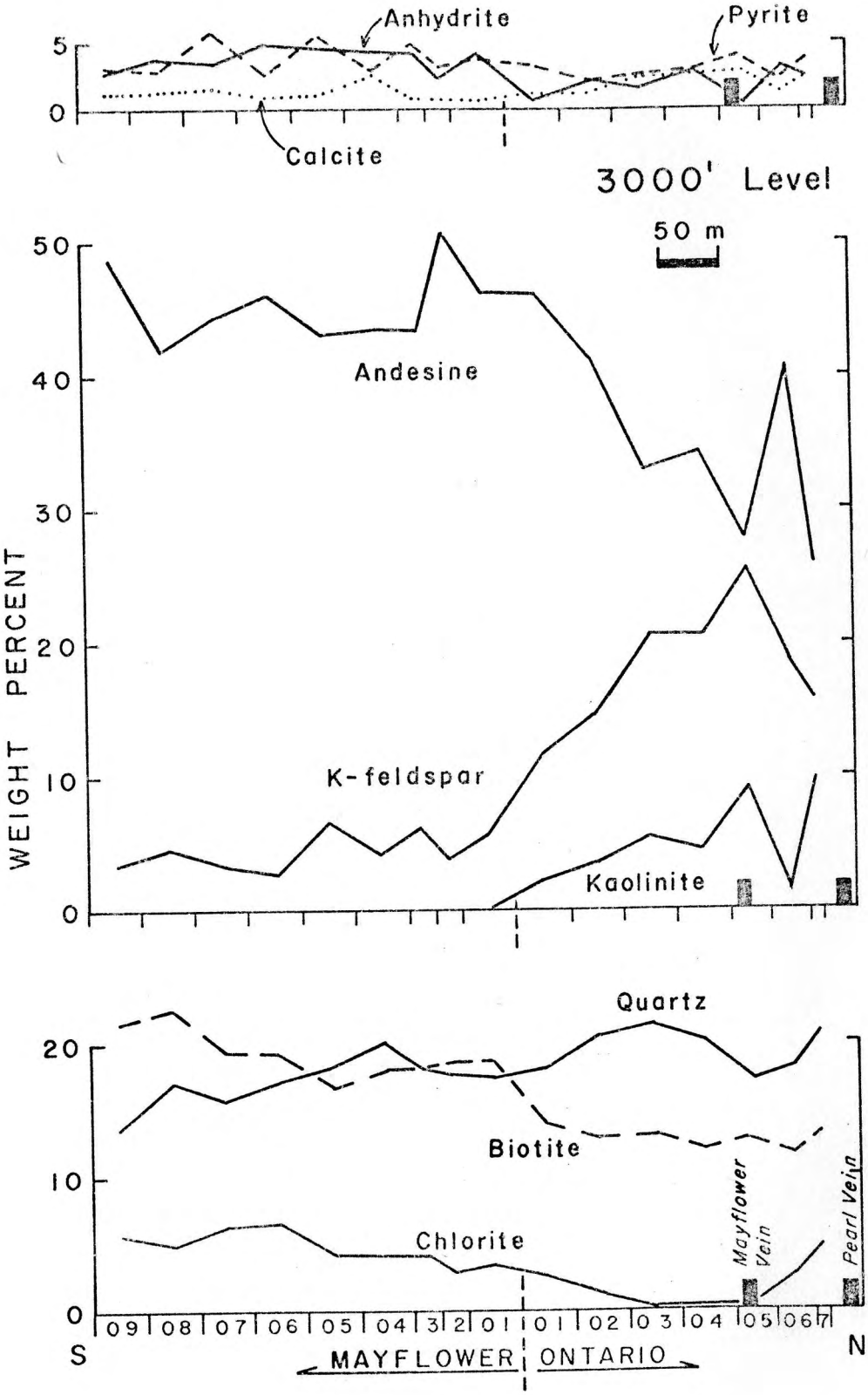
Anhydrite
Pyrite
Calcite
5
0
3000' Level
50 m
50
40
30
20
10
0
WEIGHT PERCENT
Andesine
K-feldspar
Kaolinite
Quartz
Biotite
Chlorite
20
10
0
Mayflower Vein
Pearl Vein
09 08 07 06 05 04 3 2 01 01 02 03 04 05 06 7
S
N
MAYFLOWER
ONTARIO

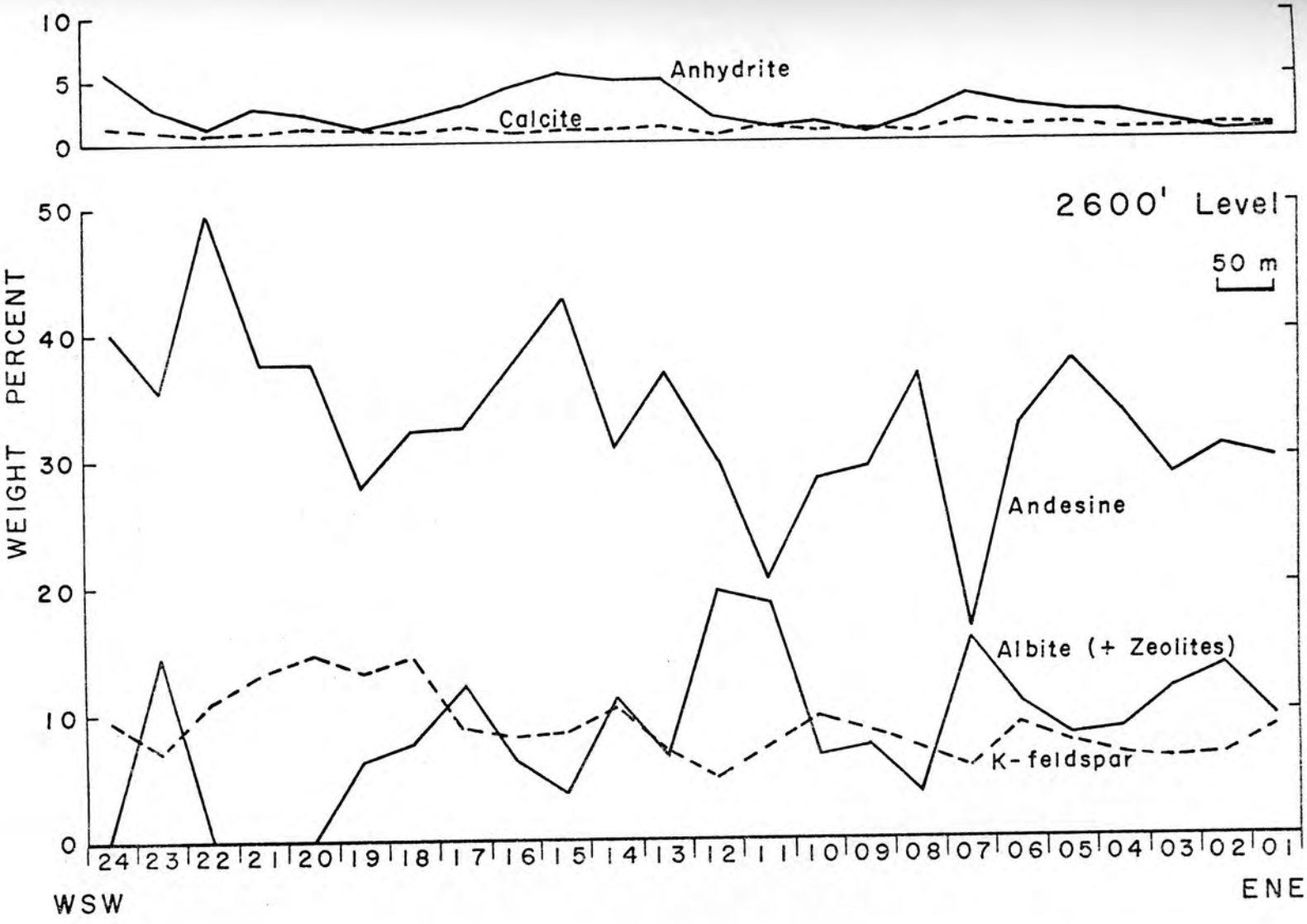
10
5
0
Anhydrite
Calcite
2600' Level
50 m
WEIGHT PERCENT
50
40
30
20
10
0
Andesine
Albite (+ Zeolites)
K-feldspar
24 23 22 21 20 19 18 17 16 15 14 13 12 11 10 09 08 07 06 05 04 03 02 01
WSW
ENE

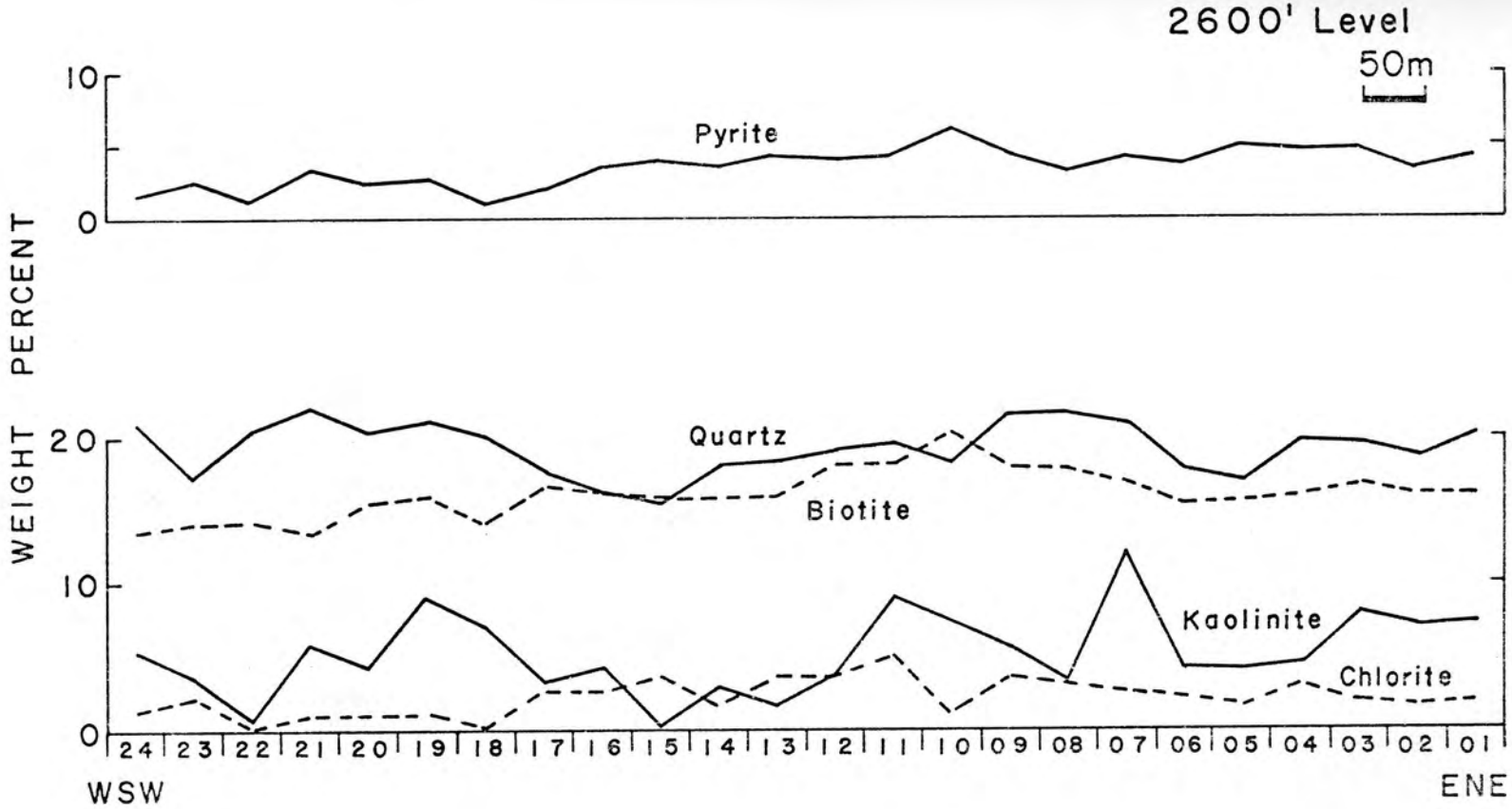
2600' Level
50m
Pyrite
Quartz
Biotite
Kaolinite
Chlorite
WEIGHT PERCENT
10
0
20
10
0
24 23 22 21 20 19 18 17 16 15 14 13 12 11 10 09 08 07 06 05 04 03 02 01
WSW
ENE

regardless of the contact between the two stocks nearby.

On the 2,600' level 365 meters of wall rock sampling was done along an ENE-WSW lateral at approximately 15 meters south of the Mayflower vein. The distribution of abundance of ten major mineral constituents (Figs. 35 and 36) shows a wide variational range for some minerals, but does not indicate any important trend to either ENE or WSW over the sampled distance.

Description of Phase Relationships

The mineral assemblages precipitated during a hydrothermal event are a result of irreversible chemical reactions between rocks and aqueous solutions. Nevertheless, the relationships between coexisting phases can be described in terms of reversible chemical reactions representing their hydrolyses (Helgeson 1970). A convenient way to portray these relationships is by means of activity diagrams. These diagrams depict chemical equilibria among minerals and aqueous solutions and are, therefore, useful to interpret the chemical environment in which product mineral assemblages are formed.

The thermodynamic data for mineral and aqueous species used in the construction of the activity diagrams presented in this research were compiled from Helgeson (1969a), except for annite, phlogopite and Mg-chlorite (clinochlore) which were obtained from Beane (1972). Thermochemical data for the Mayflower plagioclase and biotite were calculated as described in Appendix G. Equilibrium constants (K) of hydrolysis reactions not provided in Helgeson's paper were calculated at different temperatures with the aid of equation (19) (Appendix Ga).

All hydrolysis reaction equations used to determine phase boundaries were balanced on Al_2O_3 and were calculated on the basis of quartz saturation at the temperature in question. All diagrams were constructed by a CDC 6400 computer (from a program written by T. H. Brown 1970) using a CALCOMP Model 665 plotter. They were based on a standard state of unity activity of the solids at 1 bar and temperatures of 100°C, 200°C and 300°C. Equilibrium constant values from 1 to 500 bars at the temperatures of interest in this research do not show any significant change, so that the diagrams can be used for pressures up to approximately 500 bars. The activity of water was considered constant with a value of unity in all calculations, since it departs insignificantly from unity in most natural aqueous solutions at pressures below 500 bars and temperatures below 300°C (Helgeson 1969b).

Thermodynamic data do not exist on chlorites with a composition similar to the ones found in the Mayflower igneous rocks. Mg-chlorite was then chosen to represent the Mayflower chlorite. As a result the phase boundaries with clinochlore are only an approximation of the true equilibrium relationships of the Mayflower chlorite and may be misleading in case the account of iron in the thermochemical data causes considerable shift of those boundaries.

Initial solution

Nash (1973) recognized veinlets with "a distinctive structure, mineralogy and fluid inclusions" in the Mayflower stock rocks that he believed to be earlier than the Mayflower ore zone. Some fluid inclusions in quartz crystals from these veinlets revealed high salinity

content (approximately 35 wt%) and were found to contain halite, sylvite, anhydrite and hematite as the most important daughter minerals. Nash estimated 350° ± 50°C as the filling temperatures for these high salinity inclusions.

Halite- and sylvite-bearing inclusions were observed, but inclusions containing these two minerals together were not seen. Phase diagram for the simple system NaCl-KCl-H_2O (Roedder 1971) indicates that at 25°C halite and sylvite coexist for solution compositions of 21 wt% NaCl and 11 wt% KCl. These values, evidently, do not represent the true univariant point at that temperature, since chloride complexes were excluded from the ideal system. In any case, departures from the univariant conditions are very likely to occur in natural environments. Therefore, if solutions capable of precipitating either halite or sylvite were trapped in some Mayflower veinlets, small deviations in the relative proportions of NaCl and KCl could account for this selectiveness. Nonetheless, the NaCl/KCl ratio may not have deviated significantly from 2 in the overall chemical composition of the aqueous solutions at that early hydrothermal stage. Consequently, fluid inclusions characterized by 35 wt% salinity should contain approximately 5.3 molal NaCl and 2.2 molal KCl if these chlorides are mostly responsible for the total salinity. More realistic values should add an estimated error as to have 5.3 ± 0.7 m NaCl and 2.2 ± 1.3 m KCl.

These molalities represent upper limits for the concentrations of NaCl and KCl in the hydrothermal alteration of the Mayflower Mine rocks. The resulting high ionic strength places this early solution beyond treatment with the available models for solution chemistry.

However, the geological setting of the Mayflower pluton indicates that water solutions in equilibrium with the surrounding country rocks flowed into the pluton as it fractured, causing the dilution of the early brine. Nash (1973) arrived at the same conclusion based upon his studies on fluid inclusions in quartz and sphalerite crystals present in the Mayflower, Pearl and Number Three veins. In similar geologic environments, oxygen isotope studies (Taylor 1974) have indicated δO^{18} values with progressive O^{18} depletion from the interior to the margins of some stocks, suggesting interaction of meteoric waters with the pluton rocks. Furthermore, constraints imposed by equilibrium relationships of the alteration assemblages at 300°C (the lower filling temperature limit for the high salinity inclusions) required a dilution of the early solutions (Villas et al. in preparation). These chemical constraints led to an initial solution composition (Table 11) in which chlorine was the ion chosen for electrical neutrality adjustments. Distribution of these species among their most important complexes (Table 12) was done by a computer program (DIST) described in Appendix F. The pH of the solution was assumed to be 4.5 to prevent the precipitation of montmorillonite in any appreciable amount as field observations demanded.

Phase stability relationships

Two broad zonings were apparent from the major mineral distribution patterns: 1) one lateral, characterized by both an increase of the K-feldspar, kaolinite and quartz abundances and a decrease of andesine, biotite and chlorite towards the main veins and 2) one vertical, characterized by major deposition of K-feldspar, anhydrite, pyrite and

TABLE 11

ESTIMATED INITIAL SOLUTION COMPOSITION OF THE

MAYFLOWER HYDROTHERMAL SYSTEM

Species	Total Molality
AL+++	.100000E-08
K+	.250000E+01
NA+	.320000E+01
CA++	.370000E-02
MG++	.370000E-04
FE++	.120000E-06
CU+	.100000E-01
H4SIO4	.114800E-01
S--	.500000E-02
SO4--	.500000E-01
CO3--	.100000E-02
CL-	.440000E+01
OH-	.295121E-06
H+	.316228E-04

NOTE: The table follows the format of a computer print-out.

TABLE 12

INITIAL SOLUTION COMPOSITION AT 300°C AFTER

PARTITIONING AMONG MOST IMPORTANT COMPLEXES

Species	Molality	Activity
AL+++	.63591E-16	.88007E-19
K+	.21058E+01	.35548E+00
NA+	.22653E+01	.53877E+00
CA++	.36842E-02	.58279E-04
MG++	.36104E-04	.14082E-05
FE++	.12000E-06	.18983E-08
FE+++	.16941E-18	.23446E-21
CU+	.31451E-11	.41718E-12
CU++	.48312E-17	.76424E-19
H4SIO4	.11480E-01	.11480E-01
S--	.28255E-06	.22872E-08
SO4--	.46544E-02	.14893E-04
CO3--	.30020E-13	.15914E-15
CL-	.43040E+01	.72654E+00
OH-	.14462E-05	.29512E-06
H+	.65713E-04	.31623E-04
H2O	.55508E+02	.10000E+01
AL(OH)++	.82289E-09	.13017E-10
AL(OH)4-	.17711E-09	.42123E-10
KCL	.37161E+00	.10282E+01
KSO4-	.22595E-01	.46109E-02
NACL	.93471E+00	.25862E+01
CASO4	.15722E-04	.43500E-04
CUCL2-	.23258E-04	.55315E-05
CUCL3--	.99767E-02	.31923E-04
H3SIO4-	.65112E-07	.15486E-07
HSO4-	.22735E-01	.54072E-02
HS-	.18601E-04	.37959E-05
H2S	.49811E-02	.13782E-01
HCO3-	.44740E-06	.12072E-06
H2CO3	.99955E-03	.27656E-02
HCL	.14430E-03	.39926E-03
MG(OH)+	.89617E-06	.21314E-06
CA(OH)+	.11461E-06	.27259E-07

NOTE: The table follows the format of a computer print-out.

kaolinite below the 2,200' level whereas calcite, quartz and biotite were more abundantly precipitated on the upper levels.

These zonings express variations in the relative proportions of the major mineral constituents which are basically present all over the sampled vertical section of the mine. Moreover, the zonings reflect differences in the chemical and/or physical conditions of the Mayflower hydrothermal environment. The chemical differences are difficult to ascertain quantitatively. Changes in the solution chemistry can be estimated in terms of individual aqueous species variations but require information on the ferrous to ferric iron ratio in the rocks and minerals as well as computed reaction path in order to understand the solution evolution in time and space. Such provisions were not sought during the course of this research and an interpretation of the zonings based on quantitative variation of the solution chemistry was not possible. Some qualitative chemical aspects, however, could be deduced. The increase of the pH of the solutions with distance from the major veins is perhaps the most evident, as it is indicated by larger amounts of alteration minerals in zones surrounding the veins (Fig. 37). Similarly evident was the greater availability of sulfate ions in the solutions circulating through the rocks of the lower levels as opposed to their greater carbonate contents while moving through rocks on the upper levels. The physical differences, in turn, relate especially to temperature and CO_2 pressure, the latter controlling particularly the carbonate deposition.

On the other hand, an attempt was made to explain the mineral distribution patterns based on purely temperature changes as fluid flow

Fig. 37. Distribution of overall mass of alteration products in relation to the mass of unaltered rocks over a N-S 670-meter cross-section of the Mayflower Mine.

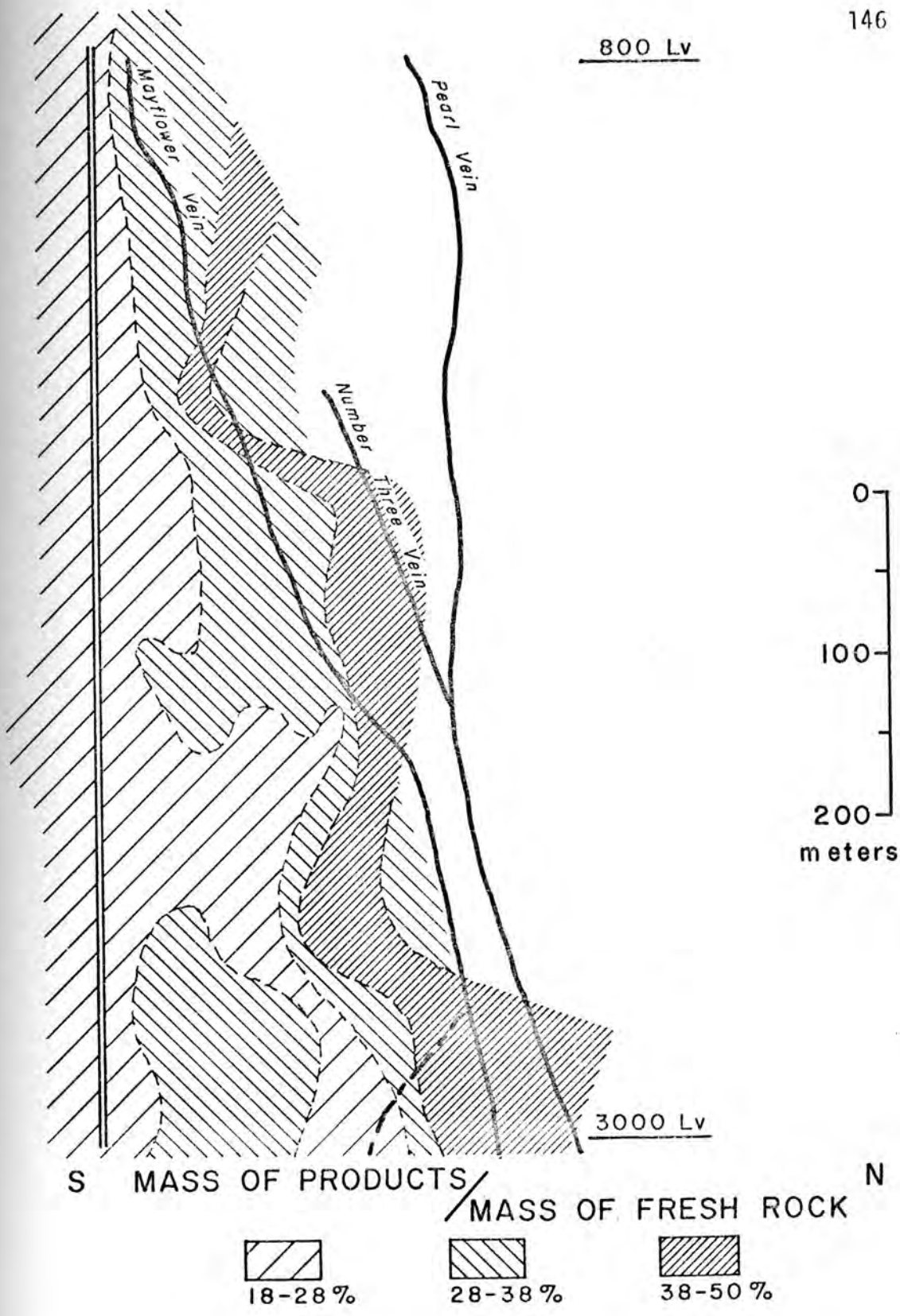
800 Lv
Mayflower Vein
Pearl Vein
Number Three Vein
0
100
200
meters
3000 Lv
S
N
MASS OF PRODUCTS / MASS OF FRESH ROCK
18-28 %
28-38 %
38-50 %

in the Mayflower hydrothermal system decreased. The interpretation rested upon the approximation that the sampled volume of rock was subjected to a sequence of isothermal conditions and that changes in the complex ion stabilities were not accounted for. The ensuing discussion, therefore, deals with the effects resulting from decreasing the temperature of the hydrothermal system with provisions at each isotherm for the chemical changes of the solutions as their reactions with the rocks progressed. This implies that, for the purposes of interpreting the alteration assemblages, the solution composition is constant. Qualitative chemical variations, however, are pointed out whenever supported by geological evidence.

The stability relations of the major mineral constituents of the altered igneous rocks of the Mayflower Mine are shown in a series of activity diagrams (Figs. 38 through 42) representing various chemical systems at different temperatures. The small hexagon drawn on the diagrams stands for the initial solution composition (at this point no ion complexing was considered) whereas the arrows suggest possible trends followed by the solutions as reactions with rocks decreased H+. The encircled areas on the diagrams, in turn, are intended to express the uncertainties of the solution composition in equilibrium with the minerals in the stability fields.

The system MgO-FeO-K_2O-Al_2O_3-SiO_2-HCl-H_2O. Biotite, microcline, quartz, albite, anhydrite, calcite and pyrite were considered to be the representative product assemblage of the hydrothermal alteration of the igneous wall rocks at 300°C.

The stability relations of phlogopite, Mayflower biotite (hereafter referred to as biotite), annite, Mg-montmorillonite and microcline (Fig. 38A) are presented as functions of the $\log(a_{Mg^{++}}/a^2_{H^+})$ and $\log(a_{Fe^{++}}/a^2_{H^+})$. Additional minerals considered in the equilibrium calculations, but not appearing in the diagram at 300°C, were kaolinite, K-montmorillonite, muscovite and Mg-chlorite. The observed alteration mineralogy (microcline, biotite, Mg-montmorillonite and quartz) requires fluids with the indicated composition. Equilibrium with quartz is implicit since the diagrams were constructed at quartz saturation conditions. The equilibrium with Mg-montmorillonite, however, must have been brief as its small amounts as an alteration product imply.

As the solution reacted with the rocks, H^+ was consumed and the solution moved toward point A at a 45° slope within the biotite stability field. As the temperature dropped to 200°C, the former mineral assemblage was preserved except for microcline which gave way to muscovite (Fig. 38B). Under this new temperature condition the solution was in equilibrium with Mg-montmorillonite and muscovite (sericite). Neither of these two minerals was precipitated in large amounts, although sericite was found to be locally abundant in the vicinity of the major veins. Similar chemical variations for the solutions may have happened at this temperature to allow for the precipitation of biotite as the solutions reacted with the rocks. Further decrease in the temperature to 100°C stabilized kaolinite over the other phases (Fig. 38C) and the solutions might have been directed towards the biotite field as H+ was consumed.

Figure 39A relates to the same chemical system but it is now

Fig. 38. Phase stability relations in the system MgO-FeO-K_2O-Al_2O_3-SiO_2-H_2O as a function of the log $(a_{Mg^{++}}/a^2_{H^+})$ and log $(a_{Fe^{++}}/a^2_{H^+})$. A. Phlogopite-Biotite-Annite-Mg-montmorillonite-Microcline at 300°C. B. Phlogopite-Biotite-Annite-Mg-Montmorillonite-Muscovite at 200°C. C. Phlogopite-Biotite-Annite-Kaolinite at 100°C.

Fig. 39. Phase stability relations in the system MgO-FeO-K_2O-Al_2O_3-SiO_2-HCl-H_2O as a function of the log $(a_{Mg^{++}}/a^2_{H^+})$ and log (a_{K^+}/a_{H^+}). A. Chlorite-Phlogopite-Biotite-Annite-Mg-montmorillonite at 300°C. B. Chlorite-Phlogopite-Microcline-Muscovite-K-montmorillonite-Mg-montmorillonite at 200°C. C. Chlorite-Phlogopite-Microcline-Muscovite- Kaolinite at 100°C.

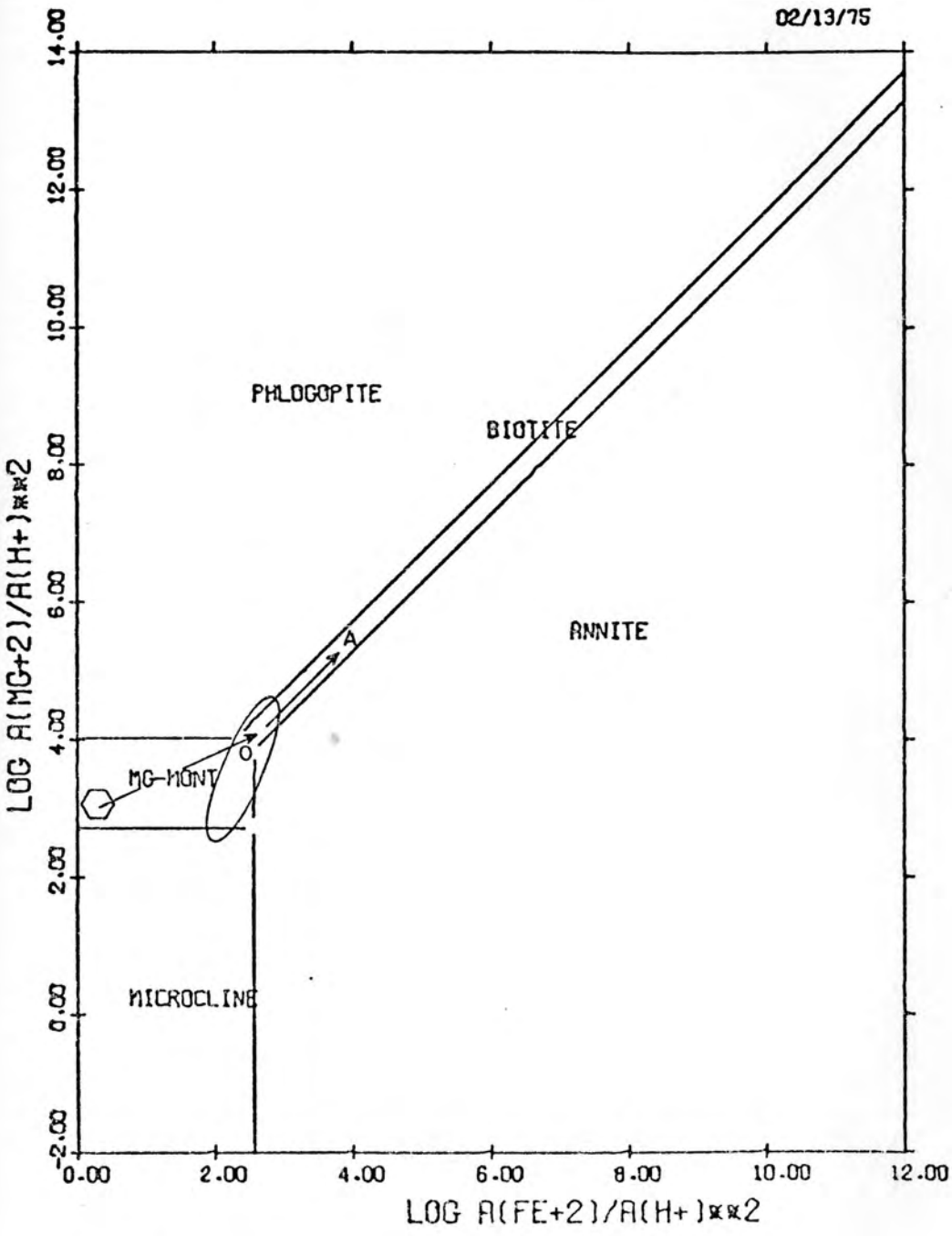

FIGURE 38A .SYSTEM MGO-FEO-K2O-AL2O3-SIO2-HCL-H2O
T = 300.C P = 1.0 BAR A(H2O) = 1.0
LOG A(H4SIO4) = -1.94 (QTZ. SAT.)
LOG A(K+)/A(H+) = 4.0

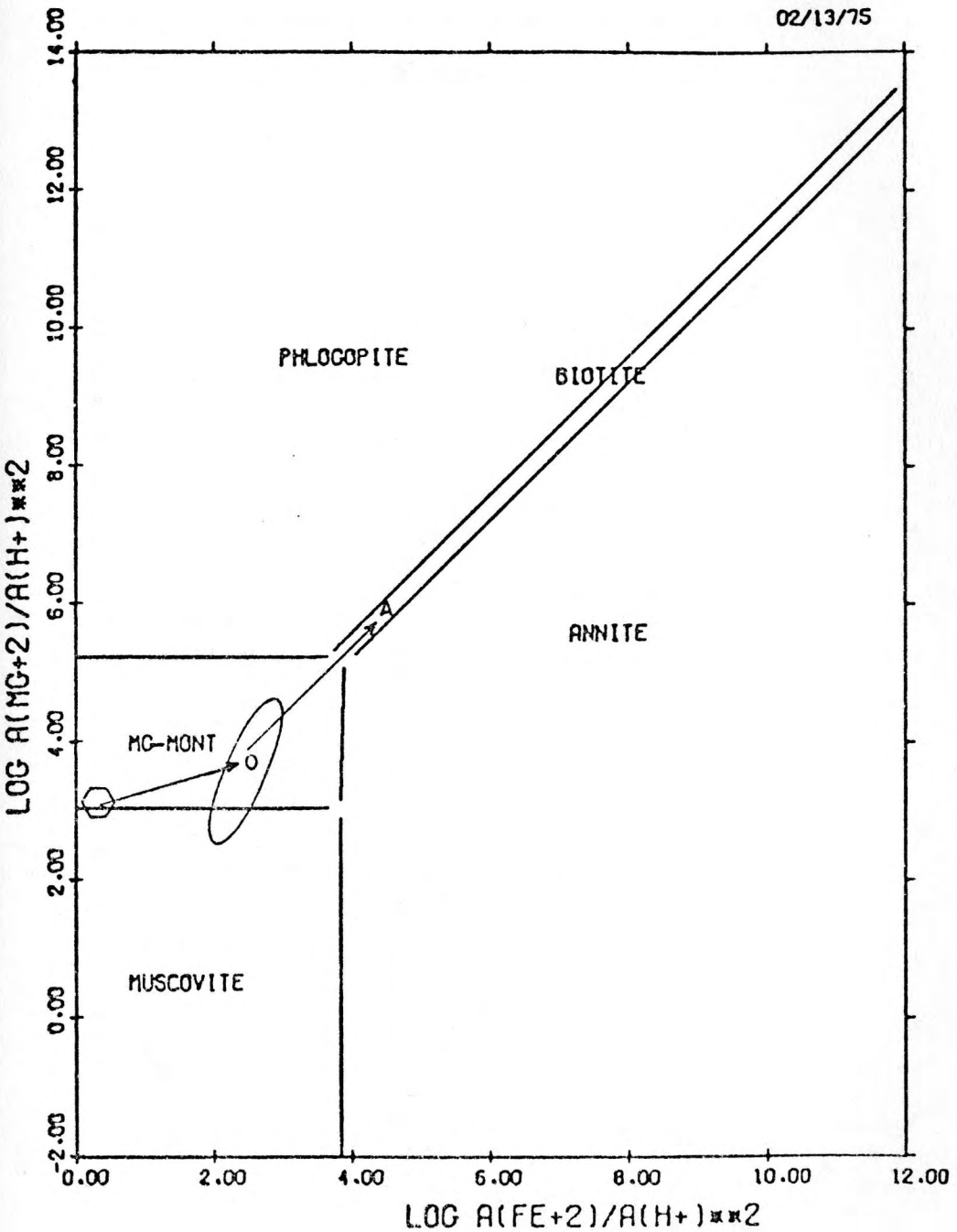

FIGURE 38B .SYSTEM MGO-FEO-K2O-AL2O3-SIO2-HCL-H2O
T = 200.C P = 1.0 BAR A(H2O) = 1.0
LOG A(H4SIO4) = -2.35 (QTZ. SAT.)
LOG A(K+)/A(H+) = 4.0

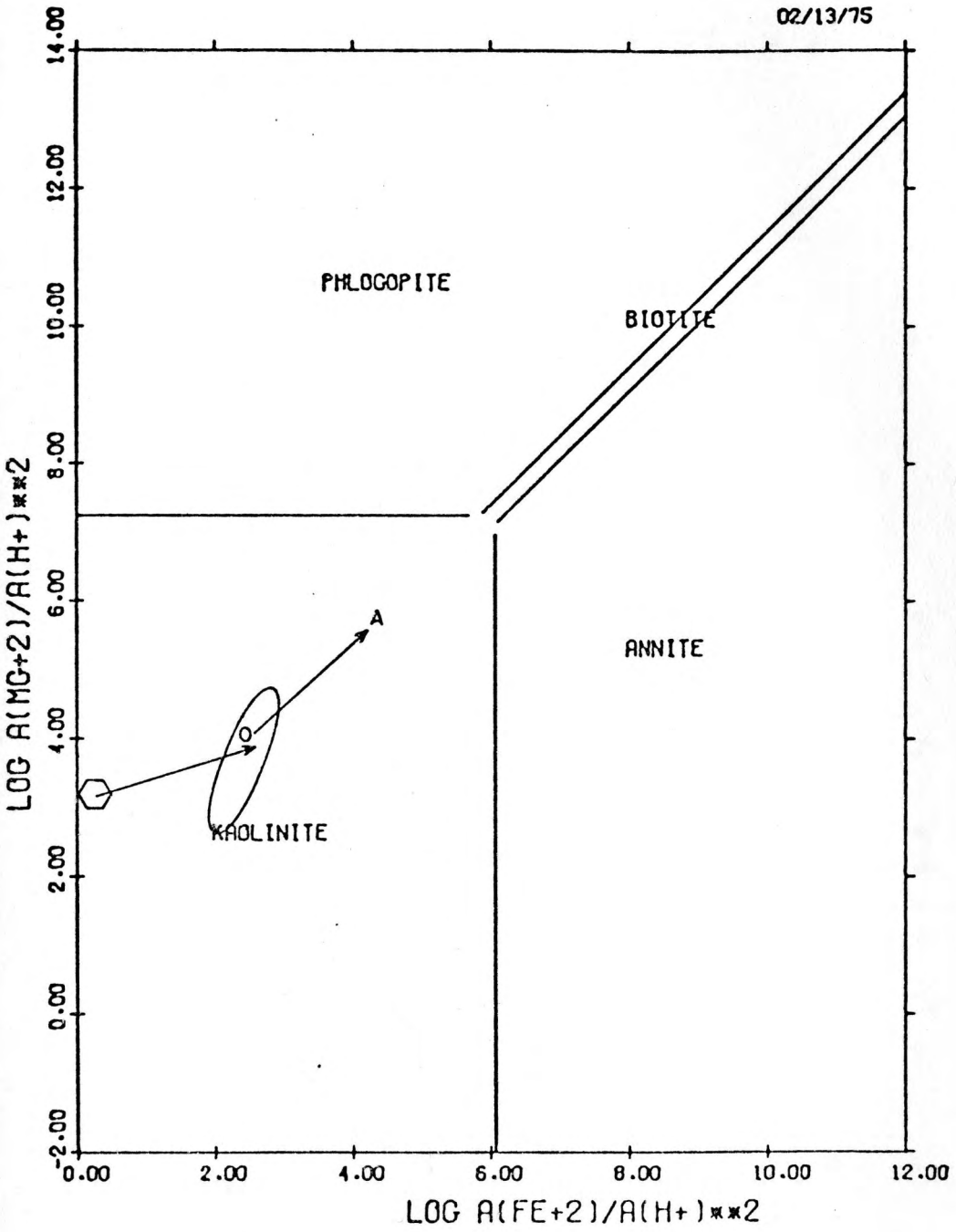

FIGURE 38C .SYSTEM MGO-FEO-K2O-AL2O3-SIO2-HCL-H2O
T = 100.C P = 1.0 BAR A(H2O) = 1.0
LOG A(H4SIO4) = -3.08 (QTZ. SAT.)
LOG A(K+)/A(H+) = 4.0

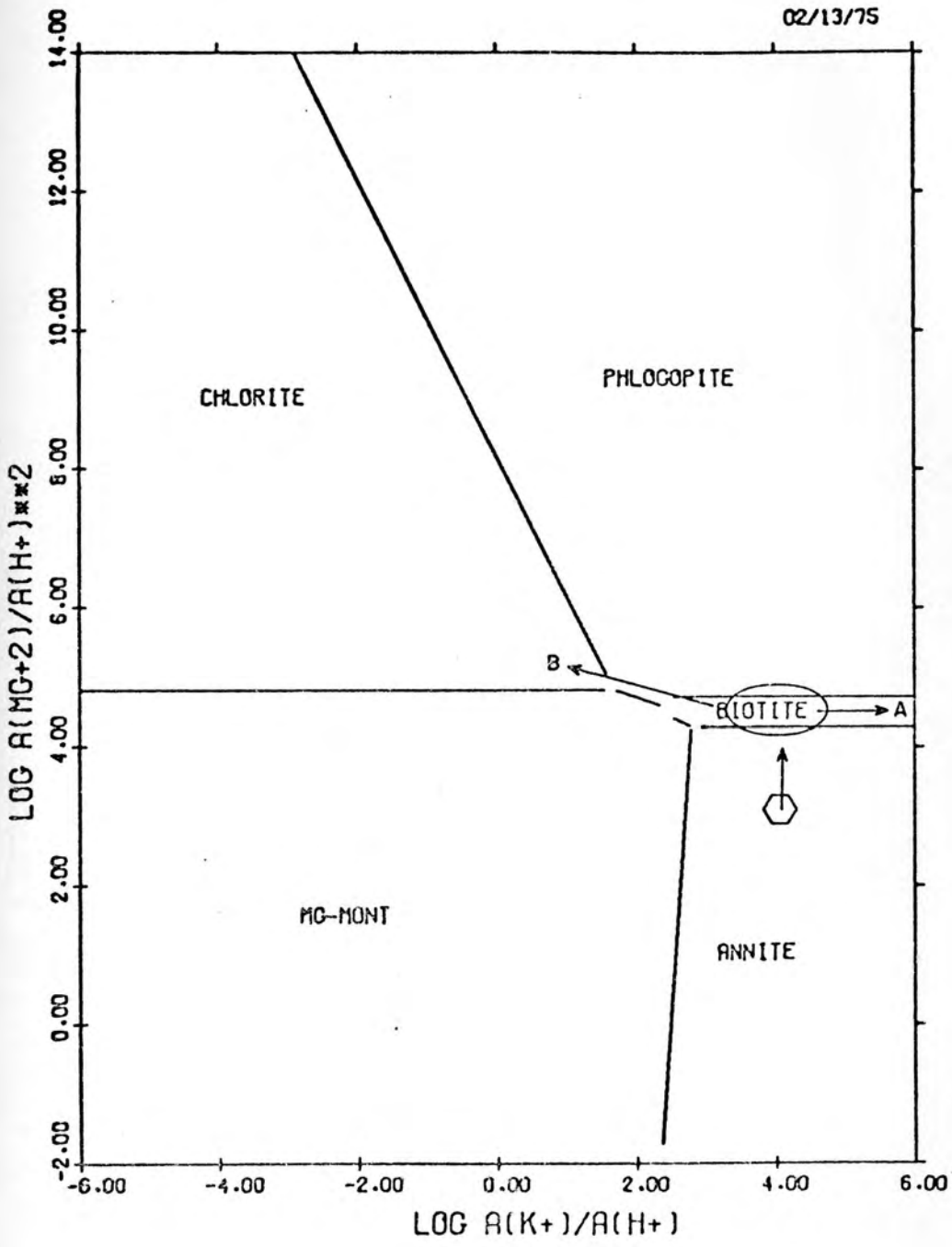

FIGURE 39A .SYSTEM MGO-K2O-FEO-AL2O3-SIO2-HCL-H2O

T = 300.C P = 1.0 BAR A(H2O) = 1.0

LOG A(H4SIO4) = -1.94 (QTZ. SAT.)

LOG (A(FE+2)/A(H+)**2) = 3.0

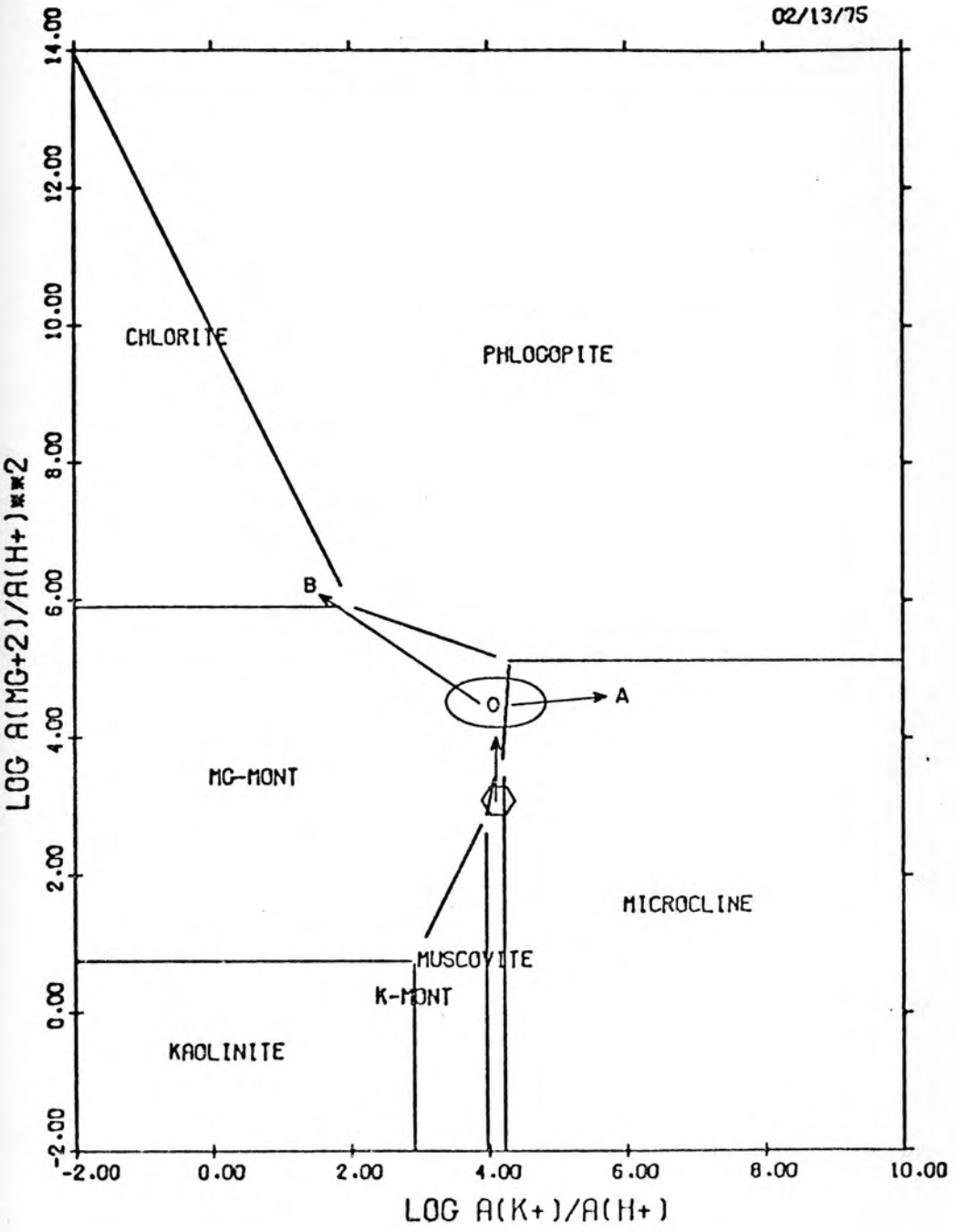

FIGURE 39B .SYSTEM MGO-K2O-FEO-AL2O3-SIO2-HCL-H2O

T = 200.C P = 1.0 BAR A(H2O) = 1.0

LOG A(H4SIO4) = -2.35 (QTZ. SAT.)

LOG (A(FE+2)/A(H+)**2) = 3.0

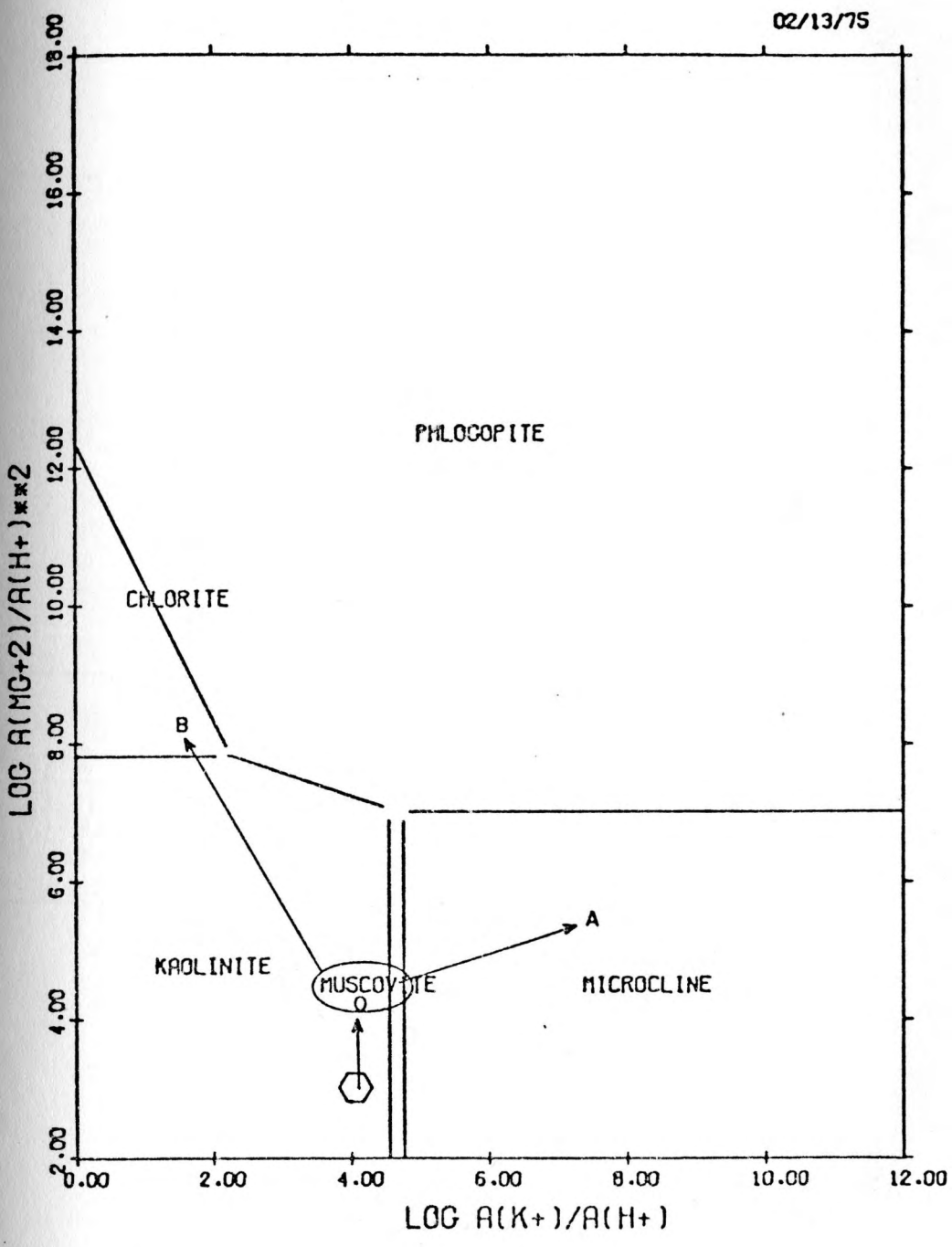

FIGURE 39C .SYSTEM MGO-K2O-FEO-AL2O3-SIO2-HCL-H2O

T = 100.C P = 1.0 BAR A(H2O) = 1.0

LOG A(H4SIO4) = -3.08 (QTZ. SAT.)

LOG (A(FE+2)/A(H+)**2) = 3.0

represented as a function of the $\log(a_{Mg^{++}}/a^2_{H^+})$ and $\log(a_{K^+}/a_{H^+})$ at a $\log(a_{Fe^{++}}/a^2_{H^+})$ equal to 3.0 and shows that the solutions might have moved either within the biotite field (from 0 to A) or towards the chlorite field (from 0 to B) at 300°C. In the first case the consumption of H+ due to rock-solution interaction should have been buffered by a decrease in the $a_{Mg^{++}}$ as to maintain the $a_{Mg^{++}}/a^2_{H^+}$ constant and, as a consequence, restrict the solution to the biotite field. In the second case the consumption of H+ increased the $a_{Mg^{++}}/a^2_{H^+}$ ratio but, at the same time, a_{K^+} must have decreased at a faster rate than a_{H^+} in order to move the solutions towards the chlorite field. Most likely, however, chlorite was not a stable phase in the Mayflower rocks at 300°C. Mg-montmorillonite and microcline started precipitating together with quartz at 200°C but biotite was left out of equilibrium (Fig. 39B). Chlorite may have become a stable phase if similar chemical variations of the solutions (from 0 to B) prevailed. Otherwise microcline kept precipitating as the solutions reacted with the rocks (from 0 to A) with consumption of H+ being buffered by decrease of $a_{Mg^{++}}$. At 100°C a similar picture might have existed for the trend of the solutions, although kaolinite and muscovite formed at the expense of Mg-montmorillonite (Fig. 39C).

The system K_2O-Na_2O-Al_2O_3-SiO_2-HCl-H_2O. Kaolinite, K-montmorillonite, Na-montmorillonite, microcline, low albite and muscovite were considered in the equilibrium calculations for this system at 300°C (Fig. 40A). The composition of the solutions was described with respect to the $\log(a_{Na^+}/a_{H^+})$ and $\log(a_{K^+}/a_{H^+})$. The fluids in equilibrium with microline and low albite had to have a composition indicated on the

diagram. As the solution reacted with the rocks it may have continued depositing quartz, microcline and/or low albite as the arrows on the diagram suggest. The trend O-A is characterized by a 1:1 slope and can be explained by the simple consumption of H+. Quartz, microcline and low albite would then be the equilibrium assemblage. Equilibrium with only microcline and quartz or with only low albite and quartz would have required the solutions to follow trends such as O-B, for which the a_{K+} increased at a faster rate than a_{Na+}, or O-C, for which the a_{Na+} increased at a faster rate than a_{K+}, respectively.

At 200°C no significant change was observed, except that the solution composition was almost totally in the microcline stability field (Fig. 40B). Again, the suggested solution trends would have precipitated only quartz, microcline and low albite under similar solution chemistry variations indicated for 300°C. At this time, however, trends O-A and O-B would have precipitated only quartz and microcline whereas trend O-C would have also precipitated low albite.

As the temperature fell to 100°C, the solution equilibrated with Na-montimorillonite, muscovite and kaolinite, besides microcline (Fig. 40C). The indicated trend of the solutions might have produced the same mineral assemblages as for the last case.

The system $CaO-Na_2O-SiO_2-Al_2O_3-HCl-H_2O$. The stability relations of kaolinite, Ca-montmorillonite, Na-montmorillonite, low albite, anorthite and the Mayflower plagioclase (hereafter referred to as plagioclase) are depicted in the system at 300°C (Fig. 41A) as functions of the log $(a_{Ca}{}^{++}/a^2{}_{H}{}^{+})$ and log $(a_{Na}{}^{+}/a_{H}{}^{+})$. Included in the diagram are the surface boundaries of anhydrite and calcite corresponding to the

Fig. 40. Phase stability relations in the system K_2O-Na_2O-Al_2O_3-SiO_2-HCl-H_2O as a function of the log (a_{Na+}/a_{H+}) and log (a_{K+}/a_{H+}). A. Low-albite-microcline-Na-montmorillonite-K-montmorillonite-kaolinite at 300°C. B. Low-albite-microcline-muscovite-K-montmorillonite-Na-montimorillonite-kaolinite at 200°C. C. Low-albite-microcline-muscovite-Na-montmorillonite-kaolinite at 100°C.

Fig. 41. Phase stability relations in the system CaO-Na_2O-SiO_2-Al_2O_3-HCl-H_2O as a function of the log (a_{Ca++}/a^2_{H+}) and log (a_{Na+}/a_{H+}). A. Anorthite-plagioclase-low-albite-Na-montmorillonite-Ca-montmorillonite-kaolinite at 300°C. B. Anorthite-plagioclase-low-albite-Na-montmorillonite-Ca-montmorillonite-kaolinite at 200°C. C. Ca-montmorillonite-low-albite-Na-montmorillonite-kaolinite at 100°C.

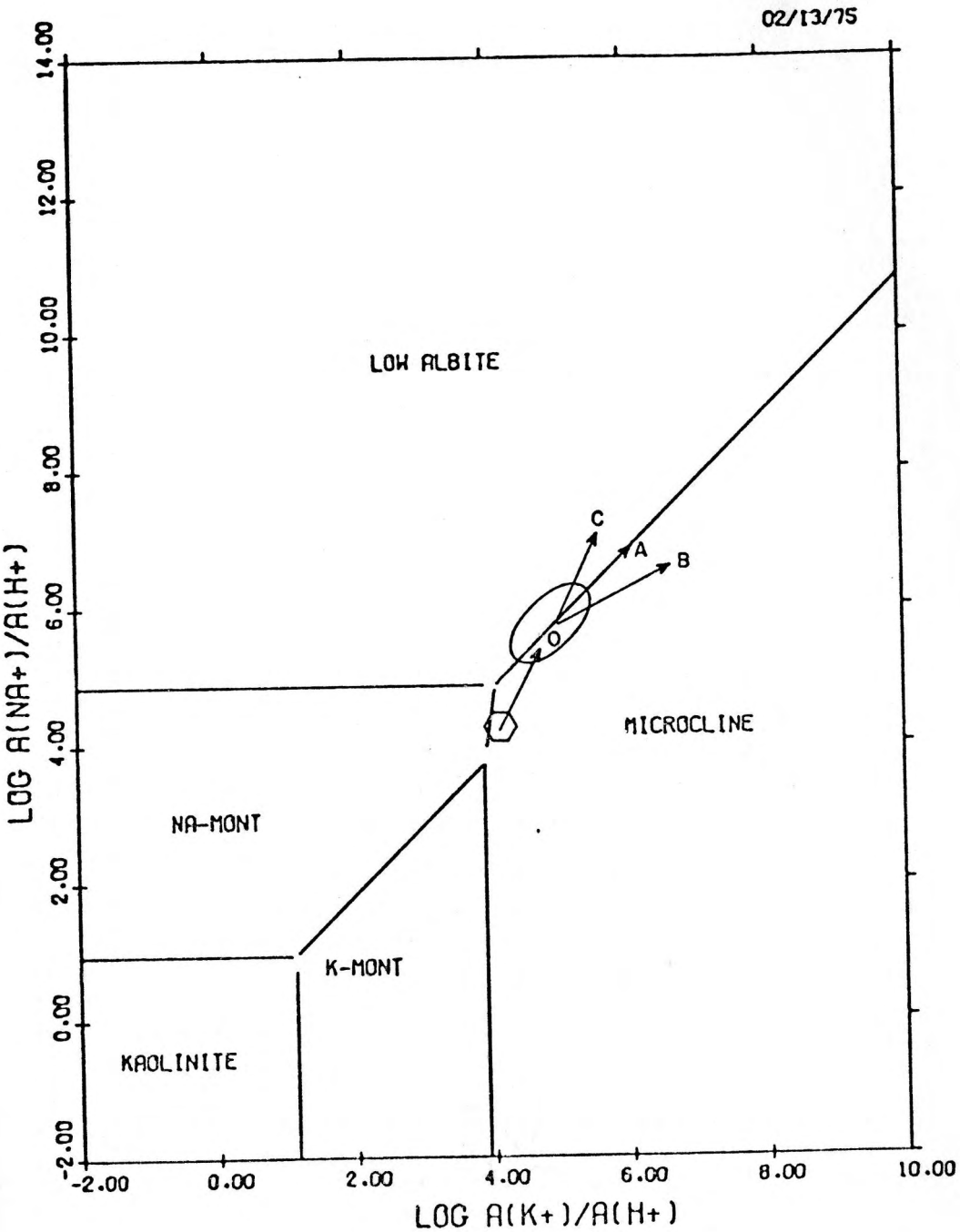

FIGURE 40A .SYSTEM K2O-NA2O-AL2O3-SIO2-HCL-H2O
T = 300.C P = 1.0 BAR A(H2O) = 1.0
LOG A(H4SIO4) = -1.94 (QTZ. SAT.)

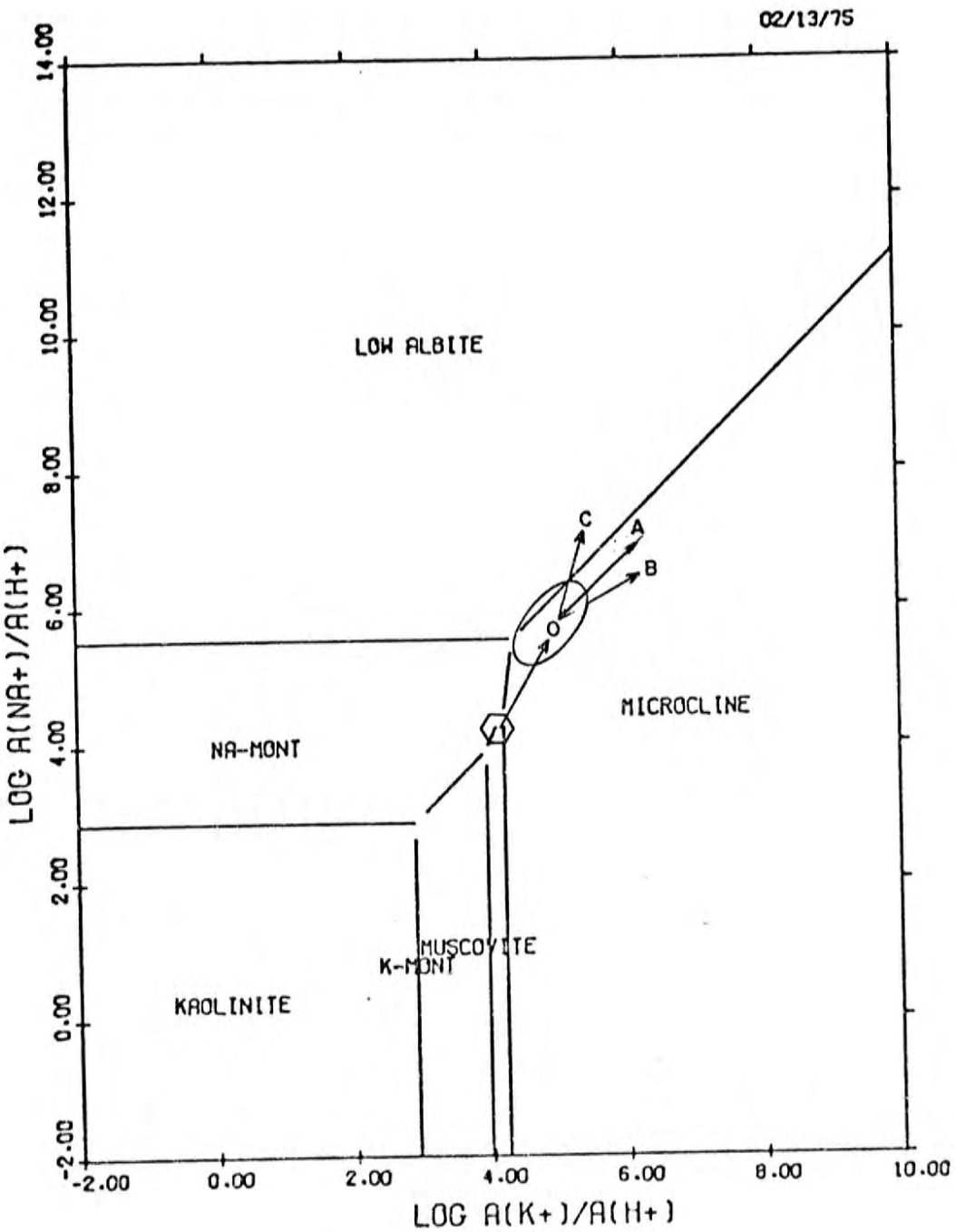

FIGURE 40B .SYSTEM K2O-NA2O-AL2O3-SIO2-HCL-H2O
T = 200.C P = 1.0 BAR A(H2O) = 1.0
LOG A(H4SIO4) = -2.35 (QTZ. SAT.)

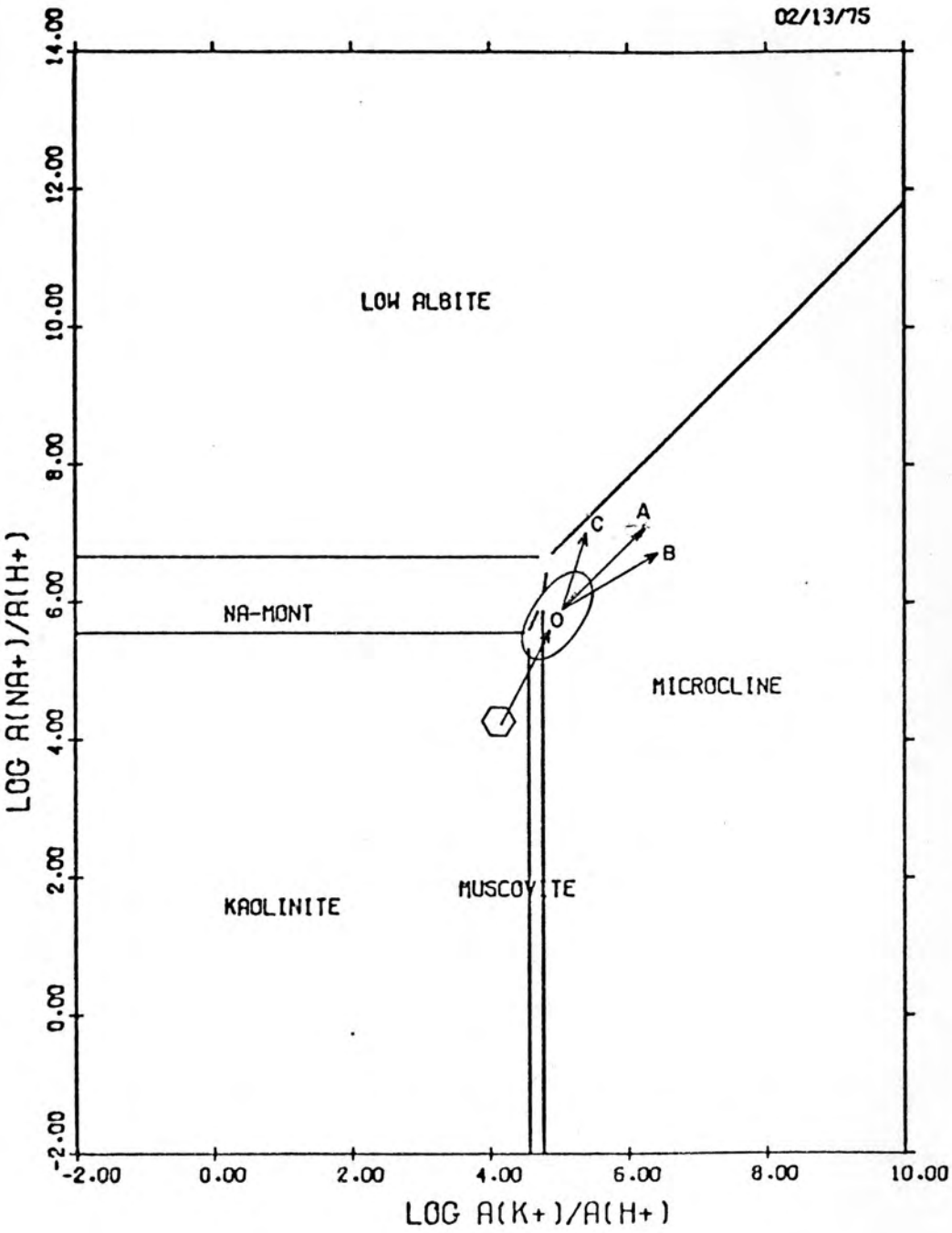

FIGURE 40C .SYSTEM K2O-NA2O-AL2O3-SIO2-HCL-H2O
T = 100.C P = 1.0 BAR A(H2O) = 1.0
LOG A(H4SIO4) = -3.08 (QTZ. SAT.)

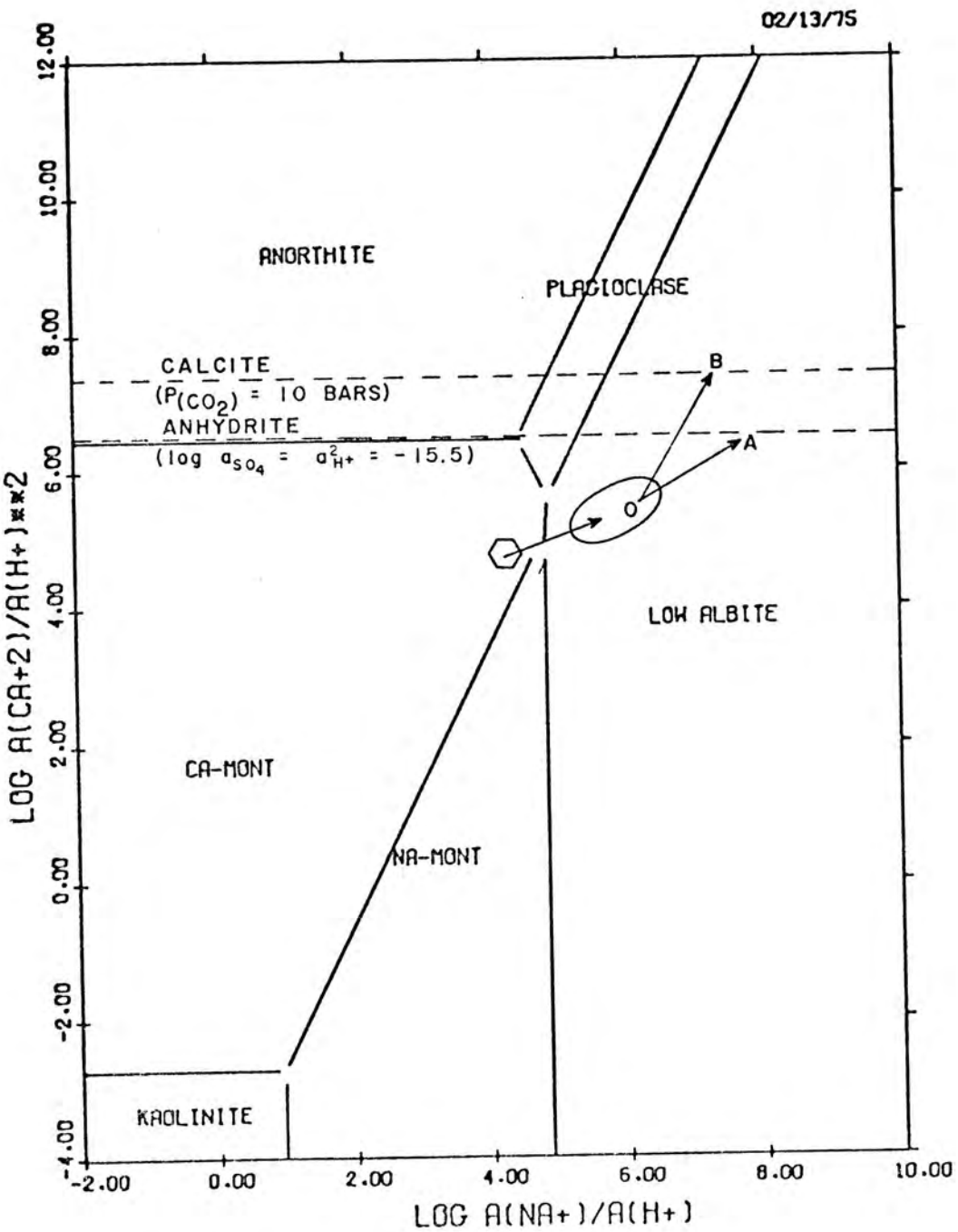

FIGURE 41A .SYSTEM CAO-NA2O-SIO2-AL2O3-HCL-H2O
T = 300.C P = 1.0 BAR A(H2O) = 1.0
LOG A(H4SIO4) = -1.94 (QTZ. SAT.)

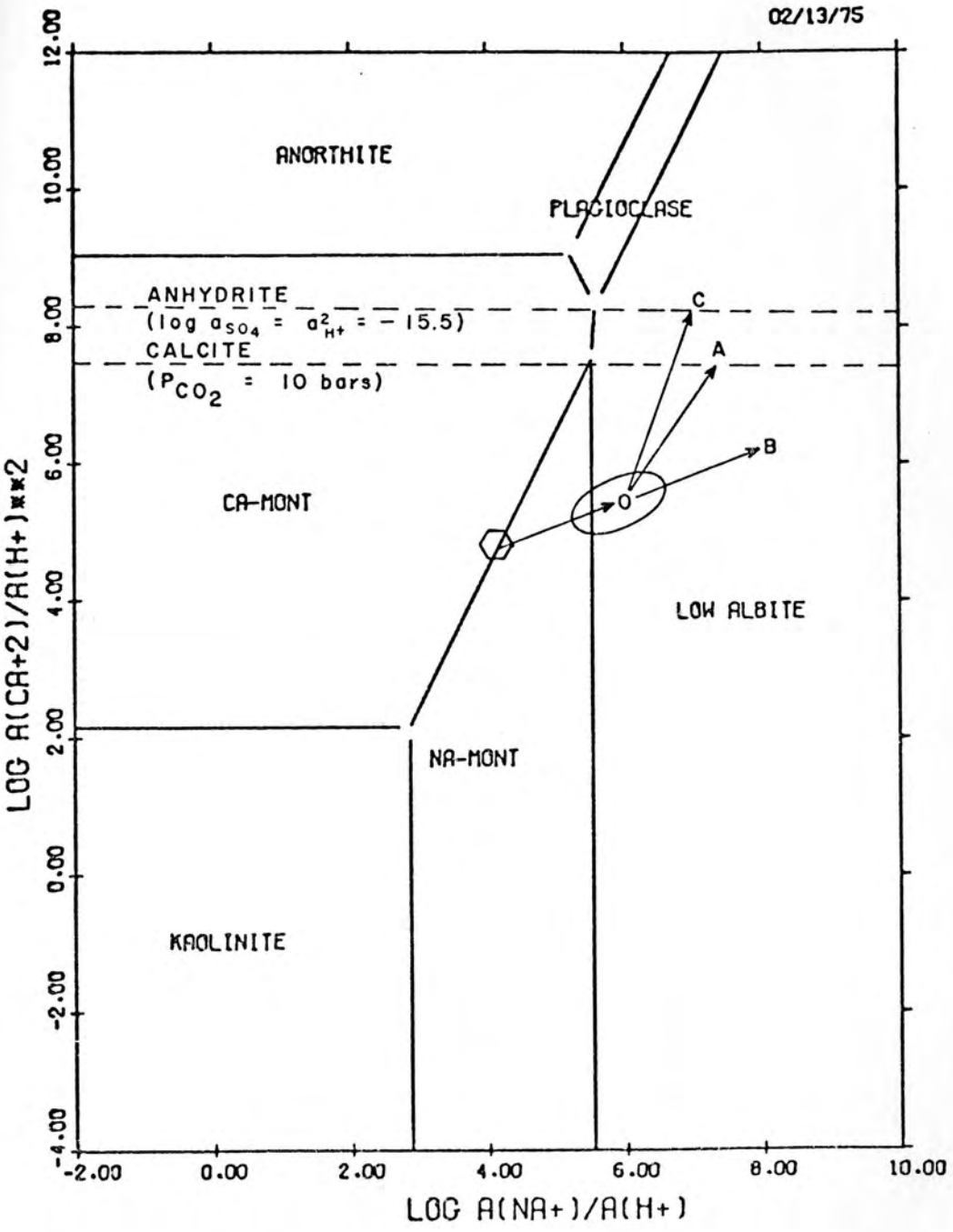

FIGURE 41B .SYSTEM CAO-NA2O-SIO2-AL2O3-HCL-H2O

T = 200.C P = 1.0 BAR A(H2O) = 1.0

LOG A(H4SIO4) = -2.35 (QTZ. SAT.)

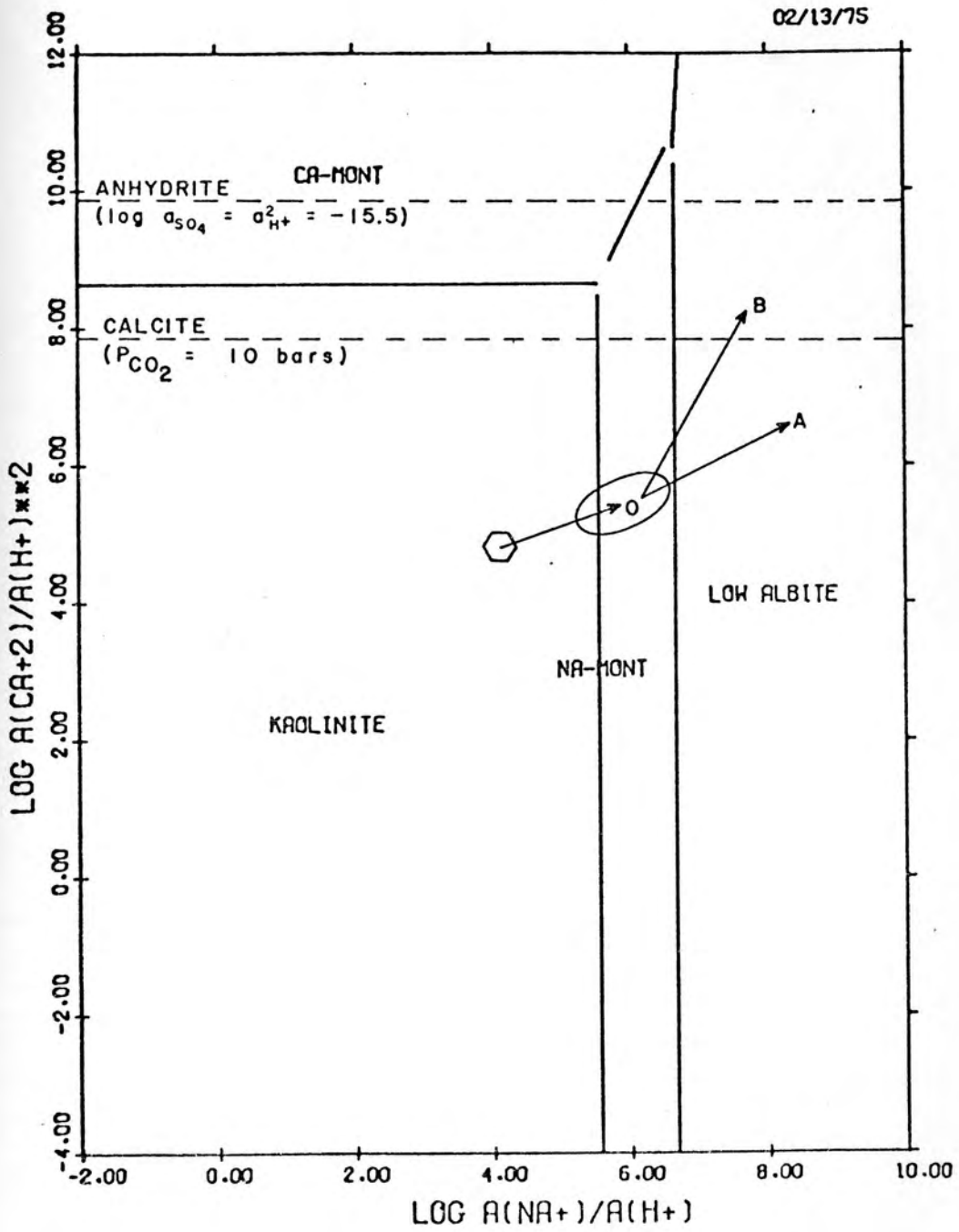

FIGURE 41C .SYSTEM CAO-NA2O-SIO2-AL2O3-HCL-H2O

T = 100.C P = 1.0 BAR A(H2O) = 1.0

LOG A(H4SIO4) = -3.08 (QTZ. SAT.)

equilibrium equations below:

$$CaSO_4 \rightleftarrows Ca^{++} + SO_4^{=}$$

for which

$$\log K_{CaSO_4} = \log(a_{Ca^{++}}/a^2_{H^+}) + \log(a_{SO_4^{=}}\ a^2_{H^+})$$

and

$$CaCO_3 + 2H^+ \rightleftarrows Ca^{++} + CO_2 + H_2O$$

for which

$$\log K_{CaCO_3} = \log(a_{C\ ^{++}}/a^2_{H^+}) + \log\ (\gamma_{CO_2}\ P_{CO_2})$$

The anhydrite boundary assumes a value of $\log\ (a_{SO_4^{=}}\ .\ a^2_{H+})$ equal to -15.5 (Table 11), whereas the calcite boundary is for a CO_2 pressure of 10 bars. Fluid inclusion studies (Nash 1973) indicated 10 bars to be the prevailing CO_2 pressure in the Mayflower hydrothermal system. For γ_{CO_2} a value of 2.29 was used corresponding to a 3m NaCl solution (Helgeson 1969a).

Low albite is the only mineral in equilibrium with the solutions characterized by the indicated composition. As more reactant minerals (particularly plagioclase) were destroyed, the solutions may have moved towards the anhydrite boundary causing this mineral to be deposited aside with albite and quartz. Subsequent changes continued depositing anhydrite, quartz and albite, but may have directed the fluid composition towards stabilization of calcite which would then start precipitating.

The decrease of the temperature fo 200°C brought Na-montmorillonite into equilibrium with the solutions together with albite and quartz (Fig. 41B). Changes in the solution composition, as indicated

on the diagram, would first equilibrate with calcite and subsequently with anhydrite. A similar situation may have occurred at 100°C, although the solutions at this time were in equilibrium with kaolinite, Na-montmorillonite and quartz (Fig. 41C).

The sole effect of temperature decrease cannot explain the relative proportions of calcite and anhydrite on the upper and lower levels of the Mayflower Mine, despite the major deposition of anhydrite at 300°C and dominant precipitation of calcite below 200°C as inferred from the diagrams. The relative positions of the surface boundaries of these two minerals are also controlled by CO_2 pressure, pH and $SO_4^{=}$ activity. Accordingly, increases of CO_2 pressure would bring the calcite boundary to lower values of $\log(a_{Ca}{}^{++}/a^2{}_{H}{}^{+})$. Increases of the pH or decreases of $SO_4^{=}$ activity would move the anhydrite boundary to higher values of $\log(a_{Ca}{}^{++}/a^2{}_{H}{}^{+})$. Increases CO_2 pressures in the upper mine levels would cause calcite to dominate over anhydrite. Conversely, relatively lower CO_2 pressure and pH or relatively higher $SO_4^{=}$ activity may have prevailed on the lower levels to account for more abundant precipitation of anhydrite over calcite.

The system Cu_2S-FeS-H_2S-H_2SO_4-HCl-H_2O. Stability relations of pyrite, magnetite, chalcopyrite, bornite and covellite are represented in this system as functions of the $\log(a_{Cu^+}/a_{H^+})$ and the $\log(a_{Fe^{++}}/a^2{}_{H^+})$. Hematite and tenorite were additional minerals included in the equilibrium calculations but do not have stability fields in the diagrams. Among the stable phases, pyrite was the only mineral to occur in significant amounts in the igneous rocks of the mine. Magnetite,

however, was found to be particularly abundant in some veinlets transecting the wall rocks. The solutions precipitating pyrite and occasionally magnetite, therefore, should have been characterized by a relatively high H_2S activity (log a_{H_2S} higher than -3.0) to prevent hematite from being formed. Occasionally, however, hematite is present in some veinlets implying that the H_2S activity might have fluctuated at times.

At 300°C (Fig. 42A) the indicated solution composition was in equilibrium with pyrite and magnetite. If only the H+ comsumption accounted for the solution-rock interaction, the solutions should move approximately as shown by the arrow OB and would precipitate pyrite and magnetite. In general magnetite was more a reactant mineral than a product phase as indicated by its almost complete absence in the rocks of the lateral sampled on the 2,600' level and its relative increase away from the major veins. Consequently, the fluids should have preferentially moved towards the chalcopyrite field (from O to A). In this case the a_{Fe++}/a^2_{H+} should have increased at a slower rate (concomitant decrease of a_{Fe++} as H+ was being consumed) than the a_{Cu+}/a_{H+}. This may have been particularly true in the zones surrounding the main veins.

At 200°C (Fig. 42B) the solutions were in equilibrium with pyrite and chalcopyrite and may have been directed towards the bornite field as suggested by arrow OA. As the temperature fell to 100°C (Fig. 42C) bornite was the only mineral in equilibrium with the solutions. Bornite, however, does not occur in the Mayflower igneous rocks in any significant amount. This fact implies that at least at lower

Fig. 42. Phase stability relations in the system Cu_2S-FeS-H_2S-H_2SO_4-HCl-H_2O as a function of the $\log(a_{Fe^{++}}/a^2_{H^+})$ and $\log(a_{Cu^+}/a_{H^+})$. A. Magnetite-chalcopyrite-bornite-covelite-pyrite at 300°C. B. Magnetite-chalcopyrite-bornite-covelite-pyrite at 200°C. C. Chalcopyrite-bornite-covelite-pyrite at 100°C.

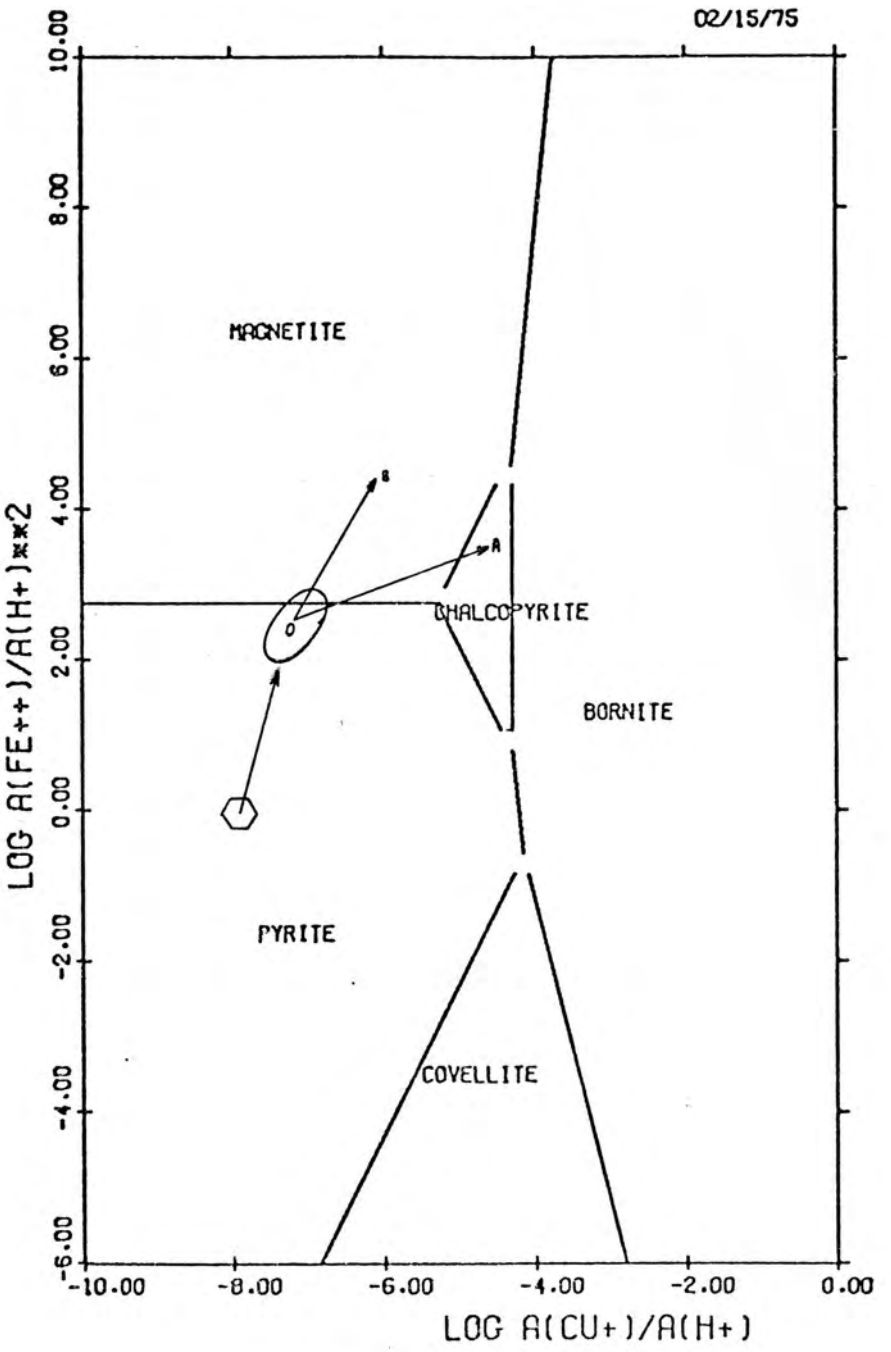

SYSTEM CU2S - FES -H2S - H2SO4 - HCL - H2O

TEMPERATURE = 300. DEG C. PRESSURE = 1 BAR

LOG ACTIVITY H2S = -2.50 , A(H2O) = 1.0

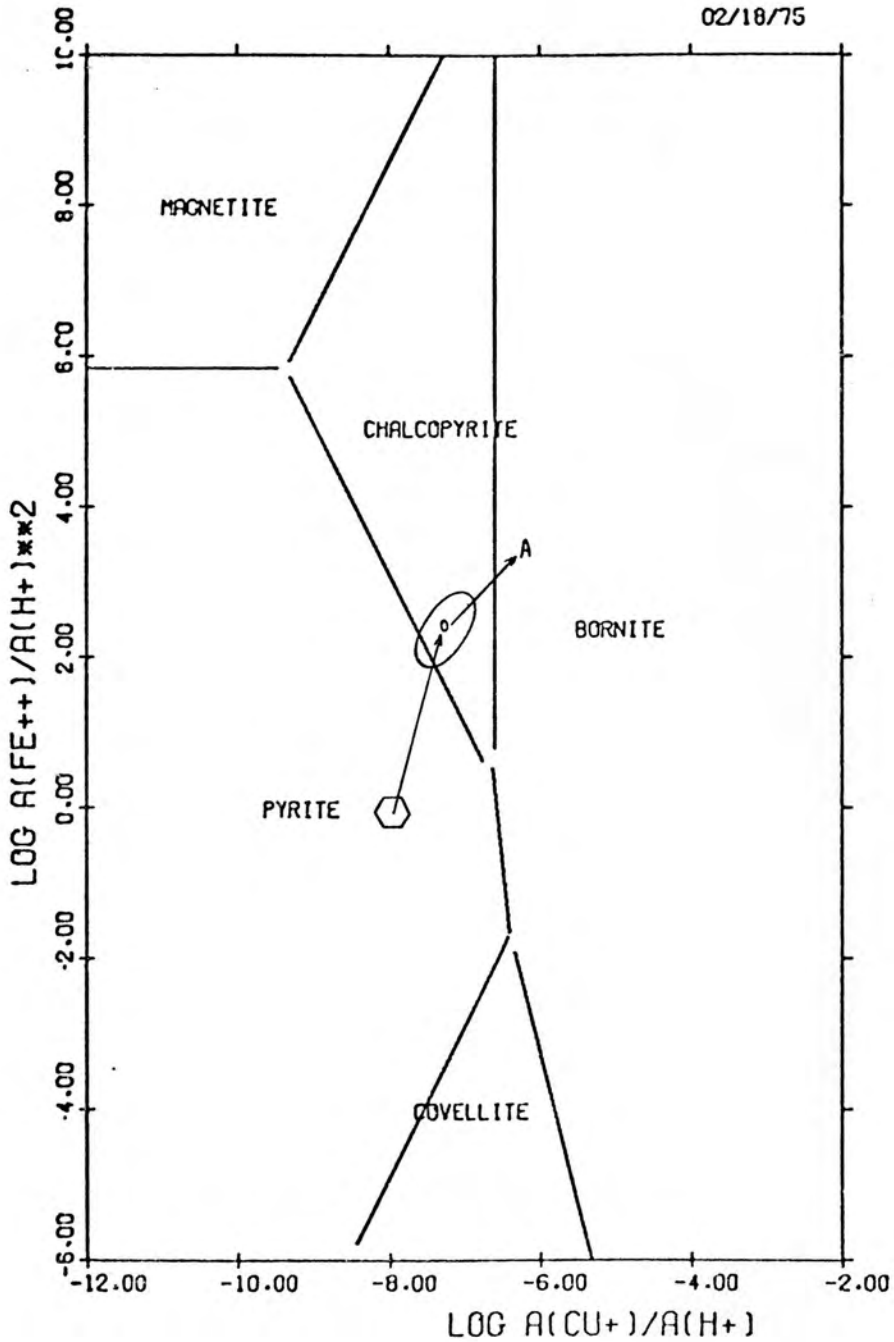

SYSTEM CU2S - FES -H2S - H2SO4 - HCL - H2O

TEMPERATURE = 200. DEG C. PRESSURE = 1 BAR

LOG ACTIVITY H2S = -2.50 , A(H2O) = 1.0

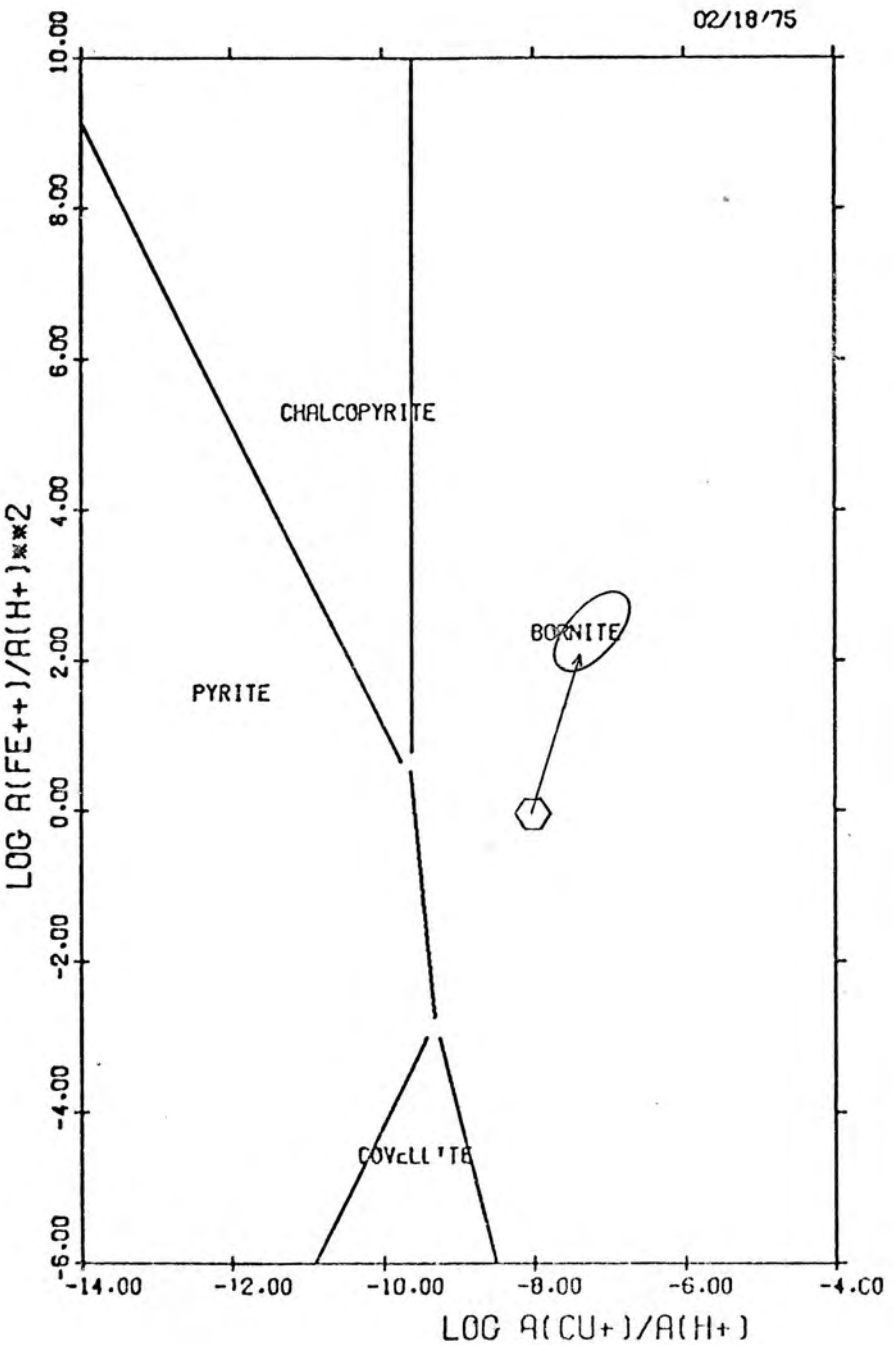

SYSTEM CU2S - FES -H2S - H2SO4 - HCL - H2O

TEMPERATURE = 100. DEG C. PRESSURE = 1 BAR

LOG ACTIVITY H2S = 2.50 , A(H2O) = 1.0

temperatures, the log a_{H_2S} might have been greater than -2.5 to cause the expansion of the pyrite field over the bornite field on the diagrams and have pyrite in equilibrium with the solutions at 300°C, 200°C and 100°C.

The proposed physico-chemical model assuming H+ ion consumption as the major chemical change of the solution composition and a sequence of isothermal conditions for the igneous wall rocks offered, therefore, a preliminary interpretation for the observed alteration mineralogy of the Mayflower and Ontario rocks. Likewise, the series of activity diagrams proved to be useful to characterize the chemical environment in which the major alteration minerals were produced.

Gains and Losses

An important result from the mineral abundance determinations was the possibility of expressing the alteration of the Mayflower and Ontario rocks in terms of gains and losses of minerals, from which the traditional gains and losses of components can be automatically deduced. Assuming no significant mass transfer subsequent to the close of the hydrothermal activity, a comparison of the modal compositions between unaltered and altered rocks affords a quantitative evaluation of the reactions that took place between the hydrothermal solutions and the stocks. The extent of these reactions is shown in a cross-section of the mine as the variation of the ratio between the mass of product minerals and mass of reactant phases (Fig. 37) with respect to the major flux of the solutions which occurred along the Mayflower-Pearl structure. This figure was prepared assuming constancy of volume of the

stock rocks despite the alteration they underwent. Apparently, most hydrothermal reactions occur under nearly isometric conditions and no significant change in volume is a valid assumption if deformational effects are not evident in the altered rock zones (Meyer 1950). Therefore, the variation of densities found among different samples of altered rocks was due only to mass changes if a uniform density distribution characterized the unaltered stocks.

The mineralogical and chemical gains and losses (Table 19) were computed with respect to the assigned modal and chemical compositions of the unaltered Mayflower and Ontario rocks. The assigned bulk chemical composition entailed the knowledge of the chemical compositions of the original igneous mineral phases, of which only primary biotite was apparently not available for analysis. As a consequence, the composition of the present-day biotite crystals was used as an approximation of the composition of the primary mica. Primary orthoclase was assumed to be stoichiometric.

For convenience of comparison, these gains and losses were expressed in grams of minerals or components per cubic centimeter of rock. Evidently, a density value had to be ascribed to the unaltered rocks. Again, the least altered Mayflower rocks (interval MF-2018) was taken as the representative unaltered counterpart and its density was found to be 2.75 g/cm^3. As intuition demands, positive values correspond to gains whereas negative values correspond to losses. The figures listed under the column "residual" in the table refer to the difference between the computed and the observed weight per cent proportions of individual components in the rocks. The residual values compare the

bulk chemical analyses of the rocks and the total compositions of the phases chosen to represent their mineral assemblages.

Hornblende was assumed to be totally destroyed for the purposes of calculating the modal compositions of the rocks. As a result, a loss of 0.0825 g/cm^3 of hornblende is implicit in all reported results. Likewise, a loss of 0.0275 g/cm^3 of magnetite is understood for the rocks in which this mineral is not reported.

From the mineralogical gain and loss tabulation, it can be seen that greater masses of andesine were destroyed than any other reactant mineral, followed by hornblende and magnetite. The other reactant phases were either consumed or re-equilibrated with the hydrothermal solutions. In both cases, they were subsequently added to the rocks carrying at this time, however, the signature of alteration products. Primary quartz may never have been destroyed, but it was precipitated as a hydrothermal phase. Anhydrite, calcite, pyrite, kaolinite, chlorite, and albite (+ zeolites) occur exclusively as alteration products and, obviously, were computed as mineral gains. Table 13 summarized the overall gain-loss range of minerals verified in the sampled volume of the Mayflower and Ontario stocks.

Figures 24 through 32 show the distinct zones of occurrence of the reactant and product phases with respect to the major veins.

In terms of gains and losses of components, the mass balance for the sampled rocks indicates an overall loss of Si, Al, Na and Ca and an overall gain of Fe(total), Mg, K, S, C, SO_3 and Ti according to Table 14. The loss values for components are in accordance with the role played by andesine as the quantitatively most significant reactant

TABLE 13

RANGE OF MINERAL GAINS AND LOSSES RESULTING FROM THE ALTERATION OF THE MAYFLOWER AND ONTARIO STOCKS

(g/cm^3)

	Gains		Losses
Andesine			0.208 to 1.452
K-feldspar	0.465	to	0.1375
Quartz	0.454	to	0.005
Biotite	0.400	to	0.034
Hornblende			0.0875
Magnetite			0.003 to 0.0275
Pyrite	0.060 to 0.181		
Calcite	0.014 to 0.599		
Anhydrite	0.000 to 0.238		
Chlorite	0.000 to 0.289		
Kaolinite	0.000 to 0.408		
Albite (+zeolites)	0.000 to 0.428		

TABLE 14

OVERALL COMPONENT GAINS AND LOSSES RESULTING FROM THE ALTERATION OF THE MAYFLOWER AND ONTARIO STOCKS

(g/cm^3)

	Gains	Losses
Si	. .	0.0026
Al	. .	0.0552
Fe (total)	0.0036	. .
Mg	0.0258	. .
Ca	. .	0.0138
Na	. .	0.0345
K	0.0205	. .
S	0.0380	. .
C	0.0070	. .
SO_3	0.0374	. .
Ti	0.0052	. .

mineral. Leaching was an important process in the alteration of the rocks especially in the vicinity of the main veins. Consumption of andesine implies the removal of lime, soda, alumina and silica which were, however, partially fixed as clay minerals and albite as well as calcite and anhydrite. Higher losses of silica may have been prevented due to the large deposition of quartz, particularly along veins. On the other hand, the considerable gain of phlogopitic biotite reflects the introduction of magnesium and potassium into the rocks, the latter element controlling also the large deposition of K-feldspar in the zones surrounding the major veins. The relatively insignificant addition of iron indicates that this metal was basically recycled in the system, from early mafic minerals and magnetite to later biotite, chlorite, pyrite, etc. If the primary igneous biotite had a higher iron content than the alteration biotite, iron gains would have been still lower and magnesium gains probably even higher. Large quantities of sulfur were added to the altered rocks from the hydrothermal solutions by reaction with indigeneous iron of the wall rocks and with other metals. The latter were almost exclusively deposited in the ore zone as sulfides. A portion of the total sulfur was in the form of sulfate which was incorporated into the altered rocks mainly as anhydrite. Considerable addition of carbon was also evident as the widespread occurrence of calcite indicates.

Alteration and Its Relation To Fracturing

The fluid flow through the rocks exposed in the Mayflower Mine

required the existence of open continuous fractures which rendered a permeable character to the rocks. Most aqueous solutions supplied through these continuous fractures were channeled by the Mayflower and Pearl fissures, along which the largest fluid flow occurred. The hydrothermal fluids also came in contact with impervious zones between flow fractures by means of diffusion channels.

The distribution of the alteration products was largely controlled by flow fractures. Discrete halos of alteration (1-2 cm wide) envelope most flow fractures but are never wide enough to give a pervasive character to the alteration, except perhaps in the vicinity of the ore zone. These fractures are also invariably filled with pyrite and other gangue minerals. As a consequence, the igneous walls are characterized by blocks of relatively unaltered rocks bounded by flow fractures. Non-continuous fractures, emanating from the flow channels, cut across these blocks, but seldom show appreciable amounts of filling products between their walls. Instead, their presence is marked by a generally tortuous alteration path of millimeter width. This general picture implies that the largest amount of alteration should occur in the vicinity of the main veins and, although in lesser amounts, in the zones displaying higher frequencies of flow fractures per unit length if their apertures are essentially the same all over the sampled volume of rocks. The former implication was manifested in the Mayflower Mine, but the latter was found only above the 2,005' level. On the lower levels the fracture abundance decreases significantly, but the alteration zones persist without much change, except that the second most abundantly altered zone is displaced southward so as to constitute a

distinct region between the 2,600' and 3,000' levels (Fig. 37). A possible explanation could be that the flow fractures on the lower levels at the time of the hydrothermal activity had a wider aperture which induced higher flow rates. If the present-day fracture openings used to describe the porosity model are a reasonable approximation of the paleo-apertures, that explanation does not hold since no appreciable aperture variation was found throughout the studied vertical section of the mine. An alternative to this could be that the diffusion channels played a significant role in the alteration of the matrix between flow fractures. Neither field observations nor analytical work were especially directed towards testing this alternative. However, comparison between Figs. 15 and 18 shows that the southwardly displaced alteration zone mentioned above coincides fairly well with a region characterized by rocks with relatively higher total porosities but with relatively lower flow porosities. As earlier discussed, residual porosity is the dominant factor contributing to the total porosity. Locally, however, the diffusion porosity can be increased as the abundance of diffusion channels increases so that it can provide a greater than normal contribution to the total porosity. As a consequence, more rock material is exposed to interaction with the solutions, thereby allowing the ions to diffuse more profusely into the matrix to account for its abundant alteration. In the absence of better evidence, the last alternative seems to be a satisfactory working hypothesis.

CHAPTER VIII

CONCLUSIONS

The present research was proposed to document quantitative data on important parameters controlling ore-forming processes. Hydrothermal ore deposits are a result of heat anomalies in the earth's crust caused by igneous intrusions which induce fluids to interact with rocks while flowing through fractures. Data on hydrodynamic parameters of fractured media and on the chemistry of altered rocks are, therefore, fundamental to test hypotheses of hydrothermal mineral deposit formation.

Several sets of mineralized fractures intersect the igneous rocks exposed in the Mayflower Mine. The most abundant sets are represented by two structural planes, N50°E/80°NW and N50°W/80°SW, the former corresponding to the Mayflower-Pearl fissure system. These structural planes were assumed to form a conjugate set of shear fractures with an average shear angle of 80°. The stress field was characterized by the intermediate principal stress direction vertically oriented and was conducive to the development of strike-slip faults. The present-day normal faulting character of the Mayflower and Pearl fissures was modified by the subsequent strike-slip faulting activity. Moreover, the igneous rocks were believed to have been fractured at their solidus temperature (750° ± 50°) under a high confining pressure to account for the large 2θ angle relating those two structural planes.

Fracture abundances and apertures determined for several intervals of igneous wall rocks of the mine were used to test a model for directional permeability and flow porosity developed by Snow (1968). The calculated permeability data ranged from 0.4 to 10 darcies whereas flow porosity values ranged from 0.05 to 0.4%. The high values found for these hydrodynamic parameters may have been the result of using present-day fracture openings to simulate the fracture apertures at the time of the hydrothermal activity and of a probable overestimation of the abundance of the continuous fractures. Nonetheless, their order of magnitude seems compatible with more realistic values despite the simplification of the mathematical model.

Measured bulk and grain densities of altered igneous rocks allowed the determination of total porosities and their subsequent application to a model in which total porosity of a fractured crystalline rock is given by the sum of the flow, diffusion and residual porosities (Norton 1975). The significant aspect derived from these results is that the residual porosity accounts for most of the total porosity of an igneous rock, even when highly fractured. Values of the calculated total porosities for the Mayflower and Ontario rocks ranged from 0.3 to 6.0% and indicated that the potential for alteration of these rocks was only partially used since most alteration per unit volume of rock is confined to zones enveloping flow fractures.

The abundance of both reactant and product minerals making up the Mayflower and Ontario altered rocks was obtained by means of a computer technique. Necessary input data included the qualitative mineral assemblages and the bulk chemical composition of the rocks as well as

the chemical compositions of the minerals present in those assemblages. These three parameters constitute an array of independent equations which was solved for a vector matrix representing the modes of individual phases. The method proved to be very practical and inexpensive in evaluating quantitatively the mineralogy of large volumes of rocks in a relatively short period of time.

The calculated mineral modes of the altered igneous rocks of the Mayflower Mine turned out to be consistent with the field observations, especially the distribution of alteration minerals in relation to the major vein system. Accordingly, two broad zonings were apparent from the mineral distribution patterns: 1) one lateral, characterized by both an increase of the K-feldspar, kaolinite and quartz abundances and a decrease of andesine, biotite and chlorite towards the main veins and 2) one vertical, characterized by major deposition of K-feldspar, anhydrite, pyrite and kaolinite below the 2,200' level and calcite, quartz, and biotite were more abundantly precipitated above. The more abundant precipitation of calcite on the upper levels was most likely controlled by increased CO_2 pressures at these depths as solutions which were in equilibrium with the carbonate host rocks flowed into the stocks. Field evidence indicated that the largest inflow of carbonate-rich solutions occurred above the 2,200' level. Fluids precipitating anhydrite, on the other hand, were probably in equilibrium with the Cambrian and Precambrian sedimentary formations from which sulfate may have been dissolved. These sulfate-rich fluids may have been introduced into the stock at greater depth where more abundant deposition of anhydrite took place.

The assumption of a chemical and a modal composition for the unaltered igneous rocks permitted the computation of both the mineral and component gains and losses. Andesine was by far the quantitatively most important reactant mineral as its less abundant occurrence in the vicinity of the major veins and the overall loss of Si, Al, Ca and Na indicate. The overall gain of K, Mg, Fe, SO_3, C, S, and Ti was expressed by the general addition of hydrothermal biotite, chlorite, anhydrite, calcite, and pyrite. Locally, significant amounts of actinolite, salite and epidote associate with the other alteration products and characterize mineral assemblages of an endoskarn.

Fluid inclusion data (Nash 1973) as well as constraints imposed by equilibrium relations among coexisting phases led to an initial solution composition which turned out to be compatible with the observed overall gains and losses of components. Reactions between solutions and rocks were considered to be essentially related to consumption of hydrogen ion. Interpretation of the alteration assemblages rested upon the approximation that the sampled volume of rock was subjected to a sequence of isothermal conditions while assuming the solution composition constant. The equilibrium relations between solutions and minerals were then discussed with the aid of activity diagrams at 100°, 200° and 300°C. This chemical model offered a preliminary interpretation for the observed mineralogy characterizing the altered Mayflower and Ontario rocks in spite of its simplification.

Significantly, the data on abundance of minerals point to an average of 0.3 for the ratio between the mass of altered rocks to mass of unaltered rocks within the sampled volume of the stocks. Such an

amount of alteration required the interaction of large quantities of hydrothermal fluids with rocks. The fracture abundance data support the evidence that these rocks were sufficiently permeable to allow the flow of aqueous solutions into the stocks. Once the stocks were emplaced into water-saturated rocks and fractured, the fluid flow started and continued until the temperature between the host rocks and the stocks equilibrated.

APPENDIX A

BULK CHEMICAL COMPOSITION OF THE ROCKS

APPENDIX A

BULK CHEMICAL COMPOSITION OF THE ROCKS

One hundred thirty-three chip rock samples were analyzed for twelve major components, namely, SiO_2, Al_2O_3, FeO (as total iron), MgO, CaO, Na_2O, K_2O, MnO, TiO_2, S, CO_2 and SO_3. The first nine were determined by X-ray fluorescence spectroscopy and the last three were analyzed using the LECO equipment available at the Department of Geosciences of the University of Arizona.

X-Ray Fluorescence Spectroscopy

Sample preparation

The chip rock samples were crushed, powdered and milled. In the last operation a tungsten disc mill (puck mill) was used. Approximately 40 grams of the pulps thus obtained were then milled again with a PICA mill or SPEX mixer-mill to assure the breakdown of the mica flakes and, as a consequence, a uniform grinding of all minerals present in the rock. Subsequently, about 15 grams of this uniform material was sifted to below 325 mesh to guarantee the homogeneity of the grain size. Utilizing the same methods employed in the preparation of the standards, one gram of the sifted material was mixed with cellulose in equal proportions in an agate mortar for twenty minutes. Finally, the two-gram mixture was placed in a spec-cap and pressed directly into pellets under

3.1 ton/cm^2 with the aid of a RIIC ring press (hydraulic press).

Analysis

A Phillips Universal X-ray Spectrometer was used for the analysis. Operational conditions for the various elements analyzed are listed on Table 15.

Two sets of standards were employed in the analyses. At first all unknown samples were run with GRLD (Geochemical Research and Laboratory Division of Kennecott Exploration, Inc.) igneous rock standards. However, the values obtained for SiO_2 and Al_2O_3 were not compatible with granitic rocks and the totals, without CO_2, SO_3 and H_2O, added to 89-93% for those rocks visibly poor in calcite and anhydrite. Even lower totals were recorded for samples in which these minerals were present in significant amounts. Inasmuch as the Mayflower rocks have been hydrothermally altered and generally contain high proportions of pyrite, calcite and anhydrite, it was thought that the cause of the relatively low values for SiO_2 and Al_2O_3 was due to matrix effects. To overcome these effects fourteen Mayflower and Ontario stock rocks were analyzed for Si, Al, Fe, Mg, Ca, Na, K and Ti by wet chemical methods at the Geochemical Laboratories of Kennecott Exploration, Inc. in Salt Lake City. Eight of them were selected for standards: MF-0804, MF-1304, MF-1711, MF-2207, MF-2805, ON-3003, ON-3004 and DDH-770.

All samples were run again and, except for SiO_2 and Al_2O_3, which revealed consistently higher contents, all other oxides showed values similar to the previous runs with a deviation of ±5%. Iron showed deviations up to 25%. However, to be consistent with other published

works, and considering the GRLD standards as more accurate, the values obtained during the first run, except for Si and Al, were favored and used in all calculations pertinent to this research.

All unknowns were calculated with equations of straight lines approximated by the least square method.

Precision

Duplicate pellets of three samples chosen at random (MF-1501, MF-1712 and MF-2204) were prepared for an indication of the precision of the analysis. Also, pellets of two samples that had been analyzed by wet chemical methods (MF-2610 and MF-2810) were made for comparison with the XRF method and therefore as an indication of the accuracy of the analyses. The results are shown in Table 16. The only discrepancy was verified with iron, suggesting good precision with the XRF method but poor accuracy between the two analytical methods.

The precision of the XRF analyses was determined by seven replicate runs of a sample which had been also analyzed by wet chemical methods (MF-2605). The arithmetic means and standards deviations of the seven analyses are listed below:

Oxide	Arithmetic Mean, %	Standard Deviation, %
SiO_2	58.60	1.29
Al_2O_3	17.28	0.43
FeO	5.32	0.23
MgO	3.29	0.16
CaO	4.53	0.24
Na_2O	3.72	0.29
K_2O	2.62	0.03
TiO_2	0.78	0.05
MnO	0.07	0.01

TABLE 15

OPERATIONAL CONDITIONS FOR ROCK CHEMICAL ANALYSIS

WITH XRF INSTRUMENTATION

Element	Detector	Target	Analyzing Crystal	Amperage MA	Voltage KV	Time (Sec)	Vacuum
Si	F.P.C.	Cr	EDDT	40	40	20	X
Al	F.P.C.	Cr	Gypsum	40	40	20	X
Fe	Scint	W	LiF	40	40	10	.
Mg	F.P.C.	Cr	Gypsum	40	40	20	X
Ca	F.P.C.	Cr	EDDT	40	40	20	.
Na	F.P.C.	Cr	Gypsum	40	40	20	X
K	F.P.C.	Cr	EDDT	40	40	20	.
Ti	Scint	W	LiF	40	40	20	.
Mn	Scint	W	LiF	40	40	10	.

NOTE: F.P.C. = flow proportional counter; scint = scintillation counter.

TABLE 16

INDICATION OF THE ACCURACY OF THE ANALYSES FOR THE MAJOR OXIDES (EXCEPT H_2O)

COMPOSING THE ALTERED MAYFLOWER AND ONTARIO ROCKS

Sample	S_1O_2			AL_2O_3			FeO			MgO		
	Wet Ch.	1st PLT	2nd PLT	Wet Ch.	1st PLT	2nd PLT	Wet Ch.	1st PLT	2nd PLT	Wet Ch.	1st PLT	2nd PLT
MF- 2610	58.10	59.30	. .	17.10	17.33	. .	4.49	6.61	. .	3.38	3.52	. .
MF- 2810	52.60	52.69	. .	14.90	15.22	. .	6.00	7.06	. .	4.85	4.97	. .
MF- 1501	. .	60.75	60.43	. .	17.11	17.65	. .	3.72	3.71	. .	2.78	2.68
MF- 1712	. .	59.29	58.92	. .	17.24	17.76	. .	4.34	4.15	. .	3.17	3.11
MF- 2004	. .	59.83	58.00	. .	17.25	17.21	. .	4.97	4.79	. .	3.86	3.64

Sample	CaO			NA_2O			K_2O			T_iO_2		
	Wet Ch.	1st PLT	2nd PLT	Wet Ch.	1st PLT	2nd PLT	Wet Ch.	1st PLT	2nd PLT	Wet Ch.	1st PLT	2nd PLT
MF- 2610	3.20	3.07	. .	3.00	3.32	. .	3.45	3.32	. .	0.82	0.86	. .
MF- 2810	6.97	5.99	. .	2.72	3.09	. .	2.89	2.78	. .	0.83	0.88	. .
MF- 1501	. .	4.87	4.82	. .	3.10	2.99	. .	3.15	3.08	. .	.072	0.70
MF- 1712	. .	5.83	5.86	. .	3.41	3.35	. .	2.99	2.89	. .	0.77	0.73
MF- 2004	. .	3.96	2.88	. .	2.16	2.26	. .	3.86	3.79	. .	0.74	0.66

Sample	MnO		
	Wet Ch.	1st PLT	2nd PLT
MF- 2610	. .	. .	. .
MF- 2810	. .	. .	. .
MF- 1501	. .	0.11	0.10
MF- 1712	. .	0.10	0.10
MF- 2004	. .	0.52	0.45

NOTE: PLT = Pellet; Wet Ch. = Wet Chemical.

LECO Equipment

A LECO automatic sulfur titrator, model DB-64, was used for sulfur determinations. Sulfur-bearing minerals are decomposed by combustion in an induction furnace, sulfur dioxide is evolved and absorbed by a solution containing hydrochloric acid, potassium iodide and starch indicator. Potassium iodate is added to this solution in sufficient amount to produce a blue color indicative of the analysis end point. This indicator color tends to fade as the sulfur dioxide is absorbed. A photo cell, sensitive to the blue color change, actuates a burette which releases potassium iodate titrant to maintain the intensity of the blue color. After a preset time has passed, both the furnace and the titrator are automatically shut off. No more sulfur dioxide is absorbed; neither is potassium iodate added. Direct reading on the titrator panel gives the amount of sulfur absorbed, provided the correct sample weight and titrant normality are used.

For carbon dioxide analyses a selective collecting-gas system was connected to the LECO induction furnace. Oxygen, after passing through a purifying train, was maintained at constant flow through the system. As sulfur dioxide, water vapor and carbon dioxide evolved from the sample under combustion, they were carried away by the oxygen flow and were successively absorbed in a series of traps. The first trap consisted of a 5% w/v solution of potassium permanganate with 3% v/v sulfuric acid and was used to collect sulfur dioxide. A frit glass bubbler was immersed in this solution to keep water and carbon dioxide from being retained. This trap was followed by a tube containing

anhydrone (magnesium perchlorate) intended to absorb water. Carbon dioxide was then collected in the next absorption tube filled with ascarite. All absorbents were changed every day or after a twenty-sample run to guarantee adequate absorption of gasses.

Analyses of sulfide-sulfur and sulfate-sulfur

Mineralogical observations indicated that sulfides, essentially pyrite, and anhydrite, gypsum and barite were the only sulfur-bearing minerals present in the igneous wall rocks of the Mayflower Mine. Therefore, the sulfur analyses were restricted to the sulfide and sulfate varieties.

The pulps were kept in an oven at a temperature of approximately 105°C for over twenty-four hours to eliminate possible moisture absorption from the environment. Initially all samples were analyzed for total sulfur. They were then stirred with deionized water for about two minutes to allow for the dissolution of the sulfate minerals. After approximately eight hours the mixture was decanted. This procedure was repeated at least four times. The sulfate-free samples were then placed back into the oven for about twenty-four hours and re-analyzed for sulfur. Assuming that the dissolution of the sulfate minerals was complete, this second total sulfur would represent, in consequence, the content of sulfide sulfur in the sample. Sulfate sulfur was determined by subtracting the values obtained for sulfur in the two runs for corresponding samples.

Carbon dioxide analyses

Calcite, rhodochrosite and siderite were the only carbon-bearing minerals identified in the Mayflower igneous rocks. Therefore, all carbon was assumed to be present as carbonate.

All samples were initially analyzed semi-quantitatively. Hydrochloric acid was used to separate the samples according to a low, medium and high carbonate content. This was done to control the amount of sample to be weighed. Largest amounts were used for carbonate-poor samples and vice-versa. Accordingly, large analytical errors were avoided and a control on the state of saturation of the absorbents was possible.

As in the case of sulfur analyses, the pulps, were kept in an oven at 105°C for over a day. A certain amount of the sample was weighed and then burnt during five minutes. The difference in weight of the CO_2- absorption tube after and before the combustion was a direct measure of the amount of carbon dioxide present in the sample.

Precision

Calibration of the sulfur automatic titrator was done by running LECO-steel ring standards. For monitoring the precision of the equipment either of the three GRLD standards (105, 114, 115) was run before and after every fifteen analyses. Standards to evaluate the precision of the carbon dioxide analytical method were prepared by using chemically pure calcium carbonate or its mixture with quartz. As before, they were run once for every fifteen samples analyzed.

The precision of the sulfur and carbon dioxide analyses was determined by six replicate runs of a randomly selected sample. The pulps MF-1304 and MF-2627 were chosen for sulfur and carbon dioxide respectively. The arithmetic means and standard deviations of the six analyses are shown below.

Compound	Arithmetic Mean, %	Standard Deviation
CO_2	1.18	0.143
S_{total}	0.90	0.016

APPENDIX B

CHEMICAL COMPOSITION OF MINERALS

APPENDIX B

CHEMICAL COMPOSITION OF MINERALS

Grains of biotite, chlorite, hornblende, actinolite, augite, salite, plagioclase, K-spar and epidote in carbon-coated, polished thin sections were analyzed with an ARL EMX-SM electron microprobe. Analyses included determinations of nine major elements for most mineral phases, namely, Si, Al, Fe, Mg, Ca, Na, K, Mn and Ti. Biotite analyses also included F, Cl and Ba, while Ca, Na and K were the only elements for which plagioclase and K-spar grains were run. Generally eight to twelve points per grain were analyzed for three elements at a time. For plagioclase grains, however, because they were invariably zoned, twenty-five to thirty points were analyzed along diagonals of each phenocryst. An average of ten grains of each mineral were examined. Count intervals were fixed by beam current termination. Raw count data were corrected for background, and calculated into percentages and averaged with the aid of a Fortran IV computer program.

APPENDIX C

BULK AND GRAIN DENSITIES OF THE ROCKS

APPENDIX C

BULK AND GRAIN DENSITIES OF THE ROCKS

One of the hand specimens collected at each interval was used for the determination of the bulk and grain densities of the rocks. The methods employed were based on Archimedes' principle.

For bulk density determinations, the samples were weighed twice with a conventional balance. The second time, however, they were immersed in water. The bulk density was calculated by the formula:

$$\rho_{\beta} = \frac{w_1}{w_1 - w_2}$$

where w_1 is the actual weight of the sample and w_2 is its weight when immersed in water.

Grain densities were determined with the aid of pycnometers. A small slab of the rock specimen used for bulk density determinations was cut, then crushed and pulverized. The grinding was to the extent that mineral grains were individually separated in order to eliminate intergranular pore spaces in the rocks (grain size is less than the minimum pore diameter). The determination of the grain density of each sample involved four weighing operations of a pycnometer as follows:

1. Empty (w_1);
2. Full with deionized water (w_2). Then the pycnometer was

emptied and left to dry;

3. With a small amount (approximately 1 g) of the pulverized sample (w_3);

4. With that amount of sample but also filled with deionized water (w_4).

Before this last weighing operation the pycnometer was placed in a vacuum chamber for about three minutes to eliminate possible trapped air bubbles.

Grain densities were calculated by the formula:

$$\rho_G = \frac{w_3 - w_1}{(w_3 - w_1) - (w_4 - w_2)}$$

From data on both densities it is possible to determine the total porosity (ϕ_T) of a rock according to the expression

$$\phi_T = 1 - \frac{\rho_\beta}{\rho_G} \qquad (13)$$

APPENDIX D

FRACTURE APERTURE DETERMINATIONS

APPENDIX D

FRACTURE APERTURE DETERMINATIONS

Large blocks of rocks (approximately 30 cm x 20 cm x 15 cm) displaying the most significant sets of mineralized fractures were collected for aperture determinations.

The method chosen required the use of fluorescent liquid penetrants which have been largely employed in the industry for detection of cracks or flaws in ceramic or metallic parts. These penetrants are sold by Magna-flux Corporation, Chicago, Illinois, under the commercial name of "Zyglo."

The instructions recommend spraying the surface to be inspected with a penetrant, a solvent and a developer successively. The solvent cleans the surface but does not remove the penetrant that infiltrated into cracks and other open spaces. When the developer is sprayed, it forms a porous white coating; this causes the penetrant inside the cracks to raise due to capillary action soaking the developer film. Under ultra-violet light the dyed developer fluoresces and reveals the presence of fractures, cracks and pores.

This technique was used to disclose open spaces in the mineralized cracks present in slabs cut with a diamond saw from the blocks of rocks. Aperture measurements were made after removing the developer coating with a new application of solvent. The slabs were then exposed to ultraviolet radiation and examined under a binocular microscope

provided with a micrometer. After calibration, each division of the micrometer was found to correspond to 182 microns at focus position. Approximately eight measurements were taken on each crack, always normally to the crack walls. The average of all measurements was indicated as the aperture for each slab.

The poor precision of the instrument used in the measurement (fractions of the micrometer division were visually estimated) added some incorrectness to the results, so that an error of 45 microns is to be expected.

APPENDIX E

QANMIN PROGRAM FUNDAMENTALS

APPENDIX E

QANMIN PROGRAM FUNDAMENTALS

(Norton, Unpublished)

The quantitative abundance of the mineral phases in a rock can be determined if the chemical composition of the rock and mineral constituents is known. A knowledge of these two qualities permits calculation of the individual phase abundances by solution of a set of equations describing the proportions in which constituent minerals must be mixed to yield the observed bulk composition.

The concentration, X_i, of the i^{th} element in a rock is determined by the relationship between the mass abundances of the n mineral phases, m_j, and the concentrations of the i^{th} element in the j^{th} mineral, $C_{i,j}$.

$$X_i = \sum_{j=1}^{n} m_j C_{i,j} \tag{14}$$

A set of such equations can be written to represent the k rock-forming elements where $n \leq k$ is a required condition. The set of equations has the form:

$$\begin{aligned}
m_1C_{11} + m_2C_{12} \cdots\cdots + M_jC_{1j} &= X_1 \\
m_1C_{21} + m_2C_{22} \cdots\cdots + m_jC_{2j} &= X_2 \\
\cdot \qquad\qquad\qquad\qquad\qquad\quad &\cdot \\
\cdot \qquad\qquad\qquad\qquad\qquad\quad &\cdot \\
m_1C_{k1} + m_2C_{k2} \cdots\cdots + m_jC_{kj} &= X_k
\end{aligned} \tag{15}$$

In matrix notation (15) becomes

$$\bar{m} \cdot \bar{C} = \bar{X} \qquad (16)$$

where $\bar{C}$ contains the chemical composition of the mineral phases, $\bar{X}$ the chemical composition of the rock and $\bar{m}$ the mineralogical composition of the sample. If the number of minerals is equal to the number of elements analyzed, i.e., if $n = k$, there will usually be a unique solution to (16). Hydrothermally altered rocks are generally disequilibrium assemblages, thus the number of phases is not constrained by the Phase Rule to be $\leq$ to the number of components. However, the number of major phases is commonly observed to be less than the components, and equation (16) is overdetermined. The solution to (16) may be obtained by a least squares approximation in which the sum of the square of the difference between actual whole rock chemical data and the value of X_i computed from (16) is minimized.

Additional constraints are imposed whereby $\Sigma m_i = 1.0$, negative values of m_i are not allowed and the solution is weighed according to the estimated absolute error in the analytical data.

APPENDIX F

DIST PROGRAM FUNDAMENTALS

APPENDIX F

DIST PROGRAM FUNDAMENTALS

(Knight, Unpublished)

The DIST program is used to solve for the molalities and activities in an aqueous solution given the pH and a chemical analysis of the solution.

The equilibrium conditions in an aqueous solution are uniquely defined by the laws of mass balance and mass action:

Law of Mass Balance:

$$m_{\varepsilon}^{T} = \sum_{s} m_{s} \nu_{\varepsilon,s} \tag{17}$$

where: $\nu_{\varepsilon,s}$ = moles of the ε^{th} element in the s^{th} aqueous species.

m_{ε}^{T} = total moles of the εth element.

m_{s} = molality of species s.

Law of Mass Action:

$$K_{j} = \prod_{s} a_{s}^{\hat{n}_{s,j}} = \prod_{s} (\gamma_{s} m_{s})^{\hat{n}_{s,j}} \tag{18}$$

where: K_{j} = equilibrium constant for the j^{th} dissociation reaction.

$\hat{n}_{s,j}$ = stoichiometric coefficient for the s^{th} species in the j^{th} reaction.

γ_{s} = activity coefficient for the s^{th} species.

a_{s} = activity of the s^{th} species.

The molality of an uncomplexed ion can be introduced into equation (17) so as to obtain ratios of the molality of a species and the molality of an uncomplexed ions. These ratios may be grouped into three types: (a) the ratio of an uncomplexed ion and itself; (b) the ratio of two different uncomplexed ions containing the same element but in different oxidation states; (c) the ratio between a complex and an uncomplexed species.

Equation (18) can be used for both complexed and uncomplexed species and be related to the above mentioned ratios by algebraic means.

The resulting equations are solved in a interative fashion. The program starts by assuming all elements are present as uncomplexed ions and the activity coefficients are equal to one. Evidently errors are introduced but they are lowered by interation. The program solved the equation to obtain an initial guess at an uncomplexed ion (m_b^a), and uses this value to resolve the equations and get a new m_b. These two values are averaged and the process repeated until the new value is closely acceptable to the old value. The program then solves for molalities of the other species in the system. These molalities are compared to previously calculated molalities. If they are closely acceptable, ionic strength and activity coefficients are calculated, otherwise the cycle is repeated. After computing ionic strength, the program checks for ionic strength convergence. If not found, the cycle is restarted.

APPENDIX G

THERMODYNAMIC DATA FOR BIOTITE AND PLAGIOCLASE COMPOSITIONS FOUND IN THE MAYFLOWER STOCK

APPENDIX G

THERMODYNAMIC DATA FOR BIOTITE AND PLAGIOCLASE COMPOSITIONS FOUND IN THE MAYFLOWER STOCK

Biotite

According to Beane (1972) the thermodynamic properties of ferromagnesian biotites can be calculated by the following equations:

$$H'_{ss,298} = -1{,}229{,}300X_{ann} - 1{,}499{,}760X_{phl} - 1{,}169{,}200X_{PDoxy}$$

$$S'_{ss,298} = 100.3X_{ann} + 75.2X_{phl} + 73.1X_{PDoxy} - 4.577(X_{ann}\log X_{ann} + X_{phl}\log X_{phl} + X_{PDoxy}\log X_{PDoxy}) - 0.61X_{ann}X_{phl} + 126.3\,X_{ann}X_{PDoxy} + 30.5X_{phl}XPDoxy$$

$$C'_{p_{ss}} = 100.88X_{ann} + 96.38X_{phl} + 87.58X_{PD\ oxy} + (37.87X_{ann} + 26.53Xphl + 49.27X_{PDoxy}) \times 10^{-3}T - (5.61X_{ann} + 27.23X_{phl} + 28.12X_{PDoxy}) \times 10^{5}\,T^{-2}$$

$$V'_{ss} = 154.3X_{ann} + 149.9X_{phl} + 136.0X_{PDoxy}$$

Where H'_{ss}, X'_{ss}, C'_{pss} and V'_{ss} are the enthalpy of formation, the entropy, the heat capacity and the molar volume respectively of the solid-solution of the ferromagnesian micas, X_{ann}, X_{phl} and X_{PDoxy} are the mole fractions of annite, phlogopite and proton-deficient oxyannite respectively in the biotite molecule and T is the absolute temperature.

The Mayflower biotite is characterized by an average composition of $0.64X_{phl}$ and $0.36X_{ann}$. No ferric and ferrous iron determinations were done, however. As a result, total iron was treated as ferrous and the X_{PDoxy} was assumed to be zero for purposes of the calculations. The substitution of the mole fractions found for the Mayflower biotite into the equations above affords:

$$H'_{biot,298} = -1,402,394.4 \text{ cal/mole}$$

$$S'_{biot,298} = 85.395 \text{ cal/mole-degree}$$

$$C'_{p_{biot}} = 98.0 + 30.61 \times 10^{-3}T - 19.45 \times 10^{5}T^{-2} \text{ (cal/mole-degree)}$$

$$V'_{biot} = 151.48 \text{ cm}^3\text{/mole}$$

The equilibrium constant for the hydrolysis of the Mayflower biotite was then calculated at different temperatures and at 1 bar pressure (Table 17) using the equation below (Helgeson 1969a):

$$\log K(T) = \log K(T_r) - \frac{\Delta H^\circ_r(Tr)}{2.303R}\left(\frac{1}{T} - \frac{1}{T_r}\right) - \frac{1}{2.303RT}\int_{T_r}^{T}\Delta C^\circ_{p,r}(T)dT$$

$$\frac{1}{2.303R}\int_{T_R}^{T}\Delta C^\circ_{p,r}(T)d\ln T \qquad (19)$$

The thermodynamic properties for the aqueous species are also found in Helgeson, 1969a.

Plagioclase

The solid solution series of the plagioclases was assumed to behave ideally. Therefore, only mixing effects were considered in the calculations of the thermodynamic properties of the Mayflower plagioclase which is characterized by an average of 60% albite and 40%

TABLE 17

EQUILIBRIUM CONSTANT (LogK) OF THE AVERAGE MAYFLOWER BIOTITE (X_{phl} = 0.64; X_{ann} = 0.36; X_{PDoxy} = 0.0) AT TEMPERATURES FROM 25°C TO 350°C.

T°C	Log K(T)
25	28.20
50	24.70
75	21.70
100	19.20
125	17.00
150	15.00
175	13.40
200	12.10
225	10.90
250	9.72
275	8.68
300	7.73
325	6.87
350	6.07

anorthite contents.

The entropy os mixing (ΔS_{mix}) and the Gibbs free energy of mixing (ΔG_{mix}) of an ideal solid solution are given by:

$$\Delta S_{mix} = - R(X_1 \ln X_1 + X_2 \ln X_2) \quad (20)$$

$$\Delta G_{mix} = RT(X_1 \ln X_1 + X_2 \ln X_2) \quad (21)$$

where X_1 and X_2 are the mole fractions of the two components in a binary system, R is the gas constant and T is the absolute temperature of the standard state (298.15°K). The substitution of X_1 and X_2 for 0.6 (albite content) and 0.4 (anorthite content) respectively in the equations (20) and (21) affords:

$$\Delta S_{mix} = 1.337 \text{ cal/mole.degree}$$

and

$$\Delta G_{mix} = -398.71 \text{ cal/mole}$$

The enthalpy of formation (ΔH°_f) of the solid solution can be written as:

$$\Delta H^\circ_f = \Delta G^\circ_f + T\Delta S^\circ_f \quad (22)$$

or for the Mayflower andesine:

$$\Delta H^\circ_{f,and} = \Delta G_{mix} + 0.6\Delta G^\circ_{f,ab} + \Delta G^\circ_{f,an} + T(\Delta S_{mix} + 0.6\Delta S^\circ_{f,ab} + 0.4\Delta S^\circ_{f,an}) \quad (23)$$

where ΔG°_f and ΔS°_f stand for the Gibbs free energy and the entropy of formation of the end members of the series. Data on ΔG°_f for albite and anorthite are available (Robie et al. 1968), but ΔS°_f values needed to be calculated by the expression:

$$\Delta S^{\circ}_{f,298.15}(\text{mineral}) = S(\text{mineral}) - \Sigma\ S(\text{elements}) \qquad (24)$$

where S is the absolute entropy. For albite and anorthite equation (24) gives:

$$\Delta S^{\circ}_{f,298.15}(\text{albite}) = -\ 178.294 \text{ cal/mole.degree}$$

$$\Delta S^{\circ}_{f,298.15}(\text{anorthite}) = -\ 180.024 \text{ cal/mole.degree}$$

The absolute entropy of the andesine can be expressed by:

$$S_{and} = S_{mix} + 0.6\ S_{ab} + 0.4\ S_{an} \qquad (25)$$

so that:

$$S_{and} = 50.84 \text{ cal/mole.degree}$$

The substitution of the unknowns in equation (23) for their corresponding values affords:

$$\Delta H^{\circ}_{f,298.15}(\text{andesine}) = -\ 966{,}088.0 \text{ cal/mole}$$

Heat capacity coefficients for andesine can be calculated by:

$$\begin{aligned} a &= 0.6\ a_{ab} + 0.4\ a_{an} \\ b &= 0.6\ b_{ab} + 0.4\ b_{an} \\ c &= 0.6\ c_{ab} + 0.4\ c_{an} \end{aligned} \qquad (26)$$

where a, b and c of the end members are known (Robie et al. 1968), so that:

$$\begin{aligned} a_{and} &= 62.79 \\ b_{and} &= 13.82 \times 10^{-3} \\ c_{and} &= -\ 15.76 \times 10^{5} \end{aligned}$$

The obtained values for $H^{\circ}_{f,298.15}$, S, and a, b and c for andesine allowed the use of equation (19) for computation of the equilibrium constant of the andesine hydrolysis at different temperatures (Table 18).

TABLE 18

EQUILIBRIUM CONSTANT (LogK) OF THE AVERAGE (0.6 Ab and 0.4 An) AT TEMPERATURES FROM FROM 25°C TO 350°C

$T^{o}C$	log (K)
25	12.00
50	9.83
75	8.01
100	6.46
125	5.09
150	3.86
175	2.87
200	2.03
225	1.32
250	0.513
275	-0.169
300	-0.801
325	-1.39
350	-1.96

APPENDIX H

TABLE 19

MINERAL ABUNDANCE AND GAINS AND LOSSES IN THE ALTERED MAYFLOWER AND ONTARIO ROCKS

MF-0801	WEIGHT		GAIN OR LOSS
MINERAL	PER CENT	G/CM**3	G/CM**3
PLAGICCLAS	47.97	1.334	-.564
K-FELDSPAR	10.59	.294	.157
QUARTZ	16.37	.455	.180
BIOTITE	15.82	.440	.110
PYRITE	1.08	.030	.030
CALCITE	2.96	.082	.082
ANHYDRITE	.32	.009	.009
CHLORITE	4.80	.133	.133
TOTALS	99.92	2.778	.138

	WT.PERCENT		GAIN OR LOSS
COMPONENT	COMPUTED	RESIDUAL	G/CM**3
SI	27.569	.363	-.0071
AL	9.469	.629	-.0541
FE++	3.345	.042	-.0001
MG	2.132	-.045	.0290
CA	4.209	.206	-.0047
NA	2.442	-.281	-.0243
K	2.693	-.021	.0275
S	.579	-.001	.0161
O	46.421	-.966	.0384
C	.355	-.005	.0100
SO3	.190	-.000	.0053
TI	.516	.001	.0077
SUM RESIDUALS**2		1.587	
STANDARD DEVIATION		.630	

MF-0802	WEIGHT		GAIN OR LOSS
MINERAL	PER CENT	G/CM**3	G/CM**3
PLAGICCLAS	49.30	1.376	-.522
K-FELDSPAR	6.34	.177	.039
QUARTZ	14.01	.391	.116
BIOTITE	17.39	.485	.155
PYRITE	1.72	.048	.048
CALCITE	4.31	.120	.120
ANHYDRITE	.37	.010	.010
CHLORITE	5.67	.158	.156
TOTALS	99.11	2.765	.125

	WT.PERCENT		GAIN OR LOSS
COMPONENT	COMPUTED	RESIDUAL	G/CM**3
SI	25.959	.529	-.0539
AL	9.448	.237	-.0428
FE++	3.990	.220	.0133
MG	2.402	-.119	.0388
CA	4.845	-.165	.0238
NA	2.464	.016	-.0317
K	2.290	-.009	.0162
S	.918	-.012	.0259
O	45.490	-1.591	.0346
C	.517	.006	.0142
SO3	.220	.000	.0061
TI	.567	-.002	.0093
SUM RESIDUALS**2		2.957	
STANDARD DEVIATION		.660	

MF-0803	WEIGHT		GAIN OR LOSS
MINERAL	PER CENT	G/CM**3	G/CM**3
PLAGICCLAS	51.70	1.417	-.491
K-FELDSPAR	4.70	.129	-.009
QUARTZ	15.55	.426	.151
BIOTITE	17.60	.482	.152
PYRITE	.64	.017	.017
CALCITE	2.75	.075	.075
ANHYDRITE	.37	.010	.010
CHLORITE	5.98	.164	.164
TOTALS	99.29	2.721	.081

	WT.PERCENT		GAIN OR LOSS
COMPONENT	COMPUTED	RESIDUAL	G/CM**3
SI	26.921	.510	-.0397
AL	9.664	.352	-.0445
FE++	3.363	-.080	.0025
MG	2.625	.026	.0397
CA	4.368	.023	.0031
NA	2.564	-.077	-.0276
K	2.109	-.008	.0100
S	.341	.001	.0093
O	46.209	-1.457	.0270
C	.330	-.000	.0090
SO3	.220	-.000	.0060
TI	.574	.005	.0090
SUM RESIDUALS**2		2.520	
STANDARD DEVIATION		.794	

MF-0804	WEIGHT		GAIN OR LOSS
MINERAL	PER CENT	G/CM**3	G/CM**3
PLAGICCLAS	51.61	1.419	-.478
K-FELDSPAR	5.36	.147	.010
QUARTZ	15.48	.426	.151
BIOTITE	17.34	.477	.147
PYRITE	1.53	.042	.042
CALCITE	3.33	.092	.092
CHLORITE	4.97	.137	.137
TOTALS	99.64	2.740	.100

	WT.PERCENT		GAIN OR LOSS
COMPONENT	COMPUTED	RESIDUAL	G/CM**3
SI	26.861	.215	-.0306
AL	9.596	.068	-.0378
FE++	3.609	-.254	.0143
MG	2.426	.074	.0332
CA	4.487	.220	.0013
NA	2.567	-.119	-.0261
K	2.171	.005	.0116
S	.820	.010	.0223
O	46.137	-.581	.0057
C	.400	-.006	.0112
TI	.566	.008	.0087
SUM RESIDUALS**2		.521	
STANDARD DEVIATION		.361	

MF-1301

MINERAL	WEIGHT PER CENT	G/CM**3	GAIN OR LOSS G/CM**3
PLAGIOCLAS	42.29	1.142	-.756
K-FELDSPAR	12.96	.360	.213
QUARTZ	21.20	.572	.297
BIOTITE	10.69	.445	.115
PYRITE	.88	.024	.024
CALCITE	2.85	.077	.077
ANHYDRITE	.03	.001	.001
KAOLINITE	2.66	.072	.072
MAGNETITE	.46	.013	-.015
TOTALS	99.07	2.696	.029

COMPONENT	WT.PERCENT COMPUTED	RESIDUAL	GAIN OR LOSS G/CM**3
SI	29.822	.273	.0128
AL	9.126	.021	-.0540
FE**	2.454	.001	-.0149
MG	1.610	.122	.0092
CA	3.697	.409	-.0245
NA	2.152	-.276	-.0345
K	3.039	.034	.0331
S	.475	-.000	.0127
O	47.045	-.661	.0091
C	.342	-.015	.0097
SO3	.029	-.000	.0005
TI	.171	-.042	.0046
SUM RESIDUALS**2		.273	
STANDARD DEVIATION		.507	

MF-1302

MINERAL	WEIGHT PER CENT	G/CM**3	GAIN OR LOSS G/CM**3
PLAGIOCLAS	40.63	1.109	-.738
K-FELDSPAR	13.60	.371	.234
QUARTZ	21.42	.598	.323
BIOTITE	16.66	.455	.125
PYRITE	.77	.021	.021
CALCITE	1.55	.042	.042
KAOLINITE	3.66	.096	.096
MAGNETITE	.76	.021	-.007
TOTALS	99.34	2.712	.045

COMPONENT	WT.PERCENT COMPUTED	RESIDUAL	GAIN OR LOSS G/CM**3
SI	29.335	.586	.0215
AL	9.150	.046	-.0512
FE**	3.026	.002	-.0044
MG	1.647	.139	.0047
CA	3.163	.304	-.0380
NA	2.079	-.266	-.0360
K	3.127	.038	.0363
S	.413	-.000	.0112
O	46.844	-1.453	.0395
C	.187	-.000	.0052
TI	.375	-.051	.0050
SUM RESIDUALS**2		2.642	
STANDARD DEVIATION		.939	

MF-1303

MINERAL	WEIGHT PER CENT	G/CM**3	GAIN OR LOSS G/CM**3
PLAGIOCLAS	33.04	.892	-1.035
K-FELDSPAR	13.84	.374	.236
QUARTZ	27.01	.729	.454
BIOTITE	13.79	.372	.042
PYRITE	3.16	.085	.085
CALCITE	2.27	.061	.061
ANHYDRITE	1.67	.045	.045
KAOLINITE	4.52	.122	.122
TOTALS	99.30	2.681	.041

COMPONENT	WT.PERCENT COMPUTED	RESIDUAL	GAIN OR LOSS G/CM**3
SI	29.476	.727	.0126
AL	8.144	.045	-.0411
FE**	3.226	.170	-.0096
MG	1.363	-.025	.0060
CA	3.467	.580	-.0180
NA	1.718	-.411	-.0425
K	2.408	.060	.0289
S	1.669	-.051	.0470
O	45.743	-1.741	.0031
C	.272	-.020	.0079
SO3	.984	-.036	.0275
TI	.310	-.007	.0020
SUM RESIDUALS**2		4.109	
STANDARD DEVIATION		1.014	

MF-1304

MINERAL	WEIGHT PER CENT	G/CM**3	GAIN OR LOSS G/CM**3
PLAGIOCLAS	38.27	1.045	-.853
K-FELDSPAR	14.18	.387	.250
QUARTZ	21.59	.589	.314
BIOTITE	18.04	.493	.163
PYRITE	1.57	.043	.043
CALCITE	1.46	.040	.040
ANHYDRITE	.19	.005	.005
KAOLINITE	4.13	.113	.113
MAGNETITE	.31	.008	-.019
TOTALS	99.74	2.723	.055

COMPONENT	WT.PERCENT COMPUTED	RESIDUAL	GAIN OR LOSS G/CM**3
SI	29.161	.319	.0240
AL	9.129	.025	-.0512
FE**	3.251	.001	-.0032
MG	1.783	.112	.0141
CA	3.033	.310	-.0417
NA	1.971	-.277	-.0186
K	3.301	.047	.0406
S	.440	-.000	.0229
O	46.581	-.754	.0132
C	.176	-.004	.0049
SO3	.110	-.000	.0030
TI	.406	-.036	.0055
SUM RESIDUALS**2		.859	
STANDARD DEVIATION		.535	

MF-1306

MINERAL	WEIGHT PER CENT	G/CM**3	GAIN OR LOSS G/CM**3
PLAGIOCLAS	49.75	1.343	-.554
K-FELDSPAR	7.81	.211	.073
QUARTZ	19.99	.540	.265
BIOTITE	16.92	.457	.127
PYRITE	1.12	.030	.030
CALCITE	2.51	.068	.068
ANHYDRITE	.59	.016	.016
MAGNETITE	.60	.016	-.011
TOTALS	99.30	2.681	.014

COMPONENT	WT.PERCENT COMPUTED	RESIDUAL	GAIN OR LOSS G/CM**3
SI	28.292	.665	-.0175
AL	9.071	.231	-.0611
FE++	3.112	.003	-.0080
MG	1.673	.153	.0095
CA	4.289	.272	-.0076
NA	2.457	-.199	-.0283
K	2.453	.004	.0181
S	.600	-.000	.0162
O	46.322	-1.767	.0194
C	.301	-.005	.0083
SO3	.349	-.001	.0094
TI	.381	-.057	.0052
SUM RESIDUALS**2		3.759	
STANDARD DEVIATION		.969	

MF-1501

MINERAL	WEIGHT PER CENT	G/CM**3	GAIN OR LOSS G/CM**3
PLAGIOCLAS	42.06	1.169	-.728
K-FELDSPAR	9.33	.259	.122
QUARTZ	22.37	.622	.347
BIOTITE	17.75	.493	.163
PYRITE	.37	.010	.010
CALCITE	2.65	.074	.074
ANHYDRITE	.27	.008	.008
KAOLINITE	3.62	.101	.101
MAGNETITE	.76	.021	-.006
TOTALS	99.19	2.757	.090

COMPONENT	WT.PERCENT COMPUTED	RESIDUAL	GAIN OR LOSS G/CM**3
SI	28.895	.660	.0215
AL	9.105	.053	-.0482
FE++	2.894	.002	-.0115
MG	1.780	.103	.0151
CA	3.712	.231	-.0192
NA	2.178	-.122	-.0361
K	2.629	.014	.0247
S	.200	-.000	.0056
O	46.915	-1.719	.0730
C	.318	-.006	.0090
SO3	.160	-.000	.0044
TI	.401	-.031	.0054
SUM RESIDUALS**2		3.472	
STANDARD DEVIATION		1.076	

MF-1502

MINERAL	WEIGHT PER CENT	G/CM**3	GAIN OR LOSS G/CM**3
PLAGIOCLAS	42.66	1.173	-.724
K-FELDSPAR	9.44	.260	.122
QUARTZ	22.55	.620	.345
BIOTITE	16.58	.456	.126
PYRITE	2.24	.062	.062
CALCITE	2.31	.063	.063
KAOLINITE	3.02	.083	.053
TOTALS	98.81	2.717	.077

COMPONENT	WT.PERCENT COMPUTED	RESIDUAL	GAIN OR LOSS G/CM**3
SI	28.809	.901	.0041
AL	8.964	.071	-.0552
FE++	3.074	.136	-.0111
MG	1.663	.028	.0135
CA	3.530	.292	-.0270
NA	2.209	-.194	-.0339
K	2.551	.019	.0216
S	1.200	-.020	.0336
O	46.159	-2.395	.0562
C	.277	-.007	.0078
TI	.374	-.021	.0043
SUM RESIDUALS**2		6.699	
STANDARD DEVIATION		1.294	

MF-1503

MINERAL	WEIGHT PER CENT	G/CM**3	GAIN OR LOSS G/CM**3
PLAGIOCLAS	37.85	1.026	-.872
K-FELDSPAR	11.60	.314	.177
QUARTZ	24.06	.652	.377
BIOTITE	16.45	.446	.116
PYRITE	1.53	.042	.042
CALCITE	1.95	.053	.053
ANHYDRITE	.29	.008	.008
CHLORITE	.55	.015	.015
KAOLINITE	4.13	.112	.112
TOTALS	98.40	2.667	.027

COMPONENT	WT.PERCENT COMPUTED	RESIDUAL	GAIN OR LOSS G/CM**3
SI	29.208	1.019	.0005
AL	8.813	.076	-.0631
FE++	2.820	-.150	-.0114
MG	1.737	.054	.0141
CA	3.177	.376	-.0401
NA	1.992	-.308	-.0377
K	2.802	.038	.0269
S	.820	.010	.0220
O	46.265	-2.700	.0480
C	.234	-.009	.0066
SO3	.169	-.001	.0046
TI	.371	-.000	.0035
SUM RESIDUALS**2		8.599	
STANDARD DEVIATION		1.693	

MF-1504	WEIGHT		GAIN OR LOSS
MINERAL	PER CENT	G/CM**3	G/CM**3
PLAGIOCLAS	37.01	1.007	-.891
K-FELDSPAR	13.41	.365	.227
QUARTZ	24.28	.660	.385
BIOTITE	16.96	.462	.132
PYRITE	1.59	.043	.043
CALCITE	1.98	.054	.054
ANHYDRITE	.25	.007	.007
KAOLINITE	3.18	.086	.086
MAGNETITE	.56	.015	-.012
TOTALS	99.24	2.699	.032

	WT.PERCENT		GAIN OR LOSS
COMPONENT	COMPUTED	RESIDUAL	G/CM**3
SI	29.410	.661	.0186
AL	8.621	.046	-.0666
FE++	3.221	.003	-.0044
MG	1.703	.062	.0131
CA	3.129	.320	-.0396
NA	1.969	-.242	-.0399
K	3.068	.038	.0344
S	.850	-.000	.0231
O	46.496	-1.625	.0299
C	.238	-.008	.0067
SO3	.150	-.000	.0041
TI	.383	-.018	.0043
SUM RESIDUALS**2		3.244	
STANDARD DEVIATION		1.040	

MF-1505	WEIGHT		GAIN OR LOSS
MINERAL	PER CENT	G/CM**3	G/CM**3
PLAGIOCLAS	52.26	1.437	-.460
K-FELDSPAR	5.61	.154	.017
QUARTZ	17.58	.483	.208
BIOTITE	21.92	.603	.273
PYRITE	.45	.012	.012
CALCITE	.96	.026	.026
ANHYDRITE	.22	.006	.006
MAGNETITE	.73	.020	-.007
TOTALS	99.73	2.743	.075

	WT.PERCENT		GAIN OR LOSS
COMPONENT	COMPUTED	RESIDUAL	G/CM**3
SI	28.140	.372	.0002
AL	9.626	.363	-.0451
FE++	3.422	.002	.0022
MG	2.198	.196	.0236
CA	3.643	-.188	-.0107
NA	2.647	.036	-.0282
K	2.511	-.021	.0216
S	.240	-.000	.0066
O	46.567	-.957	.0279
C	.115	.001	.0032
SO3	.130	.000	.0036
TI	.495	-.069	.0089
SUM RESIDUALS**2		1.266	
STANDARD DEVIATION		.563	

MF-1506	WEIGHT		GAIN OR LOSS
MINERAL	PER CENT	G/CM**3	G/CM**3
PLAGIOCLAS	20.00	.522	-1.375
K-FELDSPAR	8.14	.212	.075
QUARTZ	14.91	.389	.114
BIOTITE	11.35	.296	-.034
PYRITE	2.07	.054	.054
CALCITE	22.95	.599	.599
ANHYDRITE	3.70	.097	.097
KAOLINITE	5.07	.132	.132
EPIDOTE	11.46	.299	.299
TOTALS	99.64	2.601	-.039

	WT.PERCENT		GAIN OR LOSS
COMPONENT	COMPUTED	RESIDUAL	G/CM**3
SI	20.307	-.028	-.2327
AL	7.143	-.003	-.1133
FE++	3.631	.063	.0012
MG	1.138	.088	-.0041
CA	13.458	-.650	.2522
NA	1.073	.005	-.0721
K	1.941	-.001	.0027
S	1.105	-.005	.0290
O	44.656	.117	-.1166
C	2.753	.076	.0699
SO3	2.178	.008	.0566
TI	.256	-.032	.0009
SUM RESIDUALS**2		.456	
STANDARD DEVIATION		.390	

MF-1701V	WEIGHT		GAIN OR LOSS
MINERAL	PER CENT	G/CM**3	G/CM**3
PLAGIOCLAS	22.14	.602	-1.295
K-FELDSPAR	9.77	.266	.128
QUARTZ	29.44	.801	.526
BIOTITE	11.29	.307	-.023
PYRITE	10.64	.289	.289
CALCITE	4.74	.129	.129
ANHYDRITE	2.39	.065	.065
KAOLINITE	9.18	.250	.250
TOTALS	99.59	2.709	.069

	WT.PERCENT		GAIN OR LOSS
COMPONENT	COMPUTED	RESIDUAL	G/CM**3
SI	27.243	.645	-.0399
AL	7.075	.035	-.1083
FE++	6.361	.508	.0573
MG	1.104	.055	-.0030
CA	3.921	.762	-.0301
NA	1.231	-.179	-.0617
K	2.156	.039	.0096
S	5.687	-.493	.1681
O	42.564	-1.557	-.0789
C	.569	-.119	.0187
SO3	1.405	-.085	.0405
TI	.267	-.027	.0014
SUM RESIDUALS**2		3.982	
STANDARD DEVIATION		.998	

MF-1702 MINERAL	WEIGHT PER CENT	G/CM**3	GAIN OR LOSS G/CM**3
PLAGIOCLAS	29.91	.825	-1.072
K-FELDSPAR	15.55	.429	.292
QUARTZ	19.84	.548	.273
BIOTITE	20.21	.558	.228
PYRITE	2.64	.073	.073
CALCITE	2.16	.060	.060
ANHYDRITE	.56	.015	.015
CHLORITE	.73	.020	.020
KAOLINITE	7.25	.200	.200
TOTALS	98.85	2.728	.088

COMPONENT	WT.PERCENT COMPUTED	RESIDUAL	GAIN OR LOSS G/CM**3
SI	27.962	.756	-.0125
AL	8.956	.063	-.0544
FE++	3.884	-.127	.0188
MG	2.088	.043	.0249
CA	2.812	.182	-.0434
NA	1.691	-.097	-.0507
K	3.609	.040	.0505
S	1.414	.014	.0386
O	45.371	-2.012	.0288
C	.259	-.006	.0073
SO3	.329	-.001	.0091
TI	.478	-.002	.0066
SUM RESIDUALS**2		4.687	
STANDARD DEVIATION		1.250	

MF-1703 MINERAL	WEIGHT PER CENT	G/CM**3	GAIN OR LOSS G/CM**3
PLAGIOCLAS	41.75	1.136	-.762
K-FELDSPAR	8.87	.241	.104
QUARTZ	17.26	.470	.195
BIOTITE	21.06	.573	.243
PYRITE	.51	.014	.014
CALCITE	2.28	.062	.062
ANHYDRITE	1.13	.031	.031
CHLORITE	.89	.024	.024
KAOLINITE	4.98	.136	.136
TOTALS	98.73	2.685	.045

COMPONENT	WT.PERCENT COMPUTED	RESIDUAL	GAIN OR LOSS G/CM**3
SI	27.549	.717	-.0336
AL	9.491	.069	-.0435
FE++	3.021	-.368	.0003
MG	2.192	.160	.0238
CA	3.736	.334	-.0235
NA	2.210	-.193	-.0346
K	2.884	.028	.0297
S	.272	.002	.0073
O	45.936	-2.008	.0251
C	.274	-.007	.0076
SO3	.664	-.006	.0182
TI	.498	.000	.0069
SUM RESIDUALS**2		4.861	
STANDARD DEVIATION		1.273	

MF-1704 MINERAL	WEIGHT PER CENT	G/CM**3	GAIN OR LOSS G/CM**3
PLAGIOCLAS	46.11	1.263	-.634
K-FELDSPAR	8.20	.225	.087
QUARTZ	17.23	.472	.197
BIOTITE	21.05	.577	.247
PYRITE	.75	.021	.021
CALCITE	1.63	.045	.045
ANHYDRITE	.34	.009	.009
CHLORITE	1.20	.033	.033
KAOLINITE	2.72	.075	.075
TOTALS	99.23	2.719	.079

COMPONENT	WT.PERCENT COMPUTED	RESIDUAL	GAIN OR LOSS G/CM**3
SI	27.986	.499	-.0103
AL	9.521	.046	-.0402
FE++	3.190	-.129	-.0010
MG	2.240	.068	.0280
CA	3.502	.114	-.0232
NA	2.422	-.070	-.0317
K	2.807	.010	.0287
S	.402	.002	.0110
O	46.263	-1.313	.0246
C	.195	-.001	.0054
SO3	.230	-.000	.0055
TI	.498	.000	.0070
SUM RESIDUALS**2		2.014	
STANDARD DEVIATION		.819	

MF-1705 MINERAL	WEIGHT PER CENT	G/CM**3	GAIN OR LOSS G/CM**3
PLAGIOCLAS	41.04	1.124	-.773
K-FELDSPAR	11.36	.311	.174
QUARTZ	18.31	.502	.227
BIOTITE	19.59	.537	.207
PYRITE	.92	.025	.025
CALCITE	1.53	.042	.042
ANHYDRITE	.56	.015	.015
CHLORITE	2.04	.056	.056
KAOLINITE	3.24	.089	.089
TOTALS	98.58	2.701	.061

COMPONENT	WT.PERCENT COMPUTED	RESIDUAL	GAIN OR LOSS G/CM**3
SI	28.055	.802	-.0167
AL	9.228	.071	-.0489
FE++	3.237	-.214	.0027
MG	2.223	.100	.0267
CA	3.224	-.007	-.0275
NA	2.203	.007	-.0398
K	3.064	.001	.0359
S	.494	.004	.0134
O	45.873	-2.188	.0379
C	.183	.000	.0050
SO3	.330	.000	.0090
TI	.463	.002	.0060
SUM RESIDUALS**2		5.491	
STANDARD DEVIATION		1.353	

MF-1706

MINERAL	WEIGHT PER CENT	G/CM**3	GAIN OR LOSS G/CM**3
PLAGIOCLAS	32.92	.889	-1.008
K-FELDSPAR	13.76	.373	.235
QUARTZ	17.28	.468	.193
BIOTITE	14.36	.389	.059
PYRITE	3.10	.084	.084
CALCITE	10.18	.276	.276
CHLORITE	1.51	.041	.041
KAOLINITE	6.83	.185	.185
TOTALS	99.83	2.706	.066

COMPONENT	WT.PERCENT COMPUTED	RESIDUAL	GAIN OR LOSS G/CM**3
SI	25.900	.330	-.0704
AL	8.764	.030	-.0631
FE++	3.504	.317	-.0055
MG	1.632	-.111	.0157
CA	5.033	.459	.0351
NA	1.817	-.060	-.0491
K	2.912	.015	.0305
S	1.658	-.082	.0472
O	46.053	-.980	-.0044
C	1.221	-.080	.0353
TI	.340	-.002	.0027
SUM RESIDUALS**2		1.410	
STANDARD DEVIATION		.686	

MF-1707

MINERAL	WEIGHT PER CENT	G/CM**3	GAIN OR LOSS G/CM**3
PLAGIOCLAS	44.06	1.212	-.686
K-FELDSPAR	6.31	.173	.036
QUARTZ	17.39	.478	.203
BIOTITE	20.90	.575	.245
PYRITE	.81	.022	.022
CALCITE	3.82	.105	.105
ANHYDRITE	.51	.014	.014
CHLORITE	.70	.019	.019
KAOLINITE	4.13	.114	.114
TOTALS	98.61	2.712	.072

COMPONENT	WT.PERCENT COMPUTED	RESIDUAL	GAIN OR LOSS G/CM**3
SI	27.176	.671	-.0345
AL	9.327	.064	-.0451
FE++	3.109	-.226	-.0002
MG	2.149	.104	.0247
CA	4.307	-.124	.0059
NA	2.297	.042	-.0380
K	2.561	-.004	.0225
S	.433	.003	.0118
O	46.002	-1.924	.0390
C	.458	.005	.0125
SO3	.300	.000	.0083
TI	.494	.003	.0069
SUM RESIDUALS**2		4.236	
STANDARD DEVIATION		1.188	

MF-1708

MINERAL	WEIGHT PER CENT	G/CM**3	GAIN OR LOSS G/CM**3
PLAGIOCLAS	40.73	1.116	-.741
K-FELDSPAR	5.36	.147	.009
QUARTZ	19.50	.534	.259
BIOTITE	19.83	.543	.213
PYRITE	1.54	.042	.042
CALCITE	6.22	.170	.170
ANHYDRITE	1.28	.035	.035
CHLORITE	.23	.006	.006
KAOLINITE	3.47	.095	.095
TOTALS	98.16	2.690	.050

COMPONENT	WT.PERCENT COMPUTED	RESIDUAL	GAIN OR LOSS G/CM**3
SI	26.531	.821	-.0589
AL	8.485	.069	-.0692
FE++	3.230	-.050	-.0020
MG	1.973	.025	.0219
CA	5.297	-.270	.0365
NA	2.118	.048	-.0433
K	2.353	-.005	.0166
S	.823	.003	.0225
O	45.385	-2.499	.0330
C	.746	.018	.0200
SO3	.753	.003	.0206
TI	.469	.001	.0062
SUM RESIDUALS**2		7.002	
STANDARD DEVIATION		1.528	

MF-1709

MINERAL	WEIGHT PER CENT	G/CM**3	GAIN OR LOSS G/CM**3
PLAGIOCLAS	49.70	1.357	-.541
K-FELDSPAR	4.69	.128	-.009
QUARTZ	17.69	.483	.208
BIOTITE	21.77	.594	.264
PYRITE	.41	.011	.011
CALCITE	2.22	.061	.061
ANHYDRITE	.41	.011	.011
CHLORITE	.77	.021	.021
KAOLINITE	.60	.016	.016
TOTALS	98.27	2.683	.043

COMPONENT	WT.PERCENT COMPUTED	RESIDUAL	GAIN OR LOSS G/CM**3
SI	27.643	.763	-.0296
AL	9.173	.068	-.0512
FE++	3.047	-.366	.0013
MG	2.246	.165	.0253
CA	3.975	-.356	.0022
NA	2.563	.137	-.0338
K	2.445	-.012	.0191
S	.221	.001	.0060
O	45.933	-2.144	.0335
C	.267	.005	.0072
SO3	.241	.001	.0066
TI	.515	.005	.0073
SUM RESIDUALS**2		5.491	
STANDARD DEVIATION		1.353	

MF-1710

MINERAL	WEIGHT PER CENT	G/CM**3	GAIN OR LOSS G/CM**3
PLAGICCLAS	47.97	1.324	-.573
K-FELDSPAR	5.45	.150	.013
QUARTZ	19.50	.538	.253
BIOTITE	21.42	.591	.261
PYRITE	.92	.025	.025
CALCITE	1.56	.044	.044
ANHYDRITE	.02	.000	.000
CHLORITE	1.06	.029	.029
KAOLINITE	.61	.017	.017
TOTALS	98.53	2.719	.079

COMPONENT	WT.PERCENT COMPUTED	RESIDUAL	GAIN OR LOSS G/CM**3
SI	28.230	.790	-.0060
AL	9.011	.066	-.0529
FE++	3.290	-.169	.0036
MG	2.294	.083	.0284
CA	3.501	-.201	-.0138
NA	2.484	.103	-.0343
K	2.506	-.010	.0214
S	.493	.003	.0135
O	46.054	-2.139	.0511
C	.190	.002	.0052
SO3	.010	.000	.0003
TI	.507	.003	.0073
SUM RESIDUALS**2		5.290	
STANDARD DEVIATION		1.326	

MF-1711

MINERAL	WEIGHT PER CENT	G/CM**3	GAIN OR LOSS G/CM**3
PLAGICCLAS	52.21	1.420	-.477
K-FELDSPAR	8.37	.228	.090
QUARTZ	17.72	.482	.207
BIOTITE	19.34	.526	.196
PYRITE	.51	.014	.014
CALCITE	.91	.025	.025
ANHYDRITE	.29	.008	.008
KAOLINITE	0.00	0.000	0.000
MAGNETITE	.92	.025	-.003
TOTALS	100.26	2.727	.060

COMPONENT	WT.PERCENT COMPUTED	RESIDUAL	GAIN OR LOSS G/CM**3
SI	28.729	-.067	.0198
AL	9.493	.124	-.0450
FE++	3.311	-.000	-.0018
MG	1.891	.106	.0171
CA	3.563	.061	-.0207
NA	2.732	-.079	-.0235
K	2.636	-.002	.0254
S	.270	.000	.0073
O	45.841	.156	-.0091
C	.109	-.000	.0030
SO3	.170	-.000	.0046
TI	.457	-.034	.0068
SUM RESIDUALS**2		.066	
STANDARD DEVIATION		.149	

MF-1712

MINERAL	WEIGHT PER CENT	G/CM**3	GAIN OR LOSS G/CM**3
PLAGICCLAS	46.67	1.265	-.533
K-FELDSPAR	6.66	.180	.043
QUARTZ	18.62	.505	.230
BIOTITE	19.49	.528	.198
PYRITE	1.84	.050	.050
CALCITE	3.88	.105	.105
ANHYDRITE	.19	.005	.005
CHLORITE	.18	.005	.005
KAOLINITE	2.25	.061	.061
TOTALS	99.78	2.704	.064

COMPONENT	WT.PERCENT COMPUTED	RESIDUAL	GAIN OR LOSS G/CM**3
SI	27.750	.216	-.0172
AL	9.123	.018	-.0531
FE++	3.320	-.053	-.0005
MG	1.933	.021	.0203
CA	4.392	.225	-.0031
NA	2.433	-.097	-.0314
K	2.491	.009	.0193
S	.984	.004	.0266
O	46.322	-.549	-.0088
C	.465	-.010	.0129
SO3	.110	-.000	.0030
TI	.461	-.001	.0059
SUM RESIDUALS**2		.412	
STANDARD DEVIATION		.371	

MF-2001

MINERAL	WEIGHT PER CENT	G/CM**3	GAIN OR LOSS G/CM**3
PLAGICCLAS	35.35	.944	-.954
K-FELDSPAR	13.88	.371	.233
QUARTZ	19.26	.514	.239
BIOTITE	13.78	.368	.038
PYRITE	2.02	.054	.054
CALCITE	2.74	.073	.073
ANHYDRITE	1.41	.038	.038
KAOLINITE	9.99	.267	.267
TOTALS	98.43	2.628	-.012

COMPONENT	WT.PERCENT COMPUTED	RESIDUAL	GAIN OR LOSS G/CM**3
SI	28.296	.668	-.0258
AL	9.644	.063	-.0440
FE++	1.620	-1.077	-.0199
MG	2.075	.440	.0121
CA	3.207	.276	-.0378
NA	2.119	-.136	-.0398
K	2.981	.017	.0311
S	1.079	.119	.0256
O	46.031	-1.755	-.0031
C	.329	-.012	.0091
SO3	.829	-.011	.0224
TI	.227	-.157	.0036
SUM RESIDUALS**2		5.020	
STANDARD DEVIATION		1.120	

MF-2002	WEIGHT		GAIN OR LOSS
MINERAL	PER CENT	G/CM**3	G/CM**3
PLAGIOCLAS	33.46	.927	-.971
K-FELDSPAR	17.34	.480	.345
QUARTZ	20.37	.564	.289
BIOTITE	14.24	.396	.056
PYRITE	2.56	.071	.071
CALCITE	2.32	.064	.064
ANHYDRITE	.22	.006	.006
KAOLINITE	6.21	.261	.261
TOTALS	99.26	2.750	.115

COMPONENT	WT.PERCENT COMPUTED	RESIDUAL	GAIN OR LOSS G/CM**3
SI	28.431	.659	.0161
AL	9.587	.054	-.0359
FE**	2.456	.212	-.0159
MG	1.454	.031	.0079
CA	2.843	.431	-.0451
NA	1.476	-.401	-.0369
K	3.241	.070	.0308
S	1.359	-.050	.0306
O	46.245	-1.650	.0491
C	.279	-.019	.0042
SO3	.339	-.001	.0036
TI	.324	-.030	.0032
SUM RESIDUALS**2		3.663	
STANDARD DEVIATION		.957	

MF-2003	WEIGHT		GAIN OR LOSS
MINERAL	PER CENT	G/CM**3	G/CM**3
PLAGIOCLAS	29.15	.799	-1.009
K-FELDSPAR	13.76	.378	.240
QUARTZ	16.87	.462	.187
BIOTITE	16.95	.464	.134
PYRITE	2.53	.069	.069
CALCITE	6.38	.175	.175
ANHYDRITE	.82	.022	.022
CHLORITE	5.11	.140	.140
KAOLINITE	7.01	.192	.192
TOTALS	98.60	2.702	.062

COMPONENT	WT.PERCENT COMPUTED	RESIDUAL	GAIN OR LOSS G/CM**3
SI	25.796	.608	-.0769
AL	8.961	.059	-.0961
FE**	4.192	.272	.0192
MG	2.487	-.142	.0406
CA	4.533	-.112	.0113
NA	1.629	.018	-.0561
K	2.913	-.005	.0341
S	1.350	-.030	.0376
O	45.040	-2.140	.0172
C	.765	.012	.0206
SO3	.441	.001	.0332
TI	.364	.000	.0039
SUM RESIDUALS**2		5.353	
STANDARD DEVIATION		1.336	

MF-2004	WEIGHT		GAIN OR LOSS
MINERAL	PER CENT	G/CM**3	G/CM**3
PLAGIOCLAS	24.29	.629	-1.268
K-FELDSPAR	14.73	.382	.244
QUARTZ	21.58	.559	.284
BIOTITE	19.37	.502	.172
PYRITE	2.72	.070	.070
CALCITE	2.42	.063	.063
ANHYDRITE	.70	.018	.018
CHLORITE	2.00	.052	.052
KAOLINITE	11.14	.289	.289
TOTALS	98.96	2.563	-.077

COMPONENT	WT.PERCENT COMPUTED	RESIDUAL	GAIN OR LOSS G/CM**3
SI	27.959	.799	-.0600
AL	9.229	.071	-.0626
FE**	4.006	.143	.0182
MG	2.271	-.058	.0288
CA	2.626	.367	-.0575
NA	1.385	-.217	-.0565
K	3.283	.079	.0350
S	1.492	-.018	.0381
O	45.608	-2.171	-.0415
C	.291	-.023	.0061
SO3	.434	-.006	.0109
TI	.439	-.005	.0069
SUM RESIDUALS**2		5.568	
STANDARD DEVIATION		1.362	

MF-2005	WEIGHT		GAIN OR LOSS
MINERAL	PER CENT	G/CM**3	G/CM**3
PLAGIOCLAS	39.67	1.087	-.810
K-FELDSPAR	10.55	.289	.152
QUARTZ	21.41	.587	.312
BIOTITE	18.85	.517	.187
PYRITE	1.66	.046	.046
CALCITE	1.31	.036	.036
ANHYDRITE	.77	.021	.021
CHLORITE	.42	.012	.012
KAOLINITE	4.99	.137	.137
TOTALS	99.65	2.730	.090

COMPONENT	WT.PERCENT COMPUTED	RESIDUAL	GAIN OR LOSS G/CM**3
SI	28.692	.236	.0218
AL	9.251	.019	-.0460
FE**	3.167	.143	-.0390
MG	1.983	-.040	.0250
CA	3.118	.488	-.0439
NA	2.116	-.629	-.0245
K	2.752	.054	.0259
S	.889	-.011	.0247
O	46.410	-.556	.0079
C	.157	-.006	.0045
SO3	.455	-.007	.0126
TI	.427	-.004	.0052
SUM RESIDUALS**2		1.029	
STANDARD DEVIATION		.566	

MF-2006 MINERAL	WEIGHT PER CENT	G/CM**3	GAIN OR LOSS G/CM**3
PLAGIOCLAS	47.14	1.301	-.597
K-FELDSPAR	2.02	.056	-.082
QUARTZ	17.02	.470	.195
BIOTITE	26.46	.730	.400
PYRITE	1.23	.034	.034
CALCITE	.91	.025	.025
ANHYDRITE	1.94	.053	.053
CHLORITE	.91	.025	.025
KAOLINITE	1.10	.030	.030
TOTALS	98.72	2.725	.085

COMPONENT	WT.PERCENT COMPUTED	RESIDUAL	GAIN OR LOSS G/CM**3
SI	26.791	.753	-.0448
AL	9.176	.072	-.0485
FE++	3.986	.169	.0134
MG	2.830	-.114	.0497
CA	3.746	.016	-.0130
NA	2.401	-.003	-.0337
K	2.276	.001	.0148
S	.656	-.004	.0182
O	45.011	-2.169	.0232
C	.109	.000	.0030
SO3	1.140	-.000	.0315
TI	.600	.000	.0099
SUM RESIDUALS**2		5.320	
STANDARD DEVIATION		1.332	

MF-2007 MINERAL	WEIGHT PER CENT	G/CM**3	GAIN OR LOSS G/CM**3
PLAGIOCLAS	43.66	1.205	-.693
K-FELDSPAR	4.28	.118	-.019
QUARTZ	14.75	.407	.132
BIOTITE	24.34	.672	.342
PYRITE	1.85	.051	.051
CALCITE	1.71	.047	.047
ANHYDRITE	4.38	.121	.121
CHLORITE	.83	.023	.023
KAOLINITE	3.28	.090	.090
TOTALS	99.07	2.734	.094

COMPONENT	WT.PERCENT COMPUTED	RESIDUAL	GAIN OR LOSS G/CM**3
SI	25.611	.565	-.0721
AL	9.270	.060	-.0456
FE++	4.000	.215	.0126
MG	2.603	-.130	.0439
CA	4.576	.031	.0095
NA	2.250	-.006	-.0378
K	2.392	.002	.0180
S	.987	-.013	.0276
O	44.047	-1.650	-.0178
C	.205	-.000	.0056
SO3	2.576	-.004	.0712
TI	.552	.000	.0086
SUM RESIDUALS**2		3.108	
STANDARD DEVIATION		1.018	

MF-2008 MINERAL	WEIGHT PER CENT	G/CM**3	GAIN OR LOSS G/CM**3
PLAGIOCLAS	43.77	1.217	-.681
K-FELDSPAR	3.24	.090	-.047
QUARTZ	16.86	.469	.194
BIOTITE	23.03	.640	.310
PYRITE	1.99	.055	.055
CALCITE	1.55	.043	.043
ANHYDRITE	4.28	.119	.119
CHLORITE	.89	.025	.025
KAOLINITE	2.81	.078	.078
TOTALS	98.41	2.736	.096

COMPONENT	WT.PERCENT COMPUTED	RESIDUAL	GAIN OR LOSS G/CM**3
SI	25.952	.868	-.0661
AL	8.978	.085	-.0526
FE++	3.917	.225	.0107
MG	2.478	-.127	.0409
CA	4.490	-.020	.0094
NA	2.244	.011	-.0379
K	2.167	.000	.0122
S	1.063	-.017	.0300
O	43.899	-2.620	.0142
C	.186	.000	.0052
SO3	2.515	.005	.0698
TI	.522	.000	.0079
SUM RESIDUALS**2		7.693	
STANDARD DEVIATION		1.601	

MF-2009 MINERAL	WEIGHT PER CENT	G/CM**3	GAIN OR LOSS G/CM**3
PLAGIOCLAS	40.96	1.122	-.775
K-FELDSPAR	4.62	.127	-.011
QUARTZ	17.57	.481	.206
BIOTITE	15.92	.436	.106
PYRITE	3.51	.096	.096
CALCITE	2.56	.070	.070
ANHYDRITE	6.74	.185	.185
CHLORITE	1.49	.041	.041
KAOLINITE	4.12	.113	.113
TOTALS	97.48	2.671	.031

COMPONENT	WT.PERCENT COMPUTED	RESIDUAL	GAIN OR LOSS G/CM**3
SI	25.020	.978	-.1047
AL	8.564	.095	-.0677
FE++	3.860	.821	-.0086
MG	1.843	-.672	.0374
CA	5.452	-.451	.0458
NA	2.117	.069	-.0439
K	1.806	-.004	.0016
S	1.878	-.402	.0625
O	42.313	-3.058	-.0358
C	.307	.005	.0083
SO3	3.961	.101	.1058
TI	.361	.001	.0033
SUM RESIDUALS**2		11.823	
STANDARD DEVIATION		1.985	

MF-2019	WEIGHT		GAIN OR LOSS
MINERAL	PER CENT	G/CM**3	G/CM**3
PLAGIOCLAS	39.51	1.079	-.819
K-FELDSPAR	5.72	.156	.059
QUARTZ	26.94	.462	.197
BIOTITE	14.92	.462	.132
PYRITE	4.44	.121	.121
CALCITE	3.26	.089	.089
ANHYDRITE	5.32	.145	.145
CHLORITE	3.23	.088	.088
KAOLINITE	3.71	.101	.101
TOTALS	99.05	2.704	.064

COMPONENT	WT.PERCENT COMPUTED	RESIDUAL	GAIN OR LOSS G/CM**3
SI	25.016	.540	-.0092
AL	8.427	.052	-.0057
FE**	4.730	.029	.0119
MG	2.204	-.613	.0454
CA	5.224	.294	.0398
NA	2.096	-.091	-.0425
K	2.014	.005	.0006
S	2.375	-.445	.0770
O	42.407	-1.954	-.0642
C	.311	-.009	.0103
SO3	3.130	-.040	.0066
TI	.346	-.000	.0029
SUM RESIDUALS**2		4.245	
STANDARD DEVIATION		1.190	

MF-2017	WEIGHT		GAIN OR LOSS
MINERAL	PER CENT	G/CM**3	G/CM**3
PLAGIOCLAS	22.56	.616	-1.282
K-FELDSPAR	15.62	.426	.289
QUARTZ	26.33	.719	.444
BIOTITE	15.77	.431	.101
PYRITE	4.17	.114	.114
CALCITE	3.56	.097	.097
ANHYDRITE	1.48	.040	.040
CHLORITE	.74	.020	.020
KAOLINITE	9.38	.256	.256
TOTALS	99.61	2.719	.079

COMPONENT	WT.PERCENT COMPUTED	RESIDUAL	GAIN OR LOSS G/CM**3
SI	28.664	.536	.0045
AL	8.240	.036	-.0756
FE**	4.012	.140	.0138
MG	1.716	-.033	.0165
CA	3.207	.405	-.0395
NA	1.307	-.174	-.0469
K	3.123	.052	.0159
S	2.228	-.042	.0620
O	45.458	-1.301	-.0325
C	.427	-.037	.0127
SO3	.870	-.020	.0243
TI	.158	-.002	.0032
SUM RESIDUALS**2		2.169	
STANDARD DEVIATION		.464	

MF-2015	WEIGHT		GAIN OR LOSS
MINERAL	PER CENT	G/CM**3	G/CM**3
PLAGIOCLAS	29.70	.814	-1.044
K-FELDSPAR	11.53	.321	.233
QUARTZ	22.75	.626	.349
BIOTITE	13.36	.419	.189
PYRITE	2.61	.072	.072
CALCITE	2.83	.077	.077
CHLORITE	.33	.009	.009
KAOLINITE	8.02	.220	.220
TOTALS	99.72	2.705	.065

COMPONENT	WT.PERCENT COMPUTED	RESIDUAL	GAIN OR LOSS G/CM**3
SI	25.683	.815	-.0051
AL	5.705	.065	-.0576
FE**	3.604	-.252	.0137
MG	1.924	.078	.0206
CA	2.983	.266	-.0437
NA	1.245	-.143	-.0510
K	3.111	.034	.0342
S	1.349	.024	.0575
O	46.459	-2.159	.0363
C	.339	-.016	.0097
TI	.429	-.002	.0052
SUM RESIDUALS**2		5.493	
STANDARD DEVIATION		1.353	

MF-2013	WEIGHT		GAIN OR LOSS
MINERAL	PER CENT	G/CM**3	G/CM**3
PLAGIOCLAS	50.75	1.391	-.507
K-FELDSPAR	8.69	.238	.101
QUARTZ	15.93	.436	.181
BIOTITE	20.16	.552	.222
PYRITE	.45	.012	.012
CALCITE	1.46	.040	.040
ANHYDRITE	.69	.019	.019
CHLORITE	.95	.026	.026
TOTALS	99.06	2.714	.074

COMPONENT	WT.PERCENT COMPUTED	RESIDUAL	GAIN OR LOSS G/CM**3
SI	27.432	.532	-.0154
AL	9.598	.335	-.0460
FE**	2.859	-.515	.0005
MG	2.194	.209	.0229
CA	3.611	-.020	-.0110
NA	2.695	-.093	-.0256
K	2.835	-.013	.0246
S	.242	.002	.0066
O	46.201	-1.420	.0256
C	.175	.000	.0048
SO3	.400	.000	.0110
TI	.457	.001	.0059
SUM RESIDUALS**2		2.725	
STANDARD DEVIATION		.625	

MF-2014 MINERAL	WEIGHT PER CENT	G/CM**3	GAIN OR LOSS G/CM**3
PLAGIOCLAS	42.28	1.150	-.748
K-FELDSPAR	12.12	.330	.192
QUARTZ	18.08	.492	.217
BIOTITE	20.10	.547	.217
PYRITE	1.37	.037	.037
CALCITE	2.55	.069	.069
ANHYDRITE	.60	.016	.016
CHLORITE	.23	.006	.006
KAOLINITE	1.43	.039	.039
TOTALS	98.75	2.686	.046

COMPONENT	WT.PERCENT COMPUTED	RESIDUAL	GAIN OR LOSS G/CM**3
SI	27.827	.761	-.0272
AL	9.011	.065	-.0565
FE++	3.148	-.016	-.0058
MG	2.081	.012	.0248
CA	3.716	.021	-.0155
NA	2.264	-.006	-.0383
K	3.041	.003	.0346
S	.731	.001	.0199
O	45.817	-2.094	.0242
C	.305	-.000	.0083
SO3	.350	-.000	.0095
TI	.456	.000	.0058
SUM RESIDUALS**2		4.969	
STANDARD DEVIATION		1.287	

MF-2015 MINERAL	WEIGHT PER CENT	G/CM**3	GAIN OR LOSS G/CM**3
PLAGIOCLAS	49.09	1.355	-.543
K-FELDSPAR	4.77	.132	-.006
QUARTZ	17.42	.481	.206
BIOTITE	23.90	.660	.330
PYRITE	.52	.014	.014
CALCITE	2.01	.056	.056
CHLORITE	.65	.018	.018
KAOLINITE	.54	.015	.015
TOTALS	98.91	2.730	.090

COMPONENT	WT.PERCENT COMPUTED	RESIDUAL	GAIN OR LOSS G/CM**3
SI	27.683	.523	-.0138
AL	9.364	.048	-.0427
FE++	3.299	-.074	.0012
MG	2.531	.052	.0369
CA	3.734	-.361	-.0030
NA	2.529	.148	-.0343
K	2.428	-.013	.0194
S	.280	.000	.0077
O	46.280	-1.417	.0374
C	.242	.004	.0066
TI	.542	.002	.0083
SUM RESIDUALS**2		2.445	
STANDARD DEVIATION		.903	

MF-2016 MINERAL	WEIGHT PER CENT	G/CM**3	GAIN OR LOSS G/CM**3
PLAGIOCLAS	46.93	1.281	-.616
K-FELDSPAR	5.34	.146	.008
QUARTZ	18.40	.502	.227
BIOTITE	23.57	.643	.313
PYRITE	.30	.008	.008
CALCITE	2.22	.061	.061
ANHYDRITE	1.14	.031	.031
CHLORITE	.25	.007	.007
KAOLINITE	1.43	.039	.039
MAGNETITE	.34	.009	-.018
TOTALS	99.91	2.728	.060

COMPONENT	WT.PERCENT COMPUTED	RESIDUAL	GAIN OR LOSS G/CM**3
SI	27.828	.013	-.0041
AL	9.264	.001	-.0469
FE++	3.327	.000	-.0011
MG	2.437	.000	.0350
CA	4.024	-.114	-.0030
NA	2.426	.045	-.0350
K	2.470	-.004	.0195
S	.160	-.000	.0044
O	46.504	-.033	-.0085
C	.266	.002	.0072
SO3	.671	.001	.0183
TI	.534	.001	.0080
SUM RESIDUALS**2		.016	
STANDARD DEVIATION		.090	

MF-2017 MINERAL	WEIGHT PER CENT	G/CM**3	GAIN OR LOSS G/CM**3
PLAGIOCLAS	49.40	1.339	-.559
K-FELDSPAR	7.13	.193	.056
QUARTZ	16.72	.453	.178
BIOTITE	21.61	.586	.256
PYRITE	.41	.011	.011
CALCITE	3.04	.082	.082
KAOLINITE	1.06	.029	.029
MAGNETITE	.65	.018	-.010
TOTALS	100.03	2.711	.043

COMPONENT	WT.PERCENT COMPUTED	RESIDUAL	GAIN OR LOSS G/CM**3
SI	27.761	-.053	-.0096
AL	9.523	-.005	-.0416
FE++	3.319	-.000	-.0020
MG	2.201	.132	.0246
CA	4.165	-.223	.0129
NA	2.570	.085	-.0327
K	2.549	-.008	.0213
S	.220	.000	.0060
O	46.864	.132	-.0126
C	.365	.005	.0098
TI	.490	-.038	.0077
SUM RESIDUALS**2		.096	
STANDARD DEVIATION		.179	

MF-2018

MINERAL	WEIGHT PER CENT	G/CM**3	GAIN OR LOSS G/CM**3
PLAGIOCLAS	52.80	1.452	-.446
K-FELDSPAR	7.64	.210	.073
QUARTZ	17.33	.477	.202
BIOTITE	19.48	.536	.206
PYRITE	.22	.006	.006
CALCITE	1.08	.030	.030
ANHYDRITE	.98	.027	.027
MAGNETITE	.77	.021	-.006
TOTALS	100.30	2.758	.091

COMPONENT	WT.PERCENT COMPUTED	RESIDUAL	GAIN OR LOSS G/CM**3
SI	28.453	-.109	.0221
AL	9.633	-.001	-.0349
FE++	3.054	-.000	-.0079
MG	1.964	.150	.0189
CA	3.872	.227	-.0158
NA	2.747	-.176	-.0196
K	2.459	.010	.0193
S	.120	.000	.0033
O	46.832	.255	.0018
C	.130	-.001	.0036
SO3	.577	-.003	.0160
TI	.442	-.050	.0069
SUM RESIDUALS**2		.185	
STANDARD DEVIATION		.215	

MF-2201

MINERAL	WEIGHT PER CENT	G/CM**3	GAIN OR LOSS G/CM**3
PLAGIOCLAS	25.25	0.000	-1.898
K-FELDSPAR	18.15	0.000	-.138
QUARTZ	23.68	0.000	-.275
BIOTITE	11.32	0.000	-.330
PYRITE	2.61	0.000	0.000
CALCITE	4.60	0.000	0.000
ANHYDRITE	1.28	0.000	0.000
CHLORITE	.73	0.000	0.000
KAOLINITE	11.44	0.000	0.000
TOTALS	99.07	0.000	-2.640

COMPONENT	WT.PERCENT COMPUTED	RESIDUAL	GAIN OR LOSS G/CM**3
SI	28.775	.774	-.7634
AL	8.954	.061	-.2998
FE++	2.697	.288	-.0919
MG	1.146	-.108	-.0315
CA	3.542	.219	-.1160
NA	1.575	-.049	-.1000
K	3.174	.020	-.0480
S	1.394	-.096	0.0000
O	46.206	-2.016	-1.2790
C	.552	-.021	0.0000
SO3	.754	-.006	0.0000
TI	.295	.001	-.0066
SUM RESIDUALS**2		4.824	
STANDARD DEVIATION		1.268	

MF-2202

MINERAL	WEIGHT PER CENT	G/CM**3	GAIN OR LOSS G/CM**3
PLAGIOCLAS	30.74	.815	-1.093
K-FELDSPAR	11.47	.304	.166
QUARTZ	18.67	.495	.220
BIOTITE	13.93	.369	.039
PYRITE	1.43	.038	.038
CALCITE	1.21	.032	.032
ANHYDRITE	1.11	.029	.029
CHLORITE	1.81	.048	.048
KAOLINITE	7.82	.207	.207
ALBITE	11.61	.308	.308
TOTALS	99.79	2.645	.005

COMPONENT	WT.PERCENT COMPUTED	RESIDUAL	GAIN OR LOSS G/CM**3
SI	29.396	.189	.0106
AL	9.687	.016	-.0435
FE++	2.662	.330	-.0301
MG	1.531	-.278	.0165
CA	2.416	.000	-.0520
NA	2.812	.001	-.0255
K	2.582	.000	.0204
S	.766	-.034	.0212
O	46.783	-.434	-.0277
C	.145	.000	.0038
SO3	.650	-.000	.0172
TI	.363	.003	.0029
SUM RESIDUALS**2		.412	
STANDARD DEVIATION		.454	

MF-2203

MINERAL	WEIGHT PER CENT	G/CM**3	GAIN OR LOSS G/CM**3
PLAGIOCLAS	35.06	.926	-.972
K-FELDSPAR	7.92	.209	.072
QUARTZ	12.30	.325	.050
BIOTITE	21.07	.556	.226
PYRITE	2.73	.072	.072
CALCITE	1.14	.030	.030
ANHYDRITE	2.11	.056	.056
CHLORITE	1.61	.043	.043
KAOLINITE	3.05	.081	.081
ALBITE	12.56	.332	.332
TOTALS	99.56	2.629	-.011

COMPONENT	WT.PERCENT COMPUTED	RESIDUAL	GAIN OR LOSS G/CM**3
SI	26.959	.347	-.0608
AL	9.189	.032	-.0580
FE++	4.211	.176	.0146
MG	2.378	-.077	.0333
CA	2.910	.001	-.0392
NA	3.088	.001	-.0185
K	2.748	.001	.0245
S	1.459	-.021	.0391
O	44.772	-.896	-.0734
C	.136	.000	.0036
SO3	1.240	.000	.0327
TI	.473	-.000	.0059
SUM RESIDUALS**2		.962	
STANDARD DEVIATION		.693	

MF-2204

MINERAL	WEIGHT PER CENT	G/CM**3	GAIN OR LOSS G/CM**3
PLAGIOCLAS	49.96	0.000	-1.898
K-FELDSPAR	2.82	0.000	-.138
QUARTZ	16.18	0.000	-.275
BIOTITE	20.16	0.000	-.330
PYRITE	1.17	0.000	0.000
CALCITE	1.56	0.000	0.000
ANHYDRITE	.71	0.000	0.000
CHLORITE	3.80	0.000	0.000
KAOLINITE	3.71	0.000	0.000
TOTALS	100.06	0.000	-2.640

COMPONENT	WT.PERCENT COMPUTED	RESIDUAL	GAIN OR LOSS G/CM**3
SI	27.643	.016	-.7634
AL	9.741	.002	-.2998
FE++	3.760	.247	-.0919
MG	2.609	-.190	-.0315
CA	3.446	.323	-.1160
NA	2.731	-.295	-.1000
K	2.097	.013	-.0480
S	.623	-.007	0.0000
O	46.351	-.040	-1.2790
C	.187	-.004	0.0000
SO3	.417	-.003	0.0000
TI	.453	-.003	-.0066
SUM RESIDUALS**2		.291	
STANDARD DEVIATION		.311	

MF-2205

MINERAL	WEIGHT PER CENT	G/CM**3	GAIN OR LOSS G/CM**3
PLAGIOCLAS	38.19	1.035	-.662
K-FELDSPAR	8.14	.221	.083
QUARTZ	15.99	.433	.158
BIOTITE	19.80	.537	.207
PYRITE	2.28	.062	.062
CALCITE	1.92	.052	.052
ANHYDRITE	1.50	.041	.041
CHLORITE	4.62	.125	.125
KAOLINITE	6.41	.174	.174
TOTALS	98.85	2.679	.039

COMPONENT	WT.PERCENT COMPUTED	RESIDUAL	GAIN OR LOSS G/CM**3
SI	26.654	.616	-.0578
AL	9.378	.062	-.0473
FE++	4.391	.370	.0168
MG	2.693	-.232	.0478
CA	3.209	-.301	-.0209
NA	2.154	.103	-.0443
K	2.682	-.016	.0251
S	1.219	-.031	.0339
O	44.921	-1.736	-.0146
C	.231	.004	.0061
SO3	.879	.009	.0236
TI	.445	.001	.0054
SUM RESIDUALS**2		3.690	
STANDARD DEVIATION		1.109	

MF-2206

MINERAL	WEIGHT PER CENT	G/CM**3	GAIN OR LOSS G/CM**3
PLAGIOCLAS	54.21	1.485	-.412
K-FELDSPAR	1.33	.037	-.101
QUARTZ	14.20	.389	.114
BIOTITE	21.09	.578	.245
PYRITE	1.07	.029	.029
CALCITE	1.29	.035	.035
ANHYDRITE	3.38	.093	.093
CHLORITE	1.65	.045	.045
KAOLINITE	1.70	.046	.046
TOTALS	99.92	2.738	.098

COMPONENT	WT.PERCENT COMPUTED	RESIDUAL	GAIN OR LOSS G/CM**3
SI	26.795	.103	-.0320
AL	9.538	.010	-.0387
FE++	3.466	-.040	.0042
MG	2.307	.021	.0311
CA	4.346	.258	-.0040
NA	2.944	-.142	-.0154
K	1.998	.006	.0066
S	.571	.001	.0156
O	45.363	-.263	-.0288
C	.154	-.001	.0043
SO3	1.989	-.031	.0553
TI	.449	-.001	.0057
SUM RESIDUALS**2		.170	
STANDARD DEVIATION		.238	

MF-2207

MINERAL	WEIGHT PER CENT	G/CM**3	GAIN OR LOSS G/CM**3
PLAGIOCLAS	50.79	1.381	-.516
K-FELDSPAR	2.70	.073	-.064
QUARTZ	15.24	.415	.140
BIOTITE	22.10	.601	.271
PYRITE	1.20	.033	.033
CALCITE	1.23	.033	.033
ANHYDRITE	3.46	.094	.094
CHLORITE	.00	.000	.000
KAOLINITE	3.07	.084	.084
TOTALS	99.78	2.714	.074

COMPONENT	WT.PERCENT COMPUTED	RESIDUAL	GAIN OR LOSS G/CM**3
SI	27.032	.199	-.0336
AL	9.441	.019	-.0435
FE++	3.356	.014	-.0010
MG	2.161	.056	.0258
CA	4.167	.036	-.0036
NA	2.775	-.015	-.0241
K	2.234	.001	.0127
S	.640	-.000	.0174
O	45.321	-.510	-.0324
C	.147	-.000	.0040
SO3	2.036	-.004	.0555
TI	.470	-.015	.0066
SUM RESIDUALS**2		.306	
STANDARD DEVIATION		.319	

MF-2208

MINERAL	WEIGHT PER CENT	G/CM**3	GAIN OR LOSS G/CM**3
PLAGIOCLAS	42.31	1.168	-.730
K-FELDSPAR	2.73	.075	-.062
QUARTZ	19.99	.552	.277
BIOTITE	18.87	.521	.191
PYRITE	1.84	.051	.051
CALCITE	1.76	.049	.049
ANHYDRITE	5.35	.148	.148
CHLORITE	1.34	.037	.037
KAOLINITE	4.98	.137	.137
TOTALS	99.17	2.737	.097

COMPONENT	WT.PERCENT COMPUTED	RESIDUAL	GAIN OR LOSS G/CM**3
SI	26.976	.518	-.0331
AL	8.671	.043	-.0617
FE++	3.493	.182	-.0005
MG	2.045	-.090	.0274
CA	4.493	-.195	.0134
NA	2.317	.047	-.0373
K	1.956	-.003	.0061
S	.986	-.014	.0276
O	44.473	-1.364	-.0139
C	.212	.001	.0058
SO3	3.144	.044	.0856
TI	.401	-.000	.0045
SUM RESIDUALS**2		2.215	
STANDARD DEVIATION		.859	

MF-2209

MINERAL	WEIGHT PER CENT	G/CM**3	GAIN OR LOSS G/CM**3
PLAGIOCLAS	40.87	1.165	-.733
K-FELDSPAR	.41	.012	-.126
QUARTZ	19.48	.555	.280
BIOTITE	15.69	.447	.117
PYRITE	1.92	.055	.055
CALCITE	4.52	.129	.129
ANHYDRITE	7.98	.228	.228
CHLORITE	4.37	.125	.125
KAOLINITE	4.04	.115	.115
TOTALS	99.29	2.830	.190

COMPONENT	WT.PERCENT COMPUTED	RESIDUAL	GAIN OR LOSS G/CM**3
SI	25.244	.216	-.0501
AL	8.116	.018	-.0690
FE++	3.683	.597	-.0040
MG	2.189	-.592	.0477
CA	6.297	-.450	.0763
NA	2.212	.046	-.0383
K	1.418	-.002	-.0075
S	1.025	-.065	.0311
O	43.537	-.589	-.0214
C	.542	.010	.0192
SO3	4.695	.105	.1308
TI	.334	-.002	.0030
SUM RESIDUALS**2		1.320	
STANDARD DEVIATION		.663	

MF-2210

MINERAL	WEIGHT PER CENT	G/CM**3	GAIN OR LOSS G/CM**3
PLAGIOCLAS	52.78	1.425	-.472
K-FELDSPAR	1.13	.030	-.107
QUARTZ	14.31	.386	.111
BIOTITE	21.42	.578	.248
PYRITE	1.09	.030	.030
CALCITE	2.35	.063	.063
ANHYDRITE	1.36	.037	.037
CHLORITE	3.99	.108	.108
TOTALS	98.44	2.658	.018

COMPONENT	WT.PERCENT COMPUTED	RESIDUAL	GAIN OR LOSS G/CM**3
SI	26.289	.625	-.0705
AL	9.293	.188	-.0540
FE++	4.097	.241	.0122
MG	2.453	-.142	.0389
CA	4.103	-.857	.0179
NA	2.864	.216	-.0285
K	2.034	-.017	.0074
S	.585	-.005	.0159
O	45.053	-1.831	-.0132
C	.282	.009	.0074
SO3	.801	.011	.0213
TI	.576	.000	.0089
SUM RESIDUALS**2		4.638	
STANDARD DEVIATION		1.077	

MF-2211

MINERAL	WEIGHT PER CENT	G/CM**3	GAIN OR LOSS G/CM**3
PLAGIOCLAS	53.42	1.410	-.497
K-FELDSPAR	0.00	0.000	-.138
QUARTZ	14.60	.385	.110
BIOTITE	19.80	.523	.193
PYRITE	1.11	.029	.029
CALCITE	1.24	.033	.033
ANHYDRITE	1.23	.033	.033
CHLORITE	5.01	.132	.132
KAOLINITE	.67	.018	.018
TOTALS	97.08	2.563	-.077

COMPONENT	WT.PERCENT COMPUTED	RESIDUAL	GAIN OR LOSS G/CM**3
SI	26.278	.847	-.0920
AL	9.417	.260	-.0580
FE++	4.074	.335	.0068
MG	2.467	-.223	.0395
CA	3.656	-2.040	.0344
NA	2.885	.341	-.0328
K	1.766	.181	-.0061
S	.592	-.008	.0158
O	44.535	-2.544	-.0361
C	.149	.004	.0038
SO3	.726	.016	.0187
TI	.532	-.091	.0099
SUM RESIDUALS**2		11.738	
STANDARD DEVIATION		1.978	

MF-2212	WEIGHT		GAIN OR LOSS
MINERAL	PER CENT	G/CM**3	G/CM**3
PLAGIOCLAS	61.43	1.689	-.200
K-FELDSPAR	1.86	.051	-.036
QUARTZ	9.41	.220	-.035
BIOTITE	22.04	.606	.276
PYRITE	.55	.014	.014
CALCITE	1.04	.026	.026
ANHYDRITE	.02	.005	.005
CHLORITE	3.02	.083	.083
KAOLINITE	0.00	0.000	0.000
TOTALS	103.29	2.757	.157

COMPONENT	WT.PERCENT COMPUTED	RESIDUAL	GAIN OR LOSS G/CM**3
SI	26.773	.065	-.0204
AL	10.484	.956	-.0178
FE**	3.726	.119	.0073
MG	2.378	-.119	.0172
CA	3.733	-.577	.0241
NA	3.542	.039	-.0012
K	2.199	-.042	.0136
S	.269	-.001	.0076
O	46.262	-.214	-.0312
C	.124	.002	.0034
SO3	.322	.002	.0088
TI	.592	.005	.0096
SUM RESIDUALS**2		1.332	
STANDARD DEVIATION		.666	

MF-2213	WEIGHT		GAIN OR LOSS
MINERAL	PER CENT	G/CM**3	G/CM**3
PLAGIOCLAS	51.55	1.422	-.475
K-FELDSPAR	2.30	.064	-.074
QUARTZ	14.77	.409	.134
BIOTITE	22.45	.622	.232
PYRITE	.43	.012	.012
CALCITE	1.71	.050	.050
ANHYDRITE	.06	.018	.018
CHLORITE	4.35	.121	.121
TOTALS	98.10	2.717	.077

COMPONENT	WT.PERCENT COMPUTED	RESIDUAL	GAIN OR LOSS G/CM**3
SI	26.710	.625	-.0209
AL	9.526	.116	-.0447
FE**	3.691	.112	.0155
MG	2.466	-.066	.0425
CA	3.996	-1.192	.0186
NA	2.801	.308	-.0310
K	2.255	-.027	.0152
S	.250	-.300	.0984
O	45.178	-1.795	.0277
C	.215	.008	.0357
SO3	.334	.004	.0105
TI	.603	.004	.0160
SUM RESIDUALS**2		5.162	
STANDARD DEVIATION		1.136	

MF-2214	WEIGHT		GAIN OR LOSS
MINERAL	PER CENT	G/CM**3	G/CM**3
PLAGIOCLAS	50.74	1.380	-.517
K-FELDSPAR	2.47	.067	-.070
QUARTZ	15.25	.415	.140
BIOTITE	24.24	.659	.329
PYRITE	.82	.022	.022
CALCITE	1.98	.054	.054
ANHYDRITE	.10	.003	.003
CHLORITE	3.04	.083	.083
TOTALS	98.64	2.683	.063

COMPONENT	WT.PERCENT COMPUTED	RESIDUAL	GAIN OR LOSS G/CM**3
SI	26.950	.492	-.0437
AL	9.256	.099	-.0507
FE**	4.170	.105	.0187
MG	2.575	-.055	.0400
CA	3.477	-.097	.0030
NA	2.769	.277	-.0322
K	2.421	-.026	.0186
S	.439	-.001	.0120
O	45.635	-1.362	-.0307
C	.234	.006	.0062
SO3	.060	.000	.0016
TI	.652	.004	.0110
SUM RESIDUALS**2		3.002	
STANDARD DEVIATION		.866	

MF-2601	WEIGHT		GAIN OR LOSS
MINERAL	PER CENT	G/CM**3	G/CM**3
PLAGIOCLAS	29.90	.786	-1.111
K-FELDSPAR	8.61	.226	.069
QUARTZ	20.31	.534	.259
BIOTITE	16.25	.427	.097
PYRITE	4.22	.111	.111
CALCITE	1.02	.027	.027
ANHYDRITE	.87	.023	.023
CHLORITE	1.98	.052	.052
KAOLINITE	7.33	.193	.193
ALBITE	9.52	.250	.250
TOTALS	100.01	2.630	-.010

COMPONENT	WT.PERCENT COMPUTED	RESIDUAL	GAIN OR LOSS G/CM**3
SI	28.561	.186	-.0171
AL	9.259	.015	-.0567
FE**	4.466	.616	.0093
MG	1.733	-.143	.0178
CA	2.273	.000	-.0562
NA	2.545	.000	-.0331
K	2.408	.000	.0153
S	2.257	-.223	.6652
O	45.699	-.427	-.0711
C	.123	.000	.0032
SO3	.510	-.000	.0136
TI	.392	-.014	.0038
SUM RESIDUALS**2		.667	
STANDARD DEVIATION		.578	

MF-2602	WEIGHT		GAIN OR LOSS
MINERAL	PER CENT	G/CM**3	G/CM**3
PLAGICCLAS	33.96	.808	-1.090
K-FELDSPAR	6.53	.176	.033
QUARTZ	18.77	.498	.215
BIOTITE	16.26	.424	.096
PYRITE	3.41	.089	.089
CALCITE	1.11	.029	.029
ANHYDRITE	.59	.015	.015
CHLORITE	1.75	.046	.046
KAOLINITE	7.06	.184	.184
ALBITE	13.64	.353	.353
TOTALS	99.46	2.604	-.031

COMPONENT	WT.PERCENT COMPUTED	RESIDUAL	GAIN OR LOSS G/CM**3
SI	28.637	.218	-.0204
AL	9.520	.019	-.0518
FE**	4.051	.662	-.0036
MG	1.697	-.203	.0181
CA	2.280	.000	-.0565
NA	2.926	.001	-.0237
K	2.167	.000	.0086
S	2.823	-.207	.0530
O	45.996	-.510	-.0662
C	.134	.000	.0035
SO3	.340	-.000	.0069
TI	.302	-.019	.0039
SUM RESIDUALS**2		.630	
STANDARD DEVIATION		.644	

MF-2603	WEIGHT		GAIN OR LOSS
MINERAL	PER CENT	G/CM**3	G/CM**3
PLAGICCLAS	28.65	.746	-1.112
K-FELDSPAR	6.25	.171	.034
QUARTZ	19.66	.539	.264
BIOTITE	16.85	.462	.132
PYRITE	4.66	.126	.126
CALCITE	.82	.022	.022
ANHYDRITE	1.34	.037	.037
KAOLINITE	8.01	.219	.219
CHLORITE	1.94	.054	.054
ALBITE	11.92	.326	.326
TOTALS	100.08	2.742	.102

COMPONENT	WT.PERCENT COMPUTED	RESIDUAL	GAIN OR LOSS G/CM**3
SI	26.221	.127	.0064
AL	9.311	.031	-.0490
FE**	4.251	.569	.0227
MG	1.745	-.115	.0206
CA	2.266	.000	-.0539
NA	2.649	.000	-.0274
K	2.179	.000	.0116
S	2.493	-.207	.0740
O	45.147	-.291	-.0148
C	.056	.000	.0027
SO3	.790	-.000	.0216
TI	.396	-.011	.0046
SUM RESIDUALS**2		.460	
STANDARD DEVIATION		.490	

MF-2604	WEIGHT		GAIN OR LOSS
MINERAL	PER CENT	G/CM**3	G/CM**3
PLAGICCLAS	33.73	.917	-.980
K-FELDSPAR	6.64	.181	.043
QUARTZ	19.78	.538	.263
BIOTITE	16.09	.435	.108
PYRITE	4.58	.125	.125
CALCITE	.84	.023	.023
ANHYDRITE	2.06	.056	.056
CHLORITE	3.33	.085	.085
KAOLINITE	4.59	.128	.128
ALBITE	8.78	.239	.239
TOTALS	100.31	2.728	.068

COMPONENT	WT.PERCENT COMPUTED	RESIDUAL	GAIN OR LOSS G/CM**3
SI	26.004	-.058	-.0301
AL	8.989	-.005	-.0552
FE**	4.792	.618	.0236
MG	1.904	-.146	.0243
CA	2.751	-.000	-.0412
NA	2.686	-.000	-.0278
K	2.175	-.000	.0112
S	2.450	-.220	.0726
O	44.905	.129	-.0611
C	.101	-.000	.0027
SO3	1.200	.000	.0326
TI	.371	-.011	.0040
SUM RESIDUALS**2		.472	
STANDARD DEVIATION		.486	

MF-2605	WEIGHT		GAIN OR LOSS
MINERAL	PER CENT	G/CM**3	G/CM**3
PLAGICCLAS	37.97	1.022	-.876
K-FELDSPAR	7.57	.206	.069
QUARTZ	16.93	.461	.196
BIOTITE	15.60	.424	.094
PYRITE	4.85	.133	.133
CALCITE	1.21	.033	.033
ANHYDRITE	2.04	.056	.056
CHLORITE	1.56	.043	.043
KAOLINITE	4.01	.109	.109
ALBITE	8.10	.220	.220
TOTALS	99.46	2.705	.065

COMPONENT	WT.PERCENT COMPUTED	RESIDUAL	GAIN OR LOSS G/CM**3
SI	27.362	.436	-.0310
AL	9.037	.038	-.0590
FE**	4.310	.174	.0206
MG	1.912	-.036	.0215
CA	3.164	.002	-.0316
NA	2.413	.001	-.0235
K	2.242	.001	.0130
S	2.687	-.063	.0726
O	44.361	-1.089	-.0427
C	.145	.000	.0039
SO3	1.200	-.000	.0326
TI	.371	-.001	.0035
SUM RESIDUALS**2		1.414	
STANDARD DEVIATION		.841	

MF-2606

MINERAL	WEIGHT PER CENT	G/CM**3	GAIN OR LOSS G/CM**3
PLAGICCLAS	32.79	.682	-1.015
K-FELDSPAR	9.14	.246	.108
QUARTZ	17.82	.479	.204
BIOTITE	15.47	.416	.086
PYRITE	3.80	.102	.102
CALCITE	1.07	.029	.029
ANHYDRITE	2.60	.070	.070
CHLORITE	2.28	.061	.061
KAOLINITE	4.30	.116	.116
ALBITE	10.73	.289	.289
TOTALS	99.98	2.690	.050

COMPONENT	WT.PERCENT COMPUTED	RESIDUAL	GAIN OR LOSS G/CM**3
SI	27.882	.194	-.0186
AL	9.062	.016	-.0565
FE++	4.211	.612	.0049
MG	1.713	-.162	.0190
CA	2.952	.001	-.0366
NA	2.812	.001	-.0244
K	2.416	.000	.0170
S	2.033	-.207	.0603
O	44.890	-.456	-.0592
C	.128	.000	.0035
SO3	1.520	-.000	.0409
TI	.364	-.014	.0036
SUM RESIDUALS**2		.690	
STANDARD DEVIATION		.587	

MF-2607

MINERAL	WEIGHT PER CENT	G/CM**3	GAIN OR LOSS G/CM**3
PLAGICCLAS	16.36	.445	-1.452
K-FELDSPAR	5.60	.152	.015
QUARTZ	21.13	.575	.300
BIOTITE	16.92	.460	.130
PYRITE	4.18	.114	.114
CALCITE	1.57	.043	.043
ANHYDRITE	3.52	.096	.096
CHLORITE	2.67	.073	.073
KAOLINITE	12.35	.336	.336
ALBITE	15.75	.428	.428
TOTALS	100.06	2.722	.082

COMPONENT	WT.PERCENT COMPUTED	RESIDUAL	GAIN OR LOSS G/CM**3
SI	27.781	.154	-.0119
AL	9.107	.013	-.0524
FE++	4.643	.694	.0155
MG	1.903	-.190	.0254
CA	2.545	.000	-.0460
NA	2.330	.000	-.0366
K	2.067	.000	.0082
S	2.234	-.236	.0672
O	44.794	-.360	-.0508
C	.188	.000	.0051
SO3	2.070	-.000	.0563
TI	.398	-.016	.0047
SUM RESIDUALS**2		.727	
STANDARD DEVIATION		.603	

MF-2608

MINERAL	WEIGHT PER CENT	G/CM**3	GAIN OR LOSS G/CM**3
PLAGICCLAS	36.63	.996	-.901
K-FELDSPAR	7.19	.196	.058
QUARTZ	21.88	.595	.320
BIOTITE	17.88	.486	.156
PYRITE	3.36	.091	.091
CALCITE	.64	.017	.017
ANHYDRITE	1.94	.053	.053
CHLORITE	3.14	.086	.086
KAOLINITE	3.39	.092	.092
ALBITE	3.81	.104	.104
TOTALS	99.86	2.716	.076

COMPONENT	WT.PERCENT COMPUTED	RESIDUAL	GAIN OR LOSS G/CM**3
SI	28.360	.265	.0008
AL	8.759	.020	-.0621
FE++	4.464	.889	.0054
MG	2.062	-.417	.0359
CA	2.795	.001	-.0400
NA	2.382	.001	-.0352
K	2.391	.000	.0170
S	1.796	-.254	.0558
O	45.209	-.620	-.0325
C	.076	.000	.0021
SO3	1.140	-.000	.0310
TI	.420	-.029	.0056
SUM RESIDUALS**2		1.484	
STANDARD DEVIATION		.862	

MF-2609

MINERAL	WEIGHT PER CENT	G/CM**3	GAIN OR LOSS G/CM**3
PLAGICCLAS	29.36	.796	-1.102
K-FELDSPAR	8.50	.230	.093
QUARTZ	21.57	.584	.309
BIOTITE	17.87	.484	.154
PYRITE	4.41	.120	.120
CALCITE	.82	.022	.022
ANHYDRITE	.66	.018	.018
CHLORITE	3.66	.099	.099
KAOLINITE	5.60	.152	.152
ALBITE	7.41	.201	.201
TOTALS	99.86	2.706	.066

COMPONENT	WT.PERCENT COMPUTED	RESIDUAL	GAIN OR LOSS G/CM**3
SI	28.395	.319	-.0025
AL	8.859	.025	-.0604
FE++	5.035	.791	.0231
MG	2.145	-.244	.0332
CA	2.102	.001	-.0591
NA	2.330	.001	-.0369
K	2.524	.000	.0204
S	2.353	-.262	.0710
O	45.206	-.751	-.0336
C	.098	.000	.0027
SO3	.390	-.000	.0106
TI	.420	-.018	.0053
SUM RESIDUALS**2		1.428	
STANDARD DEVIATION		.842	

MF-2612

MINERAL	WEIGHT PER CENT	G/CM**3	GAIN OR LOSS G/CM**3
PLAGICCLAS	29.60	.814	-1.064
K-FELDSPAR	4.85	.133	-.004
QUARTZ	19.06	.524	.249
BIOTITE	18.05	.496	.166
PYRITE	4.09	.113	.113
CALCITE	.52	.014	.014
ANHYDRITE	1.87	.051	.051
CHLORITE	3.61	.099	.099
KAOLINITE	3.69	.101	.101
ALBITE	14.63	.402	.402
TOTALS	99.97	2.749	.109

COMPONENT	WT.PERCENT COMPUTED	RESIDUAL	GAIN OR LOSS G/CM**3
SI	28.032	.185	.0024
AL	8.823	.014	-.0576
FE++	4.903	.379	.0325
MG	2.153	-.091	.0302
CA	2.352	.000	-.0513
NA	2.924	.001	-.0196
K	2.139	.000	.0100
S	2.187	-.083	.0624
O	44.900	-.430	-.0324
C	.063	.000	.0017
SO3	1.100	.000	.0303
TI	.424	-.007	.0053
SUM RESIDUALS**2		.379	
STANDARD DEVIATION		.435	

MF-2610

MINERAL	WEIGHT PER CENT	G/CM**3	GAIN OR LOSS G/CM**3
PLAGICCLAS	28.32	.745	-1.153
K-FELDSPAR	9.66	.254	.117
QUARTZ	18.29	.481	.206
BIOTITE	20.44	.538	.208
PYRITE	6.00	.158	.158
CALCITE	.80	.021	.021
ANHYDRITE	1.51	.040	.040
CHLORITE	1.07	.028	.028
KAOLINITE	7.40	.195	.195
ALBITE	6.66	.175	.175
TOTALS	100.16	2.634	-.006

COMPONENT	WT.PERCENT COMPUTED	RESIDUAL	GAIN OR LOSS G/CM**3
SI	27.234	.074	-.0491
AL	9.111	.007	-.0504
FE++	5.711	.573	.0432
MG	1.951	-.088	.0221
CA	2.287	.000	-.0559
NA	2.226	.000	-.0415
K	2.864	.000	.0273
S	3.208	-.222	.0902
O	44.102	-.173	-.1146
C	.096	.000	.0025
SO3	.890	-.000	.0234
TI	.481	-.011	.0063
SUM RESIDUALS**2		.421	
STANDARD DEVIATION		.459	

MF-2613

MINERAL	WEIGHT PER CENT	G/CM**3	GAIN OR LOSS G/CM**3
PLAGICCLAS	36.56	.994	-.903
K-FELDSPAR	7.17	.195	.057
QUARTZ	18.35	.499	.224
BIOTITE	15.95	.434	.104
PYRITE	4.23	.115	.115
CALCITE	1.30	.035	.035
ANHYDRITE	4.93	.134	.134
CHLORITE	3.62	.099	.099
KAOLINITE	1.73	.047	.047
ALBITE	6.55	.178	.178
TOTALS	100.38	2.730	.090

COMPONENT	WT.PERCENT COMPUTED	RESIDUAL	GAIN OR LOSS G/CM**3
SI	25.860	-.131	-.0292
AL	8.523	-.010	-.0577
FE++	4.684	.494	.0221
MG	1.971	-.122	.0254
CA	3.937	-.001	-.0089
NA	2.618	-.000	-.0266
K	2.233	-.000	.0127
S	2.259	-.141	.0653
O	43.864	.300	-.0941
C	.156	-.000	.0042
SO3	2.900	.300	.0789
TI	.375	-.009	.0038
SUM RESIDUALS**2		.386	
STANDARD DEVIATION		.440	

MF-2611

MINERAL	WEIGHT PER CENT	G/CM**3	GAIN OR LOSS G/CM**3
PLAGICCLAS	20.41	.543	-1.355
K-FELDSPAR	7.30	.194	.057
QUARTZ	19.52	.519	.244
BIOTITE	18.31	.487	.157
PYRITE	4.32	.115	.115
CALCITE	1.11	.030	.030
ANHYDRITE	1.19	.032	.032
CHLORITE	5.18	.138	.138
KAOLINITE	9.15	.243	.243
ALBITE	13.62	.362	.362
TOTALS	100.11	2.663	.023

COMPONENT	WT.PERCENT COMPUTED	RESIDUAL	GAIN OR LOSS G/CM**3
SI	27.793	.133	-.0276
AL	9.227	.012	-.0547
FE++	5.291	.682	.0307
MG	2.428	-.220	.0389
CA	1.894	.000	-.0656
NA	2.382	.000	-.0367
K	2.391	.000	.0156
S	2.308	-.172	.0660
O	45.129	-.315	-.0702
C	.134	.000	.0036
SO3	.700	.000	.0186
TI	.430	-.013	.0052
SUM RESIDUALS**2		.660	
STANDARD DEVIATION		.574	

MF-2614 MINERAL	WEIGHT PER CENT	G/CM**3	GAIN OR LOSS G/CM**3
PLAGICCLAS	30.71	.842	-1.056
K-FELDSPAR	10.45	.286	.149
QUARTZ	17.98	.493	.218
BIOTITE	15.90	.436	.106
PYRITE	3.53	.097	.097
CALCITE	.98	.027	.027
ANHYDRITE	4.93	.135	.135
CHLORITE	1.67	.046	.046
KAOLINITE	2.85	.078	.078
ALBITE	11.18	.306	.306
TOTALS	100.18	2.745	.105

COMPONENT	WT.PERCENT COMPUTED	RESIDUAL	GAIN OR LOSS G/CM**3
SI	27.548	.024	-.0092
AL	8.566	.002	-.0651
FE++	4.046	.423	.0074
MG	1.652	-.097	.0164
CA	3.495	.000	-.0202
NA	2.760	.000	-.0244
K	2.598	.000	.0232
S	1.888	-.112	.0548
O	44.231	-.055	-.0656
C	.117	.000	.0032
SO3	2.900	-.000	.0795
TI	.374	-.010	.0039
SUM RESIDUALS**2		.205	
STANDARD DEVIATION		.320	

MF-2615 MINERAL	WEIGHT PER CENT	G/CM**3	GAIN OR LOSS G/CM**3
PLAGICCLAS	42.52	1.169	-.728
K-FELDSPAR	8.60	.236	.099
QUARTZ	15.53	.427	.152
BIOTITE	15.73	.433	.103
PYRITE	4.02	.111	.111
CALCITE	.91	.025	.025
ANHYDRITE	5.44	.150	.150
CHLORITE	3.75	.103	.103
ALBITE	3.59	.099	.099
TOTALS	100.09	2.753	.113

COMPONENT	WT.PERCENT COMPUTED	RESIDUAL	GAIN OR LOSS G/CM**3
SI	26.219	.134	-.0461
AL	8.749	.121	-.0625
FE++	4.579	.459	.0214
MG	1.973	-.120	.0261
CA	4.253	-.035	.0019
NA	2.696	-.012	-.0255
K	2.402	-.006	.0182
S	2.149	-.121	.0624
O	43.393	-.331	-.0766
C	.109	.000	.0030
SO3	3.200	.010	.0877
TI	.370	-.008	.0038
SUM RESIDUALS**2		.384	
STANDARD DEVIATION		.358	

MF-2616 MINERAL	WEIGHT PER CENT	G/CM**3	GAIN OR LOSS G/CM**3
PLAGICCLAS	37.41	1.029	-.869
K-FELDSPAR	8.26	.227	.090
QUARTZ	16.32	.449	.174
BIOTITE	16.28	.448	.118
PYRITE	3.45	.095	.095
CALCITE	.75	.021	.021
ANHYDRITE	4.46	.123	.123
CHLORITE	2.59	.071	.071
KAOLINITE	4.41	.121	.121
ALBITE	6.21	.171	.171
TOTALS	100.13	2.754	.114

COMPONENT	WT.PERCENT COMPUTED	RESIDUAL	GAIN OR LOSS G/CM**3
SI	26.956	.077	-.0242
AL	9.270	.007	-.0451
FE++	4.206	.530	.0092
MG	1.834	-.151	.0231
CA	3.624	.000	-.0164
NA	2.649	.000	-.0272
K	2.391	.000	.0177
S	1.846	-.134	.0545
O	44.262	-.185	-.0567
C	.090	.000	.0025
SO3	2.620	.000	.0721
TI	.383	-.013	.0043
SUM RESIDUALS**2		.362	
STANDARD DEVIATION		.425	

MF-2617 MINERAL	WEIGHT PER CENT	G/CM**3	GAIN OR LOSS G/CM**3
PLAGICCLAS	32.40	.901	-.997
K-FELDSPAR	8.90	.247	.110
QUARTZ	17.60	.489	.214
BIOTITE	16.66	.463	.133
PYRITE	2.20	.061	.061
CALCITE	1.43	.040	.040
ANHYDRITE	2.84	.079	.079
CHLORITE	2.65	.074	.074
KAOLINITE	3.13	.087	.087
ALBITE	12.27	.341	.341
TOTALS	100.09	2.782	.142

COMPONENT	WT.PERCENT COMPUTED	RESIDUAL	GAIN OR LOSS G/CM**3
SI	28.070	.092	.0144
AL	9.001	.007	-.0498
FE++	3.685	.475	-.0027
MG	1.876	-.193	.0260
CA	3.152	.000	-.0284
NA	2.923	.000	-.0187
K	2.482	.000	.0210
S	1.178	-.062	.0345
O	45.487	-.217	-.0084
C	.172	.000	.0048
SO3	1.670	.000	.0464
TI	.392	-.016	.0047
SUM RESIDUALS**2		.322	
STANDARD DEVIATION		.401	

MF-2618 MINERAL	WEIGHT PER CENT	G/CM**3	GAIN OR LOSS G/CM**3
PLAGIOCLAS	32.23	.851	-1.047
K-FELDSPAR	14.57	.385	.247
QUARTZ	20.05	.529	.254
BIOTITE	14.15	.374	.044
PYRITE	1.21	.032	.032
CALCITE	.96	.025	.025
ANHYDRITE	1.87	.049	.049
KAOLINITE	7.07	.187	.187
ALBITE	7.74	.204	.204
TOTALS	99.84	2.636	-.004

COMPONENT	WT.PERCENT COMPUTED	RESIDUAL	GAIN OR LOSS G/CM**3
SI	29.594	.190	.0129
AL	9.517	.016	-.0490
FE++	2.464	.078	-.0269
MG	1.231	.000	.0010
CA	2.666	.001	-.0456
NA	2.597	.000	-.0315
K	2.947	.000	.0298
S	.645	-.005	.0172
O	46.635	-.428	-.0366
C	.115	.000	.0030
SO3	1.100	-.000	.0290
TI	.333	-.009	.0024
SUM RESIDUALS**2		.225	
STANDARD DEVIATION		.274	

MF-2619 MINERAL	WEIGHT PER CENT	G/CM**3	GAIN OR LOSS G/CM**3
PLAGIOCLAS	27.71	.726	-1.172
K-FELDSPAR	13.23	.347	.209
QUARTZ	21.10	.553	.278
BIOTITE	15.97	.418	.088
PYRITE	2.78	.073	.073
CALCITE	1.07	.028	.028
ANHYDRITE	1.21	.032	.032
CHLORITE	1.19	.031	.031
KAOLINITE	8.99	.235	.235
ALBITE	6.38	.167	.167
TOTALS	99.62	2.610	-.030

COMPONENT	WT.PERCENT COMPUTED	RESIDUAL	GAIN OR LOSS G/CM**3
SI	28.981	.349	-.0132
AL	9.377	.029	-.0549
FE++	3.629	.092	.0008
MG	1.581	-.018	.0104
CA	2.273	.001	-.0565
NA	2.219	.001	-.0419
K	2.923	.001	.0286
S	1.486	-.014	.0393
O	45.939	-.517	-.0540
C	.128	.000	.0034
SO3	.710	-.000	.0186
TI	.376	-.002	.0033
SUM RESIDUALS**2		.798	
STANDARD DEVIATION		.632	

MF-2620 MINERAL	WEIGHT PER CENT	G/CM**3	GAIN OR LOSS G/CM**3
PLAGIOCLAS	37.55	1.010	-.887
K-FELDSPAR	14.72	.396	.258
QUARTZ	20.47	.551	.276
BIOTITE	15.50	.417	.087
PYRITE	2.50	.067	.067
CALCITE	1.29	.035	.035
ANHYDRITE	2.19	.059	.059
CHLORITE	1.17	.031	.031
KAOLINITE	4.29	.115	.115
TOTALS	99.69	2.682	.042

COMPONENT	WT.PERCENT COMPUTED	RESIDUAL	GAIN OR LOSS G/CM**3
SI	28.537	.279	-.0033
AL	9.031	.022	-.0575
FE++	3.434	-.056	.0020
MG	1.537	.011	.0096
CA	3.181	.358	-.0401
NA	2.204	-.281	-.0331
K	3.090	.051	.0337
S	1.337	.007	.0358
O	45.532	-.654	-.0366
C	.155	-.004	.0043
SO3	1.290	-.040	.0358
TI	.365	-.001	.0032
SUM RESIDUALS**2		.721	
STANDARD DEVIATION		.490	

MF-2621 MINERAL	WEIGHT PER CENT	G/CM**3	GAIN OR LOSS G/CM**3
PLAGIOCLAS	37.63	1.050	-.848
K-FELDSPAR	13.34	.372	.235
QUARTZ	21.95	.612	.337
BIOTITE	13.45	.375	.045
PYRITE	3.14	.088	.088
CALCITE	.85	.024	.024
ANHYDRITE	2.84	.079	.079
CHLORITE	1.00	.028	.028
KAOLINITE	5.74	.160	.160
TOTALS	99.94	2.788	.148

COMPONENT	WT.PERCENT COMPUTED	RESIDUAL	GAIN OR LOSS G/CM**3
SI	28.793	.231	.0335
AL	9.070	.018	-.0473
FE++	3.427	.271	-.0039
MG	1.331	-.050	.0070
CA	3.202	.286	-.0346
NA	2.188	-.193	-.0336
K	2.762	.031	.0282
S	1.677	-.073	.0488
O	45.399	-.524	.0023
C	.103	-.001	.0029
SO3	1.670	-.050	.0480
TI	.316	-.007	.0024
SUM RESIDUALS**2		.532	
STANDARD DEVIATION		.421	

MF-2622

MINERAL	WEIGHT PER CENT	G/CM**3	GAIN OR LOSS G/CM**3
PLAGICCLAS	49.18	1.323	-.575
K-FELDSPAR	11.03	.297	.159
QUARTZ	20.52	.552	.277
BIOTITE	14.20	.382	.052
PYRITE	1.35	.036	.036
CALCITE	.82	.022	.022
ANHYDRITE	1.46	.039	.039
CHLORITE	.08	.002	.002
KAOLINITE	.69	.019	.019
TOTALS	99.32	2.672	.032

COMPONENT	WT.PERCENT COMPUTED	RESIDUAL	GAIN OR LOSS G/CM**3
SI	29.335	.833	.0087
AL	9.154	.050	-.0549
FE++	2.552	.274	-.0306
MG	1.247	-.092	.0045
CA	3.400	.127	-.0279
NA	2.769	-.095	-.0230
K	2.584	.010	.0212
S	.724	-.026	.0202
O	46.269	-1.542	.0071
C	.098	-.000	.0026
SO3	.656	-.004	.0231
TI	.334	-.014	.0028
SUM RESIDUALS**2		2.889	
STANDARD DEVIATION		.981	

MF-2623

MINERAL	WEIGHT PER CENT	G/CM**3	GAIN OR LOSS G/CM**3
PLAGICCLAS	35.25	.952	-.946
K-FELDSPAR	7.09	.192	.054
QUARTZ	17.26	.466	.191
BIOTITE	14.04	.379	.049
PYRITE	2.37	.064	.064
CALCITE	1.02	.028	.028
ANHYDRITE	2.58	.070	.070
CHLORITE	2.21	.060	.060
KAOLINITE	3.65	.099	.099
ALBITE	14.48	.391	.391
TOTALS	99.96	2.699	.059

COMPONENT	WT.PERCENT COMPUTED	RESIDUAL	GAIN OR LOSS G/CM**3
SI	28.443	.136	.0008
AL	9.301	.012	-.0490
FE++	3.339	.230	-.0080
MG	1.578	-.062	.0128
CA	3.067	.001	-.0332
NA	3.242	.001	-.0125
K	2.067	.000	.0078
S	1.265	-.035	.0351
O	45.682	-.320	-.0370
C	.123	.000	.0033
SO3	1.520	.000	.0410
TI	.330	-.006	.0025
SUM RESIDUALS**2		.180	
STANDARD DEVIATION		.300	

MF-2624

MINERAL	WEIGHT PER CENT	G/CM**3	GAIN OR LOSS G/CM**3
PLAGICCLAS	40.02	1.053	-.845
K-FELDSPAR	9.61	.253	.115
QUARTZ	21.02	.553	.278
BIOTITE	13.49	.355	.025
PYRITE	1.58	.042	.042
CALCITE	1.45	.038	.038
ANHYDRITE	5.64	.148	.148
CHLORITE	1.34	.035	.035
KAOLINITE	5.39	.142	.142
TOTALS	99.54	2.618	-.022

COMPONENT	WT.PERCENT COMPUTED	RESIDUAL	GAIN OR LOSS G/CM**3
SI	27.849	.502	-.0442
AL	8.988	.042	-.0645
FE++	2.761	.421	-.0304
MG	1.389	-.186	.0099
CA	4.393	.219	-.0062
NA	2.262	-.067	-.0387
K	2.333	.009	.0131
S	.846	-.054	.0237
O	44.909	-1.257	-.0648
C	.173	-.001	.0046
SO3	3.319	-.071	.0892
TI	.317	-.019	.0022
SUM RESIDUALS**2		2.106	
STANDARD DEVIATION		.838	

MF-2625

MINERAL	WEIGHT PER CENT	G/CM**3	GAIN OR LOSS G/CM**3
PLAGICCLAS	36.60	.988	-.909
K-FELDSPAR	11.82	.319	.182
QUARTZ	18.35	.495	.220
BIOTITE	13.10	.354	.024
PYRITE	1.57	.042	.042
CALCITE	1.30	.035	.035
ANHYDRITE	2.55	.069	.069
KAOLINITE	6.47	.175	.175
ALBITE	7.99	.216	.216
TOTALS	99.74	2.693	.053

COMPONENT	WT.PERCENT COMPUTED	RESIDUAL	GAIN OR LOSS G/CM**3
SI	28.946	.150	.0141
AL	9.541	.013	-.0425
FE++	2.236	-.204	-.0260
MG	1.394	.121	.0029
CA	3.238	.001	-.0286
NA	2.812	.000	-.0241
K	2.540	.000	.0206
S	.840	.020	.0221
O	46.224	-.344	-.0217
C	.156	.000	.0042
SO3	1.500	-.000	.0405
TI	.312	-.018	.0023
SUM RESIDUALS**2		.198	
STANDARD DEVIATION		.257	

MF-2628	WEIGHT		GAIN OR LOSS
MINERAL	PER CENT	G/CM**3	G/CM**3
PLAGIOCLAS	27.77	.736	-1.162
K-FELDSPAR	19.85	.526	.389
QUARTZ	21.90	.580	.305
BIOTITE	11.76	.312	-.018
PYRITE	2.47	.065	.065
CALCITE	1.83	.049	.049
ANHYDRITE	3.05	.081	.081
KAOLINITE	11.53	.306	.306
TOTALS	100.17	2.654	.014

	WT.PERCENT		GAIN OR LOSS
COMPONENT	COMPUTED	RESIDUAL	G/CM**3
SI	29.086	.057	.0059
AL	9.427	.005	-.0501
FE++	2.501	.076	-.0276
MG	1.252	.063	-.0000
CA	3.127	.297	-.0410
NA	1.757	-.135	-.0499
K	3.354	.050	.0396
S	1.320	-.020	.0355
O	46.051	-.126	-.0553
C	.220	-.006	.0060
SO3	1.796	-.064	.0493
TI	.240	-.026	.0015
SUM RESIDUALS**2		.143	
STANDARD DEVIATION		.189	

MF-2629	WEIGHT		GAIN OR LOSS
MINERAL	PER CENT	G/CM**3	G/CM**3
PLAGIOCLAS	34.49	.945	-.952
K-FELDSPAR	12.21	.334	.197
QUARTZ	19.25	.528	.253
BIOTITE	14.74	.404	.074
PYRITE	1.91	.052	.052
CALCITE	2.94	.081	.081
ANHYDRITE	8.67	.238	.238
KAOLINITE	5.79	.159	.159
TOTALS	100.00	2.740	.100

	WT.PERCENT		GAIN OR LOSS
COMPONENT	COMPUTED	RESIDUAL	G/CM**3
SI	26.471	.153	-.0423
AL	8.429	.012	-.0692
FE++	2.582	.227	-.0274
MG	1.568	-.115	.0146
CA	5.585	.568	.0215
NA	2.005	-.101	-.0423
K	2.710	.020	.0257
S	1.020	-.040	.0290
O	43.828	-.379	-.0677
C	.353	-.010	.0099
SO3	5.098	-.332	.1488
TI	.351	-.003	.0031
SUM RESIDUALS**2		.677	
STANDARD DEVIATION		.412	

MF-2626	WEIGHT		GAIN OR LOSS
MINERAL	PER CENT	G/CM**3	G/CM**3
PLAGIOCLAS	52.01	1.420	-.478
K-FELDSPAR	4.80	.131	-.006
QUARTZ	15.17	.414	.139
BIOTITE	16.52	.451	.121
PYRITE	2.23	.061	.061
CALCITE	1.06	.029	.029
ANHYDRITE	6.03	.165	.165
CHLORITE	1.54	.042	.042
TOTALS	99.38	2.713	.073

	WT.PERCENT		GAIN OR LOSS
COMPONENT	COMPUTED	RESIDUAL	G/CM**3
SI	26.180	.563	-.0641
AL	9.122	.176	-.0556
FE++	3.504	.224	-.0023
MG	1.686	-.064	.0163
CA	4.999	.282	.0128
NA	2.831	-.144	-.0188
K	2.046	.004	.0078
S	1.193	-.027	.0333
O	43.755	-1.544	-.0423
C	.128	-.001	.0035
SO3	3.548	-.082	.0991
TI	.388	-.007	.0042
SUM RESIDUALS**2		2.895	
STANDARD DEVIATION		.851	

MF-2627	WEIGHT		GAIN OR LOSS
MINERAL	PER CENT	G/CM**3	G/CM**3
PLAGIOCLAS	35.17	.957	-.941
K-FELDSPAR	15.20	.414	.276
QUARTZ	21.80	.593	.318
BIOTITE	11.88	.323	-.037
PYRITE	2.27	.062	.062
CALCITE	2.61	.071	.071
ANHYDRITE	3.65	.099	.099
KAOLINITE	7.91	.215	.215
TOTALS	100.49	2.733	.093

	WT.PERCENT		GAIN OR LOSS
COMPONENT	COMPUTED	RESIDUAL	G/CM**3
SI	28.731	-.112	.0211
AL	9.201	-.009	-.0493
FE++	2.654	.268	-.0270
MG	1.033	.038	-.0044
CA	4.008	.356	-.0167
NA	2.084	-.134	-.0397
K	2.848	.026	.0288
S	1.213	-.067	.0348
O	45.983	.246	-.0350
C	.313	-.009	.0088
SO3	2.145	-.065	.0601
TI	.279	-.044	.0022
SUM RESIDUALS**2		.303	
STANDARD DEVIATION		.275	

MF-2630

MINERAL	WEIGHT PER CENT	G/CM**3	GAIN OR LOSS G/CM**3
PLAGIOCLAS	31.71	.869	-1.029
K-FELDSPAR	12.12	.332	.195
QUARTZ	22.02	.603	.328
BIOTITE	17.98	.493	.163
PYRITE	3.75	.103	.103
CALCITE	3.26	.089	.089
ANHYDRITE	.77	.021	.021
KAOLINITE	8.35	.229	.229
TOTALS	99.97	2.739	.099

COMPONENT	WT.PERCENT COMPUTED	RESIDUAL	GAIN OR LOSS G/CM**3
SI	28.222	.240	.0033
AL	8.906	.019	-.0563
FE++	3.813	.300	.0044
MG	1.913	-.102	.0237
CA	3.234	.350	-.0369
NA	1.857	-.176	-.0443
K	2.949	.044	.0316
S	2.007	-.093	.0575
O	45.793	-.577	-.0085
C	.391	-.024	.0114
SO3	.456	-.004	.0126
TI	.428	-.004	.0052
SUM RESIDUALS**2		.656	
STANDARD DEVIATION		.405	

MF-2631

MINERAL	WEIGHT PER CENT	G/CM**3	GAIN OR LOSS G/CM**3
PLAGIOCLAS	46.85	1.288	-.609
K-FELDSPAR	3.45	.095	-.043
QUARTZ	16.59	.456	.181
BIOTITE	18.70	.514	.184
PYRITE	1.91	.053	.053
CALCITE	1.88	.052	.052
ANHYDRITE	4.75	.131	.131
KAOLINITE	5.22	.144	.144
TOTALS	99.36	2.732	.092

COMPONENT	WT.PERCENT COMPUTED	RESIDUAL	GAIN OR LOSS G/CM**3
SI	26.558	.520	-.0474
AL	9.422	.053	-.0421
FE++	3.040	.070	-.0102
MG	1.330	.090	.0208
CA	4.670	.182	.0074
NA	2.538	-.059	-.0286
K	2.031	.005	.0077
S	1.023	-.007	.0283
O	44.620	-1.427	-.0127
C	.225	-.001	.0062
SO3	2.795	-.035	.0778
TI	.445	-.035	.0066
SUM RESIDUALS**2		2.361	
STANDARD DEVIATION		.768	

MF-2632

MINERAL	WEIGHT PER CENT	G/CM**3	GAIN OR LOSS G/CM**3
PLAGIOCLAS	47.59	1.314	-.584
K-FELDSPAR	6.95	.192	.054
QUARTZ	16.02	.442	.167
BIOTITE	16.71	.461	.131
PYRITE	2.15	.059	.059
CALCITE	1.45	.040	.040
ANHYDRITE	4.74	.131	.131
KAOLINITE	3.79	.104	.104
TOTALS	99.40	2.743	.103

COMPONENT	WT.PERCENT COMPUTED	RESIDUAL	GAIN OR LOSS G/CM**3
SI	26.831	.513	-.0370
AL	9.366	.050	-.0427
FE++	2.923	.124	-.0147
MG	1.778	.113	.0144
CA	4.537	.070	.0073
NA	2.627	-.022	-.0269
K	2.286	.003	.0150
S	1.151	-.019	.0323
O	44.540	-1.369	-.0119
C	.174	-.000	.0048
SO3	2.787	-.013	.0773
TI	.398	-.052	.0058
SUM RESIDUALS**2		2.178	
STANDARD DEVIATION		.738	

MF-2633

MINERAL	WEIGHT PER CENT	G/CM**3	GAIN OR LOSS G/CM**3
PLAGIOCLAS	47.71	1.317	-.581
K-FELDSPAR	3.47	.096	-.042
QUARTZ	15.48	.427	.152
BIOTITE	21.42	.591	.261
PYRITE	1.93	.053	.053
CALCITE	2.47	.068	.068
ANHYDRITE	3.06	.084	.084
KAOLINITE	3.23	.089	.089
TOTALS	98.77	2.726	.086

COMPONENT	WT.PERCENT COMPUTED	RESIDUAL	GAIN OR LOSS G/CM**3
SI	26.286	.529	-.0525
AL	9.263	.053	-.0456
FE++	3.358	.288	-.0072
MG	2.279	-.115	.0346
CA	4.455	-.633	.0244
NA	2.584	.151	-.0328
K	2.251	-.015	.0146
S	1.030	-.030	.0293
O	44.658	-1.490	-.0053
C	.296	.007	.0080
SO3	1.798	.038	.0486
TI	.510	-.012	.0078
SUM RESIDUALS**2		3.026	
STANDARD DEVIATION		.870	

MF-2634	WEIGHT		GAIN OR LOSS
MINERAL	PER CENT	G/CM**3	G/CM**3
PLAGIOCLAS	33.26	.925	-.973
K-FELDSPAR	2.74	.076	-.061
QUARTZ	18.38	.511	.236
BIOTITE	22.13	.615	.285
PYRITE	4.34	.121	.121
CALCITE	1.56	.043	.043
ANHYDRITE	4.20	.117	.117
CHLORITE	.69	.019	.019
KAOLINITE	11.02	.306	.306
TOTALS	98.33	2.734	.094

COMPONENT	WT.PERCENT COMPUTED	RESIDUAL	GAIN OR LOSS G/CM**3
SI	25.632	.716	-.0707
AL	9.233	.075	-.0452
FE++	4.692	.580	.0224
MG	2.457	-.323	.0458
CA	3.649	-.660	.0038
NA	1.806	.107	-.0528
K	2.180	-.020	.0132
S	2.322	-.180	.0698
O	43.175	-2.072	-.0211
C	.197	.004	.0051
SO3	2.471	.101	.0659
TI	.526	.011	.0077
SUM RESIDUALS**2		5.747	
STANDARD DEVIATION		1.384	

MF-2801	WEIGHT		GAIN OR LOSS
MINERAL	PER CENT	G/CM**3	G/CM**3
PLAGIOCLAS	17.08	.465	-1.433
K-FELDSPAR	22.13	.602	.465
QUARTZ	17.13	.466	.191
BIOTITE	9.65	.262	-.068
PYRITE	5.12	.139	.139
CALCITE	4.88	.133	.133
ANHYDRITE	3.07	.084	.084
CHLORITE	5.03	.137	.137
KAOLINITE	15.00	.408	.408
TOTALS	99.09	2.695	.055

COMPONENT	WT.PERCENT COMPUTED	RESIDUAL	GAIN OR LOSS G/CM**3
SI	25.987	.566	-.0741
AL	9.403	.060	-.0457
FE++	4.408	.257	.0210
MG	1.609	-.050	.0136
CA	3.728	-.046	-.0134
NA	1.252	.005	-.0661
K	3.426	-.003	.0453
S	2.735	-.105	.0772
O	43.916	-1.603	-.0409
C	.586	.005	.0158
SO3	1.806	.006	.0490
TI	.318	.000	.0020
SUM RESIDUALS**2		2.974	
STANDARD DEVIATION		.996	

MF-2802	WEIGHT		GAIN OR LOSS
MINERAL	PER CENT	G/CM**3	G/CM**3
PLAGIOCLAS	36.08	.974	-.923
K-FELDSPAR	11.52	.311	.174
QUARTZ	21.66	.585	.310
BIOTITE	12.02	.324	-.006
PYRITE	2.27	.061	.061
CALCITE	1.50	.040	.040
ANHYDRITE	3.48	.094	.094
CHLORITE	3.07	.083	.083
KAOLINITE	7.62	.206	.206
TOTALS	99.21	2.679	.039

COMPONENT	WT.PERCENT COMPUTED	RESIDUAL	GAIN OR LOSS G/CM**3
SI	26.363	.642	-.0149
AL	9.105	.053	-.0554
FE++	2.992	.325	-.0199
MG	1.540	-.167	.0146
CA	3.460	.065	-.0243
NA	2.144	-.022	-.0415
K	2.420	.004	.0172
S	1.215	-.065	.0346
O	45.345	-1.617	-.0110
C	.180	-.001	.0049
SO3	2.049	-.011	.0556
TI	.396	.000	.0041
SUM RESIDUALS**2		3.174	
STANDARD DEVIATION		1.029	

MF-2803	WEIGHT		GAIN OR LOSS
MINERAL	PER CENT	G/CM**3	G/CM**3
PLAGIOCLAS	39.08	1.075	-.823
K-FELDSPAR	11.39	.313	.176
QUARTZ	18.29	.503	.228
BIOTITE	10.91	.300	-.030
PYRITE	2.63	.072	.072
CALCITE	1.49	.041	.041
ANHYDRITE	6.45	.177	.177
CHLORITE	5.68	.156	.156
KAOLINITE	3.79	.104	.104
TOTALS	99.70	2.742	.102

COMPONENT	WT.PERCENT COMPUTED	RESIDUAL	GAIN OR LOSS G/CM**3
SI	26.797	.338	-.0358
AL	8.763	.029	-.0596
FE++	3.514	.420	-.0068
MG	1.818	-.233	.0249
CA	4.481	.257	.0002
NA	2.307	-.074	-.0345
K	2.325	.009	.0157
S	1.405	-.085	.0410
O	43.960	-.852	-.0467
C	.179	-.002	.0050
SO3	3.791	-.109	.1073
TI	.360	-.000	.0033
SUM RESIDUALS**2		1.163	
STANDARD DEVIATION		.623	

MF-2804 MINERAL	WEIGHT PER CENT	G/CM**3	GAIN OR LOSS G/CM**3
PLAGICCLAS	49.61	1.379	-.518
K-FELDSPAR	7.27	.202	.065
QUARTZ	13.75	.382	.107
BIOTITE	14.58	.405	.075
PYRITE	4.10	.114	.114
CALCITE	1.36	.038	.038
ANHYDRITE	3.27	.091	.091
CHLORITE	6.18	.172	.172
TOTALS	100.14	2.784	.144

COMPONENT	WT.PERCENT COMPUTED	RESIDUAL	GAIN OR LOSS G/CM**3
SI	26.167	-.105	-.0331
AL	9.199	.094	-.0467
FE++	4.709	.885	.0144
MG	2.225	-.640	.0481
CA	4.032	.037	-.0049
NA	2.827	-.044	-.0202
K	2.165	-.002	.0122
S	2.193	-.337	.0703
O	44.054	.255	-.0614
C	.164	-.000	.0046
SO3	1.926	-.004	.0537
TI	.481	.001	.0067
SUM RESIDUALS**2		1.395	
STANDARD DEVIATION		.591	

MF-2805 MINERAL	WEIGHT PER CENT	G/CM**3	GAIN OR LOSS G/CM**3
PLAGICCLAS	38.70	1.068	-.829
K-FELDSPAR	8.72	.241	.103
QUARTZ	14.72	.406	.131
BIOTITE	14.59	.403	.073
PYRITE	6.50	.179	.179
CALCITE	4.09	.113	.113
ANHYDRITE	3.21	.089	.089
CHLORITE	7.36	.203	.203
KAOLINITE	1.45	.040	.040
TOTALS	99.33	2.742	.102

COMPONENT	WT.PERCENT COMPUTED	RESIDUAL	GAIN OR LOSS G/CM**3
SI	24.563	.395	-.0964
AL	8.347	.036	-.0704
FE++	6.043	.718	.0551
MG	2.396	-.215	.0406
CA	4.551	-.216	.0156
NA	2.248	.045	-.0392
K	2.303	-.005	.0157
S	3.473	-.317	.1046
O	42.551	-1.134	-.0733
C	.491	.008	.0133
SO3	1.887	.017	.0516
TI	.461	.001	.0066
SUM RESIDUALS**2		2.154	
STANDARD DEVIATION		.647	

MF-2806 MINERAL	WEIGHT PER CENT	G/CM**3	GAIN OR LOSS G/CM**3
PLAGICCLAS	39.39	1.095	-.802
K-FELDSPAR	7.34	.204	.066
QUARTZ	18.21	.506	.231
BIOTITE	13.51	.376	.046
PYRITE	3.66	.102	.102
CALCITE	1.43	.040	.040
ANHYDRITE	4.23	.118	.118
CHLORITE	8.66	.241	.241
KAOLINITE	2.90	.081	.081
TOTALS	99.33	2.761	.121

COMPONENT	WT.PERCENT COMPUTED	RESIDUAL	GAIN OR LOSS G/CM**3
SI	26.322	.378	-.0421
AL	8.714	.033	-.0585
FE++	4.839	.556	.0272
MG	2.487	-.294	.0458
CA	3.820	-.404	.0014
NA	2.267	.101	-.0398
K	2.057	-.011	.0095
S	1.957	-.113	.0575
O	43.763	-.988	-.0349
C	.171	.002	.0047
SO3	2.487	.067	.0673
TI	.445	.002	.0057
SUM RESIDUALS**2		1.706	
STANDARD DEVIATION		.754	

MF-2807 MINERAL	WEIGHT PER CENT	G/CM**3	GAIN OR LOSS G/CM**3
PLAGICCLAS	38.08	1.051	-.847
K-FELDSPAR	9.39	.259	.122
QUARTZ	17.90	.494	.219
BIOTITE	14.35	.396	.066
PYRITE	2.46	.068	.068
CALCITE	2.93	.081	.081
ANHYDRITE	4.25	.117	.117
CHLORITE	8.88	.245	.245
KAOLINITE	2.08	.057	.057
TOTALS	100.33	2.769	.129

COMPONENT	WT.PERCENT COMPUTED	RESIDUAL	GAIN OR LOSS G/CM**3
SI	26.426	-.126	-.0306
AL	8.628	-.010	-.0514
FE++	4.416	.638	.0124
MG	2.595	-.572	.0559
CA	4.360	.336	-.0049
NA	2.224	-.106	-.0357
K	2.362	.013	.0168
S	1.315	-.075	.0384
O	44.676	.308	-.0544
C	.351	-.009	.0099
SO3	2.501	-.069	.0709
TI	.473	-.001	.0065
SUM RESIDUALS**2		.980	
STANDARD DEVIATION		.572	

MF-2808

MINERAL	WEIGHT PER CENT	G/CM**3	GAIN OR LOSS G/CM**3
PLAGIOCLAS	45.33	1.241	-.757
K-FELDSPAR	7.83	.216	.079
QUARTZ	19.95	.523	.246
BIOTITE	12.36	.368	.038
PYRITE	4.68	.129	.129
CALCITE	1.52	.042	.042
ANHYDRITE	3.11	.086	.086
CHLORITE	7.24	.200	.200
KAOLINITE	1.23	.034	.034
TOTALS	99.22	2.736	.048

COMPONENT	WT.PERCENT COMPUTED	RESIDUAL	GAIN OR LOSS G/CM**3
SI	26.694	.422	-.0383
AL	4.450	.031	-.0075
FE**	5.029	.846	.0235
MG	2.264	-.490	.0434
CA	3.625	-.356	-.0061
NA	2.380	-.110	-.0373
K	2.106	-.011	.0104
S	2.400	-.340	.0784
O	43.722	-1.078	-.0425
C	.183	.002	.0050
SO3	1.476	.336	.0494
TI	.439	.002	.0055
SUM RESIDUALS**2		2.018	
STANDARD DEVIATION		.916	

MF-2809

MINERAL	WEIGHT PER CENT	G/CM**3	GAIN OR LOSS G/CM**3
PLAGIOCLAS	41.54	1.109	-.766
K-FELDSPAR	7.10	.189	.052
QUARTZ	17.25	.460	.185
BIOTITE	14.76	.394	.064
PYRITE	3.68	.098	.098
CALCITE	1.27	.034	.034
ANHYDRITE	4.73	.126	.126
CHLORITE	9.07	.242	.242
KAOLINITE	.30	.008	.008
TOTALS	99.70	2.662	.022

COMPONENT	WT.PERCENT COMPUTED	RESIDUAL	GAIN OR LOSS G/CM**3
SI	26.039	.253	-.0249
AL	4.441	.021	-.0037
FE**	5.066	.760	.0231
MG	2.640	-.525	.0535
CA	4.014	.004	-.0049
NA	2.591	-.000	-.0164
K	2.114	.000	.0090
S	1.906	-.162	.0569
O	43.529	-.693	-.0994
C	.193	.000	.0041
SO3	2.779	-.001	.0742
TI	.486	.001	.0064
SUM RESIDUALS**2		1.371	
STANDARD DEVIATION		.676	

MF-2810

MINERAL	WEIGHT PER CENT	G/CM**3	GAIN OR LOSS G/CM**3
PLAGIOCLAS	35.77	.994	-.403
K-FELDSPAR	8.57	.238	.101
QUARTZ	17.24	.479	.204
BIOTITE	15.15	.421	.091
PYRITE	6.52	.181	.181
CALCITE	2.08	.058	.058
ANHYDRITE	4.83	.134	.134
CHLORITE	8.57	.238	.238
KAOLINITE	.65	.018	.018
TOTALS	99.57	2.763	.123

COMPONENT	WT.PERCENT COMPUTED	RESIDUAL	GAIN OR LOSS G/CM**3
SI	24.954	.375	-.0798
AL	7.917	.030	-.0405
FE**	6.339	.452	.0607
MG	2.623	-.303	.0498
CA	4.071	-.338	.0066
NA	2.305	.066	-.0439
K	2.323	-.010	.0188
S	3.485	-.365	.1070
O	41.985	-1.007	-.0439
C	.249	.006	.0060
SO3	2.834	.068	.0770
TI	.499	.002	.0072
SUM RESIDUALS**2		2.230	
STANDARD DEVIATION		.862	

MF-2811

MINERAL	WEIGHT PER CENT	G/CM**3	GAIN OR LOSS G/CM**3
PLAGIOCLAS	44.31	1.223	-.675
K-FELDSPAR	4.64	.128	-.009
QUARTZ	16.85	.465	.190
BIOTITE	16.13	.445	.115
PYRITE	2.65	.073	.073
CALCITE	1.41	.039	.039
ANHYDRITE	3.22	.089	.089
CHLORITE	10.46	.289	.289
TOTALS	99.66	2.751	.111

COMPONENT	WT.PERCENT COMPUTED	RESIDUAL	GAIN OR LOSS G/CM**3
SI	26.263	.226	-.0446
AL	8.804	.388	-.0675
FE**	4.999	.623	.0269
MG	2.946	-.567	.0606
CA	3.764	-.445	.0602
NA	2.499	.065	-.0328
K	1.962	-.022	.0068
S	1.414	-.062	.0408
O	44.375	-.591	-.0379
C	.169	.002	.0046
SO3	1.893	.043	.0511
TI	.512	.004	.0080
SUM RESIDUALS**2		1.469	
STANDARD DEVIATION		.606	

ON-2801	WEIGHT		GAIN OR LOSS
MINERAL	PER CENT	G/CM**3	G/CM**3
PLAGICCLAS	36.16	.976	-.921
K-FELDSPAR	17.65	.477	.339
QUARTZ	20.17	.545	.270
BIOTITE	12.62	.341	.011
PYRITE	2.34	.063	.063
CALCITE	1.69	.046	.046
ANHYDRITE	2.85	.077	.077
CHLORITE	.72	.020	.020
KAOLINITE	6.03	.163	.163
TOTALS	100.22	2.706	.066

COMPONENT	WT.PERCENT COMPUTED	RESIDUAL	GAIN OR LOSS G/CM**3
SI	28.660	.004	.0103
AL	9.264	.000	-.0497
FE++	2.826	.300	-.0237
MG	1.299	-.125	.0069
CA	3.513	.483	-.0342
NA	2.065	-.317	-.0357
K	3.319	.048	.0403
S	1.249	-.071	.0356
O	45.808	-.009	-.0419
C	.202	-.008	.0057
SO3	1.679	-.081	.0475
TI	.340	-.002	.0026
SUM RESIDUALS**2		.493	
STANDARD DEVIATION		.389	

ON-2802	WEIGHT		GAIN OR LOSS
MINERAL	PER CENT	G/CM**3	G/CM**3
PLAGICCLAS	32.07	.843	-1.054
K-FELDSPAR	16.18	.426	.288
QUARTZ	22.43	.590	.315
BIOTITE	13.00	.342	.012
PYRITE	2.42	.064	.064
CALCITE	.94	.025	.025
ANHYDRITE	1.46	.038	.038
CHLORITE	.26	.007	.007
KAOLINITE	10.84	.285	.285
TOTALS	99.60	2.620	-.020

COMPONENT	WT.PERCENT COMPUTED	RESIDUAL	GAIN OR LOSS G/CM**3
SI	29.364	.241	.0025
AL	9.708	.021	-.0450
FE++	2.827	.262	-.0244
MG	1.267	-.096	.0044
CA	2.577	.461	-.0604
NA	1.837	-.708	-.0331
K	3.155	.083	.0328
S	1.296	-.064	.0356
O	46.254	-.546	-.0482
C	.113	-.005	.0031
SO3	.858	-.042	.0237
TI	.350	-.004	.0027
SUM RESIDUALS**2		1.161	
STANDARD DEVIATION		.622	

ON-2804	WEIGHT		GAIN OR LOSS
MINERAL	PER CENT	G/CM**3	G/CM**3
PLAGICCLAS	27.16	.771	-1.126
K-FELDSPAR	15.59	.443	.305
QUARTZ	22.26	.632	.357
BIOTITE	13.04	.370	.040
PYRITE	5.26	.150	.150
CALCITE	.84	.024	.024
ANHYDRITE	1.35	.038	.038
CHLORITE	3.08	.088	.088
KAOLINITE	11.11	.315	.315
TOTALS	99.69	2.831	.191

COMPONENT	WT.PERCENT COMPUTED	RESIDUAL	GAIN OR LOSS G/CM**3
SI	28.228	.367	.0279
AL	9.348	.032	-.0352
FE++	4.696	.320	.0324
MG	1.684	-.066	.0182
CA	2.232	.310	-.0614
NA	1.574	-.318	-.0463
K	3.070	.065	.0373
S	2.814	-.126	.0435
O	44.794	-.866	.0178
C	.101	-.003	.0029
SO3	.792	-.028	.0233
TI	.351	-.003	.0034
SUM RESIDUALS**2		1.211	
STANDARD DEVIATION		.635	

MF-3001	WEIGHT		GAIN OR LOSS
MINERAL	PER CENT	G/CM**3	G/CM**3
PLAGICCLAS	46.19	1.275	-.623
K-FELDSPAR	5.61	.155	.017
QUARTZ	17.44	.481	.226
BIOTITE	18.65	.515	.185
PYRITE	3.72	.103	.103
CALCITE	.63	.017	.017
ANHYDRITE	4.14	.114	.114
CHLORITE	3.38	.093	.093
TOTALS	99.76	2.753	.113

COMPONENT	WT.PERCENT COMPUTED	RESIDUAL	GAIN OR LOSS G/CM**3
SI	26.334	.473	-.0497
AL	8.424	.355	-.0660
FE++	4.850	.613	.0250
MG	2.154	-.295	.0361
CA	4.293	.341	-.0069
NA	2.346	-.265	-.0279
K	2.332	-.001	.0164
S	1.986	-.134	.0585
O	43.676	-1.255	-.0389
C	.076	-.000	.0021
SO3	2.432	-.068	.0690
TI	.459	-.003	.0061
SUM RESIDUALS**2		2.597	
STANDARD DEVIATION		.806	

MF-3002	WEIGHT		GAIN OR LOSS
MINERAL	PER CENT	G/CM**3	G/CM**3
PLAGIOCLAS	50.75	1.406	-.492
K-FELDSPAR	3.90	.108	-.030
QUARTZ	17.66	.439	.214
BIOTITE	18.51	.513	.183
PYRITE	3.13	.087	.087
CALCITE	.75	.021	.021
ANHYDRITE	2.38	.066	.066
CHLORITE	2.81	.078	.078
TOTALS	99.88	2.767	.127

COMPONENT	WT.PERCENT COMPUTED	RESIDUAL	GAIN OR LOSS G/CM**3
SI	27.032	.452	-.0271
AL	9.230	.687	-.0631
FE++	4.449	.617	.5143
MG	2.061	-.376	.0360
CA	4.101	.028	-.0032
NA	2.555	-.205	-.0236
K	2.112	-.021	.0111
S	1.673	-.117	.0496
O	44.722	-1.143	-.0074
C	.090	-.000	.0025
SO3	1.399	-.001	.0388
TI	.455	-.001	.0060
SUM RESIDUALS**2		2.655	
STANDARD DEVIATION		.815	

MF-3003	WEIGHT		GAIN OR LOSS
MINERAL	PER CENT	G/CM**3	G/CM**3
PLAGIOCLAS	43.37	1.188	-.709
K-FELDSPAR	6.31	.173	.035
QUARTZ	18.07	.495	.220
BIOTITE	18.02	.494	.154
PYRITE	4.89	.134	.134
CALCITE	.97	.027	.027
ANHYDRITE	4.36	.120	.120
CHLORITE	4.05	.111	.111
TOTALS	100.05	2.741	.101

COMPONENT	WT.PERCENT COMPUTED	RESIDUAL	GAIN OR LOSS G/CM**3
SI	26.065	.401	-.0602
AL	8.510	.631	-.0837
FE++	5.438	.719	.0374
MG	2.190	-.319	.0373
CA	4.324	.264	-.0048
NA	2.213	-.294	-.0313
K	2.362	-.021	.0173
S	2.613	-.227	.0778
O	43.204	-1.048	-.0665
C	.117	-.001	.0032
SO3	2.566	-.054	.0718
TI	.443	-.000	.0056
SUM RESIDUALS**2		2.487	
STANDARD DEVIATION		.789	

MF-3004	WEIGHT		GAIN OR LOSS
MINERAL	PER CENT	G/CM**3	G/CM**3
PLAGIOCLAS	43.59	1.199	-.699
K-FELDSPAR	4.20	.116	-.022
QUARTZ	20.16	.554	.279
BIOTITE	18.09	.497	.167
PYRITE	2.89	.079	.079
CALCITE	2.60	.071	.071
ANHYDRITE	4.15	.114	.114
CHLORITE	4.19	.115	.115
TOTALS	99.88	2.747	.107

COMPONENT	WT.PERCENT COMPUTED	RESIDUAL	GAIN OR LOSS G/CM**3
SI	26.493	.408	-.0461
AL	8.364	.212	-.0756
FE++	4.544	.533	.0184
MG	2.216	-.293	.0375
CA	4.927	.767	-.0016
NA	2.203	-.430	-.0276
K	2.105	.013	.0095
S	1.544	-.076	.0446
O	44.287	-1.084	-.0313
C	.312	-.016	.0090
SO3	2.442	-.148	.0712
TI	.445	-.005	.0058
SUM RESIDUALS**2		2.559	
STANDARD DEVIATION		.800	

MF-3005	WEIGHT		GAIN OR LOSS
MINERAL	PER CENT	G/CM**3	G/CM**3
PLAGIOCLAS	43.09	1.198	-.700
K-FELDSPAR	6.71	.187	.049
QUARTZ	18.11	.504	.229
BIOTITE	16.79	.467	.137
PYRITE	5.51	.153	.153
CALCITE	1.08	.030	.030
ANHYDRITE	4.62	.128	.128
CHLORITE	4.21	.117	.117
TOTALS	100.13	2.784	.144

COMPONENT	WT.PERCENT COMPUTED	RESIDUAL	GAIN OR LOSS G/CM**3
SI	25.925	.355	-.0525
AL	8.442	.608	-.0820
FE++	5.595	.753	.0427
MG	2.101	-.287	.0349
CA	4.426	.352	-.0027
NA	2.203	-.341	-.0293
K	2.308	-.017	.0166
S	2.947	-.293	.0901
O	42.922	-.915	-.0603
C	.130	-.001	.0036
SO3	2.717	-.083	.0778
TI	.413	-.001	.0049
SUM RESIDUALS**2		2.316	
STANDARD DEVIATION		.761	

MF-3006	WEIGHT		GAIN OR LOSS
MINERAL	PER CENT	G/CM**3	G/CM**3
PLAGICCLAS	46.03	1.261	-.636
K-FELDSPAR	2.67	.073	-.064
QUARTZ	17.25	.473	.198
BIOTITE	19.36	.530	.200
PYRITE	2.49	.068	.068
CALCITE	.91	.025	.025
ANHYDRITE	4.84	.133	.133
CHLORITE	6.60	.181	.181
TOTALS	100.17	2.745	.105

COMPONENT	WT.PERCENT COMPUTED	RESIDUAL	GAIN OR LOSS G/CM**3
SI	25.930	.266	-.0602
AL	8.909	.757	-.0764
FE++	4.983	.381	.0342
MG	2.666	-.283	.0493
CA	4.603	.008	.0099
NA	2.309	-.199	-.0313
K	2.025	-.026	.0082
S	1.331	-.029	.0373
O	43.979	-.708	-.0546
C	.109	.000	.0030
SO3	2.849	-.001	.0781
TI	.476	.003	.0064
SUM RESIDUALS**2		1.412	
STANDARD DEVIATION		.594	

MF-3007	WEIGHT		GAIN OR LOSS
MINERAL	PER CENT	G/CM**3	G/CM**3
PLAGICCLAS	44.42	1.222	-.676
K-FELDSPAR	3.20	.088	-.049
QUARTZ	15.75	.433	.158
BIOTITE	19.44	.535	.205
PYRITE	5.82	.160	.160
CALCITE	1.59	.044	.044
ANHYDRITE	3.39	.093	.093
CHLORITE	6.36	.175	.175
TOTALS	99.97	2.749	.109

COMPONENT	WT.PERCENT COMPUTED	RESIDUAL	GAIN OR LOSS G/CM**3
SI	24.927	.292	-.0859
AL	8.712	.454	-.0727
FE++	6.499	1.128	.0558
MG	2.639	-.606	.0577
CA	4.347	.074	.0015
NA	2.234	-.125	-.0351
K	2.095	-.013	.0100
S	3.113	-.427	.0974
O	42.738	-.801	-.0817
C	.191	-.000	.0053
SO3	1.992	-.008	.0550
TI	.478	-.002	.0066
SUM RESIDUALS**2		2.775	
STANDARD DEVIATION		.833	

MF-3008	WEIGHT		GAIN OR LOSS
MINERAL	PER CENT	G/CM**3	G/CM**3
PLAGICCLAS	41.90	1.161	-.737
K-FELDSPAR	4.61	.128	-.010
QUARTZ	17.07	.473	.198
BIOTITE	22.62	.627	.297
PYRITE	2.87	.079	.079
CALCITE	1.34	.037	.037
ANHYDRITE	3.61	.100	.100
CHLORITE	4.91	.136	.136
TOTALS	98.93	2.740	.100

COMPONENT	WT.PERCENT COMPUTED	RESIDUAL	GAIN OR LOSS G/CM**3
SI	25.665	.562	-.0680
AL	8.577	-.157	-.0579
FE++	5.272	.880	.0298
MG	2.725	-.689	.0631
CA	4.160	-.007	-.0006
NA	2.124	.039	-.0423
K	2.534	.010	.0219
S	1.533	-.107	.0454
O	43.506	-1.592	-.0298
C	.161	.000	.0045
SO3	2.122	.002	.0587
TI	.556	-.007	.0090
SUM RESIDUALS**2		4.136	
STANDARD DEVIATION		1.017	

MF-3009	WEIGHT		GAIN OR LOSS
MINERAL	PER CENT	G/CM**3	G/CM**3
PLAGICCLAS	48.70	1.344	-.553
K-FELDSPAR	3.29	.091	-.047
QUARTZ	13.64	.377	.102
BIOTITE	21.59	.596	.266
PYRITE	3.10	.086	.086
CALCITE	1.19	.033	.033
ANHYDRITE	2.61	.072	.072
CHLORITE	5.68	.157	.157
TOTALS	99.80	2.755	.115

COMPONENT	WT.PERCENT COMPUTED	RESIDUAL	GAIN OR LOSS G/CM**3
SI	25.424	.227	-.0680
AL	9.414	.362	-.0500
FE++	5.389	.496	.0321
MG	2.739	-.784	.0657
CA	4.220	-.118	.0037
NA	2.447	-.023	-.0318
K	2.293	-.015	.0157
S	1.658	-.122	.0491
O	44.009	-.626	-.0471
C	.142	.000	.0039
SO3	1.537	.007	.0422
TI	.531	-.003	.0081
SUM RESIDUALS**2		2.021	
STANDARD DEVIATION		.711	

ON-3001	WEIGHT		GAIN OR LOSS
MINERAL	PER CENT	G/CM**3	G/CM**3
PLAGIOCLAS	46.05	1.285	-.613
K-FELDSPAR	11.57	.323	.165
QUARTZ	17.96	.501	.226
BIOTITE	14.03	.391	.061
PYRITE	3.28	.092	.092
CALCITE	1.05	.029	.029
ANHYDRITE	.70	.019	.019
CHLORITE	2.54	.071	.071
KAOLINITE	2.20	.061	.061
TOTALS	99.34	2.773	.133

COMPONENT	WT.PERCENT COMPUTED	RESIDUAL	GAIN OR LOSS G/CM**3
SI	26.040	.506	.0348
AL	9.415	.546	-.0384
FE**	3.735	.250	.0070
MG	1.639	-.041	.0101
CA	3.169	-.040	-.0285
NA	2.521	.026	-.0305
K	2.705	-.002	.0275
S	1.793	-.047	.0505
O	45.365	-1.274	.0723
C	.126	.000	.0035
SO3	.410	.000	.0114
TI	.376	-.000	.0034
SUM RESIDUALS**2		1.956	
STANDARD DEVIATION		.807	

ON-3002	WEIGHT		GAIN OR LOSS
MINERAL	PER CENT	G/CM**3	G/CM**3
PLAGIOCLAS	41.42	1.110	-.786
K-FELDSPAR	14.64	.391	.293
QUARTZ	20.69	.582	.277
BIOTITE	12.47	.346	.015
PYRITE	2.05	.055	.055
CALCITE	1.14	.031	.031
ANHYDRITE	2.08	.056	.056
CHLORITE	1.24	.035	.035
KAOLINITE	1.46	.043	.033
TOTALS	99.64	2.666	.026

COMPONENT	WT.PERCENT COMPUTED	RESIDUAL	GAIN OR LOSS G/CM**3
SI	28.869	.617	-.0342
AL	9.146	.642	-.0554
FE**	3.435	.295	-.0227
MG	1.636	-.114	.0042
CA	3.358	.308	-.0342
NA	2.109	-.221	-.0522
K	2.472	-.025	.0313
S	1.087	-.043	.0366
O	45.439	-1.252	-.0178
C	.137	-.002	.0037
SO3	1.224	-.026	.0135
TI	.346	-.001	.0027
SUM RESIDUALS**2		2.061	
STANDARD DEVIATION		.829	

ON-3003	WEIGHT		GAIN OR LOSS
MINERAL	PER CENT	G/CM**3	G/CM**3
PLAGIOCLAS	32.90	.888	-1.009
K-FELDSPAR	20.56	.555	.418
QUARTZ	21.45	.579	.304
BIOTITE	13.10	.354	.024
PYRITE	2.27	.061	.061
CALCITE	2.32	.063	.063
ANHYDRITE	1.52	.041	.041
CHLORITE	.13	.003	.003
KAOLINITE	5.59	.151	.151
TOTALS	99.84	2.696	.056

COMPONENT	WT.PERCENT COMPUTED	RESIDUAL	GAIN OR LOSS G/CM**3
SI	29.140	.297	-.0154
AL	8.968	.022	-.0503
FE**	2.743	.248	-.0245
MG	1.257	-.095	.0250
CA	3.193	.186	-.0348
NA	1.924	-.046	-.0457
K	3.710	.024	.0515
S	1.214	-.056	.0343
O	46.164	-.669	-.0140
C	.278	-.005	.0077
SO3	.892	-.008	.0243
TI	.353	-.001	.0038
SUM RESIDUALS**2		.679	
STANDARD DEVIATION		.476	

ON-3004	WEIGHT		GAIN OR LOSS
MINERAL	PER CENT	G/CM**3	G/CM**3
PLAGIOCLAS	34.36	.948	-.949
K-FELDSPAR	20.57	.568	.430
QUARTZ	20.09	.554	.279
BIOTITE	12.17	.336	.006
PYRITE	2.80	.077	.077
CALCITE	2.50	.069	.069
ANHYDRITE	2.88	.079	.079
CHLORITE	.28	.008	.008
KAOLINITE	4.52	.125	.125
TOTALS	100.16	2.764	.124

COMPONENT	WT.PERCENT COMPUTED	RESIDUAL	GAIN OR LOSS G/CM**3
SI	28.480	.114	.0198
AL	8.864	.009	-.0558
FE**	2.902	.415	-.0232
MG	1.191	-.160	.0098
CA	3.746	.516	-.0268
NA	2.007	-.270	-.0373
K	3.641	.056	.0510
S	1.499	-.161	.0453
O	45.522	-.261	-.0154
C	.300	-.016	.0087
SO3	1.683	-.077	.0489
TI	.328	-.002	.0025
SUM RESIDUALS**2		.654	
STANDARD DEVIATION		.467	

ON-3005	WEIGHT		GAIN OR LOSS
MINERAL	PER CENT	G/CM**3	G/CM**3
PLAGIOCLAS	27.71	.745	-1.152
K-FELDSPAR	25.60	.689	.551
QUARTZ	17.32	.466	.191
BIOTITE	12.89	.347	.017
PYRITE	3.82	.103	.103
CALCITE	2.68	.072	.072
ANHYDRITE	.46	.012	.012
CHLORITE	.21	.006	.006
KAOLINITE	9.16	.246	.246
TOTALS	99.85	2.686	.046

COMPONENT	WT.PERCENT COMPUTED	RESIDUAL	GAIN OR LOSS G/CM**3
SI	28.192	.237	-.0114
AL	9.603	.022	-.0421
FE++	3.455	.415	-.0101
MG	1.249	-.108	.0050
CA	2.740	.060	-.0439
NA	1.703	-.026	-.0535
K	4.306	.014	.0675
S	2.044	-.196	.0603
O	45.616	-.569	-.0366
C	.322	-.003	.0087
SO3	.270	-.000	.0073
TI	.347	-.001	.0028
SUM RESIDUALS**2		.608	
STANDARD DEVIATION		.450	

ON-3006	WEIGHT		GAIN OR LOSS
MINERAL	PER CENT	G/CM**3	G/CM**3
PLAGIOCLAS	40.62	1.105	-.793
K-FELDSPAR	18.89	.514	.376
QUARTZ	18.28	.497	.222
BIOTITE	11.76	.320	-.010
PYRITE	2.07	.056	.056
CALCITE	1.25	.034	.034
ANHYDRITE	3.08	.084	.084
CHLORITE	2.65	.072	.072
KAOLINITE	1.03	.028	.028
TOTALS	99.63	2.710	.070

COMPONENT	WT.PERCENT COMPUTED	RESIDUAL	GAIN OR LOSS G/CM**3
SI	28.238	.424	-.0369
AL	8.927	.034	-.0579
FE++	2.962	.281	-.0190
MG	1.499	-.135	.0130
CA	3.652	.400	-.0275
NA	2.310	-.264	-.0300
K	3.416	.038	.0439
S	1.105	-.045	.0313
O	45.241	-1.031	-.0204
C	.150	-.003	.0042
SO3	1.813	-.067	.0511
TI	.316	-.001	.0020
SUM RESIDUALS**2		1.578	
STANDARD DEVIATION		.725	

ON-3005V	WEIGHT		GAIN OR LOSS
MINERAL	PER CENT	G/CM**3	G/CM**3
PLAGIOCLAS	19.24	0.000	-1.898
K-FELDSPAR	26.07	0.000	-.138
QUARTZ	18.71	0.000	-.275
BIOTITE	12.79	0.000	-.330
PYRITE	5.29	0.000	0.000
CALCITE	2.60	0.000	0.000
ANHYDRITE	1.95	0.000	0.000
CHLORITE	.45	0.000	0.000
KAOLINITE	12.67	0.000	0.000
TOTALS	99.77	0.000	-2.640

COMPONENT	WT.PERCENT COMPUTED	RESIDUAL	GAIN OR LOSS G/CM**3
SI	27.561	.402	-.7634
AL	9.353	.037	-.2998
FE++	4.171	.603	-.0919
MG	1.274	-.120	-.0315
CA	2.677	.476	-.1160
NA	1.265	-.233	-.1000
K	4.332	.148	-.0480
S	2.829	-.441	0.0000
O	44.500	-.989	-1.2790
C	.312	-.040	0.0000
SO3	1.147	-.073	0.0000
TI	.344	-.004	-.0066
SUM RESIDUALS**2		2.022	
STANDARD DEVIATION		.821	

ON-3007	WEIGHT		GAIN OR LOSS
MINERAL	PER CENT	G/CM**3	G/CM**3
PLAGIOCLAS	26.80	.729	-1.168
K-FELDSPAR	15.88	.432	.294
QUARTZ	20.83	.567	.292
BIOTITE	13.13	.357	.027
PYRITE	3.67	.100	.100
CALCITE	2.39	.065	.065
ANHYDRITE	2.30	.063	.063
CHLORITE	4.81	.131	.131
KAOLINITE	9.75	.265	.265
TOTALS	99.56	2.708	.068

COMPONENT	WT.PERCENT COMPUTED	RESIDUAL	GAIN OR LOSS G/CM**3
SI	27.472	.405	-.0272
AL	9.194	.036	-.0507
FE++	4.295	.191	.0197
MG	1.945	-.058	.0230
CA	3.116	.078	-.0334
NA	1.559	-.022	-.0570
K	3.113	.008	.0364
S	1.960	-.040	.0546
O	44.919	-1.025	-.0293
C	.287	-.002	.0079
SO3	1.352	-.006	.0370
TI	.353	-.000	.0030
SUM RESIDUALS**2		1.265	
STANDARD DEVIATION		.649	

DDH-216

MINERAL	WEIGHT PER CENT	G/CM**3	GAIN OR LOSS G/CM**3
PLAGIOCLAS	44.97	1.250	-.647
K-FELDSPAR	0.00	0.000	-.138
QUARTZ	13.93	.387	.112
BIOTITE	24.66	.685	.355
PYRITE	.93	.026	.026
CALCITE	.87	.024	.024
ANHYDRITE	5.09	.142	.142
CHLORITE	1.37	.038	.038
ALBITE	8.07	.224	.224
TOTALS	99.88	2.777	.137

COMPONENT	WT.PERCENT COMPUTED	RESIDUAL	GAIN OR LOSS G/CM**3
SI	26.305	.220	-.0382
AL	9.060	.538	-.0629
FE++	3.274	.095	-.0035
MG	3.060	-.167	.0582
CA	4.330	-.208	.0102
NA	3.056	-.082	-.0128
K	2.059	.025	.0085
S	.498	-.302	.0139
O	44.663	-.581	-.0212
C	.104	.000	.0029
SO3	2.994	.044	.0820
TI	.478	-.002	.0067
SUM RESIDUALS**2		.764	
STANDARD DEVIATION		.505	

DDH-350

MINERAL	WEIGHT PER CENT	G/CM**3	GAIN OR LOSS G/CM**3
PLAGIOCLAS	53.62	1.491	-.407
K-FELDSPAR	.72	.020	-.117
QUARTZ	15.04	.418	.143
BIOTITE	25.66	.713	.383
PYRITE	1.43	.040	.040
CALCITE	.83	.023	.023
ANHYDRITE	1.97	.055	.055
CHLORITE	0.00	0.000	0.000
TOTALS	99.27	2.760	.120

COMPONENT	WT.PERCENT COMPUTED	RESIDUAL	GAIN OR LOSS G/CM**3
SI	26.812	.541	-.0331
AL	9.431	.644	-.0555
FE++	3.363	.075	-.0005
MG	2.972	-.062	.0528
CA	3.871	-.460	.0044
NA	2.808	.049	-.0233
K	2.253	-.030	.0155
S	.766	-.004	.0214
O	45.241	-1.499	.0204
C	.099	.001	.0027
SO3	1.156	.016	.0317
TI	.495	-.000	.0072
SUM RESIDUALS**2		3.178	
STANDARD DEVIATION		.891	

DDH-639

MINERAL	WEIGHT PER CENT	G/CM**3	GAIN OR LOSS G/CM**3
PLAGIOCLAS	38.94	1.051	-.846
K-FELDSPAR	7.41	.200	.063
QUARTZ	19.23	.519	.244
BIOTITE	13.72	.370	.040
PYRITE	.52	.014	.014
CALCITE	.75	.020	.020
ANHYDRITE	2.31	.062	.062
KAOLINITE	2.96	.080	.080
ALBITE	12.95	.350	.350
MAGNETITE	.74	.020	-.007
TOTALS	99.54	2.688	.020

COMPONENT	WT.PERCENT COMPUTED	RESIDUAL	GAIN OR LOSS G/CM**3
SI	29.442	.459	.0191
AL	9.193	.036	-.0525
FE++	2.224	.001	-.0319
MG	1.589	.226	.0353
CA	3.132	.002	-.0315
NA	3.244	.002	-.0125
K	2.109	.000	.0089
S	.280	-.000	.0076
O	46.611	-1.092	.0090
C	.090	.000	.0024
SO3	1.360	-.000	.0367
TI	.266	-.094	.0031
SUM RESIDUALS**2		1.465	
STANDARD DEVIATION		.856	

DDH-770

MINERAL	WEIGHT PER CENT	G/CM**3	GAIN OR LOSS G/CM**3
PLAGIOCLAS	34.34	.920	-.977
K-FELDSPAR	12.44	.333	.196
QUARTZ	16.77	.449	.174
BIOTITE	14.43	.387	.057
PYRITE	.52	.014	.014
CALCITE	.77	.021	.021
ANHYDRITE	2.31	.062	.062
CHLORITE	0.00	0.000	0.000
KAOLINITE	2.70	.072	.072
ALBITE	15.69	.421	.421
TOTALS	99.98	2.680	.040

COMPONENT	WT.PERCENT COMPUTED	RESIDUAL	GAIN OR LOSS G/CM**3
SI	29.464	.013	.0259
AL	9.370	.001	-.0487
FE++	2.111	-.003	-.0352
MG	1.347	.002	.0045
CA	2.887	.000	-.0386
NA	3.294	.000	-.0117
K	2.798	.000	.0270
S	.280	.000	.0075
O	46.656	-.030	-.0278
C	.093	.000	.0025
SO3	1.360	.000	.0364
TI	.324	-.000	.0021
SUM RESIDUALS**2		.001	
STANDARD DEVIATION		.023	

DDH-812	WEIGHT		GAIN OR LOSS
MINERAL	PER CENT	G/CM**3	G/CM**3
PLAGIOCLAS	24.75	.668	-1.229
K-FELDSPAR	15.24	.411	.274
QUARTZ	21.09	.570	.295
BIOTITE	10.11	.273	-.057
PYRITE	2.42	.065	.065
CALCITE	.80	.021	.021
ANHYDRITE	2.36	.064	.064
CHLORITE	0.00	0.000	0.000
KAOLINITE	8.33	.225	.225
ALBITE	13.92	.376	.376
TOTALS	99.02	2.674	.034

	WT.PERCENT		GAIN OR LOSS
COMPONENT	COMPUTED	RESIDUAL	G/CM**3
SI	29.757	.728	.0204
AL	9.161	.057	-.0540
FE++	2.435	-.161	-.0218
MG	.944	.142	-.0098
CA	2.382	.002	-.0517
NA	2.665	.002	-.0281
K	2.774	.001	.0269
S	1.203	.033	.0340
O	45.897	-1.716	.0065
C	.096	.000	.0026
SO3	1.390	.000	.0375
TI	.227	-.067	.0013
SUM RESIDUALS**2		3.528	
STANDARD DEVIATION		1.328	

DDH-992	WEIGHT		GAIN OR LOSS
MINERAL	PER CENT	G/CM**3	G/CM**3
PLAGIOCLAS	44.14	1.223	-.575
K-FELDSPAR	3.43	.095	-.042
QUARTZ	17.45	.483	.208
BIOTITE	20.58	.570	.240
PYRITE	2.11	.058	.058
CALCITE	.68	.019	.019
ANHYDRITE	5.93	.164	.164
CHLORITE	5.43	.151	.151
KAOLINITE	.14	.004	.004
TOTALS	99.90	2.767	.127

	WT.PERCENT		GAIN OR LOSS
COMPONENT	COMPUTED	RESIDUAL	G/CM**3
SI	25.950	.192	-.0499
AL	8.698	.017	-.0593
FE++	4.624	.496	.0224
MG	2.755	-.321	.0537
CA	4.456	.132	.0036
NA	2.340	-.042	-.0340
K	2.195	.003	.0127
S	1.126	-.034	.0321
O	43.724	-.498	-.0541
C	.082	-.000	.0023
SO3	3.486	-.044	.0978
TI	.462	-.006	.0064
SUM RESIDUALS**2		.657	
STANDARD DEVIATION		.468	

BIBLIOGRAPHY

AL-SHAIEB, Zuhair, 1972, Geochemical anomalies in the Igneous Wall Rocks at Mayflower Mine; Unpub. Ph.D. dissertation, University of Missouri, Rolla.

AUCOTT, J. W., 1970, Tectonics of the Galway Granite, in Mechanics of Igneous Intrusions, Geol. Journal Special Issue n. 2, Newall & Rast, ed., Gallery Press, Liverpool, p. 49-62.

ANDERSON, E. M., 1951, The Dynamics of Faulting and Dike Formation with Applications to Britain, Oliver & Boyd Publ., London, England.

BAILEY, E. H. and STEVENS, R. E., 1960, Selective Staining of K-feldspar and Plagioclase in Rock Slabs and Thin Sections: Amer. Mineral. v. 45, p. 1020-1025.

BARNES, M. P. and SIMOS, J. G., 1968, Ore Deposits of the Park City District with a Contribution on the Mayflower Lode, in Ore Deposits of the United States, 1933-1967, J. D. Ridge ed., The Granton-Sales volume, n. 2, AIME, p. 1102-1126.

BEANE, R. E., 1972, A Thermodynamic Analysis of the Effect of Solid Solution on the Hydrothermal Stability of Biotite; Unpublished Ph.D. dissertation, Northwestern University, Evanston, Illinois, 195 p.

_____, 1974, Biotite Stability in Porphyry Copper Environment: Econ. Geol. v. 69, n. 2, p. 241-256.

BETZ, C. E., 1963, Principles of Penetrants, Magnaflux Corp., Chicago, Illinois.

BIANCHI, L., 1968, Geology of the Manitou Springs-Cascade Area, El Paso County, Colorado, with a Study of the Permeability of its Crystalline Rocks: Unpublished M.Sc. Thesis, Colorado School of Mines, 197 p.

BIANCHI, L. and SNOW, D. T., 1969, Permeability of Crystalline Rocks Interpreted from Measured Orientations and Apertures of Fractures, Annals of Arid Zone, v. 8, n. 2, The Arid Zone Research of India, Jodhpur (Rajasthan), p. 231-245.

BILLINGS, M., 1972, Structural Geology, Prentice-Hall, New York. 3rd ed.

BOUTWELL, J. M., 1912, Geology and Ore Deposits of the Park City District, Utah: USGS Prof. Paper n. 77, 231 p.

BROMFIELD, C. J., 1968, General Geology of the Park City Region, Utah, in Park City District, Utah, A. J. Erickson Jr., ed. Utah Geol. Soc. Guidebook n. 22, p. 10-29.

BROMFIELD, C. J., BAKER, A. A. and CRITTENDEN Jr., M. D., 1970, Geologic Map of the Heber Quadrangle, Wasatch and Summit Counties, Utah, U. S. Geol. Survey.

BROWN, T. H., 1970, Theoretical Predictions of Equilibria and Mass Transfer in the System CaO-MgO-SiO_2-H_2O-CO_2-$NaCl$-HCl: Unpublished Ph.D. dissertation, Northwestern, Evanston, Illinois, 136 p.

CRITTENDEN Jr., M. D. STUCKLESS, J. S., KISTLER, R. W. and STERN, T. W., 1973, Radiometric Dating of Intrusive Rocks in the Cottonwood Area, Utah: Journ. Research U. S. Geol. Survey, v. 1, n. 2, p. 173-178.

EARDLEY, A. J., 1968, Regional Geologic Relations of the Park City District, in Park City District, Utah, A. J. Erickson Jr., ed., Utah Geol. Soc., Guidebook, n. 22, p. 3-9.

GARMOE, W. J. and ERICKSON Jr., A. J., 1968, Ore Deposits of the Park City District, in Park City District, Utah, A. J. Erickson Jr., ed., Utah Geol. Soc., Guidebook, n. 22, p. 30-39.

GRANT, Sheldon K., 1966, Metallization and Panagenesis in the Park City District: Unpublished Ph.D. dissertation, University of Utah, 183 p.

GRIGGS, D. T., TURNER, F. J., and HEARD, H. C., 1960, Deformation of Rocks at 500°C to 800°C, in Rock Deformation, Griggs & Handin, ed., Memoir n. 79, Geol. Soc. of Amer., p. 39-104.

HALLIMOND, A. F., 1943, On the Graphical Representation of the Calciferous Amphiboles: The Amer. Mineral., v. 28, n. 2, p. 65-89.

HASHAD, Ahmad, 1964, Geochronological Studies in the Central Wasatch Mountains, Utah: Unpublished Ph.D. dissertation, University of Utah, 98 p.

HELGESON, H., 1969a, Thermodynamics of Hydrothermal Systems at Elevated Temperatures and Pressures: Amer. Journ. Sci., v. 267, p. 729-804.

HELGESON, H., BROWN, T. H., and LEEPER, R. H., 1969b, Handbook of Theoretical Activity Diagrams Depicting Chemical Equilibria in Geologic Systems Involving an Aqueous Phase at One Atm and 0° to 300°C: Freeman, Cooper & Co., San Francisco.

HELGESON, H., 1970, A Chemical and Thermodynamic Model of Ore Deposition in Hydrothermal Systems: Mineral. Soc. Amer. Spec. Paper 3, p. 155-186.

HOLT, R. E., 1953, Structure and Petrology of the Diorite on the 800' Level Mayflower Mine, Park City, Utah: Unpublished M.Sc. Thesis, University of Utah, 35 p.

HUBBERT, M. K., 1940, The Theory of Groundwater Motion: The Journ. of Geol., v. 48, n. 8, Part I, p. 785-944.

JAEGER, J. C., 1964, Elasticity, Fracture and Flow: Methuen & Co., London.

MEIER, Charles, 1950, Hydrothermal Wall Rock Alteration at Butte, Montana: Unpublished Ph.D. dissertation, Harvard University, 329 p.

NASH, J. T., 1973, Geochemical Studies in the Park City District: I. Ore Fluids in the Mayflower Mine: Econ. Geol., v. 68, n. 1, p. 34-51.

NEW PARK MINING COMPANY, 1970, Annual Report to Shareholders, San Francisco.

NORTON, D. L., 1975, A Theoretical Model of Porosity in Fractured Media in the Context of Chemical Mass Transfer: in preparation.

QUINLAN, J. J. and SIMOS, J. G., 1968, The Mayflower Mine, in Park City District, Utah, A. J. Erickson Jr. ed., Utah Geol. Soc., Guidebook, n. 22, p. 40-55.

ROBERTS, J. L., 1970, The Intrusion of Magma Into Brittle Rocks, in Mechanism of Igneous Intrusion: Geol. Journ. Spec. Issue n. 2, Newall & Rast ed., Gallery Press, Liverpool, p. 287-338.

ROBIE, R. A. and WALDBAUM, D. R., 1968, Thermodynamic Properties of Minerals and Related Substances at 298.15°K (25.0°C) and one Atmosphere (1.013 Bars) Pressure and at Higher Temperatures: USGS Bulletin, n. 1259, 256. p.

ROEDDER, E., 1971, Fluid Inclusions Studies on Porphyry-Type Ore Deposits at Bingham, Utah, Butte, Montana and Climax, Colorado: Econ. Geol., v. 66, n. 1, p. 98-120.

SNOW, D. T., 1965, A Parallel Plate Model of Fractured Permeable Media: Unpublished Ph.D. dissertation, University of California, Berkeley, 331 p.

_____, 1968, Rock Fracture Spacings, Openings and Porosities: Journ. Soil Mech. and Found. Div., Amer. Soc. Civil Eng., v. 94, n. 1, p. 73-91.

_____, 1969, Anisotropic Permeability of Fractured Media: Water Resources Research, v. 5, n. 6, p. 1273-1288.

_____, 1970, The Frequency and Apertures of Fractures in Rock: Int. Journ. Rock Mech. Min. Sci., vol. 7, p. 23-40.

TAYLOR, Jr., H. D., 1974, The Application of Oxygen and Hydrogen Isotope Studies to Problems of Hydrothermal Alteration and Ore Deposition; Econ. Geol., v. 69, n. 6, p. 843-883.

TIMUR, A., HEMPKINS, W. B. and WEINBRANDT, R. M., 1971, Scanning Electron Microscope Study of Pore Systems in Rocks: Journ. Geoph. Research, v. 76, n. 20, p. 4932-4948.

WILLIAMS, N. C., 1952, Wall Rock Alteration, Mayflower Mine, Park City, Utah: Unpublished Ph.D. dissertation, Columbia University, 58 p.